中華民國核醫學學會
2020年會暨國際學術研討會

2020 Annual Meeting and International Symposium of The Society of Nuclear Medicine, Taiwan (R.O.C)

2020 November 21 (六)

■ 地　　點 ■ 台北榮民總醫院　致德樓

■ 主辦單位 ■ 中華民國核醫學學會

台北榮民總醫院

行政院原子能委員會核能研究所

經濟部技術處

TECAN

Freedom EVO®

(衛部醫器輸壹字第 021434 號)

全自動條碼掃描儀

獨立液面偵測系統

一個平台 多樣選擇

- 超過 **25** 年的自動分注、稀釋平台及工作流程經驗。
- 感謝 **10** 家放射免疫分析實驗室的採用與長期愛護。

Everlight Group

大昇生物科技股份有限公司

電話: 02 2695 4758　　傳真: 02 2695 6680

現代儀器股份有限公司

自動化正子FDG/NaF輸液系統

- 減少臨床人員輻射劑量
  - 大瓶裝設計不需分藥作業
  - 減少50%體部劑量
  - 減少90%手部劑量

- 給予病患安全與精準輸液
  - 以體重自動計算劑量
  - 依所設定的劑量做注射
  - 兩種流速以及saline test

- 提高工作效率
  - 靈活的排程安排
  - 無線輸出輸液記錄和輻射劑量到PACS

全球45個國家400台以上設備

超過3.5百萬次以上累計輸液

輸液過程即時活性輸出曲線圖

AFINITOR®
(everolimus) Tablets

適用於治療無法切除、局部晚期或
轉移之進展性、分化良好、

胃腸道(GI)或肺部

來源之非功能性神經內分泌腫瘤
(NET)成人病患

晚期 **胰臟** 神經內分泌腫瘤(pNET)
標靶藥物的治療優選

處方資訊摘要 [本藥須由醫師處方使用]

產品名稱: AFINITOR® 5 毫克 (許可證字號：衛部藥輸字第 025165 號) AFINITOR® 10 毫克 (許可證字號：衛部藥輸字第 025166 號) **主成分:** everolimus **適應症:** 合併 exemestane 適用於治療荷爾蒙接受體陽性、HER2 受體陰性且之前使用過 letrozole 或 anastrozole 復發或惡化之停經後晚期乳癌患者。適用於進展性，無法切除或轉移性分化良好或中度分化 (well-differentiatedor moderately-differentitated) 之胰臟神經內分泌腫瘤成人患者。適用於治療無法切除、局部晚期或轉移之進展性、分化良好、胃腸道(GI)或肺部來源之非功能性神經內分泌腫瘤(NET) 成人患者。適用於治療在經 VEGF-targeted 療法無效後之晚期腎細胞癌患者 **用法/用量:** Afinitor建議用量為 10 毫克。處理嚴重或不耐受的不良反應時可能需要暫時調降劑量或中斷 Afinitor 療法。需要調降劑量時，建議調降至每天原給予劑量的 50%，若使用的已經是最低劑量，建議將給藥頻次降低為隔天給藥。肝功能不全會增加Afinitor 曝露量。劑量調整建議如下：- 輕度肝功能不全(Child-Pugh A 類)- 建議劑量為每日 7.5 毫克；若無法忍受，劑量可調降至 5 毫克。- 中度肝功能不良(Child-Pugh B 類)- 建議劑量為每日5 毫克；若無法忍受，劑量可調降至 2.5 毫克。- 重度肝功能不良(Child-Pugh C 類)- 若期望的益處超出風險，可給予每日 2.5 毫克，但不可超過此劑量。避免同時使用強效 CYP3A4 抑制劑或強效 P-gP 抑制劑。如果患者需要併用中效 CYP3A4 或 P- 醣蛋白(P-gP) 抑制劑時，請降低 Afinitor 劑量至每日服用一次 2.5 毫克。根據患者耐受程度，可考慮將 Afinitor 劑量從每日 2.5 毫克調高到每日 5 毫克。如果停用中效抑制劑，在調高 Afinitor 劑量前應先進行約 2 至 3 天的廓清期。當停用中效抑制劑時，Afinitor 劑量應回復到開始使用中效 CYP3A4 或 P-gP 抑制劑前所用之劑量。請避免與強效 CYP3A4 誘導劑併用。若患者需要併用強效 CYP3A4 誘導劑，應考慮將Afinitor 的每日劑量加倍，以每次 5 毫克或更低劑量的方式逐步提高劑量。停用強效 CYP3A4 誘導劑，應考慮進行至少 3 到 5 天的廓清期；再將 Afinitor 劑量應恢復至使用強效CYP3A4 誘導劑前的劑量。葡萄柚、葡萄柚汁以及其他已知會影響細胞色素 P450 和 P-gP 活性之食物可能會增加 everolimus 體內曝露量，在治療期間應避免食用。聖約翰草(St. John's Wort；Hypericum perforatum) 可能會減少 everolimus 體內曝露量，在治療期間應避免食用。**禁忌:** 對於主成分、rapamycin (雷帕霉素) 衍生物或任何賦形劑過敏者。**警語:** 1. 非感染性肺炎 對於出現非特異性呼吸病徵與症狀，如缺氧、肋膜積水、咳嗽或呼吸困難，且已經以合適的檢查方式排除傳染性、腫瘤性與其他因素的病人，應考慮診斷是否患有非感染性肺炎。應告知病人於任何新的呼吸症狀出現或於現有呼吸症狀惡化時，儘速通報。在放射線造影上出現疑似非感染性肺炎但症狀輕微或甚至無症狀的病人，可以在不改變劑量的情況下，繼續 Afinitor 療法。症狀之嚴重性如為中度，可以考慮中斷治療，直到症狀改善為止，可以使用類固醇類藥物。重新開始 Afinitor 治療時，可從低於原劑量的 50% 開始。若非感染性肺炎症狀嚴重性為第 4 級，應停止使用Afinitor。2. 感染 Afinitor 具有免疫抑制特性，在使用 Afinitor 期間，應該特別注意是否出現感染跡象與症狀；如果診斷確定發生感染，應立即採取適當的治療措施，並考慮暫時中斷或完全停用 Afinitor。3. 併用血管收縮素轉化酶抑制劑(ACEI) 而引發的血管性水腫 併用ACEI 治療的病人，發生血管性水腫的風險可能提升。4. 口腔炎 病人口腔炎最常在治療開始後 8 周內發生。若發生口腔炎，建議進行局部治療，但是應避免使用含酒精含碘或含 thyme 或含過氧化氫(peroxide) 的產品，因其可能會使症狀惡化。在一個以乳癌病人為受試對象的試驗中，讓受試者在 Afinitor 併用 exemestane 治療的前 8 周以無酒精類固醇溶液漱口，結果顯示口腔炎的發生率及嚴重度都有臨床上有意義的減少。5. 腎衰竭 接受 Afinitor 治療的病人曾有腎衰竭(包括急性腎衰竭) 的案例，有些因腎衰竭導致死亡 6 受損傷口癒合。Everolimus 會延遲傷口癒合 7.老年患者 建議小心監測並依不良反應適當調整劑量 8. 實驗室檢驗與監測 肌酸酐升高與蛋白尿, 血糖及血脂升高, 血紅素、淋巴球、嗜中性球及血小板數減少。9. 藥物間交互作用 由於會使 everolimus 的曝藥量明顯升高，因此應避免與強效型 CYP3A4 抑制劑併用 9 肝功能不全 對於肝功能不全病人，everolimus 的曝藥量會增加，劑量調整方式如前所述。10 疫苗接種 於接受 Afinitor 治療期間應避免接受活性疫苗注射或與接種活性疫苗的人進行緊密接觸。11 致畸胎毒性 如施用於孕婦或於服藥中懷孕，應告知其對於胎兒之潛在危險。建議育齡婦女於使用 Afinitor 期間應採取適當之避孕措施並應持續至療程結束後 8 週。**副作用:** 最常見的不良反應(發生率 30% 以上) 為口炎、感染、皮疹、疲勞、腹瀉及食慾下降。最常見第 3 至第 4 級不良反應(發生率 2% 以上) 為口炎、感染、高血糖、疲勞、呼吸困難、肺炎及腹瀉。最常見實驗室數值異常(發生率 50% 以上)為膽固醇增加、血糖增加、天門冬胺酸轉胺酶(AST) 增加、貧血、白血球減少症、血小板減少症、淋巴球減少症、丙胺酸轉胺酶(ALT) 增加及三酸甘油脂增加。最常見第 3/4 級的實驗室數值異常(發生率 3% 以上) 為淋巴球減少、血糖增加、貧血、血鉀減少、天門冬胺酸轉胺酶(AST) 增加、丙胺酸轉胺酶(ALT)增加及血小板減少症。詳細資訊請參閱完整仿單 TW1908719121 僅限醫療專業人士參閱。

使用前詳閱說明書警語及注意事項
僅限醫療專業人士參閱
北市衛藥廣字第 108080166 號

NOVARTIS

台灣諾華股份有限公司
10480 臺北市中山區民生東路三段 2 號 8 樓
電話：(02)-2322-7777
傳真：(02)-2322-7993

諾華健康諮詢專線：0800-880-870
諾華網站：www.novartis.com.tw
使用前請詳閱說明書警語以及注意事項
詳細處方資料備索 TW1909728854

Sandostatin® LAR®
octreotide / IM INJECTION 善得定®
長效緩釋注射劑 10/20/30毫克

神經內分泌腫瘤症狀治療的領導品牌

Sandostatin® LAR® 能有效延遲晚期間腸或原位不明之神經內分泌腫瘤的疾病惡化時間

Sandostatin® LAR® 能長期控制胃、腸、胰內分泌系統功能性腫瘤的相關症狀

類癌腫瘤 Carcinoid Tumours	能改善潮紅及腹瀉等臨床症狀，並使血中血清素(serotonin)下降及尿中 5-hydroxyindole acetic acid 的排泄量減少
血管活性腸多胜肽瘤 VIPomas	能緩解嚴重分泌性腹瀉，改善低血鉀，降低血清中的VIP濃度
升糖激素瘤 Glucagonomas	能減少典型的 necrolytic migratory rash狀況，改善腹瀉、增加患者體重
胃泌素瘤 Gastrinomas	能單獨或配合使用H2受體阻斷劑及質子唧筒抑制劑以減少胃酸過度分泌，改善腹瀉、潮紅等症狀
胰島素瘤 Insulinomas	能降低血中胰島素，幫助重建及維持手術患者的術前正常血糖值，並幫助無法手術的良性或惡性腫瘤患者控制血糖有所進步

STRENGTH, BUILT ON EVIDENCE.

善得定 長效緩釋注射劑 10 毫克 (衛署藥輸字第 022656 號)/ 20 毫克 (衛署藥輸字第 022657 號)/ 30 毫克 (衛署藥輸字第 022655 號)
Sandostatin® LAR® Microspheres for Injection 10 mg/ 20 mg/ 30 mg

[適應症] 肢端肥大症，功能性胃、腸、胰臟內分泌腫瘤。治療患有晚期間腸(midgut) 或已排除原位非為間腸處而原位不明之分化良好(well-differentiated) 的神經內分泌腫瘤患者。**[用藥方式]** Sandostatin LAR 只能以臀部肌肉深層注射的方式給藥，而臀部肌肉的注射部位應左右側交替使用。**[劑量]** 晚期間腸或已排除原位為非間腸處而原位不明之分化良好的神經內分泌腫瘤患者: 建議劑量為每四週注射一次 Sandostatin LAR 30mg。在腫瘤無惡化期間仍應持續以 Sandostatin LAR 控制腫瘤。功能性胃- 腸- 胰內分泌腫瘤引起的症狀: 對於沒有接受過 Sandostatin 皮下注射的患者，建議開始接受短期(約 2 週) 的 Sandostatin 皮下注射治療，劑量為 0.1 mg，每日 3 次， 如此可以在施用 Sandostatin LAR 前評估患者對 octreotide 的反應及其全身性的耐受程度。對於經皮下注射 Sandostatin 症狀獲得良好控制的患者，建議起初每四週注射一劑 20 mg 的 Sandostatin LAR；若患者在 3 個月的療程後，症狀及生化檢驗指標都獲得控制，則 Sandostatin LAR 的劑量可以降至 10 mg，每四週注射一次。若患者在 3 個月的治療之後，症狀只有部份受到控制，則Sandostatin LAR 的使用劑量可以增加至 30 mg，每四週注射一次。**[禁忌]** 已知對 octreotide 或對本製品賦形劑之其他成份過敏者 **[警語]** 一般警語: 由於生長激素分泌性腦垂體腫瘤有時會擴大並造成嚴重的併發症(如視野缺損)，因此必須小心監控所有的病人，如果出現腫瘤擴大的跡象，建議應改變治療方式。懷孕: 在 octreotide 治療期間，若有必要則應建議具生育能力的女性患者使用合適的避孕方法。心血管相關情況: 已有肢端肥大症及類癌症候群的病人使用 octreotide 治療期間，發生心律徐緩、心律不整和傳導異常的案例報告。膽囊: Octreotide 抑制膽囊收縮素(Cholecystokinin) 的分泌，導致膽囊收縮被抑制並使膽汁分泌減少，增加膽結石形成、淤積的風險。葡萄糖代謝: Sandostatin LAR 會對生長激素、升糖激素和胰島素的釋放產生抑制作用，因此可能會影響葡萄糖的調控。營養: octreotide 會改變某些患者的食物脂肪吸收。某些接受 octreotide 治療的患者，可觀察到維他命 B12 值減少以及 Schilling 檢驗異常。**[極常見副作用]** 腹瀉，腹部疼痛，噁心，便秘，胃腸氣脹，頭痛，膽石症，血糖過高，注射部位局部性疼痛。**[衛福部食藥署網站]** https://www.fda.gov.tw　TW1908715724　僅限醫療專業人士參閱。

NOVARTIS
台灣諾華股份有限公司
10480 臺北市中山區民生東路三段 2 號 8 樓
電話：(02)-2322-7777
傳真：(02)-2322-7993
諾華健康諮詢專線：0800-880-870
諾華網站：www.novartis.com.tw

使用前請詳閱說明書警語以及注意事項
詳細處方資料備索
TW1909728854

VERITON-CT ®
D-SPECT ® CARDIO

CHANGING THE SHAPE OF NUCLEAR MEDICINE
CZT BASED SOLID STATE SPECT IMAGING

D-SPECT Series
CARDIOLOGY DIGITAL SPECT IMAGING

D-SPECT CARDIO

VERITON Series
360° TOTAL BODY DIGITAL SPECT/CT IMAGING

VERITON-CT
SPECT/CT 64

Digital SPECT Technology for Throughput and Diagnostic Efficency

- Flexibility to image in upright, semi-upright, supine and any angle in between
- Capacity to image large or heavy patient as chair supports up to 454kg
- High sensitivity and system configuration allow for dose reduction and shorter scan times
- Comprehensive clinical applications: myocardial perfusion imaging, cardiac amyloidosis, CFR or Coronary Flow Reserve analysis; Simultaneous Dual Isotope

Benefits of 360 CZT Digital SPECT/CT Imaging

- Scan head to feet in 3D for a Total Body SPECT/CT scan in less than 18 minutes
- Integrated with high resolution CT for improved image quality and absolute quantitation capabilities
- Accommodate patients of all sizes with its 80-cm bore size
- 1st ring-shaped gantry for 360-degrees simultaneous acquisition, with superior sensitivity and workflow throughput

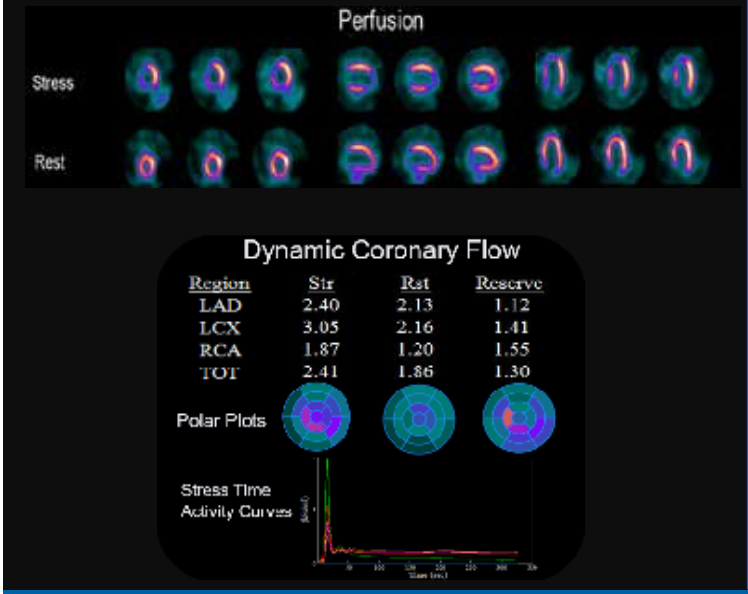

SPECTRUM DYNAMICS MEDICAL

www.spectrum-dynamics.com

常捷生醫科技股份有限公司
GreenEver Medical Systems Inc.
TEL:+886-2-2808-5960 http://www.grever.com.tw

目　次

陳 適 安 副院長

敬致 各位嘉賓及醫界先進

中華民國核醫學學會 2020 年會暨國際學術研討會於 109 年 11 月 21 日在臺北榮民總醫院致德樓舉行，謹代表承辦單位臺北榮民總醫院誠摯歡迎各位嘉賓蒞臨及指導。

臺北榮民總醫院自 1959 年建院迄今已逾一甲子，本院核子醫學部亦於今年歡慶成立 50 周年。半世紀來、見證了核子醫學在藥物發展、影像處理、造影技術、數據分析以及相關生醫領域有著長足的發展。近年來更由於多種藥物研發，診斷影像與治療合一的核醫分子診療學，在臨床應用上占有一席之地，如神經內分泌腫瘤與攝護腺癌；本次會議主軸之一便是將此一全球正蓬勃發展的技術作為議題。此外、輻射防護與輻射安全一直是核醫診療中不可或缺的一環；隨著核醫技術的精進，檢查劑量的降低，對於新領域的藥物使用也需要醫界的了解與共識，才能提供病患最好的醫療照護。

再次誠摯歡迎各位的參與，進行跨領域的整合性交流與討論，希望能夠藉此激發出更多想法與相關基礎研究及臨床應用。最後 祝

大會圓滿順利！

各位嘉賓滿載而歸！

臺北榮民總醫院副院長　陳適安

陳長盈 所長

核能研究所所長致詞

首先感謝核醫學會顏若芳理事長誠摯的邀約，核能研究所非常榮幸能參與每年一度的核醫盛會。同時感謝國內外核醫專家與學者提供的真知灼見，對於核研所未來開發新核醫藥物與中型迴旋加速器的長遠研究與發展方向，提供極具參考價值的經驗分享與指導。

世界各國（例如：美國、歐盟等國家）將精準醫療列為國家發展的重點，從個人化醫療到標靶精準治療，是全球生醫界積極投入研究領域。在總統的就職演說中將「臺灣精準健康戰略產業」列為六大核心戰略產業之一。而行政院亦將生技醫藥與醫學影像研究納入國家中長程計畫來進行規劃，這更是我們跨步向前、開創新局的極佳契機。

目前核研所積極投入我國急需解決的醫學與健康議題，專注於腦神經退化疾病診斷造影劑、腫瘤癌症診斷或治療藥物等精準核醫藥物開發與臨床前基礎研究。我們已於去年獲得「核研心交碘 -123 注射劑（碘 -123-MIBG injection）」之藥品許可證，目前於生產工廠登記階段，期盼未來對神經腫瘤及心臟交感神經功能診斷，提供更精準之診斷利器。今年已完成「鐳 -177-PSMA-617 攝護腺癌症治療新藥」製程技術開發與藥物安全性及臨床前藥毒理的評估，最終目標期望成為國內自行開發與供應之精準治療藥物。此外，「肝功能量化造影劑」預定申請 Phase II 臨床試驗申請，藉由與國內多家醫學中心的合作，整合專業量能，以肝殘存功能量化影像協助肝病病患及早確診、掌控疾病療程與療效。

今 (2020) 年因應新冠肺炎疫情，我們除緊急產製與穩定供應國內核醫藥物「氯化亞鉈 (鉈 -201) 注射劑」及「檸檬酸鎵 (鎵 -67) 注射劑」，開始著手規劃「建置本國質子與中子科學研究 70MeV 中型迴旋加速器」，並將納入明 (110) 年科技發展計畫，除了可達到穩定供藥與創新研發放射性同位素藥物的雙贏局面外，更將擴大研究發展領域，期望能滿足國內質子與中子應用的國家研究需求。

核研所除持續與國內外產、學、研、醫界組成緊密合作聯盟，共同開發卓具價值與發展潛力的核醫新藥外，亦擔當國內新藥開發的重要推手，提供各項分子造影及代謝研究與服務，以縮短新藥研發上市的時程及證實新藥的價值，並積極推動新藥技術移轉於業界，促進台灣核醫市場的投資，以及同步提供高品質核醫藥物於臨床端的應用，達成照護國民健康，落實原子能民生應用的社會福祉目標，以追求永續經營的宗旨。最後，感謝諸位先進們對核研所的支持與協助，預祝大會圓滿成功，與會先進們身體健康，平安喜樂！

核能研究所所長　陳長盈

會場平面圖

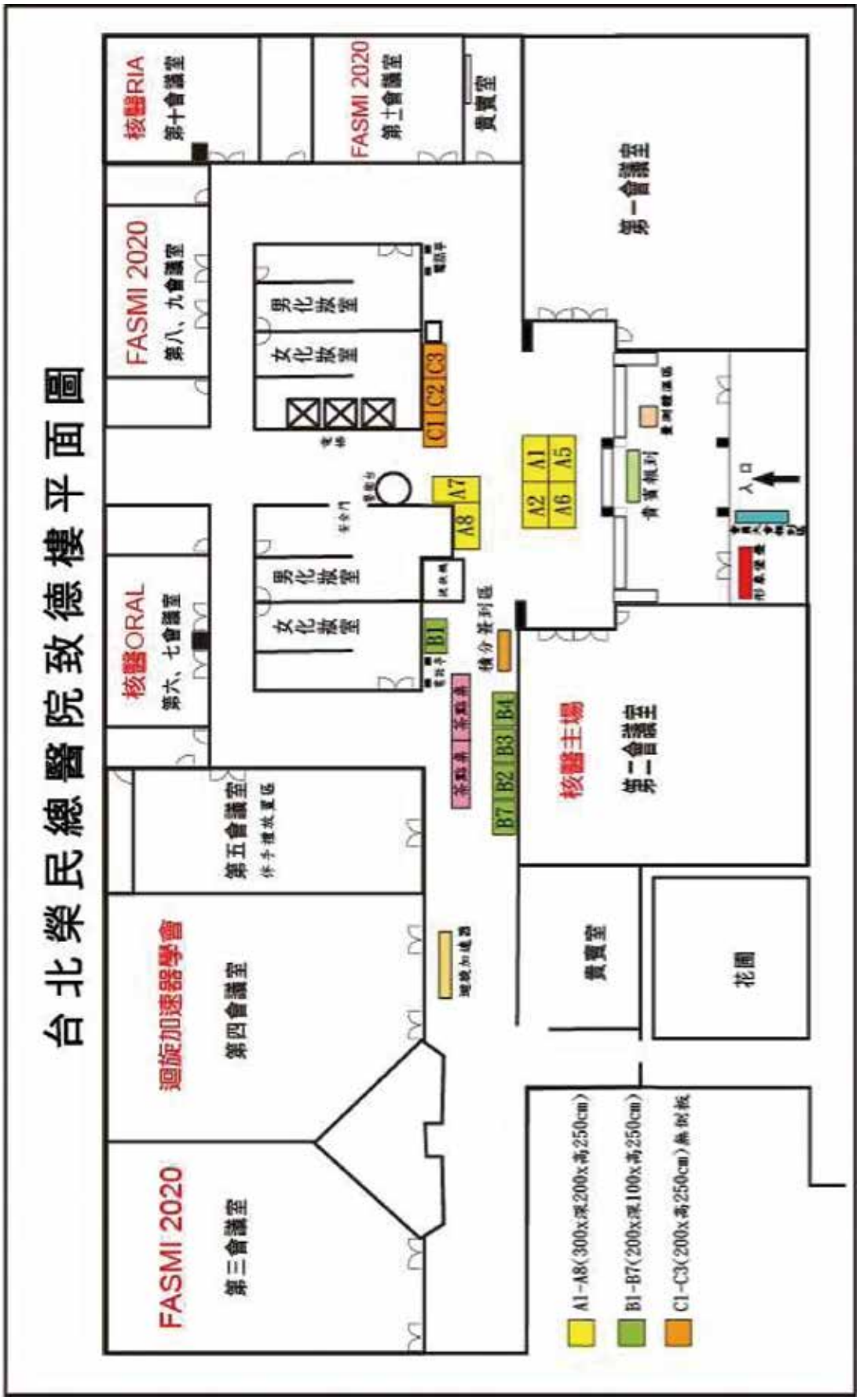
台北榮民總醫院致德樓平面圖
核醫RIA
第十會議室
FASMI 2020
第十會議室
貴賓室
FASMI 2020
第八、九會議室
核醫ORAL
第六、七會議室
第五會議室
迴旋加速器學會
第四會議室
FASMI 2020
第三會議室
男化放室
女化放室
男化放室
女化放室
C1 C2 C3
A7
A8
B1
A1
A5
A2
A6
入口
核醫主場
第一會議室
B7 B2 B3 B4
貴賓室
花園
A1~A8(300x深200x高250cm)
B1~B7(200x深100x高250cm)
C1~C3(200x高250cm)無底板

中華民國核醫學學會 2020 年會暨國際學術研討會議程

時　序	台北榮總		
08:30~9:10	大會報到		
09:10~09:20	大會開幕 (北榮副院長、核研所所長、黃文盛會長、顏若芳理事長)		
	第二會議室 (1F) (264 人)	第六、七會議室 (1F) (36 人)	第十會議室 (1F) (50 人)
09:20~10:20	抗癌藥物發展的百年省思 主講：鄭安理　教授 座長：顏若芳　理事長		09:20-10:50 內部稽核執行與管理 主講：張錦標　副教授 座長：王安美　主任
10:20~10:40	Coffee break、廠商展示		
10:40~11:10	**Fluciclovine PET for Prostate Cancer: Applications and Advice** 主講：美國 Emory 大學 Dr. Schuster 座長：林立凡　主任	口頭論文基礎	管理審查執行與管理 主講：張錦標　副教授 座長：王安美　主任
11:10~11:40	**Building clinical capacity and infra-structure for Lutetium based theranot-ics: practical experiences, pitfalls and emerging needs** 主講：雪梨利物浦醫院 Dr. Peter Lin 座長：黃文盛　教授		10:55-11:40 放射性同位素標記抗體在肝腫瘤特異性治療中的研究 主講：田育彰　教授 座長：陳宜伶　放射師
11:50~12:30	會員大會 (第二會議室)		
12:30~13:30	午餐演講 (Lunch symposium)		
	12:35-12:55 第二會議室 **Optimizing Treatment in mCRPC Pa-tients with Xofigo** 主講：劉忠一　醫師 座長：蒲永孝　教授 12:55-13:15 **Radiation Safety considerations for the use of Xofigo** 主講：邱宇莉　醫師 座長：諶鴻遠　教授	第六、七會議室 AI 人工智能與輻射防護結合運用 主講：陳繼光　總經理 座長：曹勤和　主任	第十會議室 **Brain digital PET imaging: from neurodegenerative diseases to cognitive proteinopathies** 主講：Prof. Antoine Vager 座長：王連嚴　主任
13:40~14:10	**PSMA imaging and therapy – from a urologist perspective** 主講：德國 Dr. Tobias Maurer 座長：蒲永孝　教授	住院醫師考試	13:40-14:25 PET/CT 新趨勢 主講：GE 鍾志輝經理、飛利浦張晉豪經理、西門子陳昭仁　專員 座長：黃奕珲　副理事長
14:10~14:40	**Radioiodine therapy and RAI refractori-ness in DTC: present and future** 主講：諶鴻遠　教授 座長：曾芬郁　理事長		14:25-15:10 EPAs 在核醫技術教學應用 主講：杜高瑩　放射師 座長：楊邦宏　博士
14:40~15:10	Lu-177 放射標靶治療藥物 台灣研發加值策略 主講：李銘忻　博士 座長：張志賢　博士	口頭論文臨床	
15:10~15:30	Coffee break、廠商展示		
15:30~16:00	**NETs overview: Diagnosis, and Current Treatment Strategies** 主講：陳明晃　教授 座長：田郁文　教授、吳彥雯　教授	口頭論文臨床	15:30-16:15 Ra223 治療實務經驗分享 主講：洪綾蔓　藥師 楊詩涵　放射師 座長：孫德宗　藥師
16:00~16:30	**Functional NET and NET Related Disor-ders** 主講：施翔蓉　醫師 座長：田郁文　教授、吳彥雯　教授		16:15-17:00 輻射安全課程 主講：郭俊良　放射師 座長：呂惠敏　放射師
16:30~17:00	**Current evidence and Patient Selection for PRRT** 主講：Prof. Navalkissoor 座長：田郁文　教授、吳彥雯　教授		
17:00~	閉幕 (顏若芳理事長)		

Name: **David M. Schuster**
Title: Professor
Institute: Emory University

Fluciclovine PET for Prostate Cancer: Applications and Advice

Prostate cancer is a leading cause of cancer death worldwide. Up to 50% of patients after initial therapy will develop biochemical failure. The differentiation of local from extraprostatic recurrence plays a critical role in patient management. The use of functional imaging targeting features of cancer metabolism has proven highly useful.Fluciclovine (anti-1-amino-3-F-18-fluorocyclobutane-1-carboxylic acid, FACBC, Axumin™) is an artificial amino acid PET radiotracer that was approved in 2016 by the U.S. Food and Drug Administration for detection of suspected recurrent prostate cancer.The advent of functional imaging such as with fluciclovine PET/CT, significantly changed the approach to prostate cancer. Fluciclovine PET/CT research reinforced that many patients with benign-appearing lymph nodes demonstrate abnormal fluciclovine intense uptake characteristics for malignancy. In the clinical trial setting and now with clinical use, fluciclovine PET/CT has high diagnostic performance in the localization of extraprostatic metastatic lesions in patients with biochemical recurrence and negative conventional imaging. The LOCATE multicenter prospective study (NCT02680041) evaluated the effect of fluciclovine PET/CT on the management plans among patients with BCR and no metastatic disease on conventional images. The study reported an overall 59% change in management, 78% were major. This talk will provide an overview of fluciclovine PET for recurrent prostate cancer, including published comparisons to conventional imaging and other molecular imaging agents. The talk will also review the fluciclovine PET imaging procedure and image interpretation, including physiologic and pathologic uptake patterns and pitfalls.

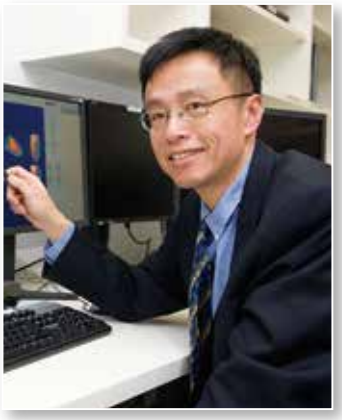

Name: **Peter Lin**
Title: Clinical Director
Institute: Liverpool Hospital

Building Clinical Capacity and Infrastructure for Lutetium Based Theranotics: Practical Experiences, Pitfalls and Emerging Needs

The presentation will provide an overview of our Medical Imaging service, and theranostics program in my Department.

I will share practical clinical experiences and pitfalls, and also lessons learnt in planning and establishing a "precision" theranostics therapy service, with particular emphasis on Lutetium labelled peptide receptor radionuclide therapy ("PRRT") and PSMA therapy.

I will discuss some of the key enablers for planning considerations to meet emerging needs and future opportunities: alternative radioisotopes, integrated biology based imaging instrumentation, developmental radiochemistry and GMP-compliant production, clinical dosimetry, development of clinical treatment capacity and infrastructure, workforce planning, engagement and be part of multidisciplinary care, translational research and patient-centric clinical trials network in combination with other therapies and emerging biotherapeutics, regulatory support and funding requirements.

Name: **Tobias Maurer**
Title: PD Dr. med.
IInstitute: University-Hospital Hamburg-Eppendorf

PSMA Imaging and Therapy – from A Urologist Perspective

PSMA-based PET has revolutionized imaging in prostate cancer in the recent years. Increasingly also theranostic approaches are pursued based on PSMA as target structure. In this overview PSMA-based PET imaging in the different clinical settings during prostate cancer diagnosis and treatment will be discussed from a urologist point-of-view. Furthermore, theranostic approaches, namely PSMA-radioligand therapy and PSMA-radioguided surgery, will be discussed and put into clinical context.

Name: **Shaunak Navalkissoor**
Title: Consultant Nuclear Medicine Physician
Institute: Royal Free London NHS Foundation Trust

Current Evidence and Patient Selection for PRRT

This talk is titled peptide receptor radionuclide therapy (PRRT) for neuroendocrine tumours. The talk is split into three parts: the evidence for lutathera, theranosticsin neuroendocrine tumoursand lastly patient selection for PRRT, practical aspects in setting up a PRRT service.

The important NETTER-1 study and other relevant studies highlighting the efficacy and safety data for Lutatherais presented. Secondly, description of theranostics and its role in patient selection for PRRT is covered: pre-treatment selection of patients who are most likely to benefit from treatment by the use of a related, specific diagnostic test are integral to the treatment of patients with NETs.

Lastly the talk describes practical aspects in setting up a PRRT service including setting up an MDT, radiation protection and logistical problems. I discuss the steps required from zero experience to administering the radiopeptide to the patient. This includes setting up an MDT, challenges in setting up a PRRT administration suite, outpatient and inpatient administrations, what precautions and checklists are required prior to administration, the administration procedure and follow up of patients.

Name: 鄭 安 理
Title: 講座教授
Institute: 國立台灣大學

抗癌藥物發展的百年省思

癌症的藥物治療自上世紀中開始，經歷半世紀以化療爲主的發展。至 21 世紀，始進入標靶治療，自此藥物治療開始與基因醫學有更緊密的結合，治療也愈加個人化。到最近的十年，新一代免疫多采多姿的各種組合，形成當前治療研究的主流。未來的世界，全新的免疫治療模式，及其他形態治療的組合，將可更大輻地提昇效果，改善病人的存活率及生活品質。

Name: 劉 忠 一
Title: 主治醫師
Institute: 土城長庚醫院泌尿科

Optimizing Treatment in mCRPC Patients with Xofigo

Radium-223 dichloride (radium-223), an alpha emitter, selectively targets bone metastaseswith alpha particles. We assessed the efficacy and safety of radium-223 asclinical outcomes men with castration-resistant prostate cancer and bone metastases in phase III study and other real world evidences.

Name: 邱 宇 莉
Title: 主治醫師
Institute: 高雄榮民總醫院核醫科

Radiation Safety Considerations for the Use of Xofigo

Radium-223 dichloride (Ra-223) is the first alpha-particle emitting radiopharmaceutical to be approved for the treatment of the patients with castration-resistant prostate cancer and associated bone metastases. Ra-223 decays by a series of alpha and beta emissions with some attendant photon emission (X and gamma rays). Therefore, there still remains radiation safety of concern with Ra-223. Highlighting the key issues of handling Ra-223 and giving proper patient and family education to reduce internal and external exposures are recommended.

Name: 諶 鴻 遠
Title: 主治醫師
Institute: 三軍總醫院核醫部

Radioiodine Therapy and RAI Refractoriness in DTC: Present and Future

Differentiated thyroid cancer (DTC) usually retains the capacity of iodide uptake and thus systemic use of radioactive iodine (RAI) can target tumor cells allowing more selective radiation killing of targeted tumors. Sodium iodide symporter (Na+/I- symporter, or NIS) is essential to mediate iodide uptake into DTC; however, mutated genes causing DTC may drive oncogenesis as well as NIS dysfunction. Therefore, progressively losing of RAI avidity of DTC might occur and lead to so called de-differentiation and cause RAI-refractoriness. Despite that the occurrence and exact mechanism of RAI-refractoriness is not fully undrstood, “re-differentiation” therapy has been proposed to restore NIS function in order to revert RAI-refractoriness. Prior studies ever reported certain treatments (e.g. MEK inhibitor) might allow DTCs regain iodine uptake and render RAI treatment effective to achieve tumor control. Also severe other approaches are proposed mainly for tumor control but may be useful to enehnce RAI sensitivity: multi-tyrosine kinase inhibitors (e.g. sorafenib and lenvatinib) and mutate gene-directed target therapy (e.g. NTRK, RET/CT, bRAF, et al). Theoretically, reduced MAPK activation can assist NIS functional expression and likely to increased RAI accumulation. Whether combination of these target therapies and RAI treatment can augment RAI effectiveness warrants for further clinical investigation.

Name: 李 銘 忻
Title: 副研究員兼副組長
Institute: 核能研究所同位素組

Lu-177 放射標靶治療藥物 台灣研發加值策略

Lu-177 核醫診療藥物具強勁躍昇動能，國際相關產業動能碁盤已臻完備，在研發核醫藥物缺乏創新模式的全球狀態下，PRRT 與 PRLT 挾帶 Lu-177 的精準診療特性分別掀起國際第二波及第三波的成長動能，進而彌補國際臨床未滿足之需求，然台灣本土患者無法享受國際研發成果紅利。核能研究所獨創 Lu-177 診療加值藥物轉譯平台，從實驗室批次生產到臨床病患，一條龍式架構協助國內產學界藥物開發爲核醫藥物加值，進而驅動當前核醫市場。Lu-177 診療加值藥物轉譯平台已進行 Lu-177-PSMA-617 及 Lu-177-PSMA-INER-56 等藥物開發，爲我國前列腺癌臨床缺口進行 Lu-177-PSMA 體內放射標靶療法在地化布局。

Name: 陳 明 晃
Title: 主治醫師
Institute: 台北榮民總醫院腫瘤醫學部

NETs Overview: Diagnosis, and Current Treatment Strategies

Neuroendocrine tumors (NETs) are rare neoplasms characterized by heterogeneous behavior, and have the ability to secrete a variety of hormones, resulting in various clinical syndromes. The prognosis of NETs is heterogeneous. Therefore, World Health Organization (WHO) classified gastroenteropancreatic neuroendocrine tumors (GEP-NETs) into NET grade 1 (G1), NET grade 2 (G2), NET G3 (G3)and neuroendocrine carcinoma (NEC) grade 3 (G3) based on their Ki-67 proliferation index and tumor differentiation.

Therapeutic options for metastatic G1, G2 and G3 GEP-NET treatments include hormone therapy with a somatostatin analog; targeted therapy; peptide receptor radiotherapy and local therapy for liver predominant metastases.

Conversely, chemotherapy is the standard frontline treatment for metastatic G3 NEC.

Name: 施 翔 蓉
Title: 副教授
Institute: 台大醫院內科

Functional NET and NET Related Disorders

Ten to ninety percent of pancreatic neuroendocrine tumors (pNETs) are functional. Functional-pNET (F-pNET) is divided in three groups: gastrinoma, insulinoma and all the rare pNET (RFT), such as VIPoma, glucagonoma, somatostatinoma, GRHoma, and ACTHoma. Gastrinoma is associated with marked gastric acid production and recurrent peptic ulceration. Diagnosis requires demonstration of elevated fasting serum gastrin when the gastric pH is < 2. Insulinoma causes hypoglycemia and the diagnostic criteria includes insulin ≥ 3.0 μU/ml and C-peptide ≥ 0.6 ng/ml when glucose < 55 mg/dl, which may be induced by 72 hour fasting test followed by oral glucose tolerance test. Multiple endocrine neoplasia type 1 and other inherited diseases should be carefully ruled out in all patients with NETs.

Name: 張 錦 標
Title: 技術長
Institute: 三軍總醫院臨床病理科

內部稽核執行與管理 / 管理審查執行與管理

醫學實驗室的專業人員受到他們個別職業道德規範的約束。每個國家對於一些或所有必需觀察的專業人員可以有特別的法規或要求。有義務要求服務與責任超過在法律最低要求之上。醫學道德的一般原則是以病人福祉至上。實驗室確保病人福祉與利益的義務，永遠是優先考慮且必需優先。因此，實驗室必需公平且沒有分別地對待病人。「檢驗醫學倫理」就是「醫學實驗室中正確的行爲，如何提升其重要性包括：回歸專業體制、提升專業形象、權力與義務並重、重視檢驗醫學倫理。

Name: 田 育 彰
Title: 教授
Institute: 高雄醫學大學

放射性同位素標記抗體在肝腫瘤特異性治療中的研究

肝癌的死亡率爲國人癌症的第二名，由於肝癌血管性豐富，目前能夠利用栓塞或手術治療。本研究目的是利用放射性同位素 ，標誌在單株抗體 Anti-Glypican-3 (GPC3) clone 9C2 上，使放射性同位素標誌之抗體在體內與肝癌細胞表面抗原進行特異性結合，分析各個器官與腫瘤之劑量，了解藥物之體內分佈與代謝途徑，並利用 所放出之 β 射線，藉以達到殺死癌細胞的目的，以探討放射免疫治療在肝癌治療上的可能性。小鼠試驗結果顯示其的確具有在體內殺死肝癌細胞的能力，且通過細胞實驗了解不同劑量下的癌細胞存活率，我們發現 標誌單株抗體 GPC3 clone 9C2 具有肝癌治療上的可能性。

Name: 陳 繼 光
Title: 總經理
Institute: 貝克西弗股份有限公司

AI 人工智能
與輻射防護結合運用

AI 人工智能及 IOT 物聯網、雲端技術能發展至今已日漸成熟，透過大數據的資料整合，已經普遍應用在生活上，提供前所未有的便利性及智能性，加上現行 5G 傳輸的新世代技術，讓所有技術能更有效率的呈現於世人。

如今，醫療領域也已經結合 AI 人工智能及相關技術，讓醫療領域更有效率及便利性，逐漸改變了傳統醫療過程及行爲，讓醫病關係、就醫環境、醫用診斷…等，更充滿前瞻性、未來感、卓越性，使人們對於醫療領域的認知及滿足感更躍進。

輻射防護領域也因應現行科技的進步，漸漸提升相關技術達到更智能應用，本課程將探討現行已有哪些智能科技應用於輻防領域，未來將以何種新的方式呈現於輻防醫療，達到輻防生態鏈。

Name: 杜 高 瑩
Title: 醫事放射師
Institute: 馬偕紀念醫院核子醫學科

EPAs 在核醫技術教學應用

現今對於醫事放射師的訓練，除了學校的基礎教育外，投入職場時還需要接受兩年期的新進人員訓練，對核子醫學科而言，其成果似乎不盡理想，檢討其原因不外乎以下幾個因素所造成核子醫學專業放射師的養成困難。

1. 學校教育受限於教育環境 (包括學分數，師資) 無法滿足核子醫學的基本專業知識建立。
2. 實習階段僅 4 周的課程無法進行專業教學。
3. 核醫科人力短缺，以致 PGY 訓練無法落實執行。

因此對於核子醫學專業放射師的人才培育就現階段的訓練方式，實在是無法達成期望的目標。

EPAs (Entrustable Professional Activities, EPAs) 可信賴專業活動是一種臨床教育的評估手法，其目的在於如何去“信賴”一位受訓的專業人員能夠獨立完成專業技能。EPA 不同於一般常用的 DOPS, Mini-CEX，是屬於觀察任務描述的專業技能執行的評估。現今的醫學教育的主流趨勢是以「能力爲本、成果導向」爲臨床教育訓練之架構，我們將醫事放射師 ACGME 五大核心能力，進展到工作中的多元評量，EPA 之核心概念就是：實地觀察受訓學員執行特定臨床任務，依據學員臨床能力給予不同層級的督導，授權決定學員是否勝任獨當一面，給予病人完善安全的照顧，這核心概念與國際醫院認證評鑑 (Joint Commission International) 分級授權準則是吻合一致的。就核子醫學專業技術訓練過程中，我們將規劃各項描述型的專業活動，如正子電腦斷層造影技術，單光子電腦斷層技術等，在過程中建立觀察面向，結合 ACGMA 的核心能力，建立各個面向須達到的態度，知識與技能 AKS (attitude, knowledge, skill)，藉由可信賴專業活動的建置我們期望可以達到以下幾個目標：

1. 讓新進人員能夠循序漸進的進入狀況。
2. 透過專業活動的過程建立新進人員的學習觀念。
3. 由資深的臨床教師直接指引學習。
4. 提升核醫專業訓練的品質，以提供更完善的臨床服務。

近年來，新的核子醫學科陸續建置，所需要的專業人員也越來越多，由於職場環境與學校培育的因素，使得所需的人才無法滿足現況。因此培育適任的醫事放射師是每個線上作業單位的當務之急，更何況原本人力就缺乏的核醫部門，整合有效的資源與方法來協助培訓，正是我們想要導入 EPAs 到核子醫學訓練的目的。

Name: 楊 詩 涵
Title: 組長
Institute: 和信治癌中心醫院核醫科

Ra-223 治療流程經驗分享

本院自 2019. 03 起健保給付 Ra-223 治療後已執行 26 人次，共完成 135 次治療。本科 Ra-223 治療團隊包含醫師、護理師、放射師及藥師，各司其職，相互合作。藉此機會分享本科治療流程、工作分配、病人照護及衛教、藥品訂購、接收、儲存及備製、輻防作業及廢棄物處理等。

Name: 郭 俊 良
Title: 醫事放射師 / 輻防師
Institute: 新竹馬偕紀念醫院核子醫學科

ICRP 103 號報告內容概要介紹

目前世界各國都是以 30 年前的 ICRP 60 號建議做爲輻射防護法規依據，而 2007 年所建議的 103 號報告則主要是對 60 號報告做強化與補充，因此爲因應未來主管機關將訂定最新之游離輻射防護安全標準，規範輻射防護作業基準及人員劑量限度等相關導則，藉由今日的分享讓各位同儕盡早瞭解以做好後續的規劃。

Name: 鍾 志 輝
Title: 經理
Institute: 奇異公司

PET/CT 新趨勢

1. GE Digital PET/CT 的發展歷程。
2. GE Digital PET/CT 的設計原理與未來發展。
3. 先進 PET/CT 組像技術 Q.Clear 與定量化的技術發展。
4. 4 公分寬度 CT 偵測器在 PET/CT 上的臨床效益。
5. GE Digital PET/CT 的臨床經驗分享。

Name: 張 晉 豪
Title: 經理
Institute: 飛利浦

PET/CT 新趨勢

Philips Vereos Digital PET/CT is the world's first and only fully digital, clinically proven PET/CT solution. With more than four years of investigational studies and over 100 published clinical studies, Vereos exemplifies an established total solution to reveal more to help you improve patient care and manage costs.

With Philips Vereos Digital PET/CT, proven accuracy inspires confidence.

Name: 陳 昭 仁
Title: 專員
Institute: 西門子

PET/CT 新趨勢

早期發現早期治療是癌症防治最重要的方法，最新 PET/CT 技術，不僅造影時的注射劑量更低、檢查速度更快，更細緻清晰的影像、多樣化最新的技術，帶領我們邁入精準醫療新紀元。

OB-001

Determination of Synthetic Impurities and Metabolic Products of F-ADAM, A Positron Emission Tomography Imaging Agent for Serotonin Transporter (SERT) using HPLC-Tandem Mass Spectrometry

Wei-Hsi Chen[1], Chyng-Yann Shiue[2,3]

[1]*Chemistry Division, Institute of Nuclear Energy Research, Taoyuan City 32546, Taiwan*
[2]*PET Center, Department of Nuclear Medicine, National Taiwan University Hospital, Taipei City 100, Taiwan*
[3]*PET Center, Department of Nuclear Medicine, Tri-Service General Hospital, Taipei City 114, Taiwan*

Introduction: Serotonin is a critical neurotransmitter in the central nervous system (CNS). Serotonin transporter (SERT) regulates serotonin levels by reuptaking serotonin from the synaptic cleft. ^{18}F labelled N,N-dimethyl-2-(2-amino-4-fluoro phenylthio)benzylamine (^{18}F-ADAM) is an important positive electron emission ligand commonly employed as an imaging agent for SERT in the brain. In the report, we determine the identity of impurities resulting from the synthesis of ^{19}F-ADAM, as well as its metabolic products by rat liver microsomes.

Methods: HPLC-MS/MS on a C4-phenyl modified silica gel column with ammonium formate aqueous buffer/acetonitrile programmed mobile phase analytical method was applied to determine the identity of impurities and metabolitees.

Results: F-ADAM is unstable in methanol, and propose the use of acetonitrile to generate optimal chromatogram. A Cl-substituted species was found to be the major impurity resulting from the F-ADAM synthetic process. The metabolic products of F-ADAM by rat liver microsomes were characterized by oxidization of the sulfur moiety to sulfoxide, demethylation of the dimethylamine moiety, and oxidative defluorination / deamination.

Conclusions: These results elucidate the by-products of F-ADAM synthetic and metabolic processes, and provide direction for the application of this imaging agent to biosystems properly.

OB-002

Drug De-Novo Design Through Deep Learning

Shih-Wei Lo[1], Liang-Hsun Huang[2], Kai-Hung Cheng[1],
Ming-Hsin Li[1], Chih-Hsien Chang[1]

[1]Isotope Application Division, Institute of Nuclear Energy Research, Taoyuan, Taiwan
[2]Planning Division, Institute of Nuclear Energy Research, Taoyuan, Taiwan

Introduction: Traditional scientists have further designed or improved drug molecules by analyzing the structure-activity relationship between drug structures and target macromolecules. The drug development process takes about 10 years and the successful development of a drug is an average of 1.3 billion US dollars, resulting in severe drug development and high threshold, while AI drug development can accelerate its process. AI is screened in the early stage. The speed of small molecules is faster than the traditional method, which can be as short as 1~2 years.

Methods: We use the Variational Auto-Encoder (VAE) as a model. VAE was trained on a subset with approximately 3M drug-like compounds extracted at random from database. In order to make the resulting compounds more novel, we add a layer of diversity before the decoding layer to produce similar but different structures. In the end of training, our model has reached 97.68% accuracy.

Results: In the forecasting phase, we use paired helical filament of tau imaging agents and beta-amyloid imaging agents as input. It is expected that generated drugs should be closed to original compounds and have similar medicinal properties. We measure our generated drugs with the following metrics: valid compound and novelty. The results shows we generated 37 valid and novel drugs.

Conclusions: Traditional drug discovery process may take a lot of effort, however, the method we propose has shorten the time. We start in drug-like dataset as input to our VAE model, and we hypothesize our model should “learn” the drug properties. Furthermore, we extend our VAE model with a diversity layer which used to raise the probability of valid drugs after generation process. The results show that the compounds we generated are both valid and novel.

OB-003

碳十四藥物代謝技術建立與平台建置

王世民　羅盛男　官孝勳　李銘忻　張志賢

核能研究所同位素組

背景介紹：新藥開發過程中，以實驗動物進行的藥物動力學研究 (包括吸收、分佈、代謝與排除，合稱 ADME)，是候選藥物安全性評估中重要的數據。利用碳十四同位素標誌藥物可偵測到極微量藥物的特性，進行藥物代謝產物、全身分佈、藥物質量 - 時間平衡分析，是目前公認的標準方法。然而目前國內仍無利用碳十四標誌藥物研究藥物代謝與分佈的執行機構，故國內進行新藥開發必須委託國外 CRO 公司執行相關研究，不僅價格高昂且耗費時程。因此，核能研究所建立碳十四標誌藥物之核心設施與代謝物分析鑑定技術，將填補此技術缺口，加速國內生技醫藥產業發展。

方法：建立碳十四藥物代謝平台必須遵循嚴格的法規管制，包括購入、保存及操作游離輻射物質、放射性廢棄物的處理與廢氣的排放等。因此，本研發完成操作碳十四實驗室的設施改善，亦規劃含碳十四的放射性放棄物處理與廢氣排放的策略，以符合游離輻射安全法規的要求。碳十四藥物代謝平台相關儀器設備完成校正確效，建立品質文件系統，符合 GLP 規範。在建立碳十四標誌藥物代謝分析技術方面，以串聯質譜儀 (結構)、高效液相層析儀 (UV) 與流式閃爍分析儀 (β 射線)，建立碳十四藥物分析方法與品管標準。透過動物餵食碳十四標誌的乙醯胺酚 (以下簡稱 C14-APAP)，以研究此藥物的藥動、分佈、代謝與排泄特性，建立藥物動力學、排除試驗、代謝物分析及全身放射自動顯影技術。

結果：小鼠餵食 C14-APAP 後 30 分鐘，以定量全身放射自動顯影技術研究藥物組織分佈，影像顯示碳 -14-APAP 主要聚集在腎臟部位。大鼠口服給藥 72 小時後，C14-APAP 主要經由尿液排泄 (84%)，並在尿液中鑑定出 3 種代謝物，皆與文獻報導一致。質量平衡研究顯示 C14-APAP 放射活度回收率達 91%。

結論：核研所已建立碳十四操作設施、碳十四排放與廢棄物處理策略，ADME 分析技術正確可靠。預計 109 年 12 月完成申請 TFDA GLP 認證，技術類別爲生物檢體中藥物濃度測試，未來將以此平台，以加速國內業界新藥之開發。

OB-004

In Vivo Investigation of a Novel Luteinizing Hormone-Releasing Hormone Antagonist for Triple Negative Breast Tumor-Bearing Model

Mao-Chi Weng, Sheng-Nan Lo, Mao-Feng Weng, Ying-Hsia Shih, Shih-Min Wang, Chung-Li Ho, Ming-Hsin Li

Institute of Nuclear Energy Research, Taoyuan, Taiwan

Introduction: Triple negative breast cancer (TNBC) was clinically considered a subtype of human breast cancer that is lack of diagnostic and effective therapeutic agents. Receptors for luteinizing hormone-releasing hormone (LHRH-R) were previously reported as potential targets for TNBC in vitro. However, as we know probes or drugs specific for LHRH-R are still under investigation as yet. In this research, we developed a novel LHRH peptide-based antagonist, DOTA-LHRH, which has been proved an effective strategy for in vivo uses by SPECT/CT imaging.

Materials and methods: The LHRH antagonist was first conjugated with a DOTA chelator; after radiolabeled with In-111, Ga-68 and Lu-177, the radiochemical purity (R.C.P.) was analyzed by both radio-TLC and radio-HPLC systems, respectively. Two kinds of TNBC cell line, HCC 1806 and MDA-MB-231, were subcutaneously inoculated on mice. After intravenous (i.v.) injection of ^{111}In-DOTA-LHRH, both HCC 1806 and MDA-MB-231-bearing mice were anesthetized and imaged at 1, 4 and 24 h by a SPECT/CT, respectively. The bio-distribution test of ^{111}In-DOTA-LHRH in HCC1806-bearing mice was also investigated at 4 and 24 h.

Results: The R.C.P. of ^{111}In-DOTA-LHRH, 68Ga-DOTA-LHRH and ^{177}Lu-DOTA-LHRH were all determined > 90% by both radio-TLC and radio-HPLC, respectively. The SPECT/CT imaging data showed that ^{111}In-DOTA-LHRH was first collected in liver, kidney and both tumors at 1 h; the activity in both tumors decreased at 4 h and showed clearance performance at 24 h. In results of bio-distribution, ^{111}In-DOTA-LHRH was mainly collected in kidney, spleen, liver and HCC 1806 tumors at 4 and 24 h; in addition, there found many signals in urine and feces. The tumor-to-muscle count ratio (T/M) were calculated as 5.80 ± 3.33 and 3.88 ± 0.34 and the tumor-to-brain count ratio (T/B) were 19.03 ± 6.22 and 17.23 ± 0.25 at 4 and 24 h, respectively.

Conclusions: This research has explored the characteristics of a novel LHRH peptide-based antagonist for LHRH-R over-expressive tumors in vivo. We suggested that DOTA-LHRH for further diagnostic research and it may also provide innovative information for development of TNBC patient's treatment strategies in the future in Taiwan.

OB-005

Automated Radiosynthesis of [^{18}F]FEPPA for PET/MRI Brain Region-Specific Imaging of TSPO *in Vivo*

Chi-Wei Chang[1], Chuang-Hsin Chiu[2], Ming Hsien Lin[3], Ya-Yao Huang[4], Chyng-Yann Shiue[4], Wen-Sheng Huang[1,2a], Skye Hsin-Hsien Yeh[5*]

[1]*Department of Nuclear Medicine, Taipei Veterans General Hospital, Taipei, Taiwan*
[2]*Department of Nuclear Medicine, Tri-Service General Hospital, National Defense Medical Center, Taipei, Taiwan*
[3]*Department of Nuclear Medicine, Cheng Hsin General Hospital, Taipei, Taiwan*
[4]*PET Center, Department of Nuclear Medicine, National Taiwan University Hospital, Taipei, Taiwan*
[5]*Brain Research Center, National Yang-Ming University, Taipei, Taiwan.*
[a]*co-corresponding author*

Background: Expression of translocator protein (TSPO) on the outer mitochondrial membrane of activated microglia is strongly associated with neuroinflammation. The second-generation PET ligand [^{18}F]FEPPA specifically binds TSPO to enable *in vivo* visualization and quantification of neuroinflammation. We optimized an automated radiosynthesis method and evaluated the utility of [^{18}F]FEPPA in a mouse model of systemic LPS challenge to detect TSPO-associated signals of central and peripheral inflammation.

Methods: Whole-body in vivo dynamic PET/MR imaging was performed in LPS-induced and control mice 30 min after [^{18}F]FEPPA administration. The relationship between the [^{18}F]FEPPA signal and the dose of LPS was also assessed. RT-PCR was used to measure cytokine levels (i.e. TNF-α, Il-1β, Il-6) in mice injected with 2.5 or 5 mg/kg LPS. Standard uptake value (SUV), total volume of distribution (VT) and area under the curve (AUC) were determined based on the metabolite-uncorrected plasma input function. Western blotting and immunostaining were used to measure TSPO expression in the brain.

Results: The optimized automated [^{18}F]FEPPA radiosynthesis produced an uncorrected radiochemical yield of 30 ± 2% within 80 min, with a radiochemical purity greater than 99% and specific activity of 148.9–216.8 GBq/μmol. Significant differences were observed in the brain 30 min after [^{18}F]FEPPA administration: SUV, VT, and AUC were 1.61 ± 0.1, 1.25 ± 0.12, and 1.58 ± 0.09-fold higher in LPS-injected mice than controls. *TNF-α, Il-1β* and *Il-6 mRNA* levels were also elevated in the brains of LPS-injected mice. Western blotting revealed TSPO ($p < 0.05$) and Iba-1 ($p < 0.01$) were upregulated in the brain 24 h after LPS administration. In LPS-injected mice, TSPO immunoactivity colocalized with Iba-1 in the cerebrum and TSPO was significantly overexpressed in the hippocampus and cerebellum. The peripheral organs (heart, lung) of LPS-injected mice had higher [^{18}F]FEPPA signal-to-noise ratios than control mice.

Conclusions: We demonstrate [^{18}F]FEPPA can be used to provide robust data on ligand specificity and selectivity in both central and peripheral tissues using 7T PET/MR imaging; pharmacological characterization is reported. The high affinity, stability and high-contrast visualization indicate detection of TSPO using [^{18}F]FEPPA represents a promising, specific biomarker for early diagnosis and neuropathological follow-up of neuroinflammatory processes.

OC-001

Comparison of Tc-99m Pertechnetate Thyroid Scan and Neck Sonography in Neonatal Hypothyroidism

Wen-Sheng Huang[1], Hong-Yin Chen[1], Dau-Ming Niu[2], Shan-Fan Yao[1], Bang-Hung Yang[1], Sing-Yung Wu[3]

[1]*Departments of Nuclear Medicine/National PET & Cyclotron Center, Taipei Veterans General Hospital, Taipei, Taiwan, ROC*
[2]*Departments of Pediatrics, Taipei Veterans General Hospital, Taipei, Taiwan, ROC*
[3]*Departments of Nuclear Medicine and Medical Services, Long Beach VA Medical Center, Long Beach, CA, USA*

Introduction: Various etiologies can cause neonatal hypothyroidism. Neonatal screening plays an important clue in this regard. Further surveys using sonography or Tc-99m thyroid scan enable us to differentiate etiologies. We compared features of Tc-99m thyroid scan (TcPT) and neck sonography in cases of neonatal hypothyroidism.

Methods: A total of 207 newborns (M/F: 97/110; mean age: 14.1 ± 8.8 / 12.8 ± 8.8 days) were recruited. Neck sonography (LOGIQ E10, GE) and TcPT [30 min after 0.5 mCi TcO4-, thigh *i.m.*, Seimens Symbia 1, pinhole (6.4 mm diameter) collimator for 5 min or 100,000 counts] were performed within 2 days. TcPT were interpreted using anterior and if needed lateral views. Adequate hydration immediate the scan was suggested. The sonographic findings were categorized into non-detectable, smaller or larger than usual by size, *e.g.* length x width x height x π/6 (Arch Dis Child Fetal Neonatal Ed 2002; 87: F209). The TcPT was interpreted visually by experienced NM physicians for location and activity of uptake and categorized as normal, ectopic, hypoplasia, dyshormonogenesis and agenesis.

Results: All hypoplasia cases seen on TcPT were small or poor demonstration (PD) in size. All ectopic cases were also PD (n = 14, 46.7%) or small (n = 16, 53.3%). Those with normal uptake were sonographic sized normal (n = 69, 62.7%), smaller (n = 37, 33.6%), larger (n = 3, 2.7%) and PD (n = 1, 0.9%). Of dyshormonogenesis, sonographic sized normal (n = 33, 61.1%), smaller (n = 20, 37.0%), larger (n = 1, 1.9%). Those with no uptake were all PD (n = 5) and classified as agenesis, of them, serum TRAb, ATG and ATPO were all negative. A case showing pyramidal lobe uptake was sonographic larger thyroid (Rt. 4.15, Lt. 3.04 mL). The estimated dose for TcPT is around 0.9 mSv (EANM, RADAR 2017).

Conclusions: Both TcPT and neck sonography were clinical complementary and valuable in evaluating neonatal hypothyroidism. Neonatal TcPT appeared clinical feasible in practice, especially in detecting ectopic, agenesis or pyramidal thyroid tissues.

OC-002

Visual Interpretation of Neonatal Thyroid Disorders using Tc-99m Pertechnetate Thyroid Scan

Chien-Hsin Ting[1], Hong-Yin Chen[1], Chia-Jung Chang[1], Dau-Ming Niu[2], Sing-Yung Wu[3], Wen-Sheng Huang[1]

[1]Departments of Nuclear Medicine/National PET & Cyclotron Center, Taipei Veterans General Hospital, Taipei, Taiwan, ROC

[2]Departments of Pediatrics, Taipei Veterans General Hospital, Taipei, Taiwan, ROC

[3]Departments of Nuclear Medicine and Medical Services, Long Beach VA Medical Center, Long Beach, CA, USA

Introduction: Tc-99m thyroid scan (TcPT) has been an importantly advanced tool to evaluate neonatal hypothyroidism. Visual interpretation of TcPT findings is a feasible means in practice. We observed the consistency in rating TcPT findings in hypothyroid newborns who presented thyroid uptake in anterior neck regions.

Methods: From 2011-2020, a total of 111 newborns (M/F: 56/55; mean age: 15.2 ± 7.7 / 14.2 ± 9.5 days) who reveal a positive neonatal thyroid screening test and present thyroid uptake seen on TcPT were recruited. Visual interpretation based on dichotomy of both uptake activity and size as normal and abnormal was performed by 2 experienced NM physicians. The kappa values were used to test the consistency of the 2 raters. Neck sonography was used to measure the size of neonatal thyroid gland and defined the size by length x width x height x π/6 (Arch Dis Child Fetal Neonatal Ed 2002; 87: F209). Both sizes measured by neck sono and TcPT were compared side by side.

Results: Our data showed the kappa value was 0.696 for agreement of thyroid uptake activity (0.61 and 0.80 means substantial agreement) and 0.821 for agreement of size seen on TcPT (0.81 and 1.00 means almost perfect agreement). Noteworthily, 38 sonographic small in size showed only 1 (2.6%) small size, 18 (47.3%) normal and 19 (50%) large on TcPT, 69 sized normal 11 (16%) normal and 58 (84%) bigger than usual on TcPT. All 3 sonographic sized larger also showed larger than usual on TcPT. One sonographic invisible case showed large size on TCPT.

Conclusions: Acceptable visual agreement of thyroid uptake activity and size seen on TcPT was observed. However, the sizes determined by neck sonography and TcPT were great discrepant. Further explore the interplay between both modalities deserves further clarification.

OC-003

Left-Ventricular Dyssynchrony in Viable Myocardium by Myocardial Perfusion SPECT is Predictive of Mechanical Response to CRT

Guang-Uei Hung[1], Weihua Zhou[2], Jin-Long Huang[3]

[1]*Department of Nuclear Medicine, Chang Bing Show Chwan Memorial Hospital, Changhua, Taiwan*
[2]*College of Computing, Michigan Technological University, Houghton, MI*
[3]*Cardiovascular Center, Taichung Veterans General Hospital, Taichung, Taiwan*

Objectives: Gated myocardial perfusion SPECT (GMPS) provides one-stop-shop evaluation for cardiac resynchronization therapy (CRT). However, conflicting results have been observed regarding whether the baseline left-ventricular (LV) mechanical dyssynchrony as assessed by phase analysis on GMPS was predictive of therapeutic response to CRT. Since dyssynchrony parameters by phase analysis spuriously increased by scarred myocardium, the purpose of this study was to explore the value of dyssynchrony after stripping off the scar region in correlation to mechanical response to CRT.

Methods: Forty-seven patients following standard indications for CRT received GMPS with phase analysis. Decrease of end systolic volume > 15% on follow-up echocardiography after CRT was considered as a mechanical response to CRT. Myocardial regions with less than 50% of maximal activity on GMPS were considered as scar. The phase standard deviation (PSD) and histogram bandwidth (BW) without or with stripping off scar were assessed by phase analysis of GMPS and were used for evaluation of LV dyssynchrony of all myocardium or only the viable myocardium, respectively.

Results: No significant difference was noted between mechanical responders (n = 31, 66%) and nonresponders (n = 16, 34%) for PSD and BW of the entire myocardium. However, responders had significantly larger PSD (40.5° ± 15.7° vs 30.5° ± 13.2°, p = 0.027) and BW (209.1° ± 91.2° vs. 156.2° ± 78.2°, p = 0.046) than non-responders after stripping off scar. The ROC curve analysis showed that the areas under the curve for predicting mechanical response were 0.70 (95% CI, 0.62 – 0.77, p = 0.029) and 0.68 (95% CI, 0.60 – 0.75, p = 0.050) for PSD and BW of viable myocardium only, respectively..

Conclusions: Our result showed that LV dyssynchrony of the entire myocardium did not predict response to CRT. However, LV dyssynchrony only in the viable myocardium was a significant predictor of CRT mechanical response.

OC-004

First-Year Bone Scan of the Newly Diagnosed Breast Cancer Patients and the Subtypes Survival data of Those with Bone Metastasis

Che Lin[1,2], Kuang-Tao Yang[3*], Ding-Ru Chen[1]

[1]*Breast cancer center, Department of Surgery, Changhua Christian Hospital, Changhua, Taiwan*
[2]*Department of Optometry, Chung Hwa University of Medical Technology, Tainan, Taiwan*
[3]*Department of Nuclear Medicine, Changhua Christian Hospital, Changhua, Taiwan*

Introduction: According to the National Comprehensive Cancer Network (NCCN)-breast cancer 2020 guideline with references, it is not recommended to use Tc-99 MDP bone scan to follow up stage 0 to stage II breast cancer patients, except clinical suspicion (such as localized bone pain or elevated alkaline phosphatase or sodium fluoride PET/CT). However, physicians in Taiwan keep using baseline Tc-99 MDP bone scan to long term follow up the newly diagnosed breast cancer patients. There are no studies yet that explore whether the NCCN Breast Cancer Guidelines and other Western studies are suitable for Asians (including Taiwan).

Methods: According to the data from Changhua Christian Hospital cancer registration service, bone scan results from 3875 breast cancer patients between January 1, 2011, and December 31 2015 were collected. Excluding patients whose primary tumor cannot be assessed or with incomplete information (pathological or surgical report), 1862 patients have their first bone scan within a year after diagnosed breast cancer: Stage 0: 119, stage I: 605, stage II: 816, stage III: 322 patients were analyzed. (Stage II upstage to IV: 4 patients, Stage III upstage to IV: 37 patients).

Results: There is no bone metastasis found in stage 0 and stage I (total 724 patients). Four bone metastases were found in stage II (0.49%, 4/816), 16 in stage III (5%, 16/322). Bone scan true positivity in stage 0 and stage I 0% (0/724), stage II 0.49% (4/812) and stage III 4% (13/322). Using bone scan typical metastasis changes as our standard, in 41 stage IV patients 20 were found to have bone metastasis, 20 with neo-adjuvant chemotherapy, 37 under hormonal receptor and her2/neu immunohistochemistry stains (2017 St. Gallen criteria, ER+ her2/neu negative A-like 7 [19%] and survival median year with 95% Confident interval [5.0, 4.8 to7.4], ER+ her2/neu negative B-like 7 [19%] and [4.5, 3.9 to-], ER+her2/neu positive 10 [27%] and [3.5, 2.5 to 5.0], ER negative her2/neu positive 6 [16%] and [2.5, 0.8 to 3.9], ER negative her2/neu negative 7 [19%] and [2.9, 1.4 to 2.9]; overall, table 5, bone scan sensitivity 85% (17/20) and specificity 99.5% (1832/1842).

Conclusions: First-year bone scan of the newly diagnosed breast cancer patients could be necessary while decision making based on stage, subtype and other breast cancer risk factors to predict survival and bone metastasis.

OC-005

Reveal Ectopic Parathyroid Gland After Parathyroidectomy in Cases with Recurrent Secondary Hyperparathyroidism

Pei-Wen Wang, Yen-Hsiang Chang, Shu-Hua Huang,
Yung-Cheng Huang, Chien-Chin Hsu

Department of Nuclear Medicine, Kaohsiung Chang Gung Memorial Hospital and Chang Gung University College of Medicine, Kaohsiung 833, Taiwan

Background: The estimated prevalence of ectopic parathyroid glands, due to aberrant migration during early stages of development, is about 2-43% in anatomical series and up to 14% in patients with secondary hyperparathyroidism (SHP). Lack of successful identification of ectopic parathyroid glands constitutes a common etiology of persistent or recurrent hyperparathyroidism after parathyroidectomy (PTX). However, recurrent SHP caused byectopic parathyroid gland detected after initial successful PTX is seldom reported.

Methods and Results: We reviewed the ^{99m}Tc-MIBI parathyroid imaging for patients with SHP at Kaohsiung Chang Gung Memorial Hospital from 2000 to 2020. The ^{99m}Tc-MIBI parathyroid imaging in 36 patients who had detectableectopic parathyroid and serial parathyroid studieswere reviewed by two nuclear medicine physicians. Among them, 8 patients' ectopic parathyroid glands were newly found after initial successful PTX. They are summarized in table 1. Briefly, the time period between negative and positive MIBI imaging for ectopic parathyroidranged from 4 years 3 months to 8 years 5 months.

Conclusion: Dynamic change of ^{99m}Tc-MIBI parathyroid imaging is observed in our series study of SHP. Prolonged stimulation of parathyroid tissue in persistent SHP patients may potentiate the enlargement of small remainder of parathyroid tissue.

OC-006

Lenvatinib for Radioiodine Refractory Thyroid Cancer: Real-World Experience in Southern Taiwan

Yen-Hsiang Chang[1], Pei-Wen Wang[1,2], He-Jiun Jiang[3], Pi-Jung Hsiao[3]

[1]Nuclear Medicine Department, Kaohsiung Chang Gung Memorial Hospital, Kaohsiung City, Taiwan
[2]Division of Endocrinology and Metabolism, Department of Internal Medicine, Kaohsiung Chang Gung Memorial Hospital, Kaohsiung City, Taiwan
[3]Division of Endocrinology and Metabolism, Department of Internal Medicine, E-DA Hospital, College of Medicine, I-Shou University

Background: Lenvatinib has significant antitumor effect on Radioiodine-refractory differentiated thyroid cancer (RRDTC). In the phase III SELECT trial, Lenvatinib showed a significant improvement in progression free survival (PFS) in patients with RRDTC compared to placebo. However, almost all the participants experienced adverse effects. In the present study, we retrospectively evaluate the efficacy and safety in patients with RRDTC in the real-world practice.

Patients and Methods: Chart records and images of 51 consecutive RRDTC patients treated with Lenvatinib from July 2016 to May 2019 in two tertiary medical centers in southern Taiwan were retrospectively reviewed. The primary objective was the progression-free survival (PFS) according to Response Evaluation Criteria In Solid Tumors v1.1 (RECIST 1.1). Disease control was defined as objective tumor response plus stable disease. The safety assessment was regularly performed according to according to Common Terminology Criteria for Adverse Events (CTCAE) v4.0.

Results: The median PFS was not reached during follow-up. Partial responses (PR) and stable disease (SD) were achieved in 9 (19%) and 34 (71%) patients, respectively. Disease control (PR + SD) of > 6 months was achieved in 31 (61%) patients. Almost all participants experienced adverse events (AEs). The most common AEs (any grade) in lenvatinib-treated patients were hypertension (60%) fatigue/asthenia/malaise (60%), and proteinuria (56%). Thirty-four (71%) and 26 (54%) patients had dose reductions or an interruption of Lenvatinib, mostly due to AEs. The mean initial and maintenance (final) dose of Lenvatinib were 13.7 and 11.2 mg/daily.

Conclusion: These results confirmed that Lenvatinib is an effective treatment for patients with RRDTC in Taiwan, even at a dose far lower than the recommended. However, more studies should be conducted to decide optimal dose for patients in Taiwan. Adverse events are frequently occurred and may cause mortality. Thus, adverse events should be identified and managed appropriately.

OC-007

髖部骨質密度用於預測良性攝護腺增生之相關性研究

陳保良[1,2] 蔡依良[1,2] 莊紫翎[1,4] 廖建國[1] 王昱豐[1,3,4*]

[1] 佛教慈濟醫療財團法人大林慈濟醫院核子醫學科
[2] 佛教慈濟醫療財團法人大林慈濟醫院醫學研究部
[3] 佛教慈濟醫療財團法人大林慈濟醫院預防醫學中心
[4] 慈濟學校財團法人慈濟大學醫學院醫學系放射線學科

目的：先前研究發現，年齡大於 65 歲，良性攝護腺增生對於腰椎骨質密度是有影響，且呈現正相關趨勢，本篇研究進一步分析，各年齡層對於髖部骨質密度與攝護腺肥大是否有相關性，髖部骨質密度是否可用於預測良性攝護腺增生。

材料方法：自 2014 年 6 月至 2020 年 07 月在臺灣南部地區醫院接受一般健康檢查的男性患者符合這項研究的條件。排除有脊柱外科手術史，全髖關節置換術，以及沒有完整病史的患者被排除在外。最後總收集 7,488 位患者中，分別通過雙能 X 射線吸收法和超音波檢查來估計骨質密度和攝護腺大小，並根據攝護腺大小將受試者分爲正常和良性攝護腺增生組。比較兩組間之髖部骨質密度和 T 分數。與相關病史，及實驗室數據間是否有差異，預測良性攝護腺增生之 ROC 結果。

結果：良性攝護腺增生患者的平均骨質密度和髖部 T 分數與正常組 T 分數有均低於正常前列腺大小的患者，推測與相關腎功能數值比起正常組高有關，我們進一步運用 ROC 曲線計算雖然預測偏低，但仍有預測之價值。

結論：我們的研究結果發現，對於無症狀之良性攝護腺增生患者應考慮監測骨質密度，未來將持續研究其機制。

OC-008

Developing an Evidence-Based-Medicine Learning in Nuclear Medicine for Medical Clerks

Bi-Fang Lee

Department of Imaging Medicine, National Cheng-Kung University Medical College and Hospital, Tainan, Taiwan

Introduction: Medical imaging, including nuclear medicine, is a powerful tool in human morphology, pathophysiology and understanding the nature of disease and response to treatment. An evidence-based-medicine (EBM) learning in nuclear medicine for medical clerks has been developing at a southern medical center in Taiwan. The purpose of this study is to create a new EBM learning model and to compare EBM and the traditional instructional approach (TIA) in a nuclear medicine clerkship.

Methods: Internal consistency and expert validity are assessed for the instrument. A quasi-experimental, two-group pretest-posttest design is used for this study. A combination of EBM and the TIA is applied to the experimental group and the TIA only to the control group. Before and after the educational intervention, students are tested with the instrument.

Results: Cronbach's coefficients of the instrument ranges from 0.79 to 0.95, indicating acceptable to strong internal consistency. For expert validity, the suitability and fitness of the instrument are verified. From 2018 June to 2019 May, Subjects are 70 undergraduate year 6 medical students in a clerkship curriculum.

Conclusions: The integration of EBM, allied with the TIA, into clinical clerkships provides medical students with the opportunity to learn a nuclear medicine curriculum in an interactive and case-based format tailored specifically for medical students.

OC-009

Radiation Safety Review in Human Research Protection Program: Preliminary Results

Lee BF[1,2,3], Liu YS[1,2], Ko WC[1], Roan JN[3], Chiou YY[3], Chang TT[3]

[1]*Department of Imaging Medicine, National Cheng Kung University Hospital, College of Medicine, National Cheng Kung University, Tainan, Taiwan*
[2]*Radiaiton Protection and management Committee, National Cheng Kung University Hospital*
[3]*Institutional Review Boards, National Cheng Kung University Hospital*

ABSTRACT

Introduction: Human research plays an important role in the translation medicine. Human research protection is required in the protection of the rights, welfare, and wellbeing of human subjects involved in research. Human research protection program (HRPP) is responsible for human subject protection. Institutional Review Boards (IRB) takes charge of reviewing research ethics. Moreover, radiation safety review is used to evaluate a HRPP of an organization to comply with national radiation safety regulations. The aim of this study is to create a grading system based on the risks, benefits, alternatives, and consequences of a proposed medical imagings involving ionising radiation.

Methods: All the applications of radiation safety review over human trails at a southern medical center in Taiwan were included. The radiation dose involved in radiation therapy, radionuclide therapy, and imagings using radionuclide, conventional radiographic, fluoroscopic and computed tomography (CT) represents a significant risk, and should have their ionising radiation risk disclosed. Pregnant subjects and paediatric subjects should be considered radiosensitive, and should have all ionising radiation risks disclosed. According to the risks, benefits, alternatives, and consequences of a proposed medical imagings involving ionising radiation, three-grading system was developed as low-risk radiation grade of ☐ 1 mSv, moderate-risk radiation grade of > 1 mSv and ☐ 3 mSv, and high-risk radiation grade of > 3 mSv.

Results: From 2018 January to 2020 August, one hundred forty-four human trials were included. The numbers of human trials with low-risk radiation grade, moderate-risk radiation grade, and high-risk radiation grade were 19, 1, and 124, respectively. The number of human trials with pediatric human subjects was three. These three human trials were belonging to low-risk radiation grade.

Conclusions: HRPP is a collaborative effort between all who develop, conduct, review, approve and facilitate Human Research. Researchers and Research Staffs have to protect the rights and welfare of the human subjects involved in research. The integration of radiation safety review, allied with the IRB review, into human research provides human subjects with the opportunity to learn about the risks, benefits, alternatives, and consequences of a proposed medical imagings involving ionising radiation.

Key words: Radiation safety review, Radiaiton Protection and management Committee, Institutional Review Boards.

OC-010

Ra-223 Treatment in Metastatic Castration-Resistant Prostate Cancer: A Single Center Preliminary Experience

Yueh Lee, Daniel H Shen, Li-Fan Lin, Chuang-Hsin Chiu*

Department of Nuclear Medicine, Tri-Service General Hospital, Taipei, Taiwan

Introduction: Radium-223, a targeted alpha-emitter, is used to treat bone metastases in patients with prostate cancer. Publications regarding the treatment experience in Taiwan population is limited. In this study, we analyzed the data of 18 patients who underwent radium-223 treatment since the reimbursement of NIH in March, 2019.

Methods: We retrospectively collected the patient's data including age, staging, treatment modalities prior to radium-223, bone scan findings, pain condition, adverse effects and blood test results including blood cell counts, PSA, LDH and ALP were collected. Eleven of the 18 patients who completed the treatment course with all 6 injections were further included for analysis of their trends of blood test results.

Results: All of the patients underwent Tc99m-MDP whole body bone scan prior to the first dose of Ra-223. The image results of treatment response were mixed. Mild decrease in the average values among the 11 patients' hemoglobin (12.4 to 10.8 g/dL), absolute neutrophil count (4150 to 3180/ mcL) and platelet (213000 to 179000/ mcL) was noted. The patients' LDH and ALP average levels revealed a slight trend of decrease, while the PSA levels oscillated and increased. Except for 1 case with bone marrow suppression that required blood transfusion, no significant treatment related adverse effect was noted. 36% of patients reported significant pain relief.

Conclusions: Ra-223 is a generally safe treatment with very rare significant adverse effects. In our study, 36% of the patients who underwent Ra-223 reported favorable response regarding pain relief, while no significant worsening of pain was complained among the rest of the patients. LDH and ALP might be promising parameters for evaluation of treatment response. More data are required for further statistical analysis.

OC-011

Lung Cancer Smaller than 3 cm with Distant Metastasis: The Relationship of F-18 Fluorodeoxyglucose Metabolism and Anatomic Structure Change

Hao-Tien Teng, Hsiao-Min Chou, Shih-Wei Chen, Sheng-Che Lin, Chia-lu Yeh, Chi-Tai Ku, I-Lin Su, Yen-Kung Chen

Department of Nuclear Medicine and PET Center, Shin Kong Wu Ho-Su Memorial Hospital, Taipei, Taiwan

Introduction: Lung cancer is one of the most common cancer with the highest morbidity and mortality. Nearly 40% of those people newly diagnosed with lung cancer already have metastases to other parts of the body. We to explore the relationship of F-18 fluorodeoxyglucose (FDG) metabolism and anatomic characteristic associated with lung cancer smaller than 3 cm with distant metastasis.

Methods: We collected patients who have the lung cancer smaller than 3 cm with distant metastasis retrospectively. All the 27 patients whose medical records and results of FDG positron emission tomography (PET)/computed tomography (CT) studies are available after the initial diagnosis are included. Among them, 14 patients (group A): lung cancer tumor size larger than 1 cm, smaller than or equal to 2 cm; 13 patients (group B): lung tumor size larger than 2 cm, smaller than or equal to 3 cm. Statistical calculations are completed using IBM SPSS Statistics, and $p < 0.05$ is considered statistically significant.

Results: A total of 27 patients, lung cancer smaller than 3 cm with distant metastasis, are analyzed. The measurement of lung cancer size-from 1.2 to 2.9 cm, SUVmax-from 2.4 to 23.2, and visual score-from 1 to 4. All of the 27 lung cancer patients have FDG uptake; associated with pleural contact in Group A and B is 5 and 4, respectively ($p = 1$). Observed patterns of lung cancer CT images vary as follows: 6 (22.2%) patients have a linear pleura tag pattern, 5 (18.5%) patients have a pleura retraction pattern, 16 (59.3%) patients have a pleura thicken and contact pattern. In addition, five patients of lung cancer involve the vessel. The metastasis of lung cancer to lymph nodes in the Group A and B is 3 (21.4%) and 10 (76.9%) respectively ($p = 0.007$). For the lung tumor size, SUVmax, visual score, metastasis to lymph node, and intrathoracic lymph node of 27 lung cancer patients, a positive correlation is found between tumor size and SUVmax of lung tumor ($r = 0.68$, $p < 0.001$); tumor size and the visual score of FDG uptake in the lung tumor ($r = 0.58$, $p = 0.002$); tumor size and metastasis to lymph node ($r = 0.53$, $p = 0.004$); tumor size and metastasis to intrathoracic lymph node ($r = 0.45$, $p = 0.018$).

Conclusion: FDG PET/CT shows for lung cancer smaller than 3 cm with FDG uptake, involving the vessel, pleura change (linear pleura tag, pleura retraction, pleura thicken and contact), and tumor nearby pleura are the risks of possibility of distant metastasis.

OC-012

Review on 3 Deep Learning Models using The SPECT Imaging for Myocardial Perfusion

Tien-Hsin Chang[1,2], Da-Chuan Cheng[2], Cing-Yuan Chen[1]

[1]*Department of Nuclear Medicine, Taichung Tzu Chi Hospital, Buddhist Tzu Chi Medical Foundation*
[2]*Department of Biomedical Imaging and Radiological Science, China Medical University, Taichung, Taiwan*

Introduction: According to statistics from the National Health Insurance in 2017, the top 10 causes of death for Taiwan, heart disease ranked 2th, and about 2 million people have heart disease, and half are consisted with coronary heart disease with symptoms including angina and myocardial infarction. In Recent years, research show using artificial intelligence (AI) is universality to improve human health with better diagnosis. Using SPECT myocardial perfusion image (MPI) is widely used for the diagnosis of coronary artery disease (CAD) and there are more than 150000 scans performed annually in Taiwan. The purpose of this review is to improve the reliability and accuracy of MPI to diagnosis CAD.

Methods: Retrospective analysis of data within 3 years and the patient has no history of heart disease. A total of sample size with 485 patients (79.7% men) were studied, patients underwent stress and rest Tl-201 MPI scan, all patients underwent cardiac catheterization within half year after MPI. The post-processing images of cardiac in nuclear medicine are analyzed using Xeleris 3.0 and it generated polar maps from 416 training datasets and 82 testing datasets. Deep analysis using MATLAB suite software and TAIWANIA 2 is a Supercomputer. The hardware specification consists of 9,072 CPUs and 2,016 GPUs, Ranked 20th in the world's top 500 supercomputer rankings released by TOP 500 at the end of 2018. The 3 Deep Learning (DL) models is ResNet101, MobileNet V2, Inception V3. Deep learning was trained using raw polar maps and evaluated for prediction of obstructive stenosis in a stratified 6-fold cross-validation procedure.

Results: The analysis for Polar map accuracy rate of prediction via AI is 79% for Pre-patient (LAD, Lcx, RCA vessels overview), the DL sensitivity is 77% and specificity is 80%.

Conclusions: Deep learning has potential for development in the future, and the applications can provide some help in medical.

PB-001

Development of DOTATATE Kit for ^{177}Lu Labeling

Shih-Ying Lee, Sheng-Nan Lo, Ming-Hsin Li, Chih-Hsien Chang

Division of Isotope Application, Institute of Nuclear Energy Research, Atomic Energy Council, Taiwan

Introduction: Peptide receptor radionuclide therapy (PRRT) is a novel treatment in theranostics that uses peptide drug as a vector to label with different nuclides. Peptide drug labeled with a diagnostic or therapeutic nuclide can be used as a diagnostic or targeting therapeutic drug. Both ^{68}Ga-DOTATATE and ^{177}Lu-DOTATAE for PRRT of neuroendocrine tumors (NETs) were approved by FDA in 2016 and 2018, and has been market in American and European. Unfortunately, due to long-distance transportation and high transportation costs. DOTATATAE PRRT drugs are still not commonly been used in Asia region. Therefore, we initiated the development of DOTATATE Kit suitable for ^{68}Ga and ^{177}Lu radio-labeling. The aim of this study was to evaluate DOTATATE Kit for ^{177}Lu labeling, and test the radioactive products stability.

Methods: The DOTATATE Kit contains with two Vials. Vial-1 contains 40 μg DOTATATE and other excipient, were lyophilized and sealed under vacuum. Vial-2 contains lyophilized ascorbic acid, we prepare with 1mL dd-H_2O before use. The ^{177}Lu labeling DOTATATE Kit was done by following steps. First, we take 1 mL buffer by 3 mL syringe from Vial-2, and transfer to Vial-1. Then, we inject with 20 mCi $^{177}LuCl_3$ solution (N.C.A) in 0.04N HCl toVial-1. After gently mixture, place the vial-1 into a dry-heater for 30 minutes at 95°C. Finally, the ^{177}Lu-DOTATATE products were filtered through sep-pak cartridge (Waters, WAT023531) and 0.22 μm syringe filter (Millipore). All ^{177}Lu-DOTATATE products were analyzed by radio-instant thin-layer chromatography (ITLC), and radio-HPLC. The stability of ^{177}Lu-DOTATATE products at room temperature for 1, 2, 3, 4, 5, 6, 7, 8 and 24 hours were test.

Results: The radiochemical purity of three batches of ^{177}Lu-DOTATATE products is 99.85 ± 0.11. The DOTATATE kit can be labeling with ^{177}Lu successfully. Three batches results show that radiochemical purity of ^{177}Lu-DOTATATE products at 1, 2, 3, 4, 5, 6, 7, 8 and 24 hours is 99.72% ± 0.11, 99.77% ± 0.09, 99.69% ± 0.06, 99.78% ± 0.02, 99.72% ± 0.11, 99.68% ± 0.09, 99.79% ± 0.06, 99.71 ± 0.12 and 99.73% ± 0.29.

Conclusions: The time-lapse stability results show that the ^{177}Lu-DOTATATE products had considerable stability within 24 hours. It demonstrated that the DOTATATE kit have high degree of product stability. By different purpose, the DOTATATE Kit can be labeled with 68Ga or ^{177}Lu for neuroendocrine tumors diagnosis or therapy as a theranostics in clinic. We hope to increase the clinical application and convenience of DOTATATE Kit products in the future.

PB-002

Automatic Semantic Segmentation of MPI Imaging Polarmap Defect Area by using Mobile-Segnet

Ta-Wei Tseng[1], Yi-Hsiang Liao[1,2], Li-Fan Lin[1,2], Yi-Fong Chen[1], Chuang-Hsin Chiu[1,2]

[1]*Department of Nuclear Medicine, Tri-Service General Hospital, Taipei, Taiwan*
[2]*Department of Nuclear Medicine, National Defense Medical Center*

Introduction: On the basis of full convolution (FCN) semantic segmentation, the method of reducing the number of neural convolution layers is used to establish a high-performance Mobile-Segnet encoding-decoding structure model, and training myocardial perfusion (MPI) Polarmap image defect area Automatic segmentation model, using TPD Map (MPI Total Defect Map) as the standard, and comparing artificially predicted blood flow defect area (Hand-ROI), using ^{avg}IOU (average intersection of Union), ^{avg}Dice (average Dice coefficient or F1 score), avgprecision, ^{avg}Sensitivity, ^{avg}PA (average pixel accuracy) and the above Object detect classification evaluation indicators are used to measure the effectiveness of automatic segmentation and prediction of myocardial blood flow defects.

Methods: Segnet is the architecture of the semantic segmentation model, which is like the Autoencoder technology. It uses encoding and decoding to identify the category (normal blood flow area or blood flow defect area) to which each pixel of the MPI Polarmap belongs. In this study, 100 MPI Polar map was used as the data set (Moderate 50%, Severe 50%), and MPI Total Perfusion Defect Map (TPD Map) image was used as the reference standard. According to the labeling of the defect area, the Mobile-Segnet training model is performed. When the best prediction model is obtained, 20 sets of Polar maps are used to artificially predict blood flow defect area ROI (Hand-ROI) and Mobile-Segnet model automatic segmentation (Auto-ROI) for Out of Sample prediction and verification. For these 20 sets of images, TPD-ROI is used as the comparison standard, and evaluation indicators (such as IOU, Dice, PPV, Sensitivity, PA, etc.) are calculated for Hand-ROI and Auto-ROI, and the generalization ability of the model is evaluated.

Results: In this study, Mobile-Segnet (Auto-ROI) semantic automatic segmentation prediction can accurately and effectively predict and segment MPI Polar map blood flow defect areas, ^{Avg}IOU: 0.81, ^{Avg}Dice: 0.92, ^{Avg}Precision: 0.90, ^{Avg}Sensitivity: 0.85, ^{Avg}Pixel Accuracy: 96%. All kinds of image segmentation evaluation indicators are better than hand-ROI prediction.

Conclusions: The characteristics of Segnet are: 1. Improve the boundary contour, 2. Reduce the amount of parameters (simplify the space complexity of the algorithm), 3. Direct end-to-end training (no need for manual feature extraction), 4. Flexible use of up-sampling decoding, adjustment Neural network training structure makes it easy to obtain better training results. Due to the relatively complex and large structure of full convolutional networks such as FCN and U-Net, the cost of training hardware and time is quite high. The cost pressure for clinical imaging research is not small, leading to a high threshold for scholars who yearn for Auto-Segmentation research. However, Segnet is a fully convolutional structure and has classification characteristics of codec. The initial development is used as a visual recognition for unmanned vehicles. The technical model has quite good results. Because MPI Defect area is usually blocky, it seems too wasteful to use “heavy” tools such as FCN, U-Net, etc. Therefore, this study confirms that the prediction effect of using Mobile-Segnet to train the MPI Defect automatic segmentation model is better than that of humans Prediction , using Polarmap single image to import the prediction model, to help physicians quickly and effectively assist in the assessment of MPI blood flow defect areas, which is believed to reduce the burden of nuclear medicine physicians in diagnosis and reporting.

PB-003

集成式機械學習應用於核醫唾液腺閃爍造影檢查異常程度預測之研究

鍾紫柔　曾大維　陳穎柔　林立凡　邱創新

三軍總醫院核子醫學部

背景介紹：在過去十幾年來，唾液腺的閃爍造影被廣泛用來評估以及診斷唾液腺異常的現象以及疾病，特別是在自體免疫疾病如：Sjögren's syndrome，長期的慢性發炎造成唾液腺分泌功能受到影響，但由於唾液腺閃爍造影現行的分析方法，須手動圈選感興趣區域(Region of Interest, ROI)，花費較多的時間。本研究將以 Pmod 軟體，快速半自動模板式圈選出唾液腺感興趣區域 (Region of Interest, ROI)，並利用機械學習 - 集成式學習預測影像結果，快速有效的輔助醫師醫療診斷。

方法：本研究預計回溯 276 位臨床病例影像，32 位正常病例，47 爲輕微病例，115 位中度病例，82 位重度病例。正常、輕、中及重度的評定是依據醫師診斷爲標準。佐以 Pmod 軟體，圈選出唾液腺感興趣區域 (Region of Interest, ROI)，圈選區域包含雙側腮腺區、下頜腺及舌下腺區、額葉 (背景) 區組織區域，共 5 個 ROI。再利用集成學習演算法將影像 ROI 數值輸出，進行單一機械學習與集成學習進行預測建模，並以醫師診斷報告之結果爲標準進行訓練。研究中，我們使用了 Random Forest、SVM、Logistic Regression、Neural Network、Decision Tree、Adaboost、KNN 等單一機械學習法訓練同時使用 Stacking 集成式學習交叉訓練方式期能求得最佳整合式模型。

結果：經過多種訓練法的訓練及建模，單一機械學習法以 Random Forest 爲最優；AUC: 0.68，集成式學習 Stacking 的部份以 Random Forest+ SVM+ Logistic Regression 的合作模式爲最佳 AUC: 0.71。

結論：單一演算法表現最出色的部份，以有多個 Decision Tree 集合概念的 Random Forest 的分類效果最佳。或許因 Random Forest 有集成式學習的概念。另外在超參數的校調上，是影響模型成效最大的因子，同樣的演算法，參數的微調仍可能造成預測差異，因此超參數的調校不可忽視。隨個案數的增加及特徵明確，可運用的集成式學習訓練的準確度肯定會更高，來將繼續收集更多個案，應可訓練多泛化能力佳的唾液腺預測模型。

PB-004

Process Development of PSMA Targeted Inhibitor (PSMA-617) and *in Vitro* Pharmacological Studies

Chun-Tang Chen, Shih-Wei Lo

Institute of Nuclear Energy Research, Taoyuan, Taiwan

Introduction: Prostate specific membrane antigen (PSMA) plays a significant role in prostate carcinogenesis and progression. Varieties of low molecular weight prostate cancer diagnostic and therapeutic radioligands have been developed. For men with metastatic castration-resistant prostate cancer (mCRPC), multiple active treatments have emerged. According clinical trial data, Lu-177-PSMA-617 has a good therapeutic value for mCRPC and has no obvious side effects. Moreover, It is being developed as PSMA-targeted radioligand therapy for mCRPC with an phase III VISION trial.

Objective: The aim of this study is to set up process development of PSMA-617 and conduct *in vitro* pharmacological studies for Lu-177-PSMA-617 IND in Taiwan.

Methods: In synthesis of DOTA-conjugated PSMA inhibitor PSMA-617, PSMA-617 precursor was dissolved in DMF and added to chelator DOTA-NHS-ester and DIPEA. After R.T. 4 hour, an amine to an amide via coupling reactions. Then, The product was precipitated by cold ether and purified by HPLC. After purification, the final product (PSMA-617) was lyophilized and confirmed by LC/MS, NMR and FT-IR. We also radiolabeled PSMA-617 with Lu-177 and conducted cellular uptake and binding competition assay to evaluate the binding affinity.

Results: In this study, we have successfully demonstrated the synthesis of four batches of PSMA-617 (100 mg process) in 95 to 98% purity range. The average yield rate is about 55%. Molecular weight, NMR and IR spectral data of PSMA-617 were confirmed by LC/MS, NMR and FT-IR. We also radiolabeled PSMA-617 with Lu-177 resulting in radioligand of high radiochemical purity (> 98%). And lastly, in vitro cellular uptake and binding competition inhibition data showed the specificity of Lu-177-PSMA-617 for PSMA positive LNCaP cells with an IC_{50} of 5 nM.

Conclusions: This study represents an important first step for the development of Lu-177-PSMA-617. We will continue to increase batch production and perform toxicological test to facilitate the application of Lu-177-PSMA-617 clinical trial, benefiting mCRPC patients in Taiwan and providing an important new treatment option.

PB-005

Imaging Evaluation of an In Vivo Long-Acting PSMA-Targeting Peptide in Prostate Cancer Mouse Model

Ming-Wei Chen, Wei-Lin Lo, Shih-Min Wang, Shih-Wei Lo, Ming-Hsin Li, Chih-Hsien Chang

Institute of Nuclear Energy Research, Taoyuan, Taiwan

Introduction: Prostate-specific membrane antigen (PSMA) is a well-known targeting for prostate cancer. The DOTA-conjugated ligand, PSMA-617, is a good choice for prostate radionuclide ligand therapy (PRLT). Referring to the structure of PSMA-617, we design a precursor MH-PC-AB-56 that has a spacer link urea-based N-Acetyl-l-aspartyl-l-glutamate (NAAG) inhibitor and albumin binder to change the pharmacokinetics of NAAG inhibitor for PSMA. This study investigated the comparison of nanoSPECT/CT imaging of radiolabeled PSMA-617 and MH-PC-AB-56 in LNCaP-xenograft BALB/c nude mice and demonstrated that MH-PC-AB-56 had more accumulation in tumor sites than PSMA-617.

Methods: MH-PC-AB-56 and PSMA-617 were labelled with ^{111}In in Institute of Nuclear Energy Research. NanoSPET/CT studies were performed in LNCaP-xenograft BALB/c nude mice. Tumor xenografts were performed in 6-wk-old male BALB/c nude mice by subcutaneous injection of 2 x 10^7 LNCaP cells. NanoSPECT/CT imaging was performed at 1 h, 4 h, 24 h, 48 h, 72 h and 96 h after injection of ^{111}In-MH-PC-AB-56 or ^{111}In-PSMA-617. The imaging analysis was performed by PMOD image analysis software.

Results: The labeling efficiencies of ^{111}In-MH-PC-AB-56 and ^{111}In-PSMA-617 were more than 90%. Compare with ^{111}In-PSMA-617, the higher tumor uptake (at 24 h, 45.87 %ID/g; and 96 h, 27.51 %ID/g) of the ^{111}In-MH-PC-AB-56 were confirmed by nanoSPECT/CT images in the LNCaP-xenograft solid tumor-bearing BALB/c nude mice.

Conclusions: These results of nanoSPECT/CT imaging showed that ^{111}In-MH-PC-AB-56 revealed long circulation and high accumulation in LNCaP tumor site. In the future, we will demonstrate that MH-PC-AB-56 may have better diagnostic/radiotherapy capabilities for prostate cancer than PSMA-617.

PB-006

Use the Results of the International Ability Test to Estimate the Application of Chromosome Analysis to Accidental Radiation Exposure Events

Wan-Chi Lin[1], Tse-Zung Liao[1], Fang-Yu Ou Yang[1], Kang-Wei Chang[2], Tsui-Jung Chang[1], Ruth C. Wilkins[3], Chin-Hsien Chang[1]

[1]*Isotope Applications Section, Institute of Nuclear Energy Research (INER), Taiwan*
[2]*Taipei Medical University (TMU), Taiwan*
[3]*Consumer and Clinical Radiation Protection Bureau, Health Canada, Ottawa, Ontario, Canada*

Introduction: The successful application of the dicentric chromosome assay in triage mode has been confirmed. The purpose of this study is to evaluate the analytical ability of DCA. The results based on the intercomparison holded by Health Canada in 2014, 2015, and 2018.

Methods: In the National Biological Dosimetry Response Plan (NBDRP) inter-comparison, two methods of conventional or QuickScan scoring could be chosen. For conventional-DCA triage scoring, cells with 46 centromeres were being counted and each scorer recorded the number of dicentrics in the first 50 metaphases or stopped scoring when it reached 30 dicentrics. And also register how much time be recorded for 50 cells in the analyzed. In QuickScan scoring, a minimum of 50 metaphase cells, and do not need to estimate 46 centromeres or not. Meantime, register how much time be recorded for 50 cells in the analyzed.

Results: In conventional-DCA triage, the result in 2014, 2015 and 2018, there is 1, 1, 3 blind sample out of the range of ± 0.5 Gy, separately. In QuickScan-DCA, the result in 2014, 2015 and 2018, there are 2, 1, 2 blind sample out of the range of ± 0.5 Gy, separately.

Conclusions: According to the results, the results of the two analysis methods have little difference. This result means that when a large-scale radiation accident occurs in the future, chromosomes can be quickly analyzed and reliable data can be obtained. This is very helpful for the follow-up evaluation of related medical treatment.

PB-007

利用 Q.Metrix 軟體定量數值分析續發性副甲狀腺亢進增生組織最佳閾值及其結果與血中 iPTH 濃度之相關性

陳恩賜　邱創新　林立凡　陳穎柔　曾大維　張議方

三軍總醫院核子醫學部

背景介紹：續發性副甲狀腺機能亢進檢查是以 99mTc-Sestamibi 雙相法副甲狀腺功能閃爍攝影進行造影分析。新一代的單光子電腦斷層機型能提供 SPECT/CT 融合影像進行定量數值分析，除病灶影像定位外，更進一步分析個別病灶之代謝強度及病灶體積，提供臨床開刀前決策的重要依據。然而分析術前副甲狀腺增生組織 (Hyperplasia) 感興趣組織體積 (Volume of interest, VOI) 的 NM 閾值 (NM threshold) 並沒有原廠確切的建議值，加上不同病人間副甲狀腺增生組織吸收影像差異很大，導致術前分析出來的 VOI 與術後實際量測副甲狀腺增生組織體積有很大的差異，造成外科醫師對於核醫影像術前分析結果信心不足。本研究的目的是利用 Q.Metrix 分析軟體，用回溯的方式以術後副甲狀腺增生組織體積爲黃金準則，找出最佳的 NM 閾值，使得分析出來的術前 VOI 與術後開刀後體積有最好的正相關性。

方法：利用回溯的方式尋找本院副甲狀腺掃描後開刀的個案，從病理切片中篩出爲副甲狀腺增生組織個案約爲 68 人。SPECT/CT 影像依照病灶攝取分布可大致分成三組：分散型 (Dispension)、單顆亮型 (Single uptake) 及稀疏型 (Few and Scatter)。利用 GE Xeleris 3.1 workstation 應用程式“Q.Metrix”進行影像後處理及分析。以病理報告副甲狀腺增生體積爲標準，對比三組病灶影像圈選 VOI，建立本院術前副甲狀腺增生組織最佳 NM 閾值。再利用 GraphPad Prism 統計軟體分析 Q.Metrix 提供的增生副甲狀腺 SUV 值與血中 iPTH、病理報告中病灶體積進行相關係數 (Pearson correlation coefficient) 分析。

結果：以病理報告副甲狀腺增生體積爲標準分別找出三組建議最佳 NM 閾值：分散型是 76%、單顆亮型是 58% 及稀疏型是 84%，三組經由 One-way ANOVA 分析 P 值小於 0.0001 是有統計上的意義。統計分析術後副甲狀腺增生體積與術前血液中 iPTH 濃度是呈現正相關性，圈選的 VOI 分析出的 SUV 數值與血液中 iPTH 濃度呈現正正相關性，但 SUV 數值與血液中 iPTH 濃度並無任何相關性 ($P = 0.24$)。

結論：利用 Q.Metrix 程式分析續發性副甲狀腺體積的最佳 NM 閾值，求得 iPTH 與副甲狀腺增生組織總體積及影像 SUV 值間的相關性，未來可提供外科醫師在擬定手術計畫時，有更精確的病灶位置及病灶體積數值，提升精準醫療的目的。

PB-008

Synthesis and Evaluate of Zr-89 Transferrin in Breast Cancer Xenograft

Fang-Yu Ou Yang[1], Mao-Chi Weng[1], Shiou-Shiow Farn[1], Jenn-Tzong Chen[1], Ting-Shien Duh[1], Ming-Hsin Li[1], Chih-Hsien Chang[1], Chien-Chih Ke[2], Ren-Shyan Liu[3,4], Cheng-Hsiu Lu[3], Yi-An Chen[5], Jeng-Jong Wang[1]

[1]*Isotope Application Department, Institute of Nuclear Energy Research, Taoyuan, 32546, Taiwan*
[2]*Department of Medical Imaging and Radiological Sciences, Kaohsiung Medical University, Kaohsiung, Taiwan*
[3]*Department of Biomedical Imaging and Radiological Sciences, National Yang-Ming University, Taipei, Taiwan*
[4]*Xi-Yun PET Center, Cheng Hsin General Hospital, Taipei, Taiwan*
[5]*Institute of Clinical Medicine, National Yang-Ming University, Taipei, Taiwan*

Introduction: Transferrin is a monomeric glycoprotein that can bind iron and transport trivalent iron ions in blood. Transferrin receptor (TfR) is responsible for transferring iron-carrying into cells. Overexpression of endogenous TfR has been qualitatively described for various cancers such as prostate cancer, hepatocellular carcinoma, lung cancer, and breast cancer. TfR may represent a potential target of small tumors. The aim of this study, we report the synthesis of ^{89}Zr-DFO-transferrin and evaluation of Zr-89 transferrin in breast cancer xenograft.

Methods: ^{89}Zr was produced via the ^{89}Y(p,n)^{89}Zr transmutation reaction on a TR15/30 cyclotron at 14.5 MeV beam energy and 20-25 μA beam current with an irradiation time of 1-15 hours. The [^{89}Zr]Zr-oxalate solution was isolated by hydroxamate resin and theoretical calculated specific activity of that was 22~106 MBq/mg (0.38–2.887 mCi/mg). Transferrin was conjugated to p-Isothiocyanatobenzyl-desferrioxamine (DFO-Bz-NCS) and radiolabeled with ^{89}Zr at room temperature and 37°C to assess the radiolabeling efficiency. The stability of DFO-Bz-NCS conjugate complex was evaluated after 15 and 30 days of storage in a dark at –20°C. PET studies were conducted at various time points of 0.5-168 h after post-injection of [^{89}Zr]Zr-DFO-transferrin in MDA-MB-231 xenografts tumor-bearing mice.

Results: ^{89}Zr was achieved in high radionuclidic purity (≥ 98%) with 30-70% recovery of the radioactivity and the appearance of [^{89}Zr]Zr-oxalic was colorless. DFO-Bz-NCS was given at ten-fold molar excess of the chelator over the molar amount of TfR. Transferrin-NCS-DFO conjugate complex still remain high purity at –20°C for 30 days of storage shielded from light. The labeling efficiency of ^{89}Zr-DFO-transferrin was 7.8% and 6.73% at room temperature and 37°C, respectively. The radiochemical purity of ^{89}Zr-DFO-transferrin was obtained with over 90% after several steps of purification. PET imaging in breast cancer xenografts showed that the T/M ratio of [^{89}Zr]Zr-DFO-transferrin was 7.58 at 72h and has significantly higher liver uptake of [^{89}Zr]Zr-DFO-transferrin than that of other organ at 0.5h-1.5h after post-injection.

Conclusions: In summary, we report a novel [^{89}Zr]Zr-DFO-transferrin synthesis based on a ten-fold molar ratio and simple cartridge procedure of purification. Furthermore, [^{89}Zr]Zr-DFO-transferrin had target tissue uptakes with T/M ratio of 2 to 6 that makes it to be a potential imaging agent for breast cancer. Suggested approach provides an optimum of [^{89}Zr]Zr-oxalic and product quality regarding radiochemical purity and separation from chelation complex.

PB-009

巴金森病人 PET/MRI 腦功能影像之量化分析

張芷瑋[1] 吳承翰[2] 陳志成[1] 傅中玲[3] 陳方佩[4]

[1] 國立陽明大學生物醫學影像暨放射科學系
[2] 臺北醫學大學雙和醫院放射科
[3] 臺北榮民總醫院一般神經
[4] 臺北榮民總醫院傳統醫學部

背景介紹：巴金森病 (Parkinson's disease, PD) 是一種神經退化性疾病，其致病機轉爲中腦黑質退化，導致紋狀體 (struatum) 之殼核 (putamen) 及尾核 (caudate) 中多巴胺神經元退化，並造成在突觸之多巴胺含量下降，逐漸失去了行動的能力。在 PET 檢查中，可以藉由注射核醫藥物，進入腦中紋狀體之殼核和尾殼區域，再經由放射藥劑在影像上分布的缺損程度評估與診斷巴金森氏症之嚴重性。透過 MRI 的影像作爲輔助，提供更爲精準之解剖資訊，使得 ROI 圈選之準確率有更大的提升。因此我們的目的是建立一個自動化定量分析系統，用於 PET / MRI 圖像，透過使用殼核和尾狀的 ROI 分割並搭配 MRI 圖像自動進行 PET 圖像的定量分析。

方法：利用開放來源 SPM (statistical parametric mapping) 軟體將針灸治療前與治療後之 PD 病人的 MRI TI 影像與 PET 影像進行對位 (co-registration) 使兩者之空間座標相符。接著將病人之 MRI TI 影像對先前建置好的 MRI T1 模板 (template) 進行空間正規化 (spatial normalization) 並獲得正規化轉換參數，最後將此參數寫入相對應完成對位之 PET 影像中來進行空間正規化。進行正規化處理過之影像，其影像空間座標軸和體素之形狀及大小皆與標準空間腦部模板一致。最後再利用同樣符合標準空間座標軸之 AAL (automated anatomical labeling) ROI 中所定義的尾核與殼核範圍對正規化後之 PET 影像進行 ROI 自動圈選來進行量化分析。採用專一攝取率 (specific uptake ratio, SUR) 與不對稱性索引 (asymmetry index, ASI) 來當作量化分析之指標。

結果：目前從台北榮總醫院神經內科招募 7 位患者進行針灸前後的治療，其中五位女性，一位男性，平均年齡約 66.6 歲。Hoehn &Yahr (H&Y) 皆在四期以下，其中一位患者中途退出此研究。將針灸前後之結果進行 T TEST 統計分析 Caudate (SUR = 0.02), Putamen (SUR = 0.006), Striatum (SUR = 0.004) 的 SUR 皆有顯著差異。

結論：自動化定量分析系統可以改善臨床傳統手工圈選方法耗時費工及再現性低和人爲主觀問題，導入 MRI 影像所提供之解剖資訊進行對 PET 影像 ROI 自動化圈選，可以提高定量分析與臨床診斷之正確率。

PB-010

運用深度學習進行 ^{18}F-FDG PET 腦部影像失智症嚴重程度分類預測

林家榆[1] 曾繁斌[1] 倪于晴[1] 林文彬[1] 蕭穎聰[2]

[1] 核能研究所保健物理組
[2] 長庚大學醫學影像暨放射科學系

背景介紹：在社會高齡化過程中失智症患者會明顯增加，失智症照顧服務的需求與成本相對其他失能者高昂。阿茲海默症 (Alzheimer's Disease, AD) 疾病發展是不可逆，部分病人會由輕度知能障礙 (Mild Cognitive Impairment, MCI) 惡化成 AD，因此強化失智症早期診斷與延緩疾病惡化成爲重要課題。核子醫學影像能靈敏反應早期腦內異常，本研究主要運用 3D 卷積神經網路 (3D Convolutional Neural Network, 3D CNN) 進行 ^{18}F-FDG 腦部影像失智症分類預測，作爲輔助診斷資訊。

方法：本研究運用 ADNI ^{18}F-FDG PET 腦部影像資料庫訓練 3D CNN 模型，影像資料包含 AD、MCI 與正常控制組 (Normal Control, NC) 等三組，分別有 545 筆、519 筆與 500 筆資料。資料在模型訓練前經過維度剪裁處理，將影像中主要資訊留下，並且將影像數值正規化，使影像數值變化量在 0-1 之間，再將影像資料以 8 比 2 隨機劃分爲訓練資料與驗證資料。本 3D CNN 模型選用交叉熵作爲損失函數，激活函數爲 ReLu，也運用 Dropout 技術避免模型過擬合 (Overfitting)。

結果：在損失函數最小時，訓練後的深度學習模型準確度爲 77%，能有效將失智症分類成 AD、MCI 與 NC，從結果顯示運用 3D CNN 模型進行 ADNI 資料庫失智症分類具可行性，可準確將 MCI 與 AD 病患分類出來。由於 NC、MCI 與 AD 的病程演進爲連續關係，因此後續將改善調整模型爲回歸架構，利用連續數值表示病患失智症嚴重程度，提供臨床診斷失智症分級參考。

結論：由目前結果顯示本 3D CNN 模型於 ADNI 影像資料之失智症分類準確率達 77%。模型分類結果可作爲臨床輔助診斷資訊。未來改善模型與調整參數進行病患失智症嚴重程度預測，給予病患不同治療方式，有效延緩失智症惡化速度。

PB-011

以心臟假體驗證病人平躺姿勢對心肌血流灌注影像重組後短軸偏轉之影響

陳在揚[1] 林立凡[1*] 邱創新[1*] 許天睿[1] 溫淑惠[2]

[1] 三軍總醫院
[2] 奇異亞洲醫療設備股份有限公司

背景介紹：心肌灌注造影是現今常用於初步篩檢冠狀動脈疾病的重要檢查工具，其可提供直觀的影像及量化數值，協助臨床擬定治療方式及判斷預後，但從偶而顯現右心室影像上，發現的心軸偏轉現象困擾著影像判讀，針對此現象成因沒有找到好的解釋，故本研究以心臟假體驗證心軸偏轉的原因，以期能避免此現象發生影響病人診斷。

方法：使用 Cardiac Insert ™ 可置入式心臟假體及其配屬胸腔假體附件，將 0.5 mCi 之 Tc-99m 注入心臟假體的心壁空腔中，此心壁空腔內置 2 個壓克力塊，模擬灌注缺損部位，其餘腔室注入純水，選取 3 公分厚的物體分別墊高胸腔假體上、下、左及右側，並以臨床使用的影像採集程序分別取像，模擬平躺有困難病人的不同造影姿勢，藉由影像灌注缺損部位觀察心軸偏轉的情形。

結果：在 Xeleris 影像工作站上以臨床參數重建四組不同傾斜姿勢的假體影像，觀察內置於心中膈部位的壓克力塊，於各組影像造成的偏轉情形，其結果可知墊高左及右側胸腔假體，灌注缺損區域仍可正確呈現在心中膈部位，而墊高上及下端胸腔假體的影像、在短軸上的灌注缺損區域則發生偏轉情形，從重組後的極座標圖觀察到，墊高胸腔假體上端將導致影像短軸逆時針方向偏轉，墊高下端則反之，因此可知病人平躺時，當軀幹屈曲或伸展，就會使心軸軸向偏轉，進而影響心肌灌注缺損部位診斷的準確性。

結論：從心假體影像的驗證結果來看，平躺困難的病人當軀幹左或右傾斜時，在影像重組的過程當中，經由調整垂直長軸及水平長軸，可以校正心軸回正確的軸向，不影響短軸影像的呈現，但是當病人因駝背或腰椎受傷而使軀幹屈曲或伸展時，現有心臟影像重組軟體未開放短軸旋轉功能，導致極座標圖及總和壓力分數 (SSS) 計算，或使灌注缺損區域發生偏轉，錯誤映照至標準模板上，進而影響量化數值判定標準；如本院實際案例，62 歲女性患者參照顯現的右心影像，調整短軸角度後，灌注缺損區域由 LCX 35% 轉變爲 RCA 6%，SSS 由調整前 8 分轉變爲 2 分，推測原因可能爲，標準模板上側壁血流灌注較下壁豐富，量化數值的變化程度已足以影響病情診斷，故放射師在執行檢查時，應注意病人是否正確平躺，並適時提醒醫師無法平躺案例短軸偏轉，影響病灶部位判斷及量化數值的可能性。

PB-012

Combining Clinical Information and Myocardial Perfusion Single-Photon Emission Tomography to Predict the Prognosis of Coronary Heart Disease with Big Data and Artificial Intelligence Technology

Cheng-Wen Huang[1], Shau-Syuan Lin[1], Li-Wei Chen[1], Wei-Chieh Huang[1], Chi-Lun Ko[3], Shan-Ying Wang[2], Kuan-Yin Ko[3], Chung-Ming Cheng[1], Yen-Wen Wu[2]

[1]*Department of Biomedical Engineering, National Taiwan University*
[2]*Department of Nuclear Medicine, Far Eastern Memorial Hospital*
[3]*Department of Nuclear Medicine, National Taiwan University Hospital*

Introduction: Myocardial perfusion single-photon emission tomography (SPECT) has gradually become the mainstream for Coronary artery disease (CAD) diagnosis and cardiovascular disease risk estimation. However, the inter-observer-variability of qualitative descriptor, and lack of reliable quantitative approach make it a difficult task to identify CAD in myocardial perfusion imaging (MPI). To overcome the shortage of MPI analysis for CAD diagnosis, we investigated the correlation between MPI and image feature by deep learning (DL) method. Presented the potential of auto-feature-learning by convolutional neural network (CNN) can exceed the expert evaluation based on traditional qualitative analysis for CAD prediction.

Methods: A model was proposed based on CNN to predict CAD in MPI, training with preprocessed rest and stress phase MPI. Data preprocessing step included image alignment between cases for benefiting the feature learning. The performance of the model was evaluated by a 5-fold cross-validation procedure.

Results: Based on 827 samples, the proposed model for LAD, LCX, and RCA prediction achieved an accuracy of 71 ± 2%, 73 ± 4%, and 76 ± 4%, respectively.

Conclusions: Identifying CAD in MPI through deep learning method showed the feasibility of auto-feature-learning by CNN. Overcome the shortages of MPI analysis using traditional qualitative analysis for CAD prediction.

PB-013

The Radiosyntheses of [^{18}F]PSMA-1007 and [^{18}F]Fallypride by Eckert-Ziegler Modular-Lab System

Chi-Wei Chang, Chun-Tse Hung, Geng-Ying Li, Shih-Pei Chen, Wen-Yi Chang, Wen-Sheng Hwang

Department of Nuclear Medicine, National PET/Cyclotron Center, Veterans General Hospital, Taipei, Taiwan

Introduction: [^{18}F]PSMA-1007 imaging agent becomes a new weapon for the diagnosis of prostate cancer. [^{18}F]Fallypride can be used to observe D2 receptors in a range of concentrations, ranging from low corticolar receptors to highly concentrated receptors in putamen, is currently a potential D2/D3 receptor contrast agent for quantitative studies of PET scans. Reliable procedure of [^{18}F]PSMA-1007 and [^{18}F]Fallypride in cGMP conditions was developed by Modular-Lab system.

Methods: For the radiosynthesis, cyclotron-produced [^{18}F]fluoride (^{18}O(p,n)^{18}F) was transferred to the Modular-Lab system and fixed on a QMA cartridge. The activity was eluted from the cartridge with 0.75 ml of 0.075 M aqueous $TBAHCO_3$ solution for [^{18}F]PSMA-1007 and 1.1 mL of a potassium carbonate and Kryptofix for [^{18}F]Fallypride then transferred to the reactor by nitrogen. Both complexes were azeotropically dried at 120°C by addition of 1.6 mL of acetonitrile. After complete drying, PSMA-1007 precursor and Fallypride precursor were added to the reactor for [^{18}F]PSMA-1007 and [^{18}F]Fallypride, respectively and heated at 80°C for 10 min. The above reactions were quenched with specific solutions and then crude products were either injected to HPLC column or passed through some cartridges to remove the chemical and radiochemical impurities. [^{18}F]PSMA-1007 product was eluted with 3 mL of 30% EtOH solution from C18 cartridge and formulated with normal saline (9 mL). [^{18}F]Fallypride product was eluted with ethanol (0.9 mL) from C18 cartridge and formulated with normal saline (9 mL).

Results: The sterile [^{18}F]PSMA-1007 and [^{18}F]Fallypride were produced in 80 min with greater than 99% radiochemical purity. The quality control was in accordance to the guidelines of the European Pharmacopoeia with a mean 24.5% EOS yield and 125 GBq/μmol (n = 2) for [^{18}F]PSMA-1007 and 25% EOS yield and 130 GBq/μmol (n = 3) for [^{18}F]Fallypride.

Conclusions: The routine production of [^{18}F]PSMA-1007 and [^{18}F]Fallypride proved to be reliable and stable. [^{18}F]PSMA-1007 and [^{18}F]Fallypride of the Ph.Eur. quality could be used for clinical study by using PET/MR in the future.

PB-014

Automated Synthesis of [^{18}F]TFAHA in the GMP-Compliant Production

Geng-Ying Li, Chi-Wei Chang, Chun-Tse Hung, Shih-Pei Chen, Wen-Yi Chang, Wen-Sheng Hwang

Department of Nuclear Medicine, National PET/Cyclotron Center, Veterans General Hospital, Taipei, Taiwan

Introduction: Herein, we produced the Good Manufacturing Practice (GMP) compliant automated synthesis of ^{18}F-labeled 6-(tri-fluoroacetamido)-1-hexanoicanilide ([^{18}F]TFAHA), a new tracer different from 6-([^{18}F]fuoroacetamido)-1-hexanoicanilide ([^{18}F]FAHA) as a positron emission tomography (PET) imaging agent for HDAC IIa enzymes, [^{18}F]TFAHA showed significantly higher selectivity for HDAC class IIa enzymes, as compared to the previously reported [^{18}F]FAHA. In the future, the TFAHA may accelerate development of novel HDAC class IIa-specific inhibitors to different disease.

Methods: [^{18}F]TFAHA was prepared from 6-(bromodifluoroacetamido)-1-hexanoicanilide precursor with Eckert-Ziegler Modular-Lab System. [^{18}F]fluoride was produced with a Scanditronix MC17F cyclotron by proton irradiation of 98% enriched [^{18}O]water with 90 μAh beam current integration then transferred to the Modular-Lab system and trapped in a pre-conditioned QMA cartridge. Elution buffer containing 11 mg Kryptofix 2.2.2 and 2.6 mg potassium carbonate in 1.1 ml solution was used to elute the activity into reaction vial then water was evaporated azeotropically to dryness by adding acetonitrile.

After complete drying, 5 mg of the precursor in 0.6 mL of acetonitrile was added to the activated and dried [^{18}F]fluoride/K2.2.2 complex and the reaction vessel was heated at 110°C for 20 min. The reaction was quenched with 2 mL of HPLC M.P. (0.9gNa_2HPO_4/CH_3CN (65/35)) and the crude product was purified by a semi-preparative HPLC column (GRACE VisionHT C18 250 x 10 mm I.D S-5 um, 12 nm) and eluted with a solution of (0.9gNa_2HPO_4/CH_3CN (65/35)) (flow at 3 mL/min). The fraction containing the product was collected and mixed with 40 mL of water. Subsequently, [^{18}F]TFAHA was trapped on a pre-conditioned (10 mL ethanol and 20 mL water) tC18plus SepPak cartridge. The product ([^{18}F]TFAHA) was eluted with ethanol (0.9 mL) and formulated with normal saline (5 mL).

Results: The GMP-Compliant [^{18}F]TFAHA was produced in 100 min, Overall yield was 4.4 ± 0.4% (n = 3) with greater than 99% radiochemical purity.

Conclusions: The automated synthesis production of [^{18}F]TFAHA proved to be reliable and stable. [^{18}F] TFAHA of the cGMP quality could be promoted to clinical study for caner diagnosis in the future.

PB-015

The Radiosynthesis of [^{11}C]SB13 by an Eckert-Ziegler Modular-Lab System

Chun-Tse Hung, Chi-Wei Chang, Geng-Ying Li, Shih-Pei Chen, Wen-Yi Chang, Wen-Sheng Hwang

Department of Nuclear Medicine, National PET/Cyclotron Center, Veterans General Hospital, Taipei, Taiwan

Introduction: [^{11}C]SB13 has been introduced as a highly promising radiotracer for imaging amyloid plaques using positron emission tomography (PET). A large number of [^{11}C]SB13 have been synthesized by an Eckert-Ziegler modular system for animal and clinical PET studies in our center. Reliable synthesis procedure of [^{11}C]SB13 in cGMP conditions was developed to meet clinical demand by Modular-Lab system.

Methods: [^{11}C]CO_2 was produced by irradiating target gas (N_2 + 1% O_2) (5.0 N_2 and 5.0 O_2) at 76 Psi target pressure. Beam current 45 μA and current integration 52 μAh were used for routine production of [^{11}C]SB13. After irradiation, [^{11}C]CO_2 was trapped in an activated charcoal. By heating activated charcoal to 60°C, [^{11}C]CO_2 was released through the hydrogenation tube (620°C, He/10% H_2 flow 150 ml/min) into [^{11}C]CH_4 trap (–10°C). After trapping of [^{11}C]CH_4, the trap was heated to 90°C and the recirculation system was evacuated by a vacuum pump simultaneously. At 60°C, [^{11}C]CH_4 trap was connected to the evacuated recirculation system and [^{11}C]CH_4 was transferred into the recirculation system with a He flow (50 ml/min). The transfer stopped at the pressure of 0.4 bar within the recirculation system and the recirculation started. The temperature of the bromination oven was set at 640°C and 660°C with the interval of 60 sec. The recirculation was stopped when [^{11}C]CH_3Br was fully trapped in [^{11}C]CH_3Br trap. [^{11}C]CH_3Br was released from [^{11}C]CH_3Br trap at 90°C, by He flow (10 ml/min) and passed through AgOTf/carbograph glass tube at 290°C. [^{11}C]CH_3OTf was swept into the HPLC loop coated with precursor solution by a stream of He gas (10 ml/min) at ambient temperature and produced [^{11}C]SB13. When the activity peaked in the loop, the flow of He was stopped and permitted the reaction to proceed for 60s, and then 1.5 ml of HPLC mobile phase (0.01 M H_3PO_4/CH_3CN, 3/2) was filled into the LC sample loop. The mobile phase containing raw [^{11}C]SB13 was injected into the HPLC column (LUNA 5μ C18 250 x 10 mm, Phenomenex). The fraction containing the product was collected and mixed with 40 mL of water. Subsequently, [^{11}C]SB13 was trapped on a pre-conditioned (10 mL ethanol and 20 mL water) tC18plus SepPak cartridge and acetonitrile was washed off by rinsing tC18plus SepPak cartridge with water. The product ([^{11}C]SB13) was eluted with ethanol (0.9 mL) and formulated with normal saline (9 mL).

Results: The sterile [^{11}C]SB13 was produced starting from [^{11}C]CO_2 in accordance with requirements of European Pharmacopoeia in 30 min with greater than 99% radiochemical purity and a mean 5% EOS yield (n = 20).

Conclusions: The production of [^{11}C]SB13 proved to be reliable in more than 180 patient productions. The procedure provides stable radiochemical yields (5% EOS) of [^{11}C]SB13 of the cGMP quality in a short synthesis time (30 min).

PB-016

Explore the dose Linearity and Dead Time of Scintillation Cameras

Tzu-Chi Chang[1,2], Li-Chun Wu[3,C]

[1]*Division of Nuclear Medicine, Department of Medical Image, Chi Mei Medical Center, Liouying, Tainan, Taiwan*
[2]*Department of Medical Imaging and Radiological Sciences, Kaohsiung Medical University*
[3,C]*Division of Nuclear Medicine, Department of Medical Image, Chi Mei Medical Center, Yongkang, Tainan, Taiwan*

Purpose: The pulse count in the random process will inevitably be affected by losses.In the detector system, the two events must be separated in the shortest time so that they can be recorded as two separate independent events.In some cases, the limiting time is determined by processes in the detector itself, but in most cases the limitation comes from related electronic devices. The shortest time interval for correct detection is usually called the resolving time. But if the two signals are too close, the detector cannot detect the signal, which is called dead time. The total dead time of a detection system is the sum of the intrinsic detector dead time (e.g. the drift time in a gas detector) the analog front end losses (e.g. the shaping time of a spectroscopy amplifier etc.) and the data acquisition dead time for example,the conversion time of ADCs (analog-to-digital converter), or the readout and storage times.

Thus, there is a need for correction at three different levels first, for the internal losses inherent in the detector itself, second, for the losses generated by the system circuitry, lastly, for the multichannel analyzer, i.e. the analog to digital conversion and storage.

Method: Different doses of ^{99m}Tc radiopharmaceutical measured by dose calibrator. The dose are 8.7 mCi, 26 mCi, 31.78 mCi, 35 mCi, 66.4 mCi, 73.5 mCi, 83.4 mCi, 84.5 mCi, 126.9 mCi respectively. The counts measured are 33.7k count, 85.5k count, 112k count, 131k count, 197.6k count, 212.2k count, 236.6k count, 248.8k count, 248.6k count respectively.

Results: It can be seen from the table and figure that the higher the dose, the higher the count, but when the dose is as high as 84.5 mCi, the count no longer increases. In addition, the linearity of dose can be seen from the line graph.

Conclusion: It can be seen from the chart that the higher the dose, the higher the count, but when the dose is as high as 84.5 mCi, the count no longer increases. This phenomenon is related to dead time. That is, when there are too many photons at a moment, the instrument cannot effectively distinguish the two signals and record them as two separate events. In addition, the linearity of the dose can be seen from the line graph. the better the linearity, the better the instrument performance.

PB-017

The Assays of Quality Control of [^{18}F]FEPPA in Clinic

Shih-Pei Chen[1,2], Chi-Wei Chang[1,2], Wen-Yi Chang[1,2], Chun-Tse Hung[1,2], Geng-Ying Li[1,2], Wen-Sheng Hwang[1,2]

[1]*Department of Nuclear Medicine, Taipei Veterans General Hospital, Taipei, Taiwan*
[2]*National PET/Cyclotron Center of Taipei Veterans General Hospital, Taipei, Taiwan*

Introduction: [^{18}F]FEPPA was a radiolabeled imaging tracer of positron emission tomography (PET) for the translocator protein of 18 kDa (TSPO) related to the brain disease. [^{18}F]FEPPA (185 MBq, 5 mCi) would not be allowed to use in clinical until cGMP regulation quality control assays passed (sterility test excepted). In stability assay, [^{18}F]FEPPA was highly stable in ethanol/saline (1/10) solution during 6 hours incubation after the end of synthesis.

Methods: [^{18}F]FEPPA had been successfully produced and qualified in seven consecutive batches in clinical. According to the specifications of [^{18}F] radiopharmaceuticals: appearance, pH value, radiochemical purity, specific activity, radionuclide identification, radionuclide purity, color spot test for kryptofix 222, residual solvent, bacterial endotoxin test, integrity test and sterility test were included in the general quality control (QC) assays. Appearance of [^{18}F]FEPPA was evaluated in visual through the lead glass. The assay of pH was determined by pH paper. Radiochemical purity (RCP) and specific activity (SA) were conducted by high performance liquid chromatography (HPLC) equipped with C18 column (4.6 * 100 mm). Radionuclide identification and radionuclide purity were assessed by multi-channel analyzer (MCA). The assay of kryptofix 222 was evaluated by TLC silica gel and iodine vapor. The calculation of residual solvent was conducted by gas chromatography (GC) equipped with capillary column (30 m * 530 μm * 1 μm). The quantitative of endotoxins was performed by PyroGene™ Recombinant Factor C Assay. Filter integrity was assessed by bubble point test. Finally, sterility was evaluated by soybean casein digest (SCD) and fluid TGC medium (FTM).

Results: The average results of QC of seven batches of [^{18}F]FEPPA were as follows: appearances were colorless and clear, pH value was 7.5 ± 0.5, radiochemical purity was greater than 99.9%, mean specific activity was 169 ± 27 GBq/μmol, half-life was 107.8 ± 0.7 minutes, radionuclidic energy was 509.4 ± 1.4 keV, radionuclidic purity was greater than 99.9%, concentration of kryptofix 222 was less than 50 μg/mL, concentration of acetone was 0.0055%, concentration of acetonitrile was 0.0011%, concentration of bacterial endotoxin was less than 1.0 EU/mL, bubble point test was 22 ± 1 psi, and sterility tests were all passed.

Conclusions: The cGMP-grade radio-pharmaceutical [^{18}F]FEPPA could be manufactured successfully and stably in National PET/Cyclotron Center of Taipei Veterans General Hospital. [^{18}F]FEPPA is ready for clinical research of translocator protein-related disease from now on.

PB-018

CA19-9 試劑混合錯誤導致實驗失效之分析檢討

王安美　陳玉蕙　林崇恩

台北馬偕紀念醫院核子醫學科

背景：

放射免疫分析試劑都是原廠套組 (Kit)，內含物包括了一組已知濃度的標準品 (standards)、和內附之品管 (inter kit control)、抗體 (Antibody coated tube)、標誌的 I-125。實驗室有時因檢體量較多，會將多盒 Kit 的內容物例如 I-125 液體物質等，先倒在同一瓶容器中混合，以利實驗之操作。此篇內容是檢討 CA19-9 實驗操作結束後，發現不能建立標準曲線，品管也偏離太大，因此展開疑難排除 (troubleshooting) 做原因分析。原因分析之結果，確認此次事件因人爲疏失，將試劑混合錯誤，導致實驗失敗。此事件也導入實驗室不符合事件，並於品管會議中檢討。

錯誤分析方法：

使用原先可能混合錯誤的試劑與新開封的試劑重做後，比對標準曲線、品管血清之 CPM，並確實點算試劑剩餘數量。

討論：

1. 從數據表一、表二之分析，可以明確查出表一的 standard bound 完全不對，而且 CPM 也沒有區分開，可以直接判定實驗失效因而全部重做。但重做前部份原因尚未釐清。
2. 詢問操作人員因其回答操作沒有問題，所以失效分析以 I-125 崩解爲主軸。
3. 然經品質主管 (組長) 盤查使用後剩餘的試劑量後，發現緩衝液 (buffer) 短缺而 I-125 量卻比較多，因此懷疑試劑被錯誤混合。
4. 爲了確認原因，採取原剩餘的試劑與全新開封的試劑做平行測試，全新開封的試劑測試結果符合標準。最後確認之前的試劑被錯誤混合。

結論：

在檢測實驗室，面對大量檢體工作非常繁忙，實驗前、實驗中、實驗後的每一個程序都非常重要。檢測前試劑的備製須格外小心，應準備的工具、試劑等皆須備妥，才不至於檢測中因加藥過程過於倉促而導致加錯試劑致使實驗失效。嚴重者影響發報告時間，亦影響病患就醫之權利。

PB-019

以 FlexLab 合成模組建立氟 -18 PSMA-1007 自動化合成方法以應用於攝護腺癌造影

詹啓仁[1] 孟凡傑[1] 李銘忻[2] 邱創新[3] 林立凡[1] 薛晴彥[1]

[1] 三軍總醫院正子中心
[2] 核能研究所同位素應用組
[3] 三軍總醫院核子醫學部

背景介紹：依 2018 流行性學調查，攝護腺癌是全球男性罹患率與死亡率第二高的惡性腫瘤，但目前僅有少數正子示蹤劑是針對攝護腺癌，其中 ^{68}Ga-PSMA 是最常見的。相較於 ^{68}Ga，^{18}F 有便利性、產量等優勢，因此許多研究著手發展 ^{18}F-PSMA-1007。^{18}F-PSMA-1007 容易被攝護腺腫瘤細胞攝取，而在泌尿系統的活性較低，成像背景干擾少，因此能夠較好地顯示攝護腺的病變以及攝護腺癌的淋巴結和骨轉移。本研究利用 FlexLab 合成模組建立 ^{18}F-PSMA-1007 自動化合成並執行品質分析，爲往後攝護腺癌診斷提供良好正子造影示蹤劑來源。

方法：使用 IBA 迴旋加速器產出 ^{18}F-，以 $PSHCO_3$ 管柱捕獲 ^{18}F-，接著以 0.65 mL $TBAHCO_3$ 將 ^{18}F- 沖提至反應瓶，加入乙腈 1.5 mL 共沸去除水分後，加入 2 mg 前趨物進行氟化反應，待反應結束後，將反應瓶內的物質傳送通過 PSH++ 與 C18ec 管柱進行純化。先以 13 mL 10% 乙醇沖提純化管柱，再以 10 mL 15% 乙醇沖提以去除副產物，接著以 3.5 mL 40% 乙醇將產物沖提至裝有 13.5 mL 生理食鹽水與 100 mg 維他命 C 混合液的無菌瓶，最後將混合液通過 GV 無菌過濾膜可得最終產品 ^{18}F-PSMA-1007。以液相層析儀分析產品的放射化學純度。

結果：產率 33.6%，放射化學純度 > 98%，合成時間約 50 分鐘。

結論：成功建立以 FlexLab 合成模組完成 ^{18}F-PSMA-1007 自動化合成之方法，可以得到良好的產率與放射化學純度。

PB-020

Validation of Automated Production of [^{18}F]F-PSMA1007 for Patients with Prostate Cancer

Ching-Hung Chiu[1], Chia-Ling Tsai[1], Ya-Yao Huang[1-3], Yu-Ning Chang[1], Ruoh-Fang Yen[1-3]

[1]PET Center, Department of Nuclear Medicine, National Taiwan University Hospital
[2]Institute of Medical Device and Imaging, National Taiwan University College of Medicine
[3]Molecular Imaging Center, National Taiwan University

Introduction: Because the prostate-specific membrane antigen (PSMA) is a key player in prostate carcinogenesis and disease progression, glutamatergic neurotransmission, and folate absorption [1], research collaborators have expressed high interest in [^{18}F]F-PSMA1007 for PET imaging studies. To implement GMP-compliant production in our laboratory (National Taiwan University Hospital, NTUH), an in-house validation of [^{18}F]F-PSMA1007 automated production is required prior to clinical use.

Methods: In this study, [^{18}F]F-PSMA1007 was full-automatic radiosynthesized with a commercial cassette and synthesizer (GE TRACERlab MXFDG). Briefly, 750 μL 0.075 M aqueous $TBAHCO_3$-solution was eluted into the reaction vessel. After drying process, precursor solved in DMSO were added to the reaction vessel for fluorination. When reaction was ended, the mixture was passed through the SPE (PS-H+ and C18ec) for purification. Finally, the product was eluted with EtOH solution into the product vial by passing through a sterile Millex-Cathivex GV 0.22-μm filter and diluted with 15 mL sterile phosphate buffered saline.

Results: The fully automated syntheses of [^{18}F]F-PSMA1007 were successfully validated under GMP conditions, resulting in radiochemical yield of 58 $\pm$ 6% (EOS) within 42 min (n = 3) of synthesis time. Radiochemical purity and specific activity of each batch were $\geqq$ 95% and 1673 $\pm$ 441 GBq/μmol (EOS, n = 3), respectively.

Conclusions: [^{18}F]F-PSMA1007 has been automatically manufactured in the NTUH cleanroom following GMP principles for use in ethics approved research projects. The manufacture of [^{18}F]F-PSMA1007 on the GE Tracerlab MXFDG consistently satisfied the defined acceptance criteria. The work instructions, standard operating procedures, training plan and related documentation developed in-house describes all aspects of [^{18}F]F-PSMA1007 production. Each batch of [^{18}F]F-PSMA1007 will produce sufficient product activity for the anticipated clinical demand. The validation process will supports the clinical use of [^{18}F]F-PSMA1007 at NTUH.

PB-021

Fully Automated GMP Production of [^{68}Ga]Ga-DOTATATE for Somatostatin Receptor Imaging

Yu-Ting Chien[1], Ya-Yao Huang[1-3], Yu-Ning Chang[1], Ming-Hsin Li[4], Shih-Ying Lee[4], Sheng-Nan Lo[4], Ruoh-Fang Yen[1,3]

[1]*PET Center, Department of Nuclear Medicine, National Taiwan University Hospital*
[2]*Institute of Medical Device and Imaging, National Taiwan University College of Medicine*
[3]*Molecular Imaging Center, National Taiwan University*
[4]*Isotope Application Division, Institute of Nuclear Energy Research*

Introduction: [^{68}Ga]Ga-DOTATATE (also known as [^{68}Ga]Ga- DOTA-octreotate) is a somatostatin receptors (SSTr)-specific radiopharmaceuticaland the corresponding monograph has been listed in European Pharmacopeia (EP)[1]. To implement [^{68}Ga]Ga-DOTATATE according to the GMP principles followed in our laboratory (National Taiwan University Hospital, NTUH) and EP specification, the verification is required prior to clinical use. The aim of this study is to setup a full-automated production of GMP-compliant [^{68}Ga]Ga-DOTATATE. Moreover, the complete QC tests of [^{68}Ga]Ga-DOTATATE based on EP monograph is prerequisites for clinical use in ethics approved research projects.

Methods: In this study, [^{68}Ga]Ga- DOTATATE was automated radiosynthesized with a commercial module (Modular-Lab Eazy, Eckert & Ziegler Eurotope GmbH). Briefly, the 5 ml of [^{68}Ga]$GaCl_3$ was eluted out form pharma-grade ^{68}Ge/^{68}Ga generator with 0.1N HCl and was then post-process with a SCX cartridge. Followed by the collection of [^{68}Ga]$GaCl_3$ elute in reaction vial, ^{68}Ga-labelling of DOTATATE acetate was conducted in the buffer mixture at 100°C for 8 minutes. After cooling, the final product was diluted with 5 mL of saline and then was sterilized by filtration through an inline 0.22 μm filter.

Results: The syntheses of [^{68}Ga]Ga-DOTATATE were successfully validated under GMP conditions, resulting in radiochemical yield of 72.5 $\pm$ 2.6% (EOS) within 20 min (n = 3) of synthesis time. Radiochemical purity and specific activity of each batch were $\geqq$ 91% and 810 $\pm$ 134 GBq/μmol, respectively.

Conclusions: In this study, we automatically produced [^{68}Ga]Ga-DOTATATE with GMP compliance. The use of disposable cassette and cartridge purification simplifies the operation and shortens the synthesis time. It will be much benefit to produce qualified [^{68}Ga]Ga-DOTATATE for clinical and pre-clinical use in NTUH.

PB-022

Four-Year Experience of Clinical [^{18}F]T807 Production with TracerLab FxN Module

Ya-Yao Huang[1-3], Chin-Hung Chiu[1], Wei-Hua Kuo[1], Lin-Wei Hsin[1,3-5], Chyng-Yann Shiue[1,3], Ruoh-Fang Yen[1,3]

[1]*PET Center, Department of Nuclear Medicine, National Taiwan University Hospital*
[2]*Institute of Medical Device and Imaging, National Taiwan University College of Medicine*
[3]*Molecular Imaging Center, National Taiwan University*
[4]*Graduate Institute of Pharmaceutical Sciences, National Taiwan University College of Medicine*
[5]*Center for Innovative Therapeutics Discovery, National Taiwan University*

Introduction: [^{18}F]T807 has been proved to be a promising PHF-tau tracer for studying AD in humans. Since April 2016, GMP-compliant automated production of [^{18}F]T807 with FxN module has been well validated and produced [^{18}F]T807 injection has been approved for clinical trial at by TFDA at NTUH. Here we report on our 4 year experience with an automated system for [^{18}F]T807 at NTUH.

Methods: In this study, [^{18}F]T807 has been radiosynthesized based on our reported method with FxN module. Analytic TLC procedure of radiochemical purity was verified in advance and all other QC tests were performed based on [^{18}F]FDG monograph of USP.

Results: Automated production of [^{18}F]T807 were successfully validated under GMP conditions, resulting in radiochemical yield of 6 ± 1% (EOS) within 62 ± 3 min (n = 60, 2016/04~2020/08) of synthesis time. For on-site produced [^{18}F]T807 injection at NTUH, all QC criteria were fully satisfied. Particularly, radiochemical purity of [^{18}F]T807 was 96 ± 2% and residual [^{18}F]Fluoride was 0.9 ± 0.9%.

Conclusions: A 4-year production experiment for clinical study supply showed that our production method of [^{18}F]T807 has the advantages of a high stable production and radiochemical yields for many patients in Taiwan.

PB-023

Whole-Body Biodistribution of [^{18}F]F-PSMA-1007 Via MicroPET/CT Imaging of Mice

Ya-Yao Huang[1-3], Yu-Ning Chang[1], Chi-Han Wu[2], Chia-Ling Tsai[1], Ruoh-Fang Yen[1,3]

[1]*PET Center, Department of Nuclear Medicine, National Taiwan University Hospital*
[2]*Institute of Medical Device and Imaging, National Taiwan University College of Medicine*
[3]*Molecular Imaging Center, National Taiwan University*

Introduction: Because PSMA is a key player in prostate carcinogenesis and disease progression, glutamatergic neurotransmission, and folate absorption, the novel compound [^{18}F]F-PSMA-1007 was developed with mimic structural modification and similar clearance kinetics compared to [^{177}Lu]Lu-PSMA-617. For the optimal strategy of molecular PET imaging for patients with prostate cancer, [^{18}F]F-PSMA-1007 has been successfully implemented at NTUH. In order to fit possible preclinical and clinical application, this study aims to evaluate whole-body biodistribution of [^{18}F]F-PSMA1007 in normal mice via microPET imaging.

Method: [^{18}F]F-PSMA1007 was synthesized by the reported method. For animal study, male ICR mice (20–30g) were used in this study and then injected with a bolus of about 150~300 μCi (n = 3) of each tracer before scanning. By using small-animal Argus PET/CT scanner, dynamic sinograms were produced for 90 min with 2 x 10 sec, 2 x 20 sec, 4 x 60 sec, 2 x 240 sec, 2 x 600 sec, 1 x 720 sec frames. VOIs were defined on co-registrated PET/CT images according to evident tracer accumulation in the area of the liver and data was expressed as standard uptake value (SUV).

Results: None of mouse developed adverse events or preclinically detectable pharmacological effects during scanning period. Prominent uptake of kidneys and bladder were seen in [^{18}F]FPSMA-1007 and it indicated primary elimination via urinary system. However, the uptake of [^{18}F]FPSMA-1007 in eyes and lymph nodes of mice were also seen.

Conclusions: Preclinical data from this study will be able to be used as a supporting evidence for safety and pharmacokinetics of in-site produced [^{18}F]FPSMA-1007 at NTUH.

PB-024

Whole-Body Biodistribution of [^{68}Ga]Ga-DOTA-TATE Via MicroPET/CT Imaging of Mice

Ya-Yao Huang[1-3], Yu-Ting Chien[1], Yu-Ning Chang[1], Chi-Han Wu[2], Shih-Ying Lee[4], Sheng-Nan Lo[4], Ming-Hsin Li[4], Ruoh-Fang Yen[1,3]

[1]PET Center, Department of Nuclear Medicine, National Taiwan University Hospital
[2]Institute of Medical Device and Imaging, National Taiwan University College of Medicine
[3]Molecular Imaging Center, National Taiwan University
[4]Isotope Application Division, Institute of Nuclear Energy Research

Introduction: With clinical implementation of "Theranostic" concept and successful development of ^{68}Ge/^{68}Ga generator system, more and more ^{68}Ga-radiopharmaceuticals have been paid attention recently, such as [^{68}Ga]Ga-DOTA-TOC and [^{68}Ga]Ga-DOTA-TATE for targeting somatostatin receptors (SSTr). In addition to [^{68}Ga]Ga-DOTA-TOC, [^{68}Ga]Ga-DOTA-TATE has been successfully implemented at NTUH recently for the optimal theranostic strategy of patients with SSTr-expressed neuroendocrine tumors. In order to fit possible preclinical and clinical application, this study aims to evaluate whole-body biodistribution of [^{68}Ga]Ga-DOTA-TATE in normal mice via microPET imaging.

Method: [^{68}Ga]Ga-DOTA-TATE was automatically synthesized by the reported method with some modifications. For animal study, male ICR mice (20–30g) were used in this study and then injected with a bolus of about 150~300 μCi (n = 3) of each tracer before scanning. By using small-animal Argus PET/CT scanner, dynamic sinograms were produced for 90 min with 2 x 10 sec, 2 x 20 sec, 4 x 60 sec, 2 x 240 sec, 2 x 600 sec, 1 x 720 sec frames. VOIs were defined on co-registrated PET/CT images according to evident tracer accumulation in the area of the liver and data was expressed as standard uptake value (SUV).

Results: None of mouse developed adverse events or preclinically detectable pharmacological effects during scanning. Similar to the uptake profiles of [^{68}Ga]Ga-DOTA-TOC, prominent uptake of kidneys and bladder of mice were seen in [^{68}Ga]Ga-DOTA-TATE and it indicated primary elimination via urinary system.

Conclusions: Preclinical data from this study will be able to used as a supporting evidence for safety and pharmacokinetics of in-site produced [^{68}Ga]Ga-DOTA-TATE at NTUH.

PB-025

Whole-Body Biodistribution of [^{68}F]Ga-MAA Via MicroPET/CT Imaging of Mice

Ya-Yao Huang[1-3], Yu-Ning Chang[1], Chi-Han Wu[2], Ching-Hung Chiu[1], Chi-Lun Ko[1], Ruoh-Fang Yen[1,3]

[1]PET Center, Department of Nuclear Medicine, National Taiwan University Hospital
[2]Institute of Medical Device and Imaging, National Taiwan University College of Medicine
[3]Molecular Imaging Center, National Taiwan University

Introduction: For pulmonary perfusion imaging agent, [^{99m}Tc]macroaggregated albumin ([^{99m}Tc]MAA) SPECT imaging has been used in clinic for a long time. Recently, [^{68}Ga]MAA has been developed for PET/CT imaging in terms of sensitivity, resolution and quantification. For the optimal strategy of molecular PET imaging for pre-clinical and clinical studies of this tracer at NTUH, whole-body biodistribution of [^{68}Ga]MAA was evaluated based on mice via microPET imaging.

Method: [^{68}Ga]MAA was synthesized by the reported method. For animal study, male ICR mice (20–30g) were used in this study and then injected with a bolus of about 150~300 μCi (n = 3) of each tracer before scanning. By using small-animal Argus PET/CT scanner, dynamic sinograms were produced for 90 min with 2 x 10 sec, 2 x 20 sec, 4 x 60 sec, 2 x 240 sec, 2 x 600 sec, 1 x 720 sec frames. VOIs were defined on co-registrated PET/CT images according to evident tracer accumulation in the area of the liver and data was expressed as standard uptake value (SUV).

Results: None of mouse developed adverse events or preclinically detectable pharmacological effects, however appropriate dilution of such [^{68}Ga]MAA injection is necessary for mice. Similar to previous report, prominent uptake of lungs were significantly seen in [^{68}Ga]MAA.

Conclusions: Preclinical data from this study will be able to be used as a supporting evidence for safety and pharmacokinetics of in-site produced [^{68}Ga]MAA at NTUH.

PB-026

First Experience of Automated Production of [^{18}F]FDOPA with Commercial FASTlab-2 Module and Developer Platform

Ya-Yao Huang[1-3], Chia-Ling Tsai[1], Ching-Hung Chiu[1], Yu-Ting Chien[1], Hsiang-Ping Wen[1], Wei-Hua Kuo[1], Yu-Ning Chang[1], Ruoh-Fang Yen[1,3]

[1]PET Center, Department of Nuclear Medicine, National Taiwan University Hospital
[2]Institute of Medical Device and Imaging, National Taiwan University College of Medicine
[3]Molecular Imaging Center, National Taiwan University

Introduction: With the increasing clinical need for [^{18}F]FDOPA in both oncology and neurology, the aim of this study was to present the experience about automated [^{18}F]FDOPA production using FASTlab-2 module and FASTlab Developer platform.

Method: In this study, [^{18}F]FDOPA will be radiosynthesized with a cassette-type FASTlab module based on Martin's method. Briefly, radiofluorination of (S)-N-Trityl-5-formyl-4-methoxy -methylene-2-nitro-phenyl-alanine tert-butyl ester with [^{18}F]TBAF in DMSO at 130°C for ~8 min followed by trapped on C18ec SPE cartridge and oxidized with m-CPBA at 55-65°C for 16 min, then hydrolyzed with 30%HCl/EtOH at 50°C for 20 min. The mixture was diluted with phosphate buffer and then passed through HR-P and Plus C18 SPE cartridges. Further the mixture was passed through WAX and Al-N light SPE cartrige and [^{18}F]FDOPA was produced. After re-formulation and sterile filtration, [^{18}F]FDOPA injection was obtained and was ready for following QC tests. Afterwards, the final product was diluted with saline and then was sterilized by filtration through an inline 0.22 μm filter.

Results: After a series of setup of FASTlab Developer platform and commercial cassette/reagent kits, related standard operation procedure has been finished. Preliminary successful results from the cold run of [^{18}F] FDOPA has been successfully completed and following hot runs are on-going at NTUH.

Conclusion: We have successfully setup the procedure for [^{18}F]FDOPA production with newly developed pharmaceutical grade cassette/reagent kits and FASTlab-2 module. Such production procedure will be beneficial to the clinical use of [^{18}F]FDOPA in Taiwan.

PB-027

Automated Synthesis of [^{18}F]-MK-6240 Analog as a Tau Imaging Agent

Ta-Kai Chou[1], Yun-Ting Jhao[2], Ming-Hsin Li[3], Chuang-Hsin Chiu[4], Li-Fan Lin[1], Chyng-Yann Shiue[1]

[1]PET Center, Department of Nuclear Medicine, Tri-Service General Hospital, National Defense Medical Center, Taipei, Taiwan
[2]Department of Biology and Anatomy, National Defense Medical Center, Taipei, Taiwan
[3]Isotope Application Division, Institute of Nuclear Energy Research, Taoyuan, Taiwan
[4]Department of Nuclear Medicine, Tri-Service General Hospital, National Defense Medical Center, Taipei, Taiwan

Introduction: Neurofibrillary tangles (NFTs) are aggregation of hyperphosphorylated tau protein, one of the pathological hallmarks of Alzheimer's disease. [^{18}F]-MK-6240 is a highly selective second generation PET tracer for NFTs imaging with low off-target binding. In order to improve its lipophilicity and brain uptake, we have synthesized one of its analogs, [^{18}F]-1 with a commercialized GE TRACERlab FX2 N module and reported herein of our preliminary results.

Methods: [^{18}F]-1 was prepared with a GE TRACERlab FX2 N module by the reaction of tosylate precursor 1 in anhydrous DMF with K[^{18}F]/Kryptofix$_{2.2.2}$ at 140°C for 5 minutes followed by dilution and purification with semi-preparative HPLC (column: Phenomenex Luna C18(2), 5 μm, 250 x 10 mm, mobile phase: 80% ACN and 20% 20 mM sodium phosphate, flow rate: 5 mL/min) and solid phase extraction to give [^{18}F]-1 (Scheme 1).

Results: The radiochemical yield (EOS) of [^{18}F]-1 was 3.6% (n = 1) with radiochemical purity > 98%. The synthesis time including HPLC purification and formulation was about 55 minutes from EOB.

Conclusions: [^{18}F]-1, an analog of [^{18}F]-MK-6240 with potentially higher uptake in brain was synthesized using a commercialized GE TRACElab FX2 N module in 3.6% yield in a synthesis time of 55 minutes from EOB. The evaluations of [^{18}F]-1 as a Tau imaging agent are ongoing.

PB-028

在西門子工作站處理右位心合併內臟反位的心肌血流灌注造影：假體實驗及案例經驗分享

蘇詩琪[1] 郭建瑋[1,2]

[1] 高雄榮民總醫院核子醫學科
[2] 高雄醫學大學醫學影像暨放射科學系

背景介紹：由於右位心合併內臟反位 (Dextrocardia with Situs Inversus) 的心臟方位與一般人剛好呈現鏡像，不僅造影及後處理影像參數需要調整，重組後影像因外壁 (lateral wall) 及側壁 (septal wall) 對調而無法直接套用 QPS 做量化分析。回顧文獻發現數篇文章描述如何利用 GE 的工作站將影像鏡像成一般人的方位並套用 QPS 分析，然而沒有討論西門子的文章。本研究利用心臟假體實驗以及一名病患，找出西門子工作站處理右位心的方法，並讓影像可以套用 QPS 做量化分析。

方法：在心臟假體的心肌上壁及下壁分別設置一塊灌流缺損區域，注入 free Tc 並確保無氣泡及滲漏，另外在側壁貼上微弱點射源。收集影像角度從左斜前 45 度順時針到右斜後 45 度 (LAO 45° → RPO 45°，CW)，重組影像的起始角度設定爲 –45 度。重組後影像呈現外壁 (lateral wall) 及側壁 (septal wall) 對調，經過鏡像處理後才能按照一般人的方位做 QPS 分析。另外在一實際病患依照上述設定造影及後處理。

結果：在假體實驗及實際病患應用中，若重組影像沒有經過鏡像處理，外壁與側壁將會呈現對調。一般會在二次截圖上做適當記號，讓判讀者不會誤認。將重組影像經過鏡像處理後，心臟方位與一般人相同，則可以適當的套用 QPS 分析。

結論：由於西門子工作站的 QPS 分析工具不提供右位心的選項，需在 workflow 中添加額外設定，將重組影像做鏡像處理，才能正確套用 QPS 分析。然而本院工作站內的正常人資料庫 (normal database) 均來自正常左位心 (levocardia) 的受檢者，未來可考慮收集更多無心肌灌流受損的右位心病患來建立右位心的資料庫，並進一步分析右位心與左位心的正常人資料庫是否有不同。

PB-029

甲狀腺攝取計數儀每日品質保證程序增加卡方檢定項目之研究

卓世傑[1] 賴法文[2] 鄭揚霖[1] 張南雄[1] 林凡珍[1] 陳興隆[1] 顏玉安[1] 李將瑄[1]

[1]奇美醫療財團法人奇美醫院核子醫學科
[2]奇美醫療財團法人奇美醫院醫工組

背景介紹：

甲狀腺攝取計數儀，是核子醫學部門常見的儀器之一，主要使用於病人甲狀腺攝取率的檢查。一般在使用前，均需使用標準射源或內部程式進行必要之品質保證程序，以確保儀器計數值之準確與穩定。而常見的每日品質保證程序通常均可自動校準 (Auto Calibration)，內容包括，高壓、增益 (Gain) 和零偏移 (Zero Offset) 的調整，能峰線性校正 (Liner)，全寬半高 (FWHM) 值計算及穩定性測試 (Constancy Test)。但本研究發現，即使每日品質保證程序達到儀器要求的標準範圍之內，其後續的計數值仍不穩定，而有相當大之落差。本研究的結果即認爲每日品質保證程序完成後，應增加非每日品保項目之卡方檢定測試 (Chi-square Test)，以觀察儀器之計數值是否穩定，並可提供計數誤差比例值以爲臨床參考。

方法：

1. 以 Capintec, Inc. 公司生產之 CAPTUS 3000 型，甲狀腺攝取計數儀，及 Eckert & Ziegler 公司生產之 GF-0008 型，Cs-137 射源以及 GF-0009 型，Eu-152 射源執行每日品保項目之自動校準及穩定性測試合格後，記錄相關數據。
2. 每日品保項目合格後，執行 3 次卡方檢定 (計數 10 次，每次 1 分鐘)，並記錄各次計數值數據。
3. 整理、統計前 2 項數據，以提出結果。

結果：

1. 以 36 日，每日 3 次，共 108 筆卡方檢定中，合格筆數爲 22 筆，比率爲 20.4%，且無連續 3 筆均合格之情形。
2. 調整次數 (Iteration)、全寬半高值及穩定性測試的結果值，與 3 次卡方檢定的相關係數均不顯著。相關係數最高的是穩定性測試與第 3 次卡方檢定的 –0.51，最低的則是穩定性測試和第 2 次卡方檢定的 0.03 (詳見表一)。
3. 卡方檢定值的 10 次數值中，最大與最小數值差距佔最小數值的比例，其第一、二、三次的平均值，分別爲 5.38%、6.46% 與 12.02% (詳見表二)。

結論：

本研究發現：

1. 每日品質保證程序執行後，即使其全寬半高值及穩定性測試均達到儀器要求的標準範圍之內，但之後進行的卡方檢定測試，均無三次皆合格之情形。顯示每日品保程序合格後，儀器之計數值仍可能不穩定。
2. 每次卡方檢定之最大與最小數值差距佔最小數值的比例，其第一次、第二次與第三次之平均值，分別

爲 5.38%、6.46% 與 12.02%。表示實際計數值之平均誤差比例值可能爲 5.38% 至 12.02%。

3. 依據以上的研究發現，由於每日品質保證程序合格後，計數值仍不穩定。

因此甲狀腺攝取計數儀每日品質程序，應增加卡方檢定項目，以觀察儀器之計數值是否穩定，並可提供計數誤差比例值以爲臨床參考。

PB-030

以人員劑量計偵測值監控核醫游離輻射作業環境評估 — 以南部某醫院爲例

陳素英[1] 卓世傑[2] 蕭莉茹[1] 陳宜伶[1] 林秋美[1] 古琴鳳[1]
陳怡如[1] 曾翠芬[1] 劉怡慶[1] 林家揚[1] 張晉銓[1]

[1] 高雄醫學大學附設醫院
[2] 奇美醫院

前言：

爲監控核醫游離輻射作業環境，利用人員劑量佩章度量評估其所接受的輻射劑量，以確保輻射工作人員與相關工作人員及病人與陪伴家屬的輻射安全。

方法：

爲監控輻射作業環境，依取樣時間分 2 個階段：第一、108-1~108-11 爲無劑量計監控階段，第二、108-12~109-7 有劑量計監控階段；設定 4 個關鍵位置，分別：a. 檔案室 (樓上造影室廁所)、b. 學生實習室 (樓上造影儀器)、c. 櫃台登記區、d. 病人等候區，各放置一個人員劑量計；各區檢查月平均使用人數；各區月累積平均劑量紀錄等。使用人員劑量計爲 Panasonic TLD，每月月初更換一次，每月提供輻射劑量紀錄，輻射劑量紀錄已扣除背景值。

結果：

監控期間紀錄：

第一、108-1~108-11 無劑量計階段：檢查月平均使用人數 a. 檔案室 1152.91±151.55 人；b. 學生實習室 73.36±28.93 人；c. 櫃台登記區 1152.91±151.55 人；d. 病人等候區 576.46±75.78 人。

第二、108-12~109-7 有劑量計階段：檢查月平均使用人數 a. 檔案室 1242.25±135.11 人、其月累積平均劑量 0.09±0.03 mSv；b. 學生實習室 92.00±21.71 人、其月累積平均劑量 0.08±0.02 mSv；c. 櫃台登記區 1242.25±135.11 人、其月累積平均劑量 0.11±0.04 mSv；d. 病人等候區 621.13±67.56 人、其月累積平均劑量 0.12±0.02 mSv。

結論：

此研究爲確保輻射工作人員與相關工作人員的輻射安全進行監控本單位輻射作業環境，分有兩個階段 (第一階段無劑量計監控、第二階段爲有劑量計監控)；設定 4 個關鍵位置；月累積平均劑量等。經研究發現，第二階段檢查月平均使用人數多於第一階段。第二階段所設置 4 個關鍵位置其最高月累積平均劑量紀錄爲 0.12 mSv，如以一般人之年劑量限度 1 mSv 爲標準，計算出可在待此輻射作業環境長達 1,389 小時。實際上這 4 個關鍵位置，對輻射工作人員與相關工作人員及病人與陪伴家屬所使用時間並不長，於是推估本單位輻射作業環境相對是安全的。

PB-031

18F-FDG PET/CT 在自發性黑色素瘤動物模型的應用

楊邦宏 [1,2] 陳冠名 [2,3] 許志全 [2] 吳東信 [2]

[1] 臺北榮民總醫院核子醫學部
[2] 國立陽明大學生物醫學影像暨放射科學系
[3] 國立陽明大學生物醫學暨工程科技產業博士學位學程

背景介紹：人類與犬類罹患的黑色素瘤同樣起源於黑色素細胞 melanocytes，且在兩個物種間都是屬於高侵襲性的皮膚癌。在健康一體 (one health) 的原則下，本研究使用自發性罹患黑色素瘤的寵物犬做爲動物模型，透過人類醫學在 18F-FDG PET/CT 經驗完成黑色素瘤在跨物種的影像定量，同時提供犬類黑色素瘤患者在疾病分期、評估治療反應全新的決策模式。

方法：本研究回溯性蒐集三例 (治療前) 及其中一例 (治療後 3 個月) 確診黑色素瘤寵物犬的 18F-FDG 影像。18F-FDG 的劑量配置原則是依據體重進行比例上的調整 (0.2 mCi/kg)。注射 18F-FDG 到 PET/CT 造影前的平均攝取時間爲 60 ± 5 min。影像定量工作站爲 Xeleris 4.0 Workstation (GE Medical System)，統一使用 axial plane 進行感興趣區域圈選。

結果：所有罹患黑色素瘤的案例，除了在原發部位有攝取 18F-FDG 的情形外，在肺臟、淋巴結等處也都發現有異常的熱點。影像定量結果顯示，黑色素瘤原發部位的平均 SUV (SUV_{mean}) 爲 9.17±0.91。其中一例治療後 3 個月黑色素瘤原發部位有明顯縮小的趨勢且量化吸收 18F-FDG 的數值相較於治療前也有明顯的下降 (SUV_{mean}: 5.26±0.93 vs. 10.25±1.1)。

結論：人類與寵物動物長期生活在同樣環境，其中寵物犬在許多癌症表現上都與人類極爲相似 (例如：黑色素瘤)，爲人類研究癌症的理想動物模型。本研究說明了黑色素瘤在跨物種間具有相同的轉移路徑，成功地完成 18F-FDG 應用於自發性罹患黑色素瘤的寵物犬進行定性與定量之評估。

PB-032

Preliminary Results of Constructing and Using Artificial Intelligence by Convolution Neural Network for Diagnosing Bone Scan Images

Yu-Chien Shiau, Chao-Chun Huang, Po-Wei Li, Fang-Shin Liu, Yen-Wen Wu, Shan-Ying Wang

Division of Nuclear Medicine, Far Eastern Memorial Hospital, New Taipei, Taiwan

Introduction: Artificial intelligence was proposed quite long ago around 1955, but its application was not well established until the progress of hardware and software. The introduction of convolution neural network (CNN) with appropriate hardware and software around 2004 made it more successful and more applications such as image recognition, and drew a lot of social attention. The term "Deep Learning" and "Artificial Intelligence" is then getting very popular. We made research and try hard to construct artificial intelligence by convolution neural network for the diagnosis of Tc-99m MDP bone scan images.

Methods: Since Dec 23, 2019, we collect retrospectively 50 bone scans randomly. Bone scans were done with Tc-99m MDP whole body images and acquiring anterior and posterior views. The diagnoses of the bone scans were divided into two groups: (1) normal or degenerative disease and (2) bone metastases. Two experienced nuclear physicians made the diagnoses for all images. The case number of group one was randomly selected to be 39, and group two was 11. We constructed software for convolution neural network in two different platforms: one system in Ubuntu 18.04.4, Python 3.7.6, TensorFlow 2.1.0, and Keras 2.3.1; and another in Windows 10 and GNU Octave 5.2.0. Posterior images were exported by the "interfile" interface. Twenty eight bone scan images were used as training data, and other 22 images were tested by the convolution neural network. The preliminary results of sensitivity, specificity, and accuracy were calculated.

Results: The preliminary results of diagnosing accuracy is 86.4%. The detailed results of sensitivity, specificity, and accuracy will be posted in the poster.

Conclusions: The preliminary results look promising. Artificial intelligence by convolution neural network for the diagnosis of Tc-99m MDP bone scan images will be valuable to help nuclear clinicians to make more efficient and more accurate diagnoses. The future development should be wonderful.

PB-033

The Effect of SGLT2 Inhibitor on Myocardial Glucose Metabolism in APOE Knockout Mice Model using Small-Animal Dynamic PET Imaging

Kuan-Yin Ko[1-2], Yen-Wen Wu[3-4], Wen-Pin Chen[5]

[1]*Department of Nuclear Medicine, National Taiwan University Cancer Center, Taipei, Taiwan*
[2]*Graduate institute of Clinical Medicine, College of Medicine, National Taiwan University, Taipei, Taiwan Department of*
[3]*Nuclear Medicine, Division of*
[4]*Cardiology, Cardiovascular Medical Center, Far Eastern Memorial Hospital, New Taipei City, Taiwan*
[5]*Institute of Pharmacology, College of Medicine, National Taiwan University, Taipei, Taiwan*

Introduction: The goal of the study is to longitudinally evaluate the myocardial glucose utilization in atherosclerosis mice model and figure out the cardiometabolic effect of SGLT2 inhibitor by non-invasive in vivo imaging.

Methods: The male atherosclerosis-prone apolipoprotein E-deficient (Apoe-/-) mice (APOE KO, n = 5) and male wild-type C57BL mice (C57BL/6JNarl, n = 5) were evaluated from 8 to 24 week age in 4 week interval. The animals on isoflurane-anesthetized were imaged by using dynamic PET for 90 minutes after intraperitoneal injection of ^{18}F-FDG. All mice were kept fasting overnight, and blood samples were collected before the scan. The ^{18}F-FDG uptake constant Ki and metabolic rate of glucose (MRGlu) were derived by Patlak plot analyses. The SGLT2 inhibitor, empagliflozin with mimicking human dosage (25 mg/day) or DMSO as control was given through mini-pump implantation. Mean left ventricular ejection fraction (LVEF), end-diastolic and end-systolic dimensions were obtained from M mode in the mid-left ventricular line after repeated measurement for 3 times.

Results: In APOE KO mice, plasma glucose, insulin, HOMA-IR index, LDL, TG and FFA levels were higher than controls ($P < 0.05$). Myocardial glucose utilization of untreated APOE KO mice increased gradually but then started to decrease at 16 week-age. However, the myocardium of control mice showed relatively steady use of glucose. APOE KO mice had higher myocardial uptake of ^{18}F-FDG than C57BL mice, most obviously at 16 week-age ($P < 0.05$). At the end of the 42-day treatment of SGLT2 inhibitor since 16 week-age, the intervention group (APOE KO with empagliflozin) had significantly lower MRGlu values than the control group (APOE KO with DMSO). No significant change of LV structure and systolic function was observed neither in untreated/treated APOE nor wild-type mice.

Conclusions: Preceding the change of LV structure and systolic function, the APOE KO mice exhibited alterations in myocardial glucose metabolism by increased glucose metabolic rate with high plasma glucose, insulin resistance and lipid profiles as compared with the wild-type mice. In addition, the preliminary result showed the cardiac fuel energetic effect of SGLT2 inhibitor on the atherosclerosis mice model.

PB-034

Simulation of a CZT Detector for Gallium-67 Imaging

Sin-Di Lee[1], Hsin-Hon Lin[2,3], Nan-Jing Peng[1,4]

[1]*Department of Nuclear Medicine, Kaohsiung Veterans General Hospital, Kaohsiung, Taiwan*
[2]*Medical Physics Research Center, Institute for Radiological Research, Chang Gung University/Chang Gung Memorial Hospital, Taoyuan, Taiwan*
[3]*Department of Radiation Oncology, Chang Gung Memorial Hospital, Tao-Yuan, Taiwan*
[4]*National Yang-Ming University, Taipei, Taiwan*

Introduction: Cadmium Zinc Telluride (CZT) is an emerging material of gamma detector. In comparison with the NaI scintillation detector, it has the characteristic of better energy resolution and spectrum resolution. However, the imaging performance on gallium-67 imaging was not well evaluated yet. GATE (GEANT4 application for tomographic emission) is the unique integrating software platform allowing for the in-silico simulation of medical imaging. This work describes the GATE simulation of gallium-67 imaging on the geometric architecture of the Siemens Symbia model and compares the performance of the traditional NaI detector.

Methods: Our gamma camera simulation model consists of a gamma camera detector comprises a medium energy collimator (hole diameter: 2.94 mm, collimator thickness: 40.64 mm and septal thickness: 1.14 mm), a 1.59 cm thick NaI crystal, a 6.5 cm thick back-compartment, and a 0.95 cm thick back lead shielding and 1.27 side shielding as per the vendor's specifications. We simulated another model with the same geometric design, except the crystal was replaced by CZT. The point spread functions of a Ga-67 point source were measured. The images were processed into the same matrix size (512 × 512). The system sensitivity was obtained. The spatial resolution was obtained as the full width at half maximum (FWHM) and the full width at tenth maximum (FWTM) along the x-axis and the y-axis.

Results: In our simulation, the sensitivity and spatial resolution (FWHM and FWTM) show good agreement between NaI detector and CZT detector.

Conclusion: In the setting of the same geometric architecture design, the CZT detector has non-inferior image performance than NaI detector.

PB-035

使用擬人假體進行心肌灌流單光子電腦斷層影像量化與重建方法的評估

鄭如金[1] 虞晁岳[2] 楊鶴廷[1] 朱麗蓉[1] 王淑芳[1] 陳世欣[1] 蘇子佩[1*] 林信宏[2]

[1] 基隆長庚醫院核子醫學科
[2] 長庚大學放射醫學研究院

Introduction: 冠狀動脈疾病爲全球排名第一的死亡主因。心肌灌流單光子電腦斷層造影 (Single Photon Emission Tomography, SPECT) 是目前協助冠狀動脈疾病診斷及預後評估的一項重要的工具。本研究主要目的爲評估目前商用 SPECT/CT 儀器中所提供的影樣重建方法及不同量化修正法對於心肌灌流影像重建品質的影響。

Methods: 本研究採用基隆長庚核醫科的 SPECT/CT 儀器 (Semiens Symbia Intevo Excel) 爲主要研究工具。爲了精確評估影像重建和量化的影響，我們使用一擬人胸腔假體 (Data Spectrum)，分別模擬 ^{99m}Tc-MIBI 或 ^{201}Tl-chloride 兩種心肌造影藥物器官比例分布進行造影。儀器掃描參數採用臨床心肌掃描程序 (雙探頭 90 度夾角，掃描 180 度，投影影像大小爲 64 x 64)。除主能窗外我們也額外增加高低的散射能窗，以評估能窗散射修正的效果。重建方法使用目前商用軟體所提供的四種重建方法 (FBP、Wallis、OSEM 2D、Flash 3D) 進行評估。最後我們將對於有 / 無散射修正、有 / 無 CT 衰減修正、以及不同影像重建方法等各項影像參數條件進行系統性的影像評估。

Results: 在不同重建方法的比較上，若無進行 CT 掃描的情況下 (無 CT 衰減修正)，Wallis 重建法相較其他重建法具有較佳的影像對比，更能分辨出心臟缺損的區域。在有 CT 掃描輔助下，Wallis 和 Flash 3D 具有較佳的影像表現，但兩者並無顯著差異。但值得強調的是，有 CT 輔助下的重建影像整體而言所有影像都具有較佳的影像品質。而對於散射修正後影像，無論使用何種方法重建，皆能夠有效降低背景區域的活度。

Conclusions: 本研究建議在無 CT 掃描下，可使用 Wallis 重建方法來達到較佳的影像表現。更進一步地，在可允許的低劑量風險下，額外的 CT 影像將能可進一步提升整體心肌灌流影像的品質。

PB-036

Effects of Potassium Iodide on Thyroid Function- A Rat Observation

Yu-An Chen[1,2], San-Fan Yao[1], Chien-Hsin Ting[1], Wen Sheng Huang[1]

[1]*Departments of Nuclear Medicine/National PET & Cyclotron Center, Taipei Veterans General Hospital, Taipei*
[2]*Department of Health and Leisure Management, YuanPei University of Medical Technology, Hsinchu*

Introduction: Potassium iodide (KI) has been widely used in prophylaxis of radioiodide thyroid uptake or control of thyroidal hyperactivity in nuclear accidents or medical applications. We observed the effects of KI ingestion on changes of rat thyroid function.

Methods: Nine 6 wks' male SD rats around 200 g in body weight were obtained from the BioLASCO. They were randomly divided into 3 treatment groups: controls (NC), low KI dosage (L-KI) and high KI dosage (H-KI), n = 3 each. Except for regular feedings, L-KI and H-KI groups were treated 167 and 500 μg KI/kg for 1 wk and blood tests for T3, T4, TSH and anti-TPO were done 1 wk after stopping feeding of KI.

Results: As compared to the controls, significant decrease of serum T4 values were noted in both low and high KI groups (6.92 ± 0.58 vs. 4.52 ± 0.19 vs. 5.16 ± 0.36 μg/dL, $p < 0.05$). No significant changes of serum T3, TSH and anti-TPO were noted among groups. Both KI treated groups were not unusual in serum T3, T4 and TSH except a significantly slow return of T3 in high KI group (53.33 ± 1.53 vs. 49.33 ± 1.53 ng/dL, $p < 0.05$).

Conclusions: Our preliminary data indicated that short-term administration of KI might only temporary reduced T4 levels. The decreased T3 level in the high KI group 1 wk after discontinuing KI deserves further clarification.

PB-037

To Compare Image Quality of SiPM-Based and Conventional PMT-Based PET Scanners with OSEM and BSREM Reconstruction Algorithms

Min-Tzu Ku[1,3], Yi-Lun Chen[2], Bang-Hung Yang[2,3], Wen-Sheng Huang[2], Ren-Shyan Liu[1,2,3*]

[1]*Xi-Yun PET Center and Department of Nuclear Medicine, Cheng Hsin General Hospital, Taipei, Taiwan*
[2]*National PET/Cyclotron Center and Department of Nuclear Medicine, Taipei Veterans General Hospital, Taipei, Taiwan*
[3]*Department of Biomedical Imaging and Radiological Science, National Yang-Ming University, Taipei, Taiwan*

Introduction: Digital PET scanner using silicon photomultiplier is considered to have higher detection capability than analog PET. In addition, a novel PET reconstruction algorithm BSREM (Q.Clear®, GE Healthcare, Waukesha, WI) controls signal at higher levels while mitigating noise amplification, correcting the problem that standard OSEM reconstruction algorithm always have. In this study, we compared maximum standard uptake value (SUV_{max}), image quality and signal-to-noise ratio (SNR) between digital and analog PET scanners with standard OSEM and BSREM reconstruction.

Methods: The ACR phantom was scanned on GE Discovery MI (digital PET/CT), Discovery MIDR (analog PET/CT) and SIGNA (digital PET/MRI) using a standard 4 minutes long acquisition protocol. According to ACR Nuclear Medicine Accreditation Program, we generated the 2.5 concentration ratio to fill the phantom. The phantom scan was obtained for 1 hour. The standard OSEM algorithm is available on the scanners with 3 iterations and 16 subsets for Discovery MI, 2 iterations and 24 subsets for Discovery MIDR, and 2 iterations and 28 subsets for SIGNA. All of them used 5.0 mm filter. The BSREM algorithm with 25 iterations and different regularization strength parameters (β value between 200 and 850) without any filter was applied. AW sever was used for data analysis.

Results: The SUVmax measured in Discovery MI and SIGNA are distinctly higher than Discovery MIDR and is independent of lesion size. The BSREM images show better quality with low noise than standard OSEM in three PET scanners. BSREM also enhances SUV_{max}, particularly in small lesion. Moreover, the SNR show the same situation, too. The BSREM algorithm regularization strength parameters (β value) in Discovery MIDR should be selected under 500, or else SUV_{max} will be lower than using standard OSEM algorithm. Otherwise, higher β value should be chosen to improve both image quality and SUV_{max} in Discovery MI and SIGNA.

Conclusions: Our preliminary data showed that BSREM algorithm is advantageous on both digital and analog PET images, especially in small lesion, but the optimal regularization strength parameters must be defined. The suitable selection of β value depends on lesion size and different type of PET scanner.

PB-038

正子放射性同位素製劑無菌性試驗取樣時機之初探－以 F-18 製劑爲例

林秀鈴[1] 蘇博仁[1] 何志豪[1] 廖曉薇[1] 彭毓婷[1] 蔡孟珊[1]
尹東傑[1] 陳輝墉[1] 羅欽瑄[2] 殷國維[1] 許耘萱[1]

[1] 義大醫院
[2] 新光醫院

背景介紹：

正子放射性同位素製劑在外釋之前必須經過嚴格的品管程序，並獲全部項目皆合格後始視爲一品管合格之產品。唯無菌性試驗 (培養基取樣接種) 作業流程依據中華藥典之規範，應在正子藥劑生產後三十小時內執行完成，但如遇到例假日或較長假期則需於生產當日完成接種，基於工作人員的輻射曝露儘可能合理抑低原則之考量，探討正子放射性同位素製劑無菌性試驗延遲取樣接種時間點之可行性，進而評估無菌性試驗取樣培養最晚容許時間。

方法：

步驟一、 進行培養基效能試驗 (Growth promotion test)：依據中華藥典選用大豆分解蛋白質 - 乾酪素培養基 (Soybean casein digest medium)、硫醇乙酸鹽培養基 (Fluid thioglycollate medium)。

步驟二、 進行無菌試驗取樣培養試驗：本試驗以標準菌株 ATCC 16404 黑麴菌 (Aspergillus brasilliensis)，ATCC 6538 金黃色葡萄球菌 (staphylococcus aureus) 爲之並以三重覆方式進行，取用 4 組藥劑小瓶上分別標示 0，24，32，72 小時，並分別注入 1 mL F-18 製劑 (單位活度濃度介於 100 ～ 130 mCi/mL)，活化標準菌株分別放入上述已標示時間點之藥劑小瓶中。

步驟三、 之後於上述每一個時間點到達時，分別加入適量的培養基，於 30 ～ 35℃及 20 ～ 25℃的溫度下培養。

步驟四、 每天定時觀察微生物生長情形並記錄之。

結果：

在培養期間經分別檢視 4 組樣本小瓶 (0，24，32，72 小時) 單位活度濃度介於 100 ～ 130 mCi/mL 之 F-18 製劑於 2 ～ 4 天呈現混濁現象，表示仍有微生物生長。

結論：

本研究以單位活度濃度介於 100 ～ 130 mCi/mL 之正子放射性同位素製劑 (F-18 製劑) 於 0，24，32，72 小時不同時間點加入培養基。結果顯示不會因時間點之延遲而抑制藥劑中可能存在的微生物的生長，因此爲了符合輻射合理抑低之原則，並依實驗室 (如例假日輻射考量因素) 設定時間範圍內執行無菌試驗。

PC-001

Primary Lung Adenocarcinoma with Sarcoidosis-Associated Mediastinal Lymphadenopathies Detected by FDG-PETCT

Ya-Ju Tsai, Deng-Yu Han

Department of Nuclear Medicine, Taipei Medical University Hospital

Introduction: Simultaneous occurrence of sarcoidosis and primary lung cancer in the same patient is rare. We reported a 76 year-old female with primary lung adenocarcinoma and sarcoidosis-associated lymphadenopathies detected by FDG-PETCT.

Case report: A 76-year-old female is a case of diabetes mellitus and dyslipidemia. Low-dose chest CT (computed tomography) found a ground-glass opacity (GGO) about 2.8 cm at right lower lobe (RLL) of lung. CT-guided biopsy proved lung adenocarcinoma in situ. Pre-operative positron emission tomography (PET) revealed a 2.8-cm lung tumor with a maximal SUV of 1.8 in RLL and lymphadenopathies with a maximal SUV of 10.5 in bilateral mediastinal, hilar & supraclavicular regions symmetrically. In addition, non-FDG avid small lung nodules were also detected in right upper, middle & lower lobes of lung. Endobronchial ultrasound-guided transbronchial needle aspiration (EBUS-TBNA) performed twice for mediastinal lymphadenopathy revealed no malignancy. Therefore, the patient received video-assisted wedge resection of the lung nodules & mediastinal lymph node dissection. Pathology revealed well differentiated, lepidic predominant (45%) adenocarcinoma in RLL, granuloma suspected sarcoidosis in other lung nodules, and sarcoidosis in dissected lymph nodes.

Discussion: Coexistence of pulmonary sarcoidosis and lung cancer is rare. Sarcoidosis is known to increase the risk of cancer. Although the relationship between sarcoidosis and cancer is unclear, the hypotheses have been suggested including cancer-associated sarcoid reaction due to immune response or chronic inflammation leading to development of cancer. Diagnosis of sarcoidosis is confirmed by tissue biopsy to excluding other possibility such as tuberculosis, lymphoma or lung cancer. FDG-PETCT is non-specific among these diseases because all of them may present intense FDG-avid lesions in lung, mediastinum and otherwhere in the body. In our causes, PETCT showed low-FDG avid lung tumor, suggesting low-grade malignancy, with intense-FDG avid lymphadenopathies symmetrically in bilateral mediastinal, hilar & supraclavicular regions. This imaging pattern is doubtful to make the diagnosis of unresectable advanced lung cancer.

Conclusion: Care must be taken when evaluation of FDG-avid lymphadenopathies in oncologic patients. Sarcoidosis as well as tuberculosis and lymphoma should be considered as the differential diagnoses. Standard pattern of lymphatic spread of lung cancer can be a clue to distinguish metastasis form benign mediastinal lymphadenopathy.

PC-002

Non-Functioning Ectopic Kidney with Backward-Filling Hydronephrosis Detected by ^{99m}Tc- DTPA SPECT/CT

Ya-Ju Tsai, Tzu-Hua, Lee

Department of Nuclear Medicine, Taipei Medical University Hospital

Introduction: We reported a case with non-functioning ectopic kidney in left pelvic cavity detected by diuretic renal function study with ^{99m}Tc- DTPA SPECT/CT.

Case report: 26-yr-old male was referred form other hospital for diuretic renal function study. Following the intravenous injection of 7 mCi of 99mTc- DTPA, a sequential renal scan and renography were obtained in the routine fashion using a gamma camera. Left kidney was not visualized during flow & cortical concentration phases, although perfusion, cortical uptake & clearance of right kidney were preserved. Focal area with tracer retention appeared in left pelvis about 4 minutes after injection of 40 mg of intravenous furosemide and the radioactivity increased over time with a short tract connecting to urinary bladder. SPECT/CT after dynamic renal study confirmed an ectopic kidney in the left pelvic cavity, which give the impression of non-functioning left pelvic kidney with vesicoureteral reflux causing backward-filling hydronephrosis.

Discussion: At present, the diagnosis of ectopic kidney mainly depends on ultrasound and CT. Renal dynamic imaging, however, provides advantages for the evaluation of the individual function of ectopic kidney. In our case, left renal fossa was empty while right kidney was visualized in normal position with persevered blood flow, cortical concentration & clearance phases. There was an unexpected pelvic area with radiotracer concentration synchronous to that of urinary bladder rather than normal right kidney. The radioactivity increased over time without clearance phase. SPECT/CT clarify the disease condition that urine collection in the bladder with backward filling to left pelvic ectopic kidney, which is almost non-functional, resulting in hydronephrosis.

Conclusion: SPECT/CT is a useful imaging modality to investigate any unexpected radioactivity during dynamic renal study and to evaluate individual function of ectopic kidney.

PC-003

意外發現 Ga-67 異常聚集於患者 Port-A

朱秀蘭[1] 莊雅雯[1] 游慧貞[2] 劉芝庭[1]

[1] 高雄醫學大學附設中和紀念醫院核子醫學部
[2] 高雄醫學大學附設中和紀念醫院影像醫學部

背景介紹：中心靜脈導管屬於血管內導管的一種，依用途細分爲 CVP、Hickman、Port A 及 PICC 等等，常用於置入中心靜脈導管之大靜脈爲內頸靜脈、外頸靜脈、鎖骨下靜脈、肱骨靜脈或股隱靜脈，適用於急需大量而快速輸液及需長期化學治療、全靜脈營養或輸血之病人，提供注射各種藥物、營養液或抽血之用。本院核醫部之放射性同位素藥物，基本上皆由週邊靜脈注射攝影，極少由中心靜脈導管注入，以避免放射性藥物於中心靜脈導管殘留，影響臨床影像判讀，而到目前爲止，在由週邊靜脈注入後，即便是與中心靜脈導管同側，放射性同位素藥物並不會累積於中心靜脈導管上，進而在影像中出現異常的放射性活性累積，造成影像之誤判。

病例報告：一位 25 歲男性患有睪丸惡性腫瘤之病患，接受鎵 -67 全身掃描，在 24 及 48 小時的全身影像中，發現右側胸腔部位上方有明顯異常的放射性活性累積 (圖一及圖二)，懷疑腫瘤轉移至胸部淋巴結，但此影像爲平面影像，容易受身體前後器官重疊而無法正確區分活性累積之位置，便進一步使用單光子電腦斷層掃描術 (SPECT/CT) 加以定位異常活性之正確解剖位置。藉由 SPECT/CT 的影像中可以證實此活性聚積並不是在淋巴結上 (圖三及圖四)，而是病患的 Port A，經本部工作人員確認此鎵 -67 藥物由病患之右手手腕注入，在圖一及圖二的影像中也可發現右手注射點處有聚積放射活性，並非由 Port A 注入。

結論：此案例之鎵 -67 全身掃描藥物並非由中心靜脈導管注入，是由右手手腕注入，但放射性活性卻累積在 Port A 之現象是較爲特殊少見的，判斷可能因同側右手腕注入血管的同時，部分放射性藥物在中心靜脈附近停留，而造成較多放射性活性聚積在 Port A。此外，上述病患影像若非藉由單光子電腦斷層掃描進一步加以確認，容易造成誤判，因此 SPECT/CT 之影像能提供準確解剖定位影像，提高核醫相關掃描判讀的正確性及臨床價值。

PC-004

Surgical Procedure with Manubrial Resection Producing Potential Pitfalls in Metastatic Work-up of Bone Scintigraphy

Ya-Wen Chuang, Chia-Yang Lin, Ying-Fong Huang, Chin-Chuan Chang, Chih-Ting Liu, Hsiu-Lan Chu

Department of Nuclear Medicine, Kaohsiung Medical University Hospital, Kaohsiung, Taiwan

Introduction: There is a surgical procedure that resection of part of manubrium, adjacent clavicles and ribs provides access to the upper thoracic esophagus and intrathoracic trachea located on the dorsal side of the sternum. It is beneficial to enlarge the thoracic inlet for reconstruction after esophagectomy, and airway reconstruction by mediastinal tracheostomy when cervical tumor dissection determines the need for a retrosternal division of the trachea. However, partial manubriectomy is a rare procedure in our institution, and the following bone scan reveals abnormal uptake around injured manubrium, mimicking the typical appearance of tumor invasion or bone metastasis to the sternum.

Case Report: The authors demonstrate 2 cases of the substernal approach involving resection of the manubrium for reconstruction after substernal route esophagectomy, and 1 case of mediastinal tracheostomy after total laryngectomy and palliative resection of advaned tumor of the lower neck, showing significantly increased uptake over the manubrium on the routine bone scan, and which may be misdiagnosed as stage-changing bone metastases without knowing the previous surgical procedure.

Discussion: It is important that this procedure is occasionally performed in few selected cases. When using esophagectomy with gastointestinal transit reconstruction, or airway reconstruction for locally advanced tumors of laryngeal, tracheal, esophageal, or thyroid origin, the possibility of with manubrial resection resulting sternal defects should be kept in mind and reviewed so that mistakes in interpretation are not made. Reference plain film radiography or CT is helpful to avoid misdiagnosis if available.

PC-005

澱粉樣蛋白沉積關節病變 在骨骼掃描與炎症掃描之影像表現

蔡雅茹　楊承頷

台北醫學大學附設醫院核子醫學科

我們報告一案例爲末期腎臟疾病引起澱粉樣蛋白沉積關節病變 (amyloid arthropathy, AA)。全身骨骼掃描與炎症掃描發現關節處有異常增加攝取放射性藥劑，且關節旁之骨骼有典型的硬化邊緣之囊性病變 (juxta-articular cystic lesions with well-defined sclerotic margin)。

個案報告：55 歲男性是一名末期腎臟疾病患者，接受規則血液透析治療。患者因不明原因發燒入院。血液檢查發現發炎指數 (ESR & CRP) 上升。感染科醫師給予抗生素並安排全身骨骼掃描 (Tc-99m MDP 20 mCi) 與炎症掃描 (Ga-67 5 mCi)。全身骨骼掃描 (bone scan) 呈現兩側肩膀及髖關節有放射性藥劑異常攝取現象。炎症掃描 (gallium scan) 亦在雙側肩關節與髖關節處有發炎檢查藥劑攝取增加。且斷層掃描 (SPECT/CT) 發現關節旁之骨骼有軟骨下囊性病變並具有明確的硬化邊緣。回顧病人過去病史，三個月前曾因澱粉樣蛋白沉積關節病變 (AA) 導致左側肩膀肌腱斷裂，進而接受手術治療。合併影像與臨床狀況判斷，此病患應是澱粉樣蛋白沉積關節病變 (AA) 引起關節炎，呈現發燒與發炎指數上升之症狀。

討論：澱粉樣蛋白沉積 (amyloidosis) 是指異常蛋白質沈積在組織引起的疾病。澱粉樣蛋白沉積可發生在多種器官中。慢性腎臟病的病人，其 beta 2-microglobulin 的清除率下降，以致於沉積在身體的各個組織中 (尤其在軟骨、關節腔、韌帶等)。澱粉樣蛋白沉積關節病變 (AA) 的特徵是侵蝕性和破壞性的骨關節炎，最常見的是髖、肩和腕骨。分佈經常是雙邊的。在大關節中類似於炎症性關節炎，伴有近關節軟組織腫脹。臨床表現關節疼痛 (尤其是肩部)、骨骼囊性病灶 (bone cysts)、腕隧道症候群、破壞性脊椎關節病 內臟的侵犯相對較爲少見。在洗腎病人中看到上述症狀，要懷疑是否爲澱粉樣蛋白沉積。臨床表現與影像特徵爲主要診斷方式。切片是黃金診斷標準。目前沒無特異性的治療，只能想辦法移除蛋白沉積來預防或延緩進展。

回顧文獻，澱粉樣蛋白沉積關節病變 (AA) 在骨骼掃描與發炎檢查時也會在病灶關節附近發現攝取異常增加。與本個案之影像表現一致。輔助斷層掃描 (SPECT/CT) 亦發現關節旁之骨骼有典型的囊性病變並具有明確的硬化邊緣。

結論：澱粉樣蛋白沉積關節病變 (AA) 與炎症性關節炎在骨骼掃描與炎症掃描之影像表現相似，皆可呈現放射性藥劑攝取增加之現象。若影像爲兩側性髖、肩和腕骨關節侵犯且骨骼有硬化邊緣之囊性病變，需考慮是否爲澱粉樣蛋白沉積關節病變 (AA)，特別是在有澱粉樣蛋白沉積 (amyloidosis) 病史或是慢性腎臟病的病人的身上。

PC-006

Skeletal Superscan in a Patient with Myeloproliferative Neoplasm

Ya-Ju Tsai, Lee-Jung Hsu

Department of Nuclear Medicine, Taipei Medical University Hospital

Introduction: Skeletal superscan can be caused by diffuse metastasis, metabolic conditions and infiltrating bone marrow diseases. We reported a case of skeletal superscan in a patient with myeloproliferative neoplasm.

Case report: 72-yr-old female is a case of myeloproliferative neoplasm with fibrosis under Jakavi treatment. She complained of persistent pain over body & limbs. Whole-body bone scan with Tc-99m MDP showed diffusely increased osteoblastic activity in axial and appendicular skeletons, associated with decreased radioactivity in soft tissues & kidneys, compatible with a skeletal superscan that was related to her underlying disease of myeloproliferative neoplasm.

Discussion: Superscan is a well-known pattern on bone scan to suggest significantly increased extraction of radiopharmaceuticals and decreased renal activity due to increased osteoblastic activity of bone. The most common cause of a skeletal superscan is extensive bone metastases from prostate cancer, although other tumors may also cause this appearance. In addition to diffuse metastasis, hyperparathyroidism, hyperthyroidism, renal osteodystrophy, Paget's disease, acromegaly, aplastic anemia, leukemia or myeloproliferative neoplasm may also result in diffuse increase of skeletal uptake on bone scan or bone PET. Superscan due to metastases shows increased uptake that is usually confined to the axial skeleton while in case of metabolic disorders, it involves entire skeleton. Increased activity primarily in the peripheral skeleton maybe seen in hematologic disorders.

Myeloproliferative neoplasms (MPNs) are a group of diseases associated with mutations leading to the growth factor-independent proliferation of bone marrow progenitors and the bone marrow makes too many blood cells. The symptoms of MPNs vary based on the type of disease. Bone pain can be one of the symptoms.

Conclusion: It is important to keep in mind that infiltrating bone marrow disease such as MPN is one of the differential diagnoses of a skeletal superscan, in addition to diffuse metastasis or metabolic bone diseases.

PC-007

Ga-67 全身掃描合併單光子電腦斷層之肝膿瘍診斷 – A Case Report

許文齡　張淑敏　莊雅雯　張晉銓　許玉春　李岱恩

高雄醫學大學附設中和紀念醫院核子醫學部

背景：肝膿瘍是肝臟實質部分受感染的一種疾病，其感染可能爲細菌、黴菌或阿米巴原蟲，初期症狀常爲腹部不適、右上腹痛，而後期常爲發燒、發冷。腹部超音波及腹部電腦斷層爲常見的診斷工具。Gallium-67 (Ga-67) 全身掃描是核醫最常用於偵測不明原因發燒及腫瘤的一項檢查，其原理是利用 Gallium 離子與鐵離子特性相似，而在發炎部位的聚集與局部微血管壁通透性增加，乳鐵蛋白增加有關，影像學上呈現爲在炎症部位會有異常放射性累積，並持續增加，搭配單光子電腦斷層 (SPECT/CT) 能對異常放射性聚集病灶定位，並獲得其相對解剖位置等資訊供臨床診斷使用。

病例報告：一位 46 歲男性，有中風 (stroke)，腦動脈瘤 (brain aneursym)，冠心病 (coronary artery disease)，副甲狀腺功能亢進症 (hyperparathyroidism)，多發性腎病 (polycystic kidney disease) 伴有末期腎病 (End-stage renal disease) 的病史，並定期進行血液透析 (hemodialysis)，因爲反覆發燒及持續性的發冷而入院接受治療。在進行腹部電腦斷層檢查中，懷疑膀胱炎及體染色體顯性多囊性腎臟病 (Autosomal dominant Polycystic Kidney Disease, ADPKD，然而發燒情況也無明顯改善，隨後的實驗室檢測，有明顯感染跡象，因而至核醫科進行 Ga-67 全身掃描。在給予 Ga-67 放射性同位素 24 小時及 48 小時後的影像中發現：左上腹部有明顯的放射性藥物聚集，合併單光子電腦斷層掃描 (SPECT/CT) 的影像，在肝臟第二區 (segment II of liver) 有一個呈卵型的病灶 (oval-shaped lesion)，高度懷疑爲膿瘍 (Abscess)。

討論：Ga-67 全身掃描是核醫常用於偵測不明原因發燒的檢查，以提供臨床進一步診斷及治療。常規進行全身及局部平面影像，然而因爲身體器官在平面影像上會有重疊的情形，因此很難區分病灶的實際位置，配合 SPECT/CT 不僅能正確指出放射性聚集病灶位置，亦能獲得病灶組成的相關資訊已提供臨床進一步診斷及後續治療。肝膿瘍如果沒有適當的治療，其死亡率是相當高，敗血症是主要的死亡原因，須格外注意。

PC-008

Kikuchi Disease Mimicking Lymphoma on F-18 FDG PET/CT: A Case Report

Chao-Jung Chen[1], Guan-Cheng Huang[2]

Departments of [1]Nuclear Medicine,
[2]Haematology-Oncology, Yuan's General Hospital, Kaohsiung, Taiwan

Introduction: Kikuchi disease is an extremely uncommon disease but with higher Japanese and Asiatic prevalence. This rare and unusual form of lymphadenitis preferentially affects young females, with a majority of patients under the age of 30 years, in a 3 to 4:1 ratio. Clinically, the most common presentation of this disorder is cervical lymphadenitis, although it may also be generalized. Other complaints include low-grade fever, malaise, fatigue, and diarrhea. The exact etiology of Kikuchi Disease is still unknown. There is limited data in patients with Kikuchi disease on F-18 fluorodeoxyglucose (FDG) positron emission tomography/computed tomography (PET/CT), we herein present a rare case of Kikuchi disease on FDG PET/CT.

Case report: A 19-year-old female patient presented with right neck lymph nodes for few days. She was referred for F-18 FDG PET/CT to exclude lymphoma. Two lymph nodes with increased FDG uptake in the right supraclavicular region were detected (the largest one, 1.0 cm in greatest dimension, SUVmax: early 16.92, delayed 18.84). No other definite abnormal FDG-avid lesion can be detected. Surgical excision was performed and the pathology showed Kikuchi disease.

Discussion: A series of 61 patients with Kikuchi disease had been reported in Taiwan. 34 women and 27 men were collected (1.26:1 ratio; age range, 6 to 46 years; mean age, 21 years). The affected cervical lymph nodes were commonly located in the posterior cervical triangle (54 of 61). Unilateral and bilateral cervical lymph nodes were affected in 54 and 7 patients, respectively. Our case is a young female with unilateral cervical lymph nodes, which is relatively compatible with the above findings. FDG-PET is useful for differentiating between benign and malignant tumors. However, several case reports have suggested that the lymph nodes of patients with Kikuchi disease exhibit FDG avidity. Indeed, Kikuchi disease was difficult to distinguish from malignant lymphoma using only the PET/CT findings, even when evaluated retrospectively. However, F-18 FDG PET/CT showed the general regions of the lymph nodes and aided decisions regarding appropriate biopsy sites.

Conclusion: In conclusion, we demonstrated the rare case of a female patient with Kikuchi disease on F-18 FDG PET/CT scan. It showed intense FDG uptake in the right cervical lymph nodes. This case emphasizes that Kikuchi disease should be considered when making a differential diagnosis of FDG-avid lymph node lesions, especially in the neck. F-18 FDG PET/CT can indicate as a guide for biopsy.

PC-009

攝護腺癌骨轉移以鐳 -223 治療後的症狀影響評估

張桂蘭　李岱恩　顏維徵　張淑敏　張晉銓

高雄醫學大學附設中和紀念醫院核子醫學科

摘要

目的：去勢抵抗性前列腺癌 (CRPC) 患者發生骨轉移轉移且尚未臟器轉移患者使用，Rad-223 治療與其發病率和改善生活品質及提升生存有其效果。高醫治療經驗近 1 年自健保啓用後 (排除經濟問題) 骨轉移共 20 名病患，完成 6 劑注射有 40%，完成 4 劑注射有 25%，3 劑注射有 20%，2 劑注射有 10%，只注射 1 劑的有 5%。經問卷統計完成注射 6 劑患者中過程中 46% 的患者疼痛得到改善有 28% 的患者沒有胃口，有 20% 的患者無症狀，中有 8% 的體重減輕。但是尚有 60% 患者未完成整組 6 劑注射者，病情因血液變化惡化，甚至輸血；噁心食慾不振等而中斷注射。因此在 CRPC 患者提供鐳 223 治療組程序使用上提升完成六劑注射完成率並增加總體存活率之參考。

研究方法：Xofigo 是一種發射 α 粒子的放射治療劑，劑量方案爲每千克體重 50 kBq (1.35 微居里)，只能行進很短的距離 (約 50-80 μm 相當於 2-10 細胞)，間隔 4 週，共注射 6 次。針對腸道，紅骨髓和骨 / 成骨細胞爲 Xofigo 提供最佳的吸收輻射劑量。

本研究在統計接受在接受鐳 -223 治療的病患中，接受藥物治療的患者中最常見的藥物不良反應爲骨髓抑制血液學異常反應，表現爲貧血，淋巴細胞減少，嗜中性白血球減少，血小板減少和中性粒細胞減少及全血球減少症；導致最常見的副作用爲：腹瀉、噁心、嘔吐、四肢水腫，體力減輕，因此每次治療前先抽血評估全血反應及病患臨床反應，決定是否連續注射治療。因此設計臨床各項症狀做統計問卷，結果可幫助評估病患能在最佳注射時機注射治療以提升生活品質及生存率。

結論：去勢抵抗性前列腺癌 (CRPC) 患者，將 Radium 223 的治療方法使用在較早的疾病狀態，或是或與其他療法聯合使用時，接受過化療後對整個患者的生理體能協助會更好。所以對整體治療過程中對目前完成 6 劑注射有 40% 生理狀況良好的患者 , 期望能再提申完成率，使有更多好的生活品質及提高存活率。在此，提供治療程序很好的參考。

PC-010

因應 Covid-19 疫情
導致免疫分析室試劑庫存調控問題之經驗分享

黃雅菁　沈珮君　劉家秀

阮綜合醫療社團法人阮綜合醫院核子醫學科

前言：醫院爲了落實有效管理，每年對實驗室試劑成本要求確實精算，今年上半年度，由於新冠肺炎疫情影響，無論病人到院或是健康檢查人數都影響甚鉅，RIA 使用之試劑因使用有效期偏短，在本次疫情中應如何調控試劑預訂，以免造成試劑短缺或過剩，以本實驗室爲例，作爲經驗分享

案例：實驗室長期與供應商訂貨皆是提前兩週預估試劑用量，但因四月歐洲疫情升溫，導致班機多次停飛，造成供應商無法每週出貨，便建議實驗室改爲每月預估下一整個月用量，所有品項更改成每月出貨方式，可避免因班機延誤而缺藥之狀況；但卻延伸出另一問題，使用月訂需求量後，再次遇到班機延遲，試劑到貨時，原本可用四週之試劑，效期縮短成三週，試劑短缺問題變成試劑過剩，故因將此狀況導入風險管理。

應變步驟：將因爲新冠肺炎引起的試劑短缺或延遲到貨導入風險管理，整理造成本次庫存問題原因有：(A) 原廠停工或班機延遲 (B) 受檢人數與去年同期相差太多，預估錯誤，導致訂貨量不足 (C) 謹慎預估後，仍因延遲到貨，使有效期縮短而無法在試劑效期內將其消耗完畢，造成嚴重浪費，檢驗成本增加；針對以上原因進行風險評估與控制，實驗室採取預防措施有：(a) 避免停工或班機延遲由每週到貨改爲每月到貨，此措施應相對兼顧實驗室有無足夠空間存放試劑，並應同時修改庫存管理作業程序內容之試劑安全庫存量 (b) 不可參考過往同期之訂貨量訂貨，參考疫情醫院管制後到院人數或健診中心是否承接大批體檢爲訂貨基準，但對於不影響之族群，例如：洗腎室，則維持正常評估量進行，也可對於不影響發報告時間的項目作集中式檢驗，避免缺藥 (c) 若因班機延遲造成效期縮短無法時間內使用完畢，實驗室可與供應商協議是否可減少出貨，並可將本次事件結果納入年度供應商評估，嚴重影響實驗室作業流程時，應考慮拒絕收貨或是更改試劑供應商。

結論：疫情期間，透過系統性鑑別與導入風險管理，對庫存作業流程做臨時的改變與調動，可有效避免缺藥狀況或讓實驗室降低成本耗損，以利實驗室成本控制，提昇實驗室檢驗效能。

PC-011

Prognostic Significance of Pretreatment Staging with Positron Emission Tomography in Esophageal Cancer: A Nationwide Population-Based Study

Hsi-Huei Lu[1], Mu-Hung Tsai[2], Nan-Ching Chiu[1]

[1]*Department of Medical Imaging, National Cheng Kung University, Tainan, Taiwan*
[2]*Department of Radiation Oncology, National Cheng Kung University, Tainan, Taiwan*

Introduction: 18F-FDG PET/CT has been established to play a role in staging esophageal malignancy other than known metastasis. However, only about half of these non-metastatic esophageal cancer undergoes PET/CT in Taiwan, which may lead to inaccurate staging and suboptimal treatment. The purpose of this study is to evaluate the prognostic significance of pretreatment PET/CT in non-metastatic esophageal cancer.

Methods: We utilized the Taiwan Cancer Registry (TCR) and National Health Insurance Research Database (NHIRD) to select newly diagnosed non-metastatic esophageal cancer patients from 2009 to 2015. Pretreatment staging PET/CT was defined by the presence of PET-CT within 90 days prior to starting treatment. Overall survival was calculated from the first day of treatment to date of death, or censored on Dec 31, 2018 if a record of death was not found. Survival curves between patients with and without staging PET/CT were compared with the log-rank test.

Results: A total of 9078 patients (1765 had pretreatment PET/CT and 7313 did not) were enrolled. The median follow-up time for all patient and surviving patients was 1.29 years and 5.46 years respectively. Patients with pretreatment PET/CT had a lower risk of death compared with those without pretreatment PET/CT [HR = 0.74, (95% % CI 0.70-0.79), $p < 0.001$]. After adjusting for age, stage, histology, and tumor location, pretreatment PET/CT remained significantly correlated with a lower risk of death [HR = 0.77 (95% CI 0.73-0.82), $p < 0.001$].

Conclusions: The utilization of pretreatment 18F FDG PET/CT in non-metastatic esophageal malignancy, which may attribute to the more accurate evaluation of nodal status, early detection of distant metastasis, incidental detection of second malignancy and precise radiotherapy simulation, was associated with reduced risk of death.

PC-012

評估注射放射性藥物時留置針的使用方式對骨骼掃描影像之影響

黃美瑩　李佳鴻　莊凱文　吳雅嵐

佛教慈濟醫療財團法人臺北慈濟醫院核子醫學科

背景介紹：骨骼掃描的影像中，放射性藥物累積過度會造成影像判讀的困擾，而住院病人的影像中，見到非生理性的藥物滯留活性過高位置常在留置針中。本研究目的爲評估注射放射性藥物時連接留置針的方式不同，是否會影響放射性藥物殘留的多寡而影響影像品質。

方法：本研究收集自 2019 年 11 月至 3 月間，進行骨骼掃描的住院病人共 142 位 (男性 73 名，女性 69 名，年齡介於 37 至 92 歲，平均年齡 64.7 ± 12 歲)，由放射師執行注射藥物 Tc-99m MDP，依照注射時連接留置針的方式分爲下列四種情形：1. 直接留有 T connect，2. 注射處延長後接 T connect，3. 注射處延長後從安全針具接 T connect，4. 核醫護理師重新放針，並記錄之。再與檢查影像做比對，依照注射處藥物殘留情形分爲以下三種等級：1. 幾乎無殘藥，2. 中等的殘藥，3. 嚴重的殘藥，並記錄之。我們將幾乎無殘藥，中等的殘藥，嚴重的殘藥分別給予 0, 1, 2 的分數以評估不同的留置針使用方式是否有影響殘留放射性藥物的嚴重程度。

結果：由 142 位病人之注射時連接留置針的方式與放射性藥物的殘留情形得知，直接留有 T connect, 注射處延長後接 T connect，注射處延長後從安全針具接 T connect 與核醫護理師重新放針之殘留放射性藥物嚴重程度分數分別爲 0.6，0.908，1.542 和 1 分。因直接留有 T connect 及核醫護理師重新放針之樣本數較少 (分別爲 5 位及 4 位)，故僅分析注射處延長後接 T connect 及注射處延長後從安全針具接 T connect 此二種情形，其 P-value < 0.001 (P-value = 0.000988)，有顯著差異。

結論：由本次研究觀察顯示，不同的注射時連接留置針方式所造成的放射性藥物殘留情形有顯著差異，且會影響影像品質。其中留置針有延長的兩種連接方式差別在於注射處與 T connect 間有無安全針具連接，我們推測放射性藥物可能容易堆積在安全針具接頭處，建議注射放射性藥物時，可以將安全針具之接頭取下直接連接 T connect 後注射藥物。並且我們也發現嚴重程度分數最低的方式爲直接留有 T connect，可以推測藥物注射位置離留置針越近，殘留藥物情形越少。選擇最適合的藥物注射位置，將大幅改善放射性藥物殘留情形，進而提升影像品質。

PC-013

Identifying Potential Predictors for the Interference of Tc-99m Bone Radiopharmaceuticals in Dual-Energy X-ray Absorptiometry Using Lasso and Logistic Regression Statistics

Ching-Lin Sung[1,2], Yu-Hung Chen[1], Kun-Han Lue[3], Shu-Hsin Liu[1,3], Sung-Chao Chu[4], Ching-Chun Ho[5]

[1]*Department of Nuclear Medicine, Hualien Tzu-Chi Hospital, Buddhist Tzu-Chi Medical Foundation, Hualien, Taiwan*
[2]*Hualien Hsien Association of Radiological Technologists*
[3]*Department of Medical Imaging and Radiological Sciences, Tzu Chi University of Science and Technology*
[4]*Department of Hematology and Oncology, Hualien Tzu Chi Hospital, Buddhist Tzu Chi Medical Foundation, Hualien, Taiwan*
[5]*Department of Surgery, Hualien Tzu Chi Hospital, Buddhist Tzu Chi Medical Foundation, Hualien, Taiwan*

Introduction: We've found that the lumbar dual-energy X-ray absorptiometry (DXA) measurement is susceptible to the interference of the Tc-99m MDP administration. We further investigate and identify possible predictors for this interference.

Methods: We conducted a prospective study investigating 74 patients who received Tc-99m MDP bone scan. All patients received lumbar DXA before and 2-4 hr after Tc-99m injection. The DXA measurement reduction exceeds the least significant change (LSC) is defined as significant BMD underestimate. We record demographics from all participants and using lasso algorism to remove redundant predictors for significant BMD underestimate. We construct the lasso fit with 10-fold cross-validation. The resulting lambda value with the minimum standard error will be used to calculate the lasso coefficient factors. The residual candidate predictors were examined with logistic regression analysis. We will further analyze each independent predictor using the ROC curve method to seek the optimal cutoff value.

Results: After lasso regularization, four candidate predictors (body weight, BMI, cigarette smoking, and the time of 2nd DXA after Tc-99m MDP injection) were selected from the initial 16 demographic variables. Among the four candidates, the logistic regression identified body weight as the only independent predictor (OR = 1.125, $p = 0.001$). The optimal cutoff bodyweight for predicting significant DXA underestimate after Tc-99m MDP administration was 62.5 kg. Patients with a bodyweight of over 62.5 kg were more likely to show significant BMD underestimate than those with bodyweight less than 62.5 kg (65% versus 13%, $p < 0.001$).

Conclusions: Our preliminary study showed that body weight is an independent predictor for significant BMD underestimate after Tc-99m MDP administration, and patients with bodyweight less than 62.5 kg may still undergo the DXA exam after Tc-99m MDP injection.

PC-014

乳腺癌患者在例行腫瘤追蹤期間逐漸變大的腦膜瘤在一系列骨骼掃描上的表現

林家揚　莊雅雯　許文齡　黃英峰　張晉銓

高雄醫學大學附設中和紀念醫院核子醫學部

引言：骨骼掃描是一項相對便宜且高度靈敏的檢查，臨床上常用在評估腫瘤的骨轉移偵測。大部分癌症病人由於臨床上症狀的表現，進行骨骼掃描，進而發現骨轉移，然而骨骼掃描的特異性相對是比較低的，其他很多情況例如外傷、感染、炎症或其他良性的情況，在骨骼掃描上也會有明顯的發現。

病例報告：這是一個現年 46 歲的女性，該患者於 12 年前因左側乳癌，於北部某醫院左側乳房全切除開刀後，後續化療及追蹤皆在本院完成。在早期的追蹤過程中，骨骼掃描並無任何明顯的異常發現。但於五年前的骨骼掃描 (該次檢查只有正面和背面影像) 突然在右側顳顬骨處，出現不正常的熱點，後來連續幾年的追蹤檢查，可以發現連續幾年右側顳顬骨病灶有緩慢變大的變化。由於病人在臨床上的腫瘤指數不高且病人無任何頭部的臨床症狀，因此沒有明顯證據以致強烈懷疑骨轉移的可能性，因此在此熱點出現的初期，認爲可能是外傷等非轉移的原因所致。接下來幾年的追蹤，病人在臨床上仍無任何症狀，但由於右側顳顬骨處的熱點持續出現在骨骼掃描上，因此於兩年前安排了頭部核磁共振掃描進一步檢查，發現了一個約 2.5 公分疑似腦膜瘤的病灶，且鄰近頭骨頭有骨質增生的現象，與骨骼掃描的位置相符。由於去年上半年，病灶逐漸變大，病人在神經外科醫師的建議下，進行手術切除，病理報告證實爲腦膜瘤，但無鄰近右側顳顬骨的侵犯。

討論：很多癌症病人透過常規的骨骼掃描追蹤，雖然無臨床症狀，但可早期偵測骨轉移病灶，但由於低特異性的關係，在癌症追蹤的族群裡，骨骼掃描上的熱點，非全然皆是骨轉移病灶。這個病患一系列的骨骼掃描，電腦斷層、核磁共振影像及最終的病理結果，讓我們了解骨骼掃描雖然是臨床上常用在癌症的追蹤檢查，但如何精準判讀骨骼掃描上的病灶，仍然是一項挑戰。

PC-015

Kinetic Evaluation of Tau PET Radiotracer ^{18}F-T807 in Non-human Primate

Chuang-Hsin Chiu[1], Kuo-Hsing Ma[2], Ta-Kai Chou[1], Yun-Ting Jhao[2], Ing-Jou Chen[1], Cheng-Yi Cheng[1], Chyng-Yann Shiue[1]

[1]*Department of Nuclear Medicine, Tri-Service General Hospital, National Defense Medical Center, Taipei, Taiwan*
[2]*Department of Biology and Anatomy, National Defense Medical Center, Taipei, Taiwan*

Introduction: ^{18}F-T807 is a PET radiotracer for tau protein imaging, which is implicated in neurologic disorders. In this study, we examined the ^{18}F-T807 pharmacokinetics in normal non-human primate (NHP) using dynamic PET imaging.

Methods: Two normal monkeys (Macaca cyclopis) underwent dynamic PET imaging for up to 90 min after bolus injection of ^{18}F-T807. Imaging was performed using GE Discovery 710 PET/CT scanner. PET imaging data were spatially normalized into INIA19 template from individual MRI images, and VOIs (frontal, temporal, parietal, occipital, caudate, putamen, precuneus and posterior cingulate gyrus and cerebellum) in the template were applied for quantitative analysis.

Reference region method analysis were performed using cerebellum as reference region including distribution volume ratio (DVR) and standard uptake ratio (SUVR).

Results: The DVR and SUVR (50-70 min, 70-90 min and 10-20 min) in one normal NHP was shown in table 1. Compared to DVR, the correlation coefficient (R^2) for SUVR in 50-70 mins and 70-90 mins were 0.95 and 0.90.

Conclusions: The kinetic of the ^{18}F-T807 tracer in cortical area showed rapid clearance. The simplified approach using DVR and SUVR (50-70 min) showed highly correlation.

PC-016

Exploring the Effect on Cerebral Blood Flow After Acupuncture and Moxibustion in Normal Subjects Using ^{99m}Tc-ECD Imaging

Chuang-Hsin Chiu[1], Ching-Heng Lin[2], Yan-Chih Liao[1], Ing-Jou Chen[1], Chen-Yu Lee[3]

[1]Department of Nuclear Medicine, Tri-Service General Hospital, National Defense Medical Center, Taipei, Taiwan
[2]Baihan Chinese Medicine Clinic, Taipei, Taiwan
[3]Yusheng Chinese Medicine Clinic, Taipei, Taiwan

Introduction: In the past few decades, there has been an increasing demand of traditional Chinese medicine. Based on general conception, traditional Chinese treatment is more focused on patients' holistic physical condition, which gradually works up to getting the whole body in balance. Acupuncture and moxibustion are widely applied in the combined treatment of cerebrovascular accident clinically, but the effect of acupuncture on cerebral blood flow is not clear. The aim of this study was to explore the effect on cerebral blood flow after acupuncture in normal subjects using ^{99m}Tc-ECD imaging.

Methods: We chosen Shousanli (LI 10) for acupuncture point in this study, which located at the radial side of the forearm and 2 inches below the transverse cubital crease. Moxibustion is a therapeutic method that consists of burning dried mugwort on acupuncture point to generate warm stimulation on the local regions. A total of 8 normal subjects received ^{99m}Tc-ECD imaging. The baseline ^{99m}Tc-ECD imaging started 30-80 minutes after ^{99m}Tc-ECD injection. The second ^{99m}Tc-ECD imaging was performed after receiving left Shousanli (LI 10) acupuncture for 20 minutes, the ^{99m}Tc-ECD imaging was also performed 30-80 minutes after ^{99m}Tc-ECD injection. The third ^{99m}Tc-ECD imaging was performed after receiving moxibustion for 20 minutes, the ^{99m}Tc-ECD imaging was also performed with same protocols as the third imaging. All images were spatially normalized into Montreal Neurological Institute (MNI) template, and 9 VOIs in the AAL template were applied for uptake ratio (global mean as reference).

Results: The results showed that the cerebral blood flow significant increase in the cerebellum and decrease in frontal cortex after acupuncture. There was significant increased cerebral blood flow in temporal cortex and cerebellum, and decreased cerebral blood flow in frontal cortex, cingulum, striatum and thalamus.

Conclusions: Preliminary results show that cerebral blood flow can be redistributed by administering acupuncture and moxibustion, which functional neuroimaging may provide scientific evidence for the therapeutic potential of acupuncture.

PC-017

The Phantom Study of Brain Dopamine Transporter SPECT Images using Different SPECT Collimators in NM 870DR

Ing-Jou Chen, Chuang-Hsin Chiu, En-Shih Chen

Department of Nuclear Medicine, Tri-Service General Hospital, National Defense Medical Center, Taipei, Taiwan

Introduction: Imaging of the dopaminergic dysfunction with radiopharmaceuticals is an important tool for evaluating neurologic disorders. There are several dopamine transporter (DAT) selective SPECT tracers for the clinical diagnosis of Parkinson's disease (PD), including ^{123}I-Iometopane (DopaScan), ^{123}I-Ioflupane (FP-CIT) (DatScan) and ^{99m}Tc-TRODAT-1 (TRODAT). TRODAT scan has obtained the national insurance coverage for clinical use, making it the most commonly utilized tool for PD patients in Taiwan. Theoretically, low energy high resolution (LEHR) collimators can be inferior to FB collimation because of lower image resolution and poorer count statistics. Recently, the new SPECT/CT systems, NM 870DR include a new low energy high resolution and sensitivity (LEHRS) collimator, which can increase sensitivity of count rate. The aim of this study was to evaluate differences in dopamine transporter SPECT images with striatal phantom between different collimators and to determine the appropriate volume of interest (VOI) for quantification.

Methods: The striatal phantom was filled with ^{99m}Tc solutions of different striatum-to-background radioactivity ratios. Five striatum-to-background radioactivity ratios (8, 6, 4, 3 and 2) were used. Phantom data were acquired using SPECT/CT devices (NM870) equipped with FB and LEHRS collimators. All images were reconstructed by OSEM with scatter correction and attenuation correction. The bilateral caudate, putamen and background VOI were determined by the contour of CT images, and then compared the recovery and linearity (R^2) of specific binding ratio (SBR).

Results: The recovery and linearity of SBR SPECT using the bilateral caudate, putamen and striatum were compared with those for true radioactivity. Recovery of SBR SPECT were 42% in FB collimators and 35% in LEHRS collimators. The linearity were 0.97 in FB collimators and 0.94 in LEHRS collimators. Preliminary results show that between different SPECT collimators, the FB collimator designed for TRODAT imaging is recommended.

Conclusions: Preliminary results show that between different SPECT collimators, the FB collimator designed for TRODAT imaging is recommended.

PC-018

南部某醫學中心 近三學年放射免疫分析實驗室檢體量之消長

曾翠芬[1] 林秋美[1] 陳怡如[1] 林家揚[1,2] 張晉銓[1,2]

[1] 高雄醫學大學附設中和紀念醫院核醫部放射免疫分析組
[2] 高雄醫學大學附設中和紀念醫院核醫部

背景介紹：本實驗室自 1977 年創立至今一直秉持著只使用放射免疫分析方法，從檢驗項目最多 51 項到目前因肝炎 RIA 試劑停產少了 15.69% 的項目，再加上檢驗方法的日新月異、各單位之營收和臨床醫師要求的快述報告等外來的競爭壓力之下，統計這近三學年本實驗室的檢體量和收入是否因此而受影響。

方法：將本實驗室所有檢驗項目分成五大類 (肝炎 hepa、婦科 obs、甲狀腺 thy、腫瘤 tumo、其它 oth) 計算 106、107、108 等 3 個學年度 (當年 8 月 1 日至隔年 7 月 31 日) 的檢體量和收入，以 106 學年度爲基準分別檢視 107 和 108 學年度之消長。每月檢體量和項次統計資料來自於本院資訊室，統計軟體使用 Microsoft office Excel 2007。

結果：這五大分類以肝炎部分因試劑停產檢體量降最多分別 107 學年減少 41.85% 和 108 學年的 61.76%，肝炎收入部分 107 學年減少 41.33% 和 108 學年的 58.87%，婦科項目檢量 108 學年少 106 學年 2.73%、比 107 學年少 4.34%，甲狀腺的項目 108 學年比 106 年增 2.13% 但少 107 學年 1.63%，剩餘二大項腫瘤標誌和其它項目於 107 學年分別增加 7.93% 和 0.11%、108 學年則爲 19.3% 和 16.44% 成長，總檢體量 107 學年減少 2.36%、108 學年減少 1.37%。

雖然這三學年的總檢體量約有 1.5 ～ 2.5% 減少，年度總營收 107 學年比 106 學年少 1.45% 但是 108 學年卻比 106 學年增加 2.13%、比 107 學年增加 3.64%。

結論：本實驗室近三學年的檢體量略爲減少但是營收卻是增加的，尤其 108 學年度還碰到新冠肺炎疫情影響醫院管控人流加上肝炎試劑停產，檢體量雖較 106 學年少尤其是肝炎部分，但是腫瘤和其它項目卻是大幅增加而且這二大項的給付也較高，108 學年腫瘤部分的收入分別高於 107 學年 9.52% 和 106 學年 18.13%、其它項目的收入 108 學年則高於 107 學年 22.0% 和 106 學年 27.24%，這些檢驗項目的消長也和臨床醫師診斷和治療需求有關，雖然較早開始使用的放射免疫分析項目如肝炎、婦科和甲狀腺等檢體量因其它科室的快速給報告和其它因素而受影響，但腫瘤標誌和其它的荷爾蒙需求卻明顯的增加，所以本實驗室會持續增開新的檢驗項目和維持良好的報告品質提供臨床醫師更多的信任和選擇。

PC-019

改善核醫科與其他檢查科室同時段排程之衝突

黃慧娥[1] 李將瑄[2] 黃俊瑋[3]

[1] 奇美醫療財團法人柳營奇美醫院核子醫學科
[2] 奇美醫療財團法人奇美醫院核子醫學科
[3] 奇美醫療財團法人奇美醫院臨床病理科

背景介紹：本院各檢查科室排程皆是獨立作業，核醫科每季平均有 3~5 件與其他科室發生同時段排程衝突，核醫藥物如不能依照表訂時間施打，會因放射活度衰減無法使用，進而增加成本支出，且在這些重疊排程個案中有一例抱怨投書案例。

方法：改善方案如下述。(一) 建置電腦排程系統提醒視窗：由資訊室協助將院內檢查科室 (核醫科、放射科及檢查室等) 的電腦排程系統設置聯結，如有同時段重複排程，電腦螢幕會出現警示視窗提醒排程人員，警示視窗內容依據各單位各項檢查需求彙整統一建立。如無特別需求，會以核醫檢查安排於其他檢查之後爲原則進行排程，以減少其他科室人員不必要的輻射曝露。(二) 病人所有檢查於檢查前一日再確認：考量病人數量太多會不易執行，主要針對高價檢查或短半衰期藥物 (如正子檢查)，排程人員於檢查前一日訂藥前，查詢病人未執行的檢驗檢查資料是否有時段重疊，如有排程衝突則電話聯繫其他科室協調。(三) 病人排程時告知如有單日多項檢查或尚未排程的其他科室的檢查，當全部排程後可電話諮詢檢查當日流程順序，排程人員可以反向查詢是否有排程衝突。

結果：在臨床實務 24 個月期間，沒有發生同時段重複事件排程，沒有因重複排程導致的核醫藥物不當浪費，沒有因重複排程導致的客訴事件，其他科室同仁抱怨接受到不必要的輻射曝露較以往減少。

結論：運用電腦排程系統提醒視窗與檢查前一日排程再確認可以有效降低檢查科室同時段排程之衝突，同時可以減少因此導致的核醫成本浪費，避免客訴醫糾發生，增加科室之間和諧。

PC-020

Sarcomatoid Carcinoma of Esophagus Presenting with Lymph Nodal Metastases of Unknown Origin Detected by FDG PET: A Case Report

Yu-Sheng Hung[1], Sheng-Yen Hsiao[2]

[1]*Division of Nuclear Medicine, Department of Medical Imaging, Chi Mei Medical Center, Liouying, Taiwan*
[2]*Division of Hematology-Oncology, Department of Internal Medicine, Chi Mei Medical Center, Liouying, Taiwan*

Introdustion: Sarcomatoid carcinoma of the esophagus is a rare malignancy composed of carcinomatous and sarcomatous elements. Identification of the primary site in carcinoma of unknown primary is challenging in clinical practice. Herein we report a clinical case of a patient who presented with metastatic sarcomatoid carcinoma of unknown origin and esophageal malignancy detected by FDG PET study.

Case report: A 44-year-old man with a history of decompensated liver cirrhosis related to hepatitis C virus, Type 2 diabetes mellitus and hypertension. Multiple enlarged lymph nodes were palpable in the physical examination. CT scan showed multiple lymphoadenopathy in bilateral lower neck, supraclavicular, mediastinum, celiac and retroperitoneal region. Excision of right lower cervical lymph nodes and metastatic sarcomatoid carcinoma proved. Reviewing the previous diagnostic CT images, however, there was no definite evidence of primary malignant lesion found. FDG PET study was further evaluation for the unknown origin and showed marked FDG uptake in low third of thoracic esophagus (SUVmax 9.6), bilateral lower cervical, supraclavicular and retroperitoneal region. Esophageal cancer with nodal metastases was favored. The gastroendoscopy showed esophageal varices, red color sign and ulcer scar, no protruding mass lesion, and biopsy performed in the FDG PET avid esophageal lesion. The pathological report showed tumorous fragments composed of mainly epithelioid tumor cells admixed with few neoplastic spindle-to-plump cells, and positive AE1/AE3 and EMA stain, consistent with sarcomatoid carcinoma.

Discussion: Sarcomatoid carcinoma of the esophagus, also termed carcinosarcoma, pseudosarcoma, spindle cell carcinoma is an unusual malignant tumor with a biphasic histological appearance containing both epithelial and mesenchymal elements. At present, sarcomatoid carcinoma of the esophagus classified as a special subtype of esophageal squamous cell carcinoma, ranges from 0.2% to 2% of all esophageal malignancy in the reported incidence of the neoplasm. In the reported cases, this malignancy can grow to a very large size but remain minimally invasive, commonly attached to the mucosal wall by a pedicle with polypoid appearance. It has a better prognosis than other malignant esophageal neoplasm, maybe due to the characteristic of exophytic growth into the lumen rather than deep invasion, more easily found in the early stage, and resulting in a lower frequency of lymph node metastasis.

Conclusion: Sarcomatoid carcinoma of esophagus is not always typically shows a lobular or polypoidal growth pattern and esophageal wall thickening in imaging studies. FDG PET study is a valuable diagnostic tool in patients with cancer of unknown primary, including sarcomatoid carcinoma of esophagus, and can assists in guiding biopsy.

PC-021

Evaluation of the Body Radiation Exposure Rate of Patients Who Stopped Thyroxine or Injected rh-TSH After I-131 Treatment

Chien-Hua Lu[1], Chiang-Hsuan Lee[2*]

[1]*Division of Nuclear Medicine, Chi Mei Medical Center, Liouying, Tainan, Taiwan*
[2]*Division of Nuclear Medicine, Chi Mei Medical Center, Tainan, Taiwan*

Purpose: This project counts patients who receive inpatient treatment in our hospital, The radiation exposure rate of the body after stopping thyroxine 4 weeks or injecting rh-TSH 2 doses for 24 hours after taking I-131 drugs as a basis for evaluation and judgment.

Method: Patients with thyroid papillary or follicular cancer were counted during the January-July 109. After surgery, they were treated with large doses of I-131 80-175 mCi. They were divided into two groups. the radiation exposure rate was 1 m at 24 hrs after taking the drug. Appropriate health education was given before admission. Using the ATOMTEX AT1121 scintillation detector to detect body radiation exposure.

Results: A total of 58 investigations, the thyroxine discontinuation group, with a total of 41 person.The average dose rate after 24 hrs was 31.17 μSv/hr. The rh-TSH injection group, with a total of 17 person.The average dose rate after 24 hrs was 22.88 μSv/hr.

Conclusion: According to R.O.C. old version of the Atomic Energy Regulations,the hospital's patient's standard for external release and discharge is based on an exposure rate of less than 11 mR/hr at a radioactive intensity of 1 m. The patient can be released and discharged after proper guidance and control. according to the results. The body exposure rate of the two groups of patients after 24 hrs of hospitalization is statistically significant ($p < 0.05$). Although they can be discharged under appropriate guidance and control, However, with the rh-TSH group, the average total-body effective half-life and residual time are shorter, and the exposure to radiation is also less.

PC-022

An Incidental Thymoma on Thallium 201 Myocardial Perfusion Imaging - A Case Report

Shu-Mei Lu, Yu-Ling Hsu

Department of Nuclear Medicine, Ditmanson Medical Foundation Chia-Yi Christian Hospital, Chia-yi, Taiwan

Case report: Here we report a 62-year-old female referred from other hospital who developed intermittent chest tightness for months; worse recently. Duration > 30 mins also combined with dizziness. A chest radiograph showed an anterior mediastinal mass that was confirmed on CT (Fig 1, 2); the mediastinal tumor is suggested by the red arrow.

She underwent a Tl 201 exercise study. Abnormally increased activity was visualized in the Tl 201 images revealed by the red arrow (Fig 3); suggesting probable mediastinal mass. Subsequently, the patient underwent resection of the tumor, which the pathology indicated a thymoma measuring 6.0 x 5.5 x 4.0 cm; type A, stage pT1a. An unanticipated focal extracardiac accumulation during myocardial scintigraphy may lead to further investigation to exclude possible mediastinal tumor. The chest X-ray after the operation can be clearly distinguished from the previous image. (Fig 4.)

Discussion: Thymoma is a rare tumor, although it is the most common primary neoplasm of the anterior mediastinum. In the majority of thymoma patients, imaging is requested for investigation of symptoms related to their tumors. However, an increasing number of asymptomatic patients are discovered incidentally due to the increased utilization of computed tomography for screening or for imaging of other unrelated diseases.

Thallium-201 (Tl-201) is widely used for myocardial perfusion imaging in the evaluation of coronary artery disease, but is also reported to have potential tumor-seeking properties. We incidentally found that the Tl 201 cardiac imaging revealed some unusual uptake, and the pathological results confirmed thymoma. Therefore, as we know, a Tl-201 scan has the potential to play an important role in tumor detection besides ischemic myocardial disease.

PC-023

右位心患者於 CZT SPECT 機器的造影方式 – 病例討論

湯淑雯　顏宏旗　鄭如伶　丁意玲　陳郁艷　邱藍儀　阮文柔　林至群

高雄長庚紀念醫院核子醫學部

背景介紹：心肌血流灌注檢查是核子醫學科常規的檢查項目之一，用於評估冠狀動脈疾病的診斷、術前評估、術後追蹤，皆有非常重要的診斷價值。右位心 (dextrocardia) 通常是心臟在胸腔的位置移至右側的總稱，發病率約爲萬分之二。本次病例討論爲右位心患者在 CZT 機器中以二種不同的造影姿勢造影，比較二種造影姿勢是否有影像上的差異，影響醫師判讀。

方法：新型半導體 (CZT) 技術採用 19 列針孔準直儀，同時採集心臟各角度影像，使用特殊演算法重組，掃描時間只需 3-5 分鐘。應用於右位心患者，採取 2 種造影方式：一種爲類似傳統造影方法請病人平躺，L 型 Detector 轉至病人正面 / 右側收集 5 分鐘影像；另一種方法病人右側躺，L 型 Detector 轉至病人正面 / 右側收集 5 分鐘影像。

結果：二種造影方式影像無明顯的差異，皆可表現心肌血流灌注情形。

結論：傳統的閃爍晶體攝影機使用 2 個低能量高解析度 (LEHR) 準直儀以 L 型，病人平躺方式以 CCW 逆時鐘方向環繞病人心臟 180 度 (RAO-LPO) 收集影像；若是右位心患者造影角度則是以 CW 順時鐘方向 (LAO-RPO) 造影，掃描時間需時 15-18 分鐘。CZT 爲較於傳統的閃爍晶體加碼攝影機具有高能量解析度、高空間解析度、高靈敏度、高對比度、高顯像速度等優點，能大幅縮短照相時間至 3-5 分鐘。此次右位心患者採取二種不同姿勢造影，是因 CZT 機器造影時間短，可以大幅減少病人因爲移動所造成的假影，在不影響醫師判讀的情況下，可採取對病患較爲舒適姿勢進行掃描。

PC-024

Intradural Extramedullary Spinal Cord Metastasis from Tongue Cancer: Detection with F-18 FDG PET/CT

Bor-Tau Hung, Pei-Ing Lee, Yu-Yi Huang

Department of Nuclear Medicine, Koo Foundation Sun Yat-Sen Cancer Center

Abstract

Spinal cord metastases are very rare in head and neck cancer and discovery often corresponds with the onset of neurologic symptoms. F-18 FDG PET and integrated PET/CT have greatly replaced other tests for detection of distant metastases and synchronous second primary tumors with good sensitivity, specificity, and negative predictive value. We present a rare case of recurrent tongue squamous cell cancer that metastasized to the spinal cord. A 44-year-old man presented with urine retention, severe back pain, and bilateral legs weakness two weeks before having a lymph node biopsy to rule out recurrent disease. Restaging F-18 FDG PET/CT examination demonstrated local recurrence, lung, and multiple lymph nodes metastases. In addition, there were multiple hypermetabolic lesions in the spinal cord at the level of T6, T10, T11, and L1, which were highly suspicious for spinal cord metastases. The findings were confirmed on MRI prior to treatment.

PC-025

動態單光子電腦斷層半定量造影技術研究

管子葳[1,3] 陳志成[1] 沈志傑[2] 杜高瑩[3] 曹勤和[3] 陳姿璇[1]

[1] 陽明大學生物醫學影像暨放射科學系
[2] 振興醫療財團法人振興醫院核子醫學科
[3] 台灣基督長老教會馬偕醫療財團法人馬偕紀念醫院核子醫學科

背景介紹：目前臨床傳統核子醫學動態功能性造影，擷取影像方式大多還是以平面式爲主；但是體內器官與組織之間重疊現象會影響分析結果之正確性。本研究以動態單光子電腦斷層造影技術 (Dynamic SPECT, D-SPECT)，克服器官空間上重疊干擾進而在進行動態影像半定量分析時，可得到較準確的生理功能資訊。

方法：本研究屬於前導行研究，以胃臟假體進行模擬胃排空並觀察其殘餘半定量的變化。胃臟假體是以聚乳酸 (polylactic acid, PLA) 爲其材料、容量大小約 750 ml 由 CR-5 3D 列印機製成。本實驗第一階段以臨床所使用之 2D 平面動態液體胃排空造影程序進行造影，2D 平面動態造影條件：30 frame/sec，total time: 90 mins，胃排空殘餘量以原廠分析軟體進行處理作爲基準值；第二階段以動態單光子電腦斷層造影技術再重複液體胃排空程序造影，用 GE INFINIA, PHILIPS BrightView, SIEMENS Symbia T-16 三台伽瑪閃爍攝影機 (gamma camera) 進行實驗。SIEMENS Symbia T-16 原廠掃描模式具有動態單光子電腦斷層造影，於一次造影內每 5 分鐘一圈連續 18 圈 (共 90 分鐘)。此外 GE INFINIA 與 PHILIPS BrightView 以傳統單光子電腦斷層造影依排空時間，收集多次斷層影像作爲模擬動態單光子電腦斷層掃描模式，一次造影：5 分鐘一圈但需要分別收 18 次 (共 90 分鐘)。每種排空速度各機台皆重複三次掃描，由單光子電腦斷層 raw data 重建後獲得 3D VOI-data 後，帶入由 MATLAB 撰寫之後處理程式，可得到胃排空殘餘量活性曲線 (time activity curve, TAC) 及殘存百分比。第三階段於造影第 75 至 90 分鐘時模擬腸道活性影響胃排空殘餘量，以 2D 平面動態造影與 D-SPECT 造影方式進行比較。

結果：馬偕醫院核子醫學科臨床液體胃排空，胃殘餘量參考值在第 60 分鐘只要低於 20% 即屬正常範圍。第一階段本實驗以 2D 平面動態造影方式液體胃排空在第 60 分鐘所得胃假體殘餘量：14.57%；第二階段 D-SPECT 所得到液體胃排空殘餘量分別爲：Siemens：3.33%，GE：15.06%，PHILIPS：1.12%。第 75 至 90 分鐘時模擬腸道活性干擾 2D 平面動態造影所得到殘餘值：(75mins：10.42%，80 mins：19.48%，85 mins：19.51%，90 mins：11.02%)；然而以 3D SPECT VOI data 所得到殘餘值：(75 mins：1.42%，80 mins：1.41%，85 mins：1.35%，90 mins：1.02%) 可以有效修正腸道重疊所造成排空數據誤差 (P = 0.017)。

結論：本研究以 D-SPECT 造影方式而得到 “3D SPECT VOI data”，可以解決因空間上器官重疊所造成胃排空殘餘半定量數據之誤差。

PC-026

核醫輻射工作人員體外輻射劑量紀錄分析—以北部某醫學中心爲例

林智偉　周榮鴻　楊邦宏　黃文盛

臺北榮民總醫院核醫部

背景介紹：「輻射工作場所管理與場所外環境輻射監測作業準則」第 15 條明定「輻射工作場所之劃定與管制，除應考量工作人員個人之劑量外，亦應合理抑低集體劑量。」本研究目的在於分析核醫輻射工作人員體外輻射劑量紀錄，提出有助於降低集體劑量的建議。

方法：選取北部某醫學中心 44 位核醫輻射工作人員熱發光劑量計 (TLD) 佩章與指環劑量記錄，採計 108 年度年累積 HP (10) 人體深度 10mm 個人佩章等效劑量 (mSv)，其中 14 名人員配置指環，紀錄年累積 HP (0.07) 手部深度 0.07 mm 等效劑量 (mSv)，34 位人員年資超過五年，另採計五年週期 HP (10) 個人等效劑量 (mSv)。後續依人員性別、年資、是否配戴指環與職別分組，分析各組間等效劑量差異。

結果：年累積 HP (10) 最大值 2.21，平均值 0.48±0.63，18 位女性與 26 位男性佩章劑量無顯著差異 (Mann-Whitney U = 204, p = ns)，配戴指環與未配戴指環人員佩章劑量亦無顯著差異 (Mann-Whitney U = 186, p = ns)。然而，10 位年資少於五年的工作人員，其年累積 HP (10) 顯著高於 34 位年資超過五年者 (Mann-Whitney U = 89, p = 0.022 < 0.05)。依職別區分爲醫師護理師、放射師、其他人員與放化製藥組，四組人員佩章劑量具顯著差異 (Kruskal-Wallis Chi-square = 21.95, df = 3, p = 0.000 < 0.05)，放射師年累積 HP (10) 平均值 1.08±0.41 顯著高於各組，其他各組間則無顯著差異。年資超過五年者，年累積 HP (10) 與五年週期 HP (10) 劑量紀錄達顯著正相關 (Pearson's r = 0.98, p = 0.000 < 0.05)。14 名配置指環人員分屬醫師護理師與放化製藥組，年累積指環 HP (0.07) 最大值 57.49，平均值 17.90±17.29，指環劑量不因性別、職別或年資有所差異。

結論：本研究之核醫輻射工作人員職業曝露符合「游離輻射防護安全標準」，仍建議定期檢視並分析人員劑量記錄，適時調派工作任務分配，加強不同職別人員輻射防護專業知能，落實各項防護操作，降低集體劑量。

PC-027

促腎上腺皮質素 (ACTH) 低於放射免疫分析法最低標準液濃度之數據論證

曾翠芬[1] 劉怡慶[1] 張朝鈞[2] 古琴鳳[1] 許玉春[3] 林家揚[1,3] 張晉銓[1,3]

[1] 高雄醫學大學附設中和紀念醫院核醫部放射免疫分析組
[2] 奇美醫療財團法人奇美醫院核醫科放射免疫分析實驗室
[3] 高雄醫學大學附設中和紀念醫院核醫部閃爍攝影組

背景介紹：促腎上腺皮質激素 (Adrenocorticotrophin 或 ACTH) 由腦下垂體前葉分泌受到下視丘分泌之促腎上腺皮質激素釋放因子 (CRF) 與皮質醇負回饋調控，測定 ACTH 能夠幫助診斷腎上腺分泌不足或過量，低濃度的 ACTH 則發生於腎上腺分泌不足可能是繼發性腦下腺功能障礙所引起。本實驗室所使用套裝試劑的生物參考區間 10-50 pg/mL 但是其標準液的最低濃度爲 15 pg/mL 所以需論證 10-15 pg/mL 區間的數據發報告標準模式。

方法：泡製 CIS bio international ELSA-ACTH 套裝試劑的所有標準液和稀釋液，然後利用試劑所附之稀釋液 2X 稀釋 S1、S2 和 S3 等 3 瓶低濃度標準液 (方法一)，再取另一瓶未泡製的 S1 最低標準液加入 2X 的 H2O (方法二)，最後不使用上面二種方式直接通過原點使用原始報告 (方法三) 分別將小於 15 pg/mL 的檢體做 inter-run (N25) & intra-run (N57) 檢測。γ-counter 廠牌 Wizard、統計軟體使用 Microsoft office Excel 2007。

結果：方法一最低三點 (S1、S2、S3) 的稀釋液稀釋，其 cpm 還高於原濃度、方法二加 2 倍水泡製 S1 其 cpm 同方法一並未將其濃度降低所以上述二法不可行，只能採用通過原點方式來發報告。inter-run 的 CV% 從 1.15 ～ 43.67 (平均 14.41)、intra-run 的 CV% 從 0.63 ～ 20.41 (平均 7.02)，inter-run & intra-run 分別有 24% 和 7% 的結果沒有落在相同的 10-15 pg/mL 區間，外部品管液 RANDOX 報告一樣採用方法三，其結果 cycle 17 sample 5 和 sample 6 及 cycle 18 sample 5 結果分別爲 7.78、10.94、17.92 皆小於 2SDI 允收。

結論：ACTH 是由 39 個胺基酸所組成的多胜肽，分子量爲 4,500 道爾敦，等電點爲 pH 4.65 ～ 4.7，臨床檢體需使用含 EDTA 之 plasma 冰浴運送，因 inter-run 檢體已重複退冰操作 CV% 相對的也比 intra-run 大 2X 左右值越低 CV% 也越大，intra-run 因是同次操作所以較穩定變異也小，從 2019 年至 2020 年的 7 月本實驗室外部品管液 RANDOX 報告 3 次的低值也符合允收標準 (高值允收 OK) ，直接通過原點的報告臨床醫師尚未有質疑出現。試劑說明書提及檢體數值很高時不可用外插法算取濃度需使用試劑盒裡的稀釋液作稀釋，但未提及低濃度不可使用此方法且本試劑的偵測極限 2 pg/mL 所以方法三是本實驗室小於 15 pg/mL 的數據主要發報告的標準。

PC-028

Diagnosis Performance of Tc-99m MDP Bone Scan for Malignant Pleural Effusion in Newly Diagnosed Lung Cancer

Yu-Zhen Qiu[1], Shih-Chin Chou[1], Tzyy-Ling Chuang[1,2], Yuh-Feng Wang[1,2]

[1]*Department of Nuclear Medicine, Dalin Tzu Chi Hospital, Buddhist Tzu Chi Medical Foundation, Chiayi, Taiwan*
[2]*School of Medicine, Tzu Chi University, Hualien, Taiwan*

Introduction: Tc-99m MDP accumulation in the pleural cavity occurs occasionally in the whole-body bone scan. In this study, we want to know the diagnosis performance of Tc-99m MDP bone scan for detecting malignant pleural effusion in newly diagnosed lung cancer.

Methods: From September 7th, 2018 to July 7th, 2020, newly diagnosed lung cancer cases in our hospital with CT evidence pleural effusion and bone scan examination within 30 days were included. Positive pleural finding at bone scan was defined as asymmetrically increased Tc-99m MDP accumulation in the ipsilateral hemithorax. Diagnosis of pleural metastases was based on pathology result or clinical manifestation of pleural lesions.

Results: 43 patients, 12 women (27.9%) and 31 men (72.1%), from 49 to 96 (72±11) year-old were included and analysis. 26 (60.5%) patients was diagnosed as pleural metastases. There were 8 (18.6%) patients with positive pleural finding at bone scan and all of them were diagnosed as pleural metastases. Among 35 patients with negative pleural finding at bone scan, 18 patients were diagnosed as pleural metastases. Only 8 (30.8%) of 26 patients with pleural involvement showed positive pleural finding at bone scan. The sensitivity, specificity, positive predict value (PPV), negative predict value and accuracy for bone scan to detect pleural involvement in newly diagnosed lung cancer were 30.1%, 100%, 100%, 48.6% and 58.1%, respectively.

Conclusions: Although only 30.8% pleural metastases are detected by bone scan, Tc-99m MDP bone scan avid pleural lesion is a specific finding for pleural metastases in the newly diagnosed lung cancer.

PC-029

Radioactive Iodine-131 Might be a Helpful Therapy in Metastatic Hurthle Cell Carcinoma of Thyroid: A Case Report

Yu-Zhen Qiu[1], Shih-Chin Chou[1], Tzyy-Ling Chuang[1,2], Yuh-Feng Wang[1,2]

[1]*Department of Nuclear Medicine, Dalin Tzu Chi Hospital, Buddhist Tzu Chi Medical Foundation, Chiayi, Taiwan*
[2]*School of Medicine, Tzu Chi University, Hualien, Taiwan*

Introduction: We present a case of thyroid Hurthle cell carcinoma with multiple pulmonary metastases and discuss the utility of I-131 treatment in this clinical situation.

Case Report: This 63-year-old female case with history of Schizophrenia suffered from progressive neck swelling for one year. Head and neck CT showed bil. thyroid enlargement trachea compression and an LUL lung 0.5 cm nodule. Near total thyroidectomy was done and pathology revealed Hurthle cell carcinoma. She was then referred to radiotherapy for locoregional disease control. However, bilateral multiple pulmonary nodules/masses were noted at simulation CT. Once she cannot care herself, isolation room was not suitable for her. She also cannot swallow capsule. After adequate duration of low iodine diet and no thyroxine therapy, liquid-form I-131 145 mCi in divided five doses (29 mCi, each dose) were given by mouth, every three to four days. The I-131 whole body with SPECT/CT study at 4 days after the lase dose of I-131 showed increased I-131 uptake in the thyroid bed, neck small lymph nodes, bilateral lung nodules and masses, left parietal bone and left 9th rib. Remnant/tumor and functional metastatic lesions were suspected. Then she was under thyroxine treatment. Four months later, Tg decreased and shrinkage of bilateral lung lesions were noted by CT.

Conclusions: Thyroid Hurthle cell carcinoma, accounts about 3 to 5% of thyroid cancer, is a relative rare subtype of thyroid cancer. About 90% of thyroid Hurthle cell carcinoma cannot uptake I-131 in the literature review, and operation should be considered first in resectable cases. However, in multiple metastatic status, high-dose I-131 might be helpful for functioning metastatic lesions and still should be considered.

PC-030

Discussion on PET-CT Malfunction with the Temperature and Humidity

Chia-Hao Chang[1], Yu-Sheng Hung[1], Chiang-Hsuan Lee[2*]

[1]*Division of Nuclear Medicine, Department of Medical Imaging, Chi Mei Medical Center, Liouying, Tainan, Taiwan*
[2]*Division of Nuclear Medicine, Department of Medical Imaging, Chi Mei Medical Center, Tainan, Taiwan*

Purpose: Positron emission and computer tomography (PET-CT) scanners are commonly used equipment in nuclear medicine department. Scintillation crystals and other electronic components are very sensitive to temperature and humidity. Our department and PET-CT room is in the basement and open-air garden above it. Equipment malfunction may be related to the temperature and humidity greatly. We try to explore its relevance in this study.

Material and Method: PET-CT scanner in our division (GE, Discovery ST) was installed in 2005. Central air conditioning system in the PET-CT room was set at 22 degrees Celsius and we maintain humidity by dehumidifier (Panasonic, F-Y12ES). We record temperature and humidity by temperature and humidity recorder (TECPEL, TR-72Ui), every 30 minutes once per day. The recorder is calibrated every year.

And we retrospectively view the temperature and humidity records with equipment malfunction records to explore its relevance.

Result: Retrospectively view the temperature and humidity records from June 2019 to July 2020, we got 30290 records. GE engineer suggest that temperature should be 15-24 degrees Celsius, temperature difference every hour should be in 1 degrees Celsius; and humidity should be 30-60%. We found 81 abnormal temperature records, 2681 abnormal humidity records, and 22 PET-CT malfunctions in this period. After consulting GE engineer, we think only 5 events is likely related to temperature and humidity.

Conclusion: Cause of equipment malfunction includes service life, poor control on temperature and humidity, unstable voltage, improper operation, etc. It's difficult to confirm the malfunctions are related to abnormal temperature and humidity directly. Although abnormal temperature and humidity within a limited range may not cause equipment malfunction definitely, we should still try to control the temperature and humidity in proper range to avoid shortening the service life of equipment.

PC-031

Shorter than Standard Imaging Acquisition Time for F18 Florbetaben Amyloid Brain PET Might be Feasible (Experience of Taipei Veterans General Hospital)

Tse-Hao Lee, Chia-Jung Chang, Yi-Lun Chen, Wen-Sheng Huang

[1]*Department of Nuclear Medicine, Taipei Veterans General Hospital, Taipei, Taiwan*

Introduction: According to SNMMI-EANM Practice Guideline for Amyloid PET Imaging of the Brain. The recommended imaging acquisition time is twenty minutes when using F18 Florbetaben as the radiophamaceutical. We managed to find the feasibility of shorter acquisition time than 20 minutes, in which the image result might be acceptable.

Methods: We included 20 patients who received F18 Florbetaben amyloid brain PET. PET/CT started 90 minutes after intravenous administration of F18 Florbetaben. We used list mode for dynamic image acquisition for 20 minutes and reconstructing PET images of acquisition duration of 5, 7, 10, and 20 minutes. For each patient, we calculated the SUVR of bilateral temporal, frontal, precuneus/posterior cingulate gyrus and parietal regions to cerebellum (reference region) in PET images from different acquisition duration (5, 7, 10 and 20 minutes).

Results: We observed that the SUVR (bilateral temporal regions to cerebellum) was not significantly different between 5, 7, 10 minutes duration images and 20 minutes duration image. The similar finding was also observed for SUVR (frontal to cerebellum), SUVR (precuneus/posterior cingulated gyrus to cerebellum) and SUVR (parietal to cerebellum) in different time duration images.

Conclusions: Using list mode with shorter than standard time (20 minutes) image acquisition for F18 Florbetaben brain PET might be feasible, which might help for patients who were uncooperative for long time image study.

PC-032

Automated cGMP-Grade Production of High Specific Activity C-11 Pittsburgh Compound B (PIB) as a PET Imaging Probe for Alzheimer's Disease

Wen-Yi Chang, Shih-Pei Chen, Chun-Tse Hung, Geng-Ying Li, Chi-Wei Chang, Wen-Sheng Huang

Department of Nuclear Medicine, Veterans General Hospital, Taipei, Taiwan

Introduction: The imaging of beta amyloid (Ab) plaque is high correlation for diagnosis Alzheimer's Diseases. During the last decade, additional optimized radio-syntheses of C-11 PIB have been published in the literature. Although these radio-syntheses proved to be reliable and easily adaptable to a GMP compliant production for patients, and the specific activity (SA) of C-11 PIB were 6-74 GBq/μmol. The imaging quality of brain is high correlation with SA value. Therefore, high SA C-11 PIB (190.6±51 GBq/μmol) was produced by Automated cGMP system in Veterans General Hospital (Taipei, Taiwan).

Methods: Synthesis C-11 PIB was followed by the reported method by Mathis et al. In National PET/Cyclotron Center of Taipei Veterans General Hospital, C-11 PIB was performed by Eckert & Ziegler (EZ) synthesizer. Radio-labeling precursor and reagents were commercially available. The standard criteria for production radiopharmaceutical are according Current Good Manufacturing Practice (cGMP). Quality control included radio-chemical purity, pH value, MCA analysis and specific activity analysis, et al. Stability test was performed up to 2 hours after end of synthesis.

Results: cGMP production of C-11 PIB was successful performed in our center with 6.7±3.6% radiochemical yield. QC results of radio-chemical purity, pH value, and specific activity analysis were 99.9%, 7.5, 190.6±51 GBq/μmol, respectively. C-11 PIB was had high stability in ethanol/saline (1/9) solution (> 99%, purity after 2h incubation).

Conclusions: cGMP production of high specific activity C-11 PIB is successful setup in National PET/Cyclotron Center of Taipei Veterans General Hospital. C-11 PIB may be used as PET probes for noninvasive evaluation of beta amyloid (Ab) plaque related Alzheimer's Diseases.

PC-033

Spinal Cord Benign Psammomatous Meningioma Mimicking Malignancy on FDG PET/CT

Tzyy-Ling Chuang[1,2], Yuh-Feng Wang[1,2,3]

[1]*Department of Nuclear Medicine, Dalin Tzu Chi Hospital, Buddhist Tzu Chi Medical Foundation, Chiayi, Taiwan*
[2]*School of Medicine, Tzu Chi University, Hualien, Taiwan*
[3]*Center of Preventive Medicine, Dalin Tzu Chi Hospital, Buddhist Tzu Chi Medical Foundation, Chiayi, Taiwan*

Introduction: We present a case, with right neck pain, was found spinal cord meningioma mimicking malignancy on FDG PET/CT when undergoing cancer survey.

Case report: A 62-year-old female had progressively developed right neck throbbing pain for one year. The throbbing pain, with radiation to right suboccipital area, sometimes accompanied with breathless sensation. The episodes were noted more often in recent three months. The symptoms improved after taking medication from LMD. She received PET/CT for cancer survey in health exam and it showed an intra-spinal cord FDG-avid calcified mass at the level of 1st cervical spine, SUVmax = 7.9 (initial), 8.2 (delayed). MRI showed an extra-medullary, intracanalicular oval mass at C1 level, displacing and compressing the cord to the left anterior aspect. It is hypointense on T1WI, T2WI and STIR images. It exhibits mild parenchymal enhancement and stronger rim enhancement after IV gadolinium administration. She received laminectomy with tumor removal; pathology showed tumor with many calcified psammoma bodies within proliferative meningothelial cells and concluded psammomatous meningioma, WHO grade I.

Discussion: A meningioma is a tumor that grows in the protective lining of the brain and spinal cord, called the meninges. Most are benign, though in rare cases they can be malignant. Meningiomas account for approximately 25% of spinal canal tumors. Spinal meningiomas represent a minority of all meningiomas (approximately 12%). The majority of patients present with motor deficits as a result of compression of the spinal cord. Less common presentations include sensory deficits, pain and sphincter dysfunction. On T1WI and T2WI MRIs, meningiomas have variable signal intensity. Meningiomas enhance intensely and homogeneously after injection of gadolinium gadopentetate. The edema may be more apparent on MRI than on CT scanning. FDG PET has been commonly used in patients with primary brain tumors for tumor grading, determination of the prognosis of patients, and discrimination of tumor recurrence from radiation necrosis. Studies also show the correlations between FDG uptake and the histopathological grade and between FDG uptake and biological aggressiveness of the intracranial meningioma. Psammomatous meningioma is a histologic subtype of meningioma usually presented as a heavily calcified intracranial or spinal mass lesion. Recurrence rates of this tumor after a surgery are related also to a young age (< 50 years), multiple lesions, calcification extension, and ossification. We present an interesting case of intense FDG-avid psammomatous meningioma at spinal cord classified as a benign meningioma (WHO grade I).

PC-034

Ga-67 Scan SPECT/CT Showed Right Huge Tubo-ovarian Abscess

Tzyy-Ling Chuang[1,2], Yuh-Feng Wang[1,2,3]

[1]*Department of Nuclear Medicine, Dalin Tzu Chi Hospital, Buddhist Tzu Chi Medical Foundation, Chiayi, Taiwan*
[2]*School of Medicine, Tzu Chi University, Hualien, Taiwan*
[3]*Center of Preventive Medicine, Dalin Tzu Chi Hospital, Buddhist Tzu Chi Medical Foundation, Chiayi, Taiwan*

Introduction: We present a case with unknown infection cause showed right huge ovarian gallium-avid lesion on Ga-67 SPECT/CT and proved to be tubo-ovarian abscess by surgery.

Case report: A 58-year-old female had 1) hypertension and diabetes mellitus under medication for two years, 2) ESRD under hemodialysis (HD). She had fever and chills after HD on the admission date. Tracing her recent history, she claims no close contact to influenza patient or travel history to local transmission area recently. Her vital signs were BP 175/91 mmHg, HR 110 bpm, body temperature 39.6°C. The laboratory data showed leukocytosis with bandemia, hyponatrimia, hypokalemia, elevated CRP and Procalcitonin. Test of COVID-19 by throat swab showed negative result. The CT revealed RML pneumonia, multiple uterine calcifications, R/O right ovarian hemorrhagic cysts or cystic neoplasm. Clinical showed infections with cause unknown even under empirical antibiotic. Ga-67 scan showed a fixed uptake at the sacral/rectal region; SPECT/CT showed uterine calcifications and an enlarged gallium-avid lesion with central cold at R/O right ovarian region. Laparoscopic assisted vaginal hysterectomy and bilateral salpingo-oophorectomy were done on 2020/06/05. Surgical finding and pathological result showed right huge tubo-ovarian abscess (TOA) of right adnexa.

Discussion: A TOA is a complex infectious mass of the adnexa that forms as a sequela of pelvic inflammatory disease. Classically, a TOA manifests with an adnexal mass, fever, elevated WBC, lower abdominal-pelvic pain, and/or vaginal discharge; however, presentations of this disease can be highly variable. Should the abscess rupture, life-threatening sepsis can result, thus any clinical concern for this diagnosis requires prompt evaluation and treatment. Gallium-67 scan has been used to localize infection for over 30 years. In our case, whole body Ga-67 images showed equivocal pelvic uptake. The hybrid imaging SPECT/CT mapped functional anomaly to the anatomic structure precisely and thus helped discriminating pathologic uptake in the right ovarian abscess from the physiological uptake in rectum and guiding surgery treatment.

PC-035

Incidentally Gallbladder Uptake in Bleeding Scan

Tzyy-Ling Chuang[1,2], Yuh-Feng Wang[1,2,3]

[1]*Department of Nuclear Medicine, Dalin Tzu Chi Hospital, Buddhist Tzu Chi MedicalFoundation, Chiayi, Taiwan*
[2]*School of Medicine, Tzu Chi University, Hualien, Taiwan*
[3]*Center of Preventive Medicine, Dalin Tzu Chi Hospital, Buddhist Tzu Chi Medical Foundation, Chiayi, Taiwan*

Introduction: We present a case, with multiple morbidity, showed intense gallbladder uptake incidentally at the bleeding scan.

Case report: A 84-year-old female had 1) coronary artery disease (triple vessel disease) s/p percutaneous coronary intervention and coronary artery bypass graft, 2) old right middle cerebral artery territory cerebrovascular accident, 3) liver cirrhosis, Child A, previous HBV infection related, 4) chronic kidney disease, stage IIIB, 5) type II diabetes mellitus, 6) hypertension. According to her caregiver, bloody stool was noted this morning. Frequently vomiting was also noted recently without coffee ground. Laboratory examination reported leukocytosis with neutrophil predominance, hyponatremia, poor renal function and hyperglycemia. PES revealed gastric ulcers and duodenal ulcers. Pantoprazole was administered. However, persisted dark-red stool passage was noted. RBC bleeding scan showed faintly increased uptake of radiotracer was found around in the small bowel on the 24 hours SPECT/CT view that probably represented the small bowel bleeding. Moreover, 24 hours SPECT/CT also showed liver cirrhosis and intensely increased uptake to the gallbladder. Fortunately, the melena was improved gradually, and became brown-color stool.

Discussion: Increased gallbladder uptake of labeled red blood cells was associated with chronic renal disease, anemia, hemolysis, and earlier multiple blood transfusions. It has been described that gallbladder uptake probably is due to breakdown of hemoglobin to bilirubin. Technetium bound to the porphyrin group of degraded hemoglobin, which is consequently excreted to the biliary system through liver metabolism. This may relate to the association of renal impairment involving increased erythrocyte damage. This mechanism would be expected to result in gallbladder uptake on significantly (ie, 12–24 hour) delayed images. We should aware that radioactivity can be excreted in bile thus gallbladder activity may not represent hemobilia.

PC-036

Visible CAPD Dialysate Leakage to Right Hydrothorax

Tzyy-Ling Chuang[1,2], Yuh-Feng Wang[1,2,3]

[1]*Department of Nuclear Medicine, Dalin Tzu Chi Hospital, Buddhist Tzu Chi Medical Foundation, Chiayi, Taiwan*
[2]*School of Medicine, Tzu Chi University, Hualien, Taiwan*
[3]*Center of Preventive Medicine, Dalin Tzu Chi Hospital, Buddhist Tzu Chi Medical Foundation, Chiayi, Taiwan*

Introduction: We present a case, with systemic lupus erythematosus (SLE) and under peritoneal dialysis (PD), showed visible dialysate leakage to right hydrothorax at the peritoneal scintigraphy.

Case report: A 45-year-old female had 1) SLE with lupus nephritis with pleuritis, pericardial effusion and polyarthritis in 2005/11, loss follow up since 2006/06, 2) chronic renal failure s/p PD since 2010. Chest radiography in two months ago showed opacification in the right laterobasal hemithorax, presumably due to pleural thickening/fluid collection. Because of pleural and/or pulmonary pathology, heart size cannot be estimated accurately. Chest tapping of effusion showed transudate, no inflammation and negative for malignant cell. Pleural effusion due to PD or SLE was considered. Peritoneal scintigraphy was performed with Tc-99m DTPA added to 1.5 L peritoneal dialysate and infused into the peritoneal cavity. In addition to the radiotracer accumulation in the peritoneal cavity, the radiotracer appeared in the right lung region at 120 minutes planar images and was localized to the right pleural effusion shown on the 2nd hour SPECT/CT.

Discussion: PD is an established renal replacement therapy for patients with end-stage renal disease, and it is an effective treatment to maintain patients' residual renal function and quality of life. Although uncommon, hydrothorax is a well-recognized complication of PD. The postulated mechanisms of its pathogenesis are pleural–peritoneal communication (due to increased intra-abdominal pressure when instilling PD fluids), congenital or acquired anatomic defects of the diaphragm, and defective lymphatic drainage. Right-sided pleural effusion is more common. Many modalities have been used to diagnose pleural–peritoneal communication, including pleural fluid analysis, CT or magnetic resonance imaging peritoneography. Peritoneal scintigraphy is a rapid and adequate method for showing peritoneal leakage, and it can also be used to demonstrate areas of leakage in the pleural cavity. Moreover, fused SPECT/CT images may provide anatomical information on trans-diaphragmatic leakage.

PC-037

Ga-67 Scan with SPECT/CT Showed Generalized Hidradenitis Suppurativa

Tzyy-Ling Chuang[1,2], Yuh-Feng Wang[1,2,3]

[1]*Department of Nuclear Medicine, Dalin Tzu Chi Hospital, Buddhist Tzu Chi Medical Foundation, Chiayi, Taiwan*
[2]*School of Medicine, Tzu Chi University, Hualien, Taiwan*
[3]*Center of Preventive Medicine, Dalin Tzu Chi Hospital, Buddhist Tzu Chi Medical Foundation, Chiayi, Taiwan*

Introduction: We present a case with generalized hidradenitis suppurativa shown on Ga-67 scan with SPECT/CT.

Case report: A 42-year-old male had scalp, right calf, back and bilateral buttock nodules with leukocytosis intermittently since 2017. In 2020/06/20, he had fever and body aches for one day. Physical examination showed hidradenitis suppurativa over buttock for years - now right buttock redness noted. The laboratory data showed leukocytosis (21.42*10^3/ul) with elevated CRP (25.06 mg/dl). He was treated by debridement and antibiotics (Oxacillin and Ceftriaxone). Debridement of right buttock hidradenitis suppurativa (2020/06/26) showed acute inflammation with abscess formation; wound culture grew Prevotella disiens and Peptostreptococcus magnus (Finegoldia magna). Due to unresolved inflammatory markers (WBC 18.56*10^3/ul, CRP 20.67 mg/dl), Ga-67 scan was arranged and antibiotics were adjusted to Linezolid and Meropenem. Ga-67 scan with SPECT/CT (2020/06/29) showed multiple sites (skin/subcutaneous lesions of right posterior neck, right axilla, left groin, bilateral buttock and right medial thigh) of enhanced uptake which compatible with his generalized hidradenitis suppurativa. Debridement of right thigh and bilateral inguinal regions (2020/06/30) showed right thigh and bilateral inguinal hidradenitis suppurativa; wound culture grew Prevotella disiens and Prevotella bivia. His conditions improved gradually ten days later (WBC 8.25*10^3/ul and CRP 2.85 mg/dl).

Discussion: Hidradenitis suppurativa is a chronic, recurrent, and debilitating skin condition. It is an inflammatory disorder of the follicular epithelium, but secondary bacterial infection can often occur. The diagnosis is made clinically based on typical lesions (nodules, abscesses, sinus tracts), locations (skin folds), and nature of relapses and chronicity. Hidradenitis suppurativa with serious infection can present with fever and septicemia. Staphylococci, streptococci, peptostreptococci, Prevotella, Fusobacterium and Bacteroides spp. were the majority of the isolated bacteria. Apart from binding to lactoferrin, Ga-67 may localize in sites of infection by exchanging with iron in siderophores secreted by bacteria. Ga-67 scan with SPECT/CT with its anatomic localization of suggestive foci of increased tracer uptake enabled the diagnosis of infection sites of hidradenitis suppurativa more precisely.

PC-038

A Subcortical Tumor Incidentally Found in A Cognitive Impairment Patient using ^{18}F-FDG PET/MR

Jiun-Ying Chern[1], Jong-Ling Fuh[2], Bang-Hong Yang[1], Chien-Yin Lee[1], Yu Kuo[3], Wen-Sheng Huang[1]

Departments of [1]Nuclear Medicine/National PET & Cyclotron Center, [2]Neurology and [3]Radiology, Taipei Veterans General Hospital, Taipei, Taiwan

Introduction: Except for detecting malignancies, ^{18}F-FDG is useful in evaluating different kinds of dementia. PET/MR on the other hand, is more capable to detect brain lesions than PET/CT. We represent a patient with mild cognitive impairment incidentally found a subcortical tumor seen on ^{18}F-FDG PET/MR and its characteristic imaging patterns.

Method: The patient was referred from a neurologist for evaluating the status of dementia using ^{18}F-FDG PET/MR. The patient fasted 6 hr and laid in supine position with a head holder fixation. The PET and MR imaging were acquired simultaneously 30 min after 5 mCi ^{18}F-FDG iv injection using a GE SIGNA 3T PET/MR machine equipped with cortex ID software. The imagines were displayed in coronal, sagittal and transverse views and also 3D rendering imaging for quantitative analyses.

Result: Except for a generalized decrease of ^{18}F-FDG uptake in the left hemisphere, an unusually ring shaped high metabolic area was incidentally found in the right thalamic/subthalamic area. The concomitant MR showed a heterogenous space occupying lesion about 41 x 37 x 36 mm in size involving thalamus, right aspect of midbrain and invading into the third ventricle. The previous brain CT was normal 2 years ago with normal cognitive status. The patient received surgical removal of the tumor and resolved the mental problems.

Discussion and Conclusion: Although the high physiologic ^{18}F-FDG uptake will be found in the normal brain and will potentially mask neoplastic lesions, it will be less affected in the subcortical areas. The MR imaging provided additional information in delineating lesion margin and involved subtle structure that might enable us to realize the interplay between lesion characteristics and presented clinical symptoms/signs. A previous study showed a 94% sensitivity and 77% specificity for ^{18}F-FDG PET in detecting high grade gliomas. Combined MR increased its specificity and might provide an important role in the management of brain malignancies in the visible near future.

PC-039

Tc-99m Heat-damaged Red Blood Cell Scintigraphy with SPECT/CT for Hepatic Splenosis: Cases Report

Chun-Pang Huang, Hong-Jie Chen, Chien-Chin Hsu

Department of Nuclear Medicine, Kaohsiung Chang Gung Memorial Hospital, Kaohsiung, Taiwan

Introduction: Splenosis is autotransplantation of splenic tissue after traumatic splenic rupture or splenectomy. Hepatic splenosis refers to a heterotopic implantation of splenic tissue in the liver or perihepatic region. To distinguish intra- or peri-hepatic splenosis from a malignant liver tumor with sonography, CT or MRI is difficult. Tc-99m heat-damaged red blood cell (RBC) scintigraphy is a method of high specificity for splenic tissue. With a SPECT/CT technique, intra- or peri-hepatic splenosis can be accurately demonstrated to avoid invasive biopsy, resection, or treatment.

Case 1: A 42-year old man has history of splenectomy after blunt abdominal trauma. A S6 liver tumor was found by sonography incidentally. The CT and MRI revealed early enhanced and early washout tumors in the S6 and perihepatic region. Tc-99m heat-damaged RBC SPECT/CT demonstrated that all the S6 and perihepatic tumors are splenosis. The lesions have been stable for 7 years without treatment.

Case 2: A 71-year-old male patient is a case of hepatitis B and C virus related liver disease. He has history of splenectomy after blunt abdominal trauma. Liver tumors were found by sonography and AFP level was rising to 105 ng/ml. The CT and MRI revealed three tumors in the S6, S2 of liver and left subphrenic region. Tc-99m heat-damaged RBC SPECT/CT demonstrated that S2 and left subphrenic tumors are splenosis. After treatment for the S6 tumor, the AFP level returned to normal range.

Conclusion: Tc-99m heat-damaged RBC scintigraphy with SPECT/CT can accurately demonstrate hepatic splenosis to avoid invasive biopsy, resection, or treatment.

PC-040

Preliminary Experiences Using Ga-68 PSMA-11 PET/CT as A Treatment Response Evaluation Modality in Treatment-Naïve Prostate Cancer Patients

Jing-Ren Tseng[1,2], Shu-Ju Tu[2], Tzu-Chen Yen[3]

[1]*Department of Nuclear Medicine, New Taipei Municipal TuCheng Hospital (Built and Operated by Chang Gung Medical Foundation), New Taipei City, Taiwan*
[2]*Department of Medical Imaging and Radiological Science, College of Medicine, Chang Gung University, Taoyuan, Taiwan*
[3]*Nuclear Medicine and Molecular Imaging Center, Chang Gung Memorial Hospital at Linkou, Taoyuan, Taiwan*

Introduction: The role of using molecular imaging as a treatment response evaluation modality in prostate cancer patients remains unclear. This prospective trial was designed to identify the ability of Ga68-PSMA-11 PET to evaluate the patients with prostate cancer, especially under the circumstance of advanced stage patients will undergo long-term androgen deprivation therapy.

Methods: Between July 1, 2019 and April 30, 2020, a total of 22 patients diagnosed with prostate cancer has been enrolled in this study. Three participators withdrew and one subject expired during follow-up period. Total 12 cases completed two stage Ga-68 PSMA-11 PET scan before the end of the April. To be eligible for inclusion, each patient must fulfill all of the following criteria: (1) Males with 40-85 years of age and life expectancy more than 3 months. (2) Pathology-proved prostate cancer patients and classified as clinical stage III and IV (including lymph node or bone metastasis) (3) Willing to sign the informed consent. Patients with previous cancer history and impaired renal functions will be excluded from the trial.

For Ga-68 PSMA-11 PET/CT scan, the subject will have catheter(s) placed for intravenous administration of [68Ga]PSMA-11. Subjects will receive a single intravenous bolus of 2-5 mCi [68Ga]PSMA-11 and received PET/CT scan 60 minutes later. The data acquisition begin with non-contrast CT at 120kVp, automated mAs, and a pitch of 1.5, followed by PET acquisition from the mid-thigh to vertex, 3 minutes each bed. After image acquisition, the subject will be observed for half an hour, and will be discharged if no adverse event happens. EKG, blood and biochemistry test will be performed before and after scan no more than two weeks. Patient will underwent two times of PSMA-11 PET/CT scans before and under androgen deprivation therapy within a 10-14 weeks interval.

Results: Of the 12 studied patients, all had positive Ga-68 PSMA-11 PET/CT findings. Of them, 8 (66%) had their clinical staging status changed after PET scan. We also measured the SUVmax value of representative lesions before and underwent treatment. The percentage of decreased value change of each lesion was measured. The SUVmax change of main tumor is between 22% to 100%; the change of nodal lesion is between 70%-100%; and bone lesion is between -7%-100%.

Conclusions: Ga-68 PSMA-11 PET/CT scan is possible to replace conventional imaging by giving additional diagnostic information. Different lesions types may show different treatment response while using Ga-68 PSMA-11 PET/CT scan as evaluation modality. The nodal lesions had best treatment response rate between 70%-100%, whereas bone lesions showed greatest variation between -7%-100%. PET imaging indices using the concept of metabolic volume should be considered as alternative imaging biomarker based on the results that some prostate tumor have significant tumor volume change but less SUVmax value change.

PC-041

I-131 治療病人外釋廢棄物之輻射安全性

陸建華[1] 李將瑄[2]

[1] 奇美醫療財團法人柳營奇美醫院核子醫學科
[2] 奇美醫療財團法人奇美醫院核子醫學科

目的：探查 I-131 治療病人住院期間釋出之廢棄物其輻射污染情形，以瞭解外釋之輻射安全性。

方法：I-131 治療病人外釋之廢棄物因可能被唾液或尿液汙染而具有輻射，如隨一般垃圾丟棄因可能具有輻射而被環保局焚化廠偵測到而退運或開罰，因此著手改善，首先於病人住院前針對廢棄物丟棄流程給予充分之分類衛教，並告知將廚餘、資源回收垃圾、衣物及一般廢棄物等分開丟棄，並於病人出院後分別偵測其輻射量，將超過 0.5 微西弗 / 小時之廢棄物攜回核醫科配藥室靜置衰減，另購置一冷藏冰箱將置衰減過程中會產生之腐敗臭味及滋生果蠅之廢棄物放入冷藏冰箱，如此可以確保外釋廢棄物之輻射安全性及改善管理流程，過程中以 ATOMTEX AT1121 閃爍偵檢器偵測廢棄物之輻射暴露劑量。

結果：自 105 年實施至今均無環保局通知輻射垃圾超標事件並同時改善了廢棄物靜置產生之異味及果蠅孳生問題。

結論：以往 I-131 病人之輻射廢棄物未予分類丟棄，以致於垃圾量多且輻射值高，現將其分類丟棄後，輻射垃圾量可以減少，一方面可節省靜置衰減儲存空間，並確保了輻射廢棄物外釋之安全性。

PC-042

Arterial Thrombosis Detected by Bone Scan

Sin-Di Lee, Chin Hu

Department of Nuclear Medicine, Kaohsiung Veterans General Hospital, Kaohsiung, Taiwan

Abstract

Introduction: We present a case of arterial thrombosis of right lower limb detected by whole-body bone scan.

Case: An 80-year-old woman presented with progressive right lower leg pain within one week. She has the underlying disease of essential thrombocythemia under Anagrelide and aspirin treatment for decades and left breast cancer complicated with disseminated intravascular coagulation (DIC) status post mastectomy 1 year ago, followed by chemotherapy and undergoing Tamoxifen treatment. The bone scan showed a non-visualized right lower leg and mild muscular uptake of the lower end of the right thigh. Physical examination showed cold and local pain. MRA showed the right iliac artery occlusion. Urgent PTA for revascularization was performed. However, she received amputation 3 days later due to a high risk of sepsis, reperfusion injury, and DIC.

Discussion: There is a struggle in treating patients with essential thrombocythemia (ET) and breast cancer. Essential thrombocythemia is a rare chronic myeloproliferative neoplasm, characterized by the overproduction of platelet. Patients with ET have a higher risk to develop another cancer. Besides, tamoxifen for treating patients with breast cancer increases the risk of thrombosis.

PC-043

Tc-99m ECD SPECT 的 eZIS 影像分析軟體輔助辨別失智症類型之診斷

劉宛如　林娜宜　陳慶元

台中慈濟醫院

背景介紹：根據 WHO 全球十大死因統計，失智症已由 2000 年的第 14 名竄升至 2016 年第 5 名，衛生福利部依據 WHO 定義之失智症範圍進行統計 2017 年全民健保申報資料中，因失智症就醫者約 17 萬人，其中 65 歲以上約 16.8 萬人。隨著年齡增加，因失智症就診比例亦隨之增加。失智症是腦部疾病的其中一類，它的症狀除了導致思考能力和記憶力長期而逐漸的退化，還會影響到其他的認知功能，包括語言能力、空間感、判斷力…等各方面的功能，同時可能出現個性改變、妄想或幻覺等症狀，這些症狀會影響患者的人際關係與工作能力。失智症因發病位置及症狀分爲不同類型之失智症，例如退化性失智症、血管性失智症、其他因素導致之失智症，且因病因不同，病變部位也不相同，所以不同的失智症，所使用之治療方式不一定相同。近年老年病患人口增加快速，通常老年人又有許多慢性疾病共存，慢性病本身與多重藥物皆會影響認知功能，使得失智症的正確診斷愈加困難。使用 eZIS 分析 ECD 及臨床上相關檢查報告結果分析失智症相關性評估，可提供臨床醫師進一步評估時之參考。

方法：患者爲一位 67 歲男性，因最近出現忘東忘西、重心不穩、走路加速的情況。因此至本院就診，經醫師評估後懷疑可能爲阿茲海默症，於是安排磁振照影 (MRI)、生化檢查及核醫腦部血流灌注掃描 (Cerebral perfusion scan) 檢查輔助診斷。先請患者在暗室休息 10 分鐘後，注射 25 mCi 的 ECD 藥物，經過 30 分鐘休息後，請患者至掃描室執行檢查，檢查使用 GE SPECT/CT 儀器搭配 fan beam collimator 執行 60 分鐘腦部掃描。

結果：磁振照影結果顯示患者腦室增大，懷疑爲腦積水，腦部血流灌注掃描影像經由 eZIS 軟體分析發現患者並非爲阿茲海默症，而抽血檢查結果發現患者的葉酸指數較低，因此主治醫生決定先補充葉酸，而經過一段時間後，患者的葉酸指數恢復正常，其臨床徵狀也改善許多。

結論：失智症疾病分類有許多種類，不能依據臨床上病患失的行爲表徵來下定論，需透過不同的檢查才能鑑別診斷對症下藥，亂投藥只會導致疾病更惡化。經由 eZIS 影像分析可以清楚知道患者是否爲阿茲海默症及腦部血流供應之情形，可輔助臨床醫師診斷失智症之參考。

PC-044

施行 Dipyridamole 心肌血流灌注壓力檢查誘發不適之探討

林娜宜　張添信　陳慶元

佛教慈濟醫療財團法人台中慈濟醫院

背景介紹：核醫心肌血流檢查 (MPI) 爲檢測冠心病中的一項快速篩檢冠狀心臟疾病的檢測工具，在台灣根據 2016 年健保資料庫分析 MPI 一年約施行約 15 萬餘件，而在 MPI 檢測中扮演重要 -Dipyridamole (商品名 Persantin) 爲最常用於使病人達到足夠運動量的冠狀動脈擴張劑，靜脈注射 Dipyridamole 所引起的不良反應被討論著，症狀包括：胸悶、頭痛、頭昏、腹部不適、低血壓等症狀，本篇也將探討病人在施打 Dipyridamole 時發生不良反應與處理方式之分析。

方法：回朔分析總共收納 101 位病人資料，收集資料時間爲一個月 (5/19 ～ 6/11)，共 50 位男性及 51 位女性，均施行 MPI 壓力測試，由檢查單上紀錄作爲分析資料，並由核醫科醫師報告作爲依據分析。

結果：根據檢查單張記錄分析，101 位病人，年紀比例 60-70 歲 (30%)、50-60 歲 (26%) 爲多數，BMI 大於 22 有 77%，此次受檢目的原因胸悶 (55%)、胸痛 (27%)、喘 (23%) 等因素，心臟壓力測試後發生不適比例爲 43%，主要發生不適爲頭暈 (44%)、胸悶 (33%)、四肢無力 (19%)、心跳快速 (19%)、頭痛 (12%)，給予結抗劑 aminophylline 靜脈注射 (100%)、葡萄糖水飲用 (12%)、硝酸甘油片使用 (7%)，核醫報告上分析有 24% 爲冠狀動脈疾病高風險病人，發生不適與報告異常無顯著關係 (P 值等於 0.547)。

結論：Aminophylline 爲 Dipyridamole 的結抗劑，當發生病人不適時給予使用，可緩解病人因藥物引起的不良反應，但須注意病人受檢前問診，詢問疾病史，如有 CAD、氣喘、COPD 等病史時，需提高緊戒隨時注意病人狀況，因此目前臨床上使用，仍相對安全。

關鍵字：心肌血流灌注檢查、心臟壓力測試、藥物不良反應。

PC-045

GOT/GPT 比率與骨質密度之相關性研究

蔡依良 [1,2] 莊紫翎 [1,3] 陳保良 [1,2] 王昱豐 [1,3]

[1] 佛教慈濟醫療財團法人大林慈濟醫院核子醫學科
[2] 佛教慈濟醫療財團法人大林慈濟醫院醫學研究部
[3] 慈濟學校財團法人慈濟大學醫學院醫學系放射線學科

背景介紹：目前有許多研究指出肝臟疾病，如 B 型肝炎、C 型肝炎、喝酒及脂肪肝等，皆與骨質密度 (BMD) 有相關性。GOT (Glutamic oxaloacetic transaminase) 及 GPT (Glutamic pyruvic transaminase) 是表示肝臟受損的指標之一，數值越高，受損的程度越嚴重。正常情況下，GPT 的數值會大於 GOT。然而，脂肪肝的患者往往呈現 GOT > GPT 的相反現象。非酒精性肝硬化的病患，其肝臟中的 GOT 活性將顯著降低；而酒精性肝硬化的病患，則是 GPT 活性顯著降低。綜合上述之病因，若單獨讀取 GPT、GOT，可能造成統計數值的偏離。因此我們欲透過 GOT/GPT 比率，來探討肝臟與骨質密度之間的相關性爲何。

方法：回溯性收集本院預防醫學中心，2014 年 6 月至 2020 年 7 月接受健康檢查的受檢者。並排除腰椎、髖骨有手術史及資料不完整的人，共收集 19,162 位受檢者。統計方法以 GOT/GPT 比率作爲依變數 (y)，使用簡單線性回歸來分析與骨質密度 (x) 的相關性。

結果：共收案 19,162 位平均年齡 56.3 歲、平均 BMI 爲 24.1 kg/m^2 的受檢者，喝酒的人共 2,839 名，占了總人口的 14.8%。其中罹患 B 型及 C 型肝炎的比例分別爲 12.0% 和 2.5%。經簡單線性回歸統計結果發現，不論腰椎或是髖骨的骨質密度皆與 GOT/GPT 比率呈現負相關的關係，r 值介於 – 0.138 至 – 0.214 之間，且都有顯著性的差異 p value < 0.001。當 GOT/GPT 比率愈高時，骨骼的骨質密度將隨之降低，其中以右側總髖骨的骨質密度 (r = – 0.214) 下降最快。然而，單以骨質密度與 GOT/GPT 比率做迴歸分析，模型的 R^2 數值只有 0.019 至 0.046，預測能力可能有稍嫌不足的現象。

結論：研究結果顯示 GOT/GPT 比率與骨質密度有高度的相關性。肝臟嚴重受損的病患，其骨質密度也會隨之降低，病患需多加留意本身的骨骼健康。未來研究將朝向找尋共同因子，以提升模型預測能力的方向前進。

PC-046

11C-Acetate Uptake in a Case of Adrenal Incidentaloma: A Case Report

Shih-Ya Ma, Tso-An Liang

Department of Nuclear Medicine, Yuan's General Hospital, Kaohsiung, Taiwan

Introduction: Adrenal incidentaloma, defined as an adrenal lesion found incidentally on autopsy or imaging, is a fairly frequent phenomenon. We report a case of hepatocellular carcinoma (HCC) with a synchronous adrenal tumor which had high uptake of 11C-Acetate (AC) on a PET/CT scan mimicking malignant metastasis.

Case Report: A 61-year-old man had history of chronic non-A, non-B hepatitis for years. Abdominal CT and MR images detected a left hepatic tumor (2.0 cm) and suspected to be HCC. Serum level of AFP, CA-199 and CEA were within normal limits. The left hepatic tumor had normal uptake of 18F-FDG but increased uptake of 11C-AC (standard uptake value, SUVmax, 6.35), consistent to typical HCC uptake pattern. Incidentally, right adrenal tumor (1.9 cm) was found. In PET/CT images, the right adrenal tumor had much higher uptake of 11C-AC (SUVmax, 10.11) than of 18F-FDG (SUVmax, 3.79) and was highly suspicious for malignant metastasis. Then, the patient underwent the surgical resection of left hepatic and right adrenal tumors. Finally, the pathology demonstrated the presence of moderate differentiated HCC and adrenocortical adenoma.

Conclusion: High 11C-AC uptake by an adrenal tumor on PET/CT scan usually suggests a metastatic lesion. However, adrenocortical adenoma should be considered in patients with solitary adrenal lesion with high uptake on PET/CT scan, even in the presence of a malignancy.

PC-047

運用 ROC 曲線與 Cut off 值分析前列腺肥大與腰椎骨質密度相關性研究

陳保良[1,2] 莊紫翎[1,4] 周詩瑾[1] 廖建國[1] 王昱豐[1,3,4]

[1] 佛教慈濟醫療財團法人大林慈濟醫院核子醫學科
[2] 佛教慈濟醫療財團法人大林慈濟醫院醫學研究部
[3] 佛教慈濟醫療財團法人大林慈濟醫院預防醫學中心
[4] 慈濟學校財團法人慈濟大學醫學院醫學系放射線學科

摘要

研究目的：目前研究良性前列腺肥大與腰椎骨質密度相關性甚少，我們先前研究發現骨質密度變化與前良性前列腺肥大有關且僅影響腰椎骨質密度，因此本篇研究進一步探討兩者是否有預測價值，並找出腰椎骨質密度與良性前列腺肥大之間 Cut off 值。

材料方法：本篇研究收集自 2014 年 6 月至 2017 年 12 月，於本院預防醫學中心接受健康檢查之患者，同時要有骨質密度檢查與超音波掃描前列腺，年齡 > 60 歲，根據臨床醫師報告判讀為良性前列腺肥大我們就將其分為良性前列腺肥大組，若無前列腺肥大則分為正常組。排除骨質密度數據不完整與病歷資料不完整者，我們將其排除於研究中。最後總計納入 1,997 位進行研究分析。

結果：良性前列腺肥大患者，平均骨質密度和腰椎 T 值與正常組 T 值有顯著高於正常前列腺大的患者，進一步分析相關性發現正常組與良性前列腺肥大之腰椎骨質密度相比為正相關，且腰椎骨質密度，P 值為 0.013；腰椎 T 值，*P* 值為 0.042。另外利用 ROC 曲線分析 AUC 腰椎骨質密度為 53.0%，95% CI (0.504-0.555)，*P* 值為 0.022，Cut off 值為 1.0935。根據 AUC 結果判斷 0.5 < AUC < 1，優於隨機猜測。

結論：我們研究發現，良性前列腺肥大與腰椎骨質密度分析之結果都為高於正常很多，但是兩側髖部骨質密度與 T 值為正常或骨質流失的結果。當男性受檢者腰椎骨質密度 > 1.0935 時可以預測此患者為良性前列腺肥大，未來我們可以運用於無症狀之良性前列腺肥大患者診斷，至於造成原因尚需更多研究來找出之間的機制。

PC-048

正子造影室血糖機品管異常率分析及探討

廖建國[1] 許幼青[1] 莊紫翎[1,2] 王昱豐[1,2]

[1] 佛教大林慈濟醫院核子醫學科
[2] 慈濟大學醫學系

背景：血糖機爲核醫正子造影作業中必要的重要設備，其主要的功能爲監測病人的血糖值，以確保造影品質。由於血糖機例行的品管至爲重要，因此，多年來本科每月例行監控血糖機品管結果，若有異常，則於品保會議中進行檢討。本研究目的爲分析近 3 年血糖機品管異常情形，並探討其發生原因，以作爲持續改進之參考。

方法：回溯性收集 2018 年 1 月至 2020 年 6 月本科血糖機例行品管結果，分析各月份之品管異常率，並回顧其發生原因，進行探討。由於本科正子造影並非每日均有操作，因此現行品管的執行方式爲每次使用前先以品管液 (QC1、QC2、QC3) 執行檢測，並檢視其結果是否符合允收標準，若通過測試始可執行病人的檢測。血糖機允收標準由本院臨床病理科整合全院血糖機之品質後訂定，並視使用現況進行調整，目前各濃度品管液之允收標準，分別爲 QC1 CV 值 < 8.95、QC2 CV 值 < 5.0、QC3 CV 值 < 6.0。

結果：總計收集 1,141 件品管個案，其中品管異常之個案計 9 件，分別爲 QC1 4 件、QC2 2 件、QC3 3 件。分析其異常率，發現近 3 年異常率最高爲 2018 年 (1.31%)，其次爲 2020 年 (0.41%)、2019 年 (0.4%)。顯示近 2 年之異常率與 2018 年比較，已有明顯的下降。進一步分析其發生原因，發現品管液未混合均勻有 4 件、品管液開瓶過久 3 件、血糖機問題 1 件、品管液濃度錯誤 1 件。顯示品管液未混合均勻及品管液開瓶過久爲主要發生原因 (合計佔 78%)，其他原因則相對較少。另外，分析發現近 2 年發生異常的原因皆爲品管液開瓶過久，顯示品管液未混合均勻的現象已有大幅的改善。

結論：本科近 3 年之品管異常率平均爲 0.71%，其中近 2 年較 2018 年有明顯的改善。核醫造影作業使用之血糖機，透過每月品管結果的監控與檢討機制，可有效降低品管異常率，提升整體作業品質。

PC-049

改善靜脈留置管注射品質成效分析

廖建國[1] 許幼青[1] 吳佳莉[1] 莊紫翎[1,2] 王昱豐[1,2]

[1] 佛教大林慈濟醫院核子醫學科
[2] 慈濟大學醫學系

背景：核醫造影過程中，放射性藥物殘留 (或滲透) 的個案，並不少見，其中使用靜脈留置管 (IV cathether; IC) 注射佔相當大比率。由於使用靜脈留置管注射的藥物殘留可以在推藥後透過多次的沖洗而改善。因此本研究目的即爲分析使用不同沖洗方法之初步改善成效，以爲持續改進之參考。

方法：於 2020 年 5 月 21 日至 2020 年 6 月 15 日 (改善前) 及至 2020 年 6 月 18 日至 2020 年 7 月 15 日 (改善後) 期間，收集例行作業中使用靜脈留置管注射之個案。改善前沖洗方法爲使用 10 mL 空針沖洗 1 次；而改善後沖洗方式則爲使用 3 mL 空計沖洗 10-20 mL。分析比較改善前後之藥物殘留率、殘留影像平均計數 (counts)，並探討藥物殘留與 IC 留置天數的相關性。

結果：總計收集改善前及改善後各 20 件注射個案，其中藥物殘留之個案計 9 件 (改善前 6 件；改善後 3 件)。整理結果發現，改善後之藥物殘留率 (15%) 較改善前 (30%) 有明顯的下降。進一步比較改善前後之藥物殘留平均計數 (counts)，結果發現改善後之藥物殘留計數 (823) 也較改善前 (1544) 有明顯的減少。顯示改變沖洗方式 (使用 3 mL 空計沖洗 10-20 mL) 的確可以改善藥物注射的殘留情形。另外，再分析藥物殘留個案中 IC 留置天數之分佈情形，結果分別爲 0 天 2 件 (22%)、1 天 5 件 (56%)、2 天 2 件 (22%)、3 天 0 件 (0%)，顯示藥物殘留件數並不會因 IC 留置天數較高而變得比較多。

結論：初步分析結果顯示，本科改變靜脈留置管注射後的沖洗方式，可以有效改善藥物殘留情形，而藥物殘留與 IC 留置天數的多寡並無明顯的相關。因此，注射人員不必因爲擔心 IC 留置天數較高，可能較容易導致殘留，而放棄使用靜脈留置管，讓病人多扎 1 針。

PC-050

核醫造影報告修改率分析及探討

廖建國[1] 許幼青[1] 莊紫翎[1,2] 王昱豐[1,2]

[1] 佛教大林慈濟醫院核子醫學科
[2] 慈濟大學醫學系

背景：核醫造影之報告修改個案並不少見，其中可能原因包括配合臨床醫師需求、輸入疏漏、文字修潤等。本科例行每月統計核醫醫師報告修改件數，並於品保會議中檢討。本研究目的即爲分析近 4 年報告修改件數及其比率，以爲持續改進之參考。

方法：回溯性收集 2017 年 1 月至 2020 年 6 月，例行造影檢查之報告修改紀錄資料，分析各月份之報告修改率，並整理其發生原因及檢查項目，進行探討。報告修改之定義爲報告經主治醫師確認發出後再進行修改之個案，由醫師列印修改後之報告後註記發生原因，並留存修改前之報告，以利檢討。

結果：總計收集 36,530 件報告個案，其中報告修改之個案計 38 件。整理結果發現，近 4 年之平均報告修改率爲 0.1%，其中以 2019 年 (0.13%) 爲最高，其次分別爲 2018 年 (0.11%)、2017 年 (0.09%)、2020 年 (0.08%)，顯示本科報告修改率均控制在 0.13% 以下，雖然前 3 年略有上升趨勢，但經過持續的改善，2020 年已降至 0.1% 以下。在各項目報告修改率方面，作業量較大的 4 項檢查中以正子造影 (0.46%) 最高，其次分別爲骨骼掃描 (0.18%)、心肌灌注掃描 (0.13%)、骨密檢查 (0.02%)，而作業量較小的其他項目則合計佔 0.25%，其中發現骨密檢查及骨骼掃描雖爲爲檢查作業中最大量的前 2 位，但其報告修改率相對而言並不是最高，顯示這 2 項的報告品質管控得不錯，而正子造影則還有改進的空間。至於報告修改原因，則以與臨床醫師討論後修改 (43%) 佔最多，其次分別爲文字輸入錯誤 (30%)、補 (加) 照後修改 (11%)、臨床醫師要求 (5%)、文字輸入遺漏 (5%)、重新分析後修改 (3%)、修潤文字 (3%)，顯示大多數的修改均非核醫醫師打報告的疏漏，而醫師可持續改善的項目爲文字輸入的正確性。

結論：分析結果顯示，本科近 4 年之平均報告修改率爲 0.1%，各項目中以正子造影之報告修改率 (0.46%) 最高，而骨密檢查 (0.02%) 則最低。針對核醫造影報告之輸入品質，管理階層可建立管理機制，每月定期分析報告修改率，並進行檢討改善，以持續提升報告品質。

PC-051

RIA 實驗室改善檢體管理品質成效分析

廖建國[1] 張素雲[1] 莊紫翎[1] 王昱豐[1,2]

[1] 佛教大林慈濟醫院核子醫學科
[2] 慈濟大學醫學系

背景：實驗室檢體管理的優劣，攸關臨床檢驗的整體品質。因此在接收檢體時，若發現檢體不良，同仁會進行退件處理，以確保檢驗前各項檢體的品質。本研究目的即爲分析近 6 年本科放射免疫分析實驗室之退檢率，以作爲持續改進之參考。

方法：回溯性收集 2015 年 1 月至 2020 年 6 月之檢體退檢紀錄，分析每月退檢件數、退檢率及其退檢原因，再進一步比較各年度的退檢率，是否有所進步。另外，也分析各項退檢原因所佔的比率，並比對檢驗系統中常見退檢原因的選項，以了解應列入優先改善的項目以及實驗室做得較好的部份。

結果：分析結果顯示，2015-2020 年 (1-6 月) 之平均退檢率爲 0.04%，其中以 2015 年之退檢率最高 (0.05%)，而 2020 年 (1-6 月) 最低 (0.02%)。退檢原因中居前 5 位者，分別爲檢驗取消 (27 件；36%)、檢體量不足 (10 件；13%)、簽收異常 (9 件；12%)、醫師開單錯誤 (6 件；8%)、重覆開單 (6 件；8%) 等，顯示此 5 項退檢原因應列入主要優先改善的項目。進一步比對檢驗系統中常見退檢原因的選項，發現檢體容器錯誤、檢體運送錯誤及有檢體無檢驗單等 3 項均未有退檢紀錄，其中檢體容器錯誤、檢體運送錯誤近 5 年未再發生，這可能由於本科 RIA 實驗室主要使用的檢體容器均爲未加抗凝劑的紅頭試管，且各項採檢容器均已於檢驗單註記說明，而有檢體無檢驗單近 5 年均無紀錄，判斷可能因同仁接收之檢體無檢驗單時，皆會以電話詢問並進行跟催補單所致。

結論：不良檢體所產生的檢驗結果，可能造成臨床醫師的誤判。爲持續提升實驗室之檢體管理品質，管理階層可定期監控分析檢體退檢率，以了解主要優先應改善的項目，並持續要求檢體的採檢及送檢品質，嚴格執行不良檢體的退件工作，以確保檢驗品質。

PC-052

放射免疫分析人員間檢驗結果差異比較

廖建國[1] 張素雲[1] 莊紫翎[1,2] 王昱豐[1,2]

[1] 佛教大林慈濟醫院核子醫學科
[2] 慈濟大學醫學系

背景：實驗室人員間檢驗結果之可比較性，爲認證實驗室要求的項目之一。一般而言，人員間檢驗結果之差異，均以不超過 ±2 倍 CV 值爲允收標準。本科每半年會進行人員工作輪替，也有輪替前後人員間檢驗結果的評估紀錄，但其平均數據爲何，其中差異大於 1 倍 CV 值的比率有多少，我們有興趣進一步了解。本研究目的即爲分析近 3 年人員間檢驗結果之差異，進行比較及探討。

方法：回溯性收集 2018 年 1 月至 2020 年 7 月，實驗室每半年進行人員工作輪替之評估紀錄。分析人員間檢驗結果差異大於 1 倍 CV 值的比率、人員間平均差異 %、各項目之平均差異 %，並比較人員間與各項目之差異 %。其中 CV 值以本科實驗室各項目的長期 CV 值 (long term CV) 爲依據，計算差異大於 1 倍 CV 值的比率。

結果：總計收集 252 件檢驗差異比較個案，經分析發現人員間差異大於 1 倍 CV 值的比率佔 9%，顯示大部份的檢驗結果差異均落在 1 倍 CV 值以內。進一步分析各項目的平均差異，發現 T4 (6.35%)、CEA (6.23%)、Free T4 (5.99%) 之平均差異較大 (居前 3 位)，而差異較小的項目爲 PSA (2.85%)、CA 125 (2.94%)、Thyroglobulin (3.12%)，其中差異較大的項目其差異大於 1 倍 CV 值的比率相對也較高。若不分項目來看，人員間檢驗結果的差異，3 組人員之平均值落在 4.2-5.3% 間，顯示人員間之檢驗值並無明顯的差異。

結論：分析結果顯示，本科 RIA 實驗室人員間的平均差異爲 4.6%，各項目中差異較大的項目其差異大於 1 倍 CV 值的比率相對也較高。因此未來可再針對差異較大的項目，進行監控與改善，以持續提升檢驗品質。

PC-053

放射免疫分析實驗室報告複驗率分析

廖建國[1] 張素雲[1] 莊紫翎[1,2] 王昱豐[1,2]

[1] 佛教大林慈濟醫院核子醫學科
[2] 慈濟大學醫學系

背景：放射免疫分析例行作業上，當對檢驗結果之正確性有懷疑時，例如檢體溶血、與前次結果差異較大、批次品管結果不合格等，醫檢師均會進行複驗 (重複分析)。雖然 RIA 實驗室進行複驗已爲可接受且必要的例行作業，但複驗的次數愈高則所消耗的成本也愈高。本研究目的即爲分析近年實驗室複驗的比率，以了解各項目複驗情形，並進行比較與探討。

方法：回溯性收集 2019 年 1 月至 2020 年 6 月間，實驗室每月試劑進出及庫存紀錄之資料，分析每月各項目之報告複驗率，並進行比較與探討。報告複驗率之計算，以每月試劑進出及庫存紀錄表中所記錄重複分析之次數爲分子，當月總檢體數爲分母，計算而得。

結果：總計收集 18 個月的檢驗個案，分析項目計 15 項。整理結果發現，2019 年平均複驗率爲 7.49%，而 2020 年上半年則爲 7.85%，與 2019 年相近，顯示例行作業中約有 8% 的試劑消耗在重複分析上。再分析各項目之複驗率，發現明顯較高的項目有 5 項，依序分別爲 CA-19-9 (18.35%)、CA-125 (16.35%)、PSA (12.95%)、Thyroglobulin (12.15%)、TSH (11.85%)。而複驗率明顯較低的項目有 3 項，分別爲 Cortisol (1.6%)、PTH (2.45%)、Free T4 (3.35%)。進一步進行整理及探討，報告複驗的可能原因可包括檢體不良 (溶血 / 黃疸 / 高血脂)、批次品管結果不合格、結果落在參考範圍外且無歷史資料、結果超出重要異常值、結果落在線性範圍 / 可報告範圍外、懷疑可能有 Hook effect、與前次結果差異較大、不符合疾病群組關聯性 (Thyroid function profile) 等。

結論：本科近 2 年之平均報告複驗率爲 7.67%，由於報告複驗的原因有很多，例行檢驗作業上，雖然有需要複驗時就應進行複驗，但實驗室若能定期分析其複驗率，可觀察每月或每年複驗率的變化，以判斷複驗率是否合理，若發現異常可適時找出原因進行改善，如此則可在追求檢驗品質的狀況下，也能兼顧試劑成本的管控。

PC-054

核醫造影室參與 TAF 認證持續改善品質 – 經驗分享

廖建國[1] 許幼青[1] 莊紫翎[1] 王昱豐[1,2]

[1] 佛教大林慈濟醫院核子醫學科
[2] 慈濟大學醫學系

背景：國內醫學實驗室的認證已推動約 20 年，核醫界絕大多數的 RIA 實驗室也已參與認證。近年影像醫學檢查之認證也逐漸受到各界關注，自全國認證基金會於 2016 年 4 月公告影像醫學 (Medical Image) 之核子醫學影像檢查項目開放認證申請後，至今也有 5 家核醫造影之認可單位，本科即爲其中 1 家。本文目的即爲將本科透過參與 TAF 認證持續改善品質之經驗，整理發表，希望能提供各醫院參考。

品質管理系統：提供優質的服務爲本科一直以來的目標，而其中首要的工作就是建構優良的品質管理系統。目前全國認證基金會 (TAF) 提供的認證系統，係依據「醫學檢驗室認證規範 - 品質與能力要求」(ISO 15189)，並搭配運用「醫學領域之核子醫學影像檢查技術規範」作爲認證評鑑要求之規範。本科多年前準備 RIA 實驗室認證時，即一併將核醫造影室納入管理。

落實執行：依據 ISO 15189 以及核醫技術規範所撰寫之管理文件與技術文件，其目的就是要讓造影作業符合國際規範的要求。因此，管理階層必須要求同仁落實執行，並透過訂定各項品質指標、自主查檢與內部稽核之機制，監控檢查前、檢查中以及檢查後各流程之執行情形，以評估並了解作業之品質。

定期檢討：每月定期召開品保會議，針對各項品質指標、查檢及稽核結果進行檢討，有異常時，儘速擬訂改善措施，進行改善，並持續追蹤改善成效，以確認發生之異常已確實改善。另外，亦於品保會議中檢討或討論所有有關技術品質、管理品質、醫院評鑑、認證要求、病人安全等議題，以持續提升作業品質。

持續改善：持續改進品質管理系統的有效性，包括檢查前、檢查中及檢查後流程，經由管理審查將造影室之評估活動 (例如品質指標、風險評估、內外部稽核等)、矯正措施與預防措施的實際執行成效，與本科之品質政策與品質目標相互比較，以確認所推行之持續改善活動，符合科室之品質要求。由本科參與認證前後之成果分析資料顯示，作業相關之異常率均能持續降低，病人滿意度也有逐年提升。

結論：依據本科的經驗，造影室參與 TAF 認證，將 ISO 15189 導入造影作業，並搭配運用核醫技術規範，可建構優良的品質管理系統，不僅能夠打造符合國際標準的核醫造影檢查服務，也有利於持續改善，追求卓越品質。

PC-055

放射師的挑戰 — 小兒麻痺患者之心肌灌注造影

張秀瑛[1] 許幼青[1] 莊紫翎[1,2] 王昱豐[1,2]

[1] 佛教慈濟醫療財團法人大林慈濟醫院核子醫學科
[2] 慈濟學校財團法人慈濟大學醫學系

背景介紹：現行的心肌灌注掃描多採平躺、雙手舉高的姿勢來執行，除少部分醫院使用 D-SPECT (可配合患者身體因素採坐姿) 之外，絕大多數傳統 Gamma camera 皆需以平躺姿勢完成，因此臨床如遇患者因身體因素而無法配合，通常就無法執行檢查。在此我們介紹一例用機器附屬延長板來克服因下肢無力且攣縮的小兒麻痺患者順利以平躺姿執行心肌灌注造影檢查的病例。

案例報告：一名 61 歲男性小兒麻痺患者於 2006 年開始因不穩定的心絞痛，及因身體因素無法執行運動心電圖而被轉介到核醫科來執行心肌灌注造影。該名患者當時的小兒痲痺症狀是表現在下肢無力、攣縮且呈小 <> 形。本科爲隨時可觀察患者執行心肌灌注造影時有無異常反應，其造影姿勢一律採頭在外、腳進機器端進行，以利工作人員監測患者狀態，如遇特殊狀況則可採腳在外、頭進機器端，但因機器限制，所有心肌灌注掃描只能以平躺姿勢執行。該名患者首次執行心肌灌注造影時，工作人員係利用束縛帶將其因外擴而無法伸直的雙腳綁緊後方能順利完成檢查。在今年 5 月患者再次來到本科進行心肌灌注掃描的追蹤。欲進行造影時發現患者的雙腳無力外擴症狀加劇，從原先的小 <> 變成大 <>，其外擴程度遠超過檢查床的寬度導致平躺時雙腳無法安放於檢查床上，束縛帶也因患者雙腳反射變嚴重而無法順利綁緊，工作人員隨即請患者採腳在外、頭進機器端，並在確保患者安全及徵求患者同意後將機器附屬延長板以橫放姿墊在患者屁股下方支持，避免不平衡及病人安全，如此一來患者成大 <> 狀的雙腳便安放在延長板上，順利地完成檢查。

結論：核醫工作人員執行每項造影檢查時皆由其標準作業流程所建議或必須的造影姿勢來執行，但偶而患者因生理、病理因素無法配合時，如何順利完成檢查都在在地考驗著工作人員的應變能力，此次介紹在患者身體因素及機器的限制下，我們如何克難的利用機器延長板幫助患者執行檢查，藉此經驗分享給大家。

PC-056

全身骨骼掃描上發現之惡性心包膜積水

張秀瑛[1] 陳薇璇[1] 王昱豐[1,2]

[1] 佛教慈濟醫療財團法人大林慈濟醫院核子醫學科
[2] 慈濟學校財團法人慈濟大學醫學系

背景介紹：全身骨骼掃描可用來診斷懷疑患有惡性腫瘤、感染、炎症、外傷或代謝性骨病，以確定骨骼有無病變，有時也可在骨外發現因腫瘤、激素、炎性、局部缺血、外傷及人爲導致的軟組織攝取異常。 在此，我們介紹一位在全身骨骼掃描中因爲心包膜積水惡性轉移而導致活性攝取異常增加的案例。

影像報告：一名 60 歲女性患者於 2013 年 9 月被診斷出惡性乳癌，並自 2014 年 3 月開始進行全身骨骼掃描的常規追蹤。患者於 2017 年的追蹤掃描中發現在第三、第四節腰椎有退化性的變化，其餘並無異常。但在 2020 年 5 月的全身骨骼掃描追蹤檢查中卻發現在第二、第三及第七節胸椎與左側的薦骼關節有新的、異常活性增加，除此之外，其心臟區域也呈現了異常的活性攝取。經針對胸部加照 SPECT/CT 之後發現，該心臟區域的活性疑似是由心包膜積水所導致，在後續的病理切片結果顯示出其心包膜有源自乳癌的惡性轉移。

結論：心包膜積水及心包炎可能原因包括：感染 (例如病毒，細菌或結核病)、炎性疾病、由癌症轉移至心包膜、腎臟衰竭，血液中氮含量過多及心臟手術等因素。雖機轉未明，文獻僅發現心包膜聚積骨掃描示蹤劑與惡性腫瘤有關；此次我們所介紹的即是因癌症轉移至心包膜，進而在骨掃描中呈現心臟異常活性攝取的案例，藉由 SPECT/CT 所提供的解剖定位，可得知病灶位於心包膜，提高診斷準確性。

PC-057

Uncommon F-18 FDG Uptake Pattern in a Patient with Recurrent Desmoplastic Small Round Cell Tumor: A Case Report

Shiou-Chi Cherng[1,2], Tsung-Han Yang[1], Yu-Hsiang Chou[1]

[1]Department of Nuclear Medicine, Taipei Tzu Chi Hospital, Buddhist Tzu Chi Medical Foundation, Taiwan
[2]School of Medicine, Buddhist Tzu Chi University, Hualien, Taiwan

Abstract:

Desmoplastic small round cell tumor (DSRCT) is a very rare and aggressive malignant tumor of the small round blue cell tumor family that mainly affects male adolescents and young adults. Due to its glucose hypermetabolism nature, fluorine-18-fluorodeoxyglucose (F-18-FDG) positron emission tomography with computed tomography (PET/CT) scan has been shown as a useful tool in the pre-treatment survey and post-treatment response evaluation. Most commonly reported F-18 PET/ CT scan findings are hypermetaboilc lesions in the abdominal and pelvic cavities with regional lymphadenopathy. Here we report a young male patient with recurrent DSRCT, whose PET/CT scan revealed glucose hypermetabolism in multiple lymph node regions in the left supraclavicular fossa, right axilla, mediastinum, bilateral pulmonary hila, para-aortic and para-caval spaces in the abdomen, and bilateral iliac regions. Glucose hypermetabolic lesions in the right humeral head and in the lower abdominal wall were also noted. This unpredicted picture of PET/CT scan in our patient suggested that much is left to be discovered regarding how DSRCT spread and metastasize within the organization and again accentuated on the importance of F-18-FDG PET/CT in the management of DSRCT.

PC-058

頭頸癌患者於正子照影時提供吸唾管 – 案例報告

吳佳莉[1,2] 廖建國[1] 周詩瑾[1] 王昱豐[1,2,3]

[1] 佛教慈濟醫療財團法人大林慈濟醫院核子醫學科
[2] 佛教慈濟醫療財團法人大林慈濟醫院預防醫學中心
[3] 慈濟學校財團法人慈濟大學醫學系

背景介紹：多數惡性腫瘤細胞其葡萄糖代謝較正常細胞旺盛，利用此特性，氟化去氧葡萄糖正子造影 (F-18 FDG PET/CT) 在協助醫師準確鑑別腫瘤之分期、評估治療效果、或疑似復發時尤其重要。造影時受檢者須平躺約 30 分鐘，造影過程中若有移動，將影響正子及電腦斷層影像對位，而無法正確判讀。本篇個案將探討患者因無法吞入唾液、無法平躺 30 分鐘，採取吸唾管 (Suction tube) 方式來協助造影。

病例報告：本案例爲一位 50 歲男性，有酒精性胰腺炎、酒精性肝硬化之病史，2019 年 06 月因雙側下咽癌伴隨頸部轉移，經同步化學放射治療後使用口服化療藥物來控制病情。2019 年 11 月個案因呼吸道壓迫引起呼吸衰竭，而作了氣切 (tracheostomy)、並使用鼻胃管灌食；2020 年 3 月底個案開始產生漸歇性鼻腔、口腔出血、無法吞嚥唾液之症狀，CT 發現下咽有大小約 10 公分之腫瘤，並侵襲鄰近之食道 / 喉 / 氣管 / 甲狀腺雙葉 / 左側甲狀腺軟骨，爲了評估有無遠處轉移及決定後續治療策略，安排正子造影檢查。在造影前之衛教時，個案表示因唾液無法吞下，平躺時唾液滯留於口腔及鼻腔亦流不出來，擔心無法平躺 30 分鐘完成造影；護理師於造影時，利用吸唾管固定於臉頰，將另一端連接到檢查室牆上醫用氣體設備之抽吸設備，並以 60 mmHg 負壓抽吸唾液，個案也因此順利完成造影。

結論：臨床上常見頭頸部癌病人安排正子造影檢查，一般而言，請病人自然流出唾液、墊高頭部及放毛巾吸收唾液即可，本案例因擔心唾液無法吞下亦流不出來，無法完成造影，護理師利用吸唾管抽吸唾液完成造影，解決病人的問題，提升醫療品質。若他院遇到此類受檢者，期此方法能提供他院核醫護理師參考。

PC-059

亞急性甲狀腺炎在鎵 -67 炎症掃描上的表現

陳薇璇[1] 許幼青[1] 張秀瑛[1] 莊紫翎[1,3] 王昱豐[1,2,3]

[1] 慈濟醫療財團法人大林慈濟醫院核子醫學科
[2] 慈濟學校財團法人大林慈濟醫院預防醫學中心
[3] 慈濟學校財團法人慈濟大學醫學系

背景介紹：臨床上因內分泌性發燒的原因很少，其中最常見的是亞急性甲狀腺炎和甲狀腺毒症。亞急性甲狀腺炎是甲狀腺自發性炎症，可引起發燒。而在 94 例亞急性甲狀腺炎患者中，有 96% 的患者有疼痛的症狀。亞急性甲狀腺炎是一種常被當做不明熱或誤診爲咽喉炎。其臨床特點爲甲狀腺壓痛、ESR 上升、thyroglobulin 上升等，可經甲狀腺超音波檢查之局部低回音及細針抽吸細胞學檢查之退化性濾泡細胞及多核巨細胞，來證實是否爲亞急性甲狀腺炎。核醫學檢查則會經由鎵 -99m 或碘 -131 甲狀腺掃描檢查和 radioactive iodine uptake (RAIU) 下降來確認。

影像報告：一名 69 歲女性，因間歇性發燒以及上腹痛就醫，體重減輕 (三個月內減輕 6 公斤)。醫師安排鎵 -67 全身炎症掃描檢查，平面及 SPECT/CT 影像結果顯示在 6 小時、24 小時及 48 小時均有雙側甲狀腺瀰漫性攝取，另外 6 小時的影像結果顯示上升結腸有活性攝取。在鎵 -67 炎症掃描中，甲狀腺瀰漫性攝取，原因可能是 amiodarone 引起的甲狀腺功能亢進、sacroidosis、甲狀腺炎 - 亞急性和慢性。之後問診確定病人無甲狀腺病史或家族史，沒有服用 amiodarone，雙手顫抖，但有甲狀腺壓痛，醫師另外安排鎝 -99m 甲狀腺掃描檢查，影像結果顯示甲狀腺區域示摂劑的攝取量極低。甲狀腺攝取值：0.0% (右側：0.0%，左側：0.0%)。鎝 -99m 甲狀腺掃描攝取值的正常範圍在 0.4% 至 2.4% 之間。病人之實驗室檢查數據：TSH：< 0.03 uIU/mL、T3：1.12 ng/ml、游離 T4：3.44 ng/dl，診斷結果爲亞急性甲狀腺炎。

結論：鎵 -67 全身炎症掃描檢查可用來診斷不明熱，因此當病人發燒不斷時，常會做此檢查。鎵 -67 全身炎症掃描檢查中如有出現甲狀腺活性攝取，主要可分爲亞急性甲狀腺炎和慢性甲狀腺炎，此外還要排除許多條件，才能更加確定病因，此個案在全身炎症掃描檢查診斷結果疑似爲亞急性甲狀腺炎或葛雷夫氏症 Graves' disease，因此再做鎝 -99m 甲狀腺掃描檢查來協助鑑別診斷。這樣醫師就能精確的用藥，讓病人及早痊癒。不用另外用細針抽吸細胞學檢查，暴露在侵入性檢查的風險中。

PC-060

全身骨骼掃描意外發現膀胱壓跡

陳薇璇[1] 許幼青[1] 張秀瑛[1] 莊紫翎[1,3] 王昱豐[1,2,3]

[1] 慈濟醫療財團法人大林慈濟醫院核子醫學科
[2] 慈濟學校財團法人大林慈濟醫院預防醫學中心
[3] 慈濟學校財團法人慈濟大學醫學系

背景介紹：根據衛生福利部 2019 年統計資料，國人的十大癌症死亡率，攝護腺癌排名第六，攝護腺癌已成爲男性國人常見的泌尿道癌症。隨著年齡的增長，罹患的機率也越來越高。攝護腺癌臨床診斷可用血液篩檢、全身骨骼檢查、電腦斷層檢查和切片檢查等。不僅是攝護腺癌，攝護腺肥大的比例也高居不下，攝護腺肥大臨床診斷可用肛門指診、攝護腺超音波、尿流動力學檢查等。如果病人積極接受治療，也能重新擁有良好的生活品質。

影像報告：一名 84 歲男性，經臨床證實爲乙狀結腸癌，醫師安排進行全身骨骼掃描檢查，影像結果顯示在額骨有活性攝取，另外在膀胱中心發現冷區，呈甜甜圈的形狀。起初醫師以爲是異物假影，經檢查過後確認並非異物造成，進一步比對電腦斷層影像，發現是攝護腺肥大造成膀胱擠壓。經臨床抽血檢驗報告證實爲非攝護腺癌。

結論：臨床上偶爾可看到在全身骨骼掃描檢查影像中，膀胱不是完整橢圓形狀的活性攝取，有可能是甜甜圈形式，或者是從上面或下面往內呈凹陷狀，除了先確認是否爲異物阻擋外，再來就要考慮體內器官影響導致。患者如果是女性，有可能是子宮肌瘤造成；如果是男性，那攝護腺肥大或者是攝護腺癌都有很大的機率。這時候醫師可以進一步進行確認，也能協助病人提早警覺未知的疾病，及早治療。

PC-061

Quantitative Myocardial Perfusion Imaging in Fabry Cardiomyopathy

Kuan-Hsiu Lin, Gin Hu

Nuclear Medicine, Kaohsiung Veteran Hospital, Taiwan

Abstract :

Fabry disease is an X-linked recessive lysosomal storage disorder, resulting in progressive accumulation of glycosphingolipids in variety of cells such as cardiomyocytes, vascular smooth muscle cells, renal cells and neuron cells. We presented a 66-year-old male case of Fabry cardiomyopathy with typical angina and diastolic heart failure. Conventional myocardial perfusion imaging showed a small non-specific fixed defect in apical-inferior segment. However, quantitative myocardial perfusion with dynamic SPECT/CT (MyoFlow Q) showed diffuse and severe reduction of coronary flow capacity, including stress blood flow (SBF) and myocardial flow reserve (MFR). Coronary microvascular dysfunction with balanced ischemia was considered, because coronary angiography (CAG) showed no significant stenosis in all epicardial coronary arteries, and cardiac magnetic resonance (CMR) showed diffuse myocardial fibrosis.

PC-062

胸腔出血之特殊造影 – 影像報告

許幼青[1] 廖建國[1] 陳薇璇[1] 莊紫翎[1,3] 王昱豐[1,2,3]

[1] 佛教慈濟醫療財團法人大林慈濟醫院核子醫學科
[2] 佛教慈濟醫療財團法人大林慈濟醫院預防醫學中心
[3] 慈濟學校財團法人慈濟大學醫學系

背景介紹：咳血在胸腔疾病的症狀中並不算少見，若以出血量來分類，可以分爲大咳血和一般咳血，其需要臨床醫師使用檢查來幫助查明眞正出血的原因，當臨床醫師使用各種檢查如胸部電腦斷層檢查、支氣管鏡檢查…等查無任何結果，則會使用核子醫學科的出血檢查來查明出血原因。一般核子醫學科常見的出血檢查爲腸胃道出血檢查，採用的方式各家醫院有所差異，本科使用改良式的體內標記法進行腸胃道出血檢查，故此個案出血位置爲胸腔，使用腸胃道出血檢查方式，照野位置更改爲胸腔進行掃描。

影像報告：一名罹患 HCC 轉移至肺臟的 54 歲男性，在 3-4 年前有接受過 2 次 TACE，由於患者不希望進行手術治療而自行轉至本院，此次患者出現咳血越來越嚴重而住院。醫師安排出血掃描檢查，由於患者呼吸困難無法平躺，故採用特殊擺位進行造影。在出血掃描影像中由於無法執行單光子電腦斷層掃描，故無法確切心臟位置，但在平面影像上顯示胸部除主要血管之外，在雙側肺野上的輕度放射性示蹤劑蓄積的情形，表示高度懷疑雙側肺區域發生出血現象。

結論：有些患者會來至核子醫學科做腸胃道出血檢查，可能的原因是胃鏡及大腸鏡檢查無法偵測出來，且大多患者出血時間不一定，而核子醫學科腸胃道出血掃描屬於間歇性掃描，有較高靈敏偵測出血量的能力，並且可連續造影，除了腸胃道處的出血外，其他地方的出血也可運用此方式得到結果，當患者無法配合常規模式時，放射師的角色就很重要，放射師需要讓機器可以運作的模式去符合患者眞正的需求，提高檢查的品質和效益，讓醫師得到最好的結果是很重要的。

PC-063

前瞻性的 Ra-223 注射方法 – 個案報告

許幼青[1] 廖建國[1] 陳薇璇[1] 莊紫翎[1,3] 王昱豐[1,2,3]

[1] 佛教慈濟醫療財團法人大林慈濟醫院核子醫學科
[2] 佛教慈濟醫療財團法人大林慈濟醫院預防醫學中心
[3] 慈濟學校財團法人慈濟大學醫學系

背景介紹：前列腺癌的患者容易產生骨骼轉移，當骨骼轉移時容易發生病理性骨折，甚至於若患者年紀較大，更容易有骨質疏鬆的問題。而近期有一個治療新選擇的藥物 Ra-223，此藥物可以運用於治療前列腺癌骨骼轉移的患者身上，其藥物本身會釋放出阿法粒子，所以可短距離及高能量的治療標的器官，且 Ra-223 大多集中在骨表面，所以對於周遭的正常骨髓組織不會造成太大的傷害，反而更加安全。

個案報告：一名罹患前列腺癌的 70 歲男性，沒有其他器官轉移只有骨骼轉移，患者定期使用骨骼掃描追蹤檢查，臨床醫師評估後符合 Ra-223 之給付規定，通過事審安排 Ra-223 治療方案。每次療程前先靜脈注射留置針，施打 Ra-223 前先給予 1 mCi 的 Tc99m，並用 10 c.c. N/S 沖洗，注射後進行照影，使用中能量的準直儀，能峰設定 140 keV (10%)，影像上呈現均勻且淡淡的活性攝取，看起來如血液的背景活性，表示在注射部位無藥物堆積無滲漏的現象。另外準備好三路活塞，從三路活塞處施打 Ra-223 時間需大於 1 分鐘，接續 Ra-223 的針筒反覆沖洗，並且重複 3 次，完成注射後移除留置針，再進行照影，使用中能量的準直儀，能峰設定 82 keV (20%)、154 keV (15%)、270 keV (10%)，影像上如同 Tc99m 之影像，表示在注射部位無藥物堆積無滲漏。

結論：Ra-223 副作用的反應會有紅腫熱痛，嚴重的會有組織壞死的狀況，所以有無滲漏是一件非常值得討論的事情，因此本科在治療 Ra-223 前開會討論各種可能的方案，最後決議在施打 Ra-223 治療前先給予 1 mCi 的 Tc99m，Tc99m 注射後進行照影，觀察有無藥物堆積，如果有藥物堆積，就必須移除留置針，再尋找其他注射部位，主要原因是避免組織受損；若無藥物堆積後則給予 Ra-223 治療，主要用意爲治療前可前瞻性得知留置針是否有百分之百在血管內，而非部分在血管內，如此可避免患者因藥物滲漏引發不必要的傷害

PC-064

SPECT/CT 用於診斷惡性腹膜積水之角色

林昱璁[1] 許幼青[1] 張秀瑛[1] 陳薇璇[1] 莊紫翎[1,3] 廖建國[1] 王昱豐[1,2,3]

[1] 佛教慈濟醫療財團法人大林慈濟醫院核子醫學科
[2] 佛教慈濟醫療財團法人大林慈濟醫院預防醫學中心
[3] 慈濟學校財團法人慈濟大學醫學院醫學系放射線學科

背景介紹：腹水 (ascites) 是晚期癌症常見的臨床症狀。約有 15-50% 的癌症病患，在臨床病程中會產生惡性腹水 (malignant ascites)，惡性腹水可能肇因於原發性腹膜腫瘤，也會因繼發轉移性腫瘤或淋巴結侵犯等而發生。當惡性腫瘤造成微血管的通透性增加，富含蛋白質的細胞外液，便會滲入腹膜腔，形成腹膜積水。

案例介紹：一名 60 歲男性，經臨床診斷爲肺癌，已戒菸五年，在 2016 年時進行肺葉切除術。近期經由醫師安排全身骨骼掃描，影像發現大約在腹部的地方有異常活性攝取，所以我們高度懷疑病患有使用民俗尿療法的可能性，爲進一步了解病情，針對腹部執行 SPECT/CT 的檢查，結果發現其腹部活性攝取爲惡性腹膜積水所造成，並非使用民俗尿療法所致。

結論：骨骼掃描主要針對癌症骨轉移之篩檢相當重要且最常用的檢查，藉由骨骼掃描的高靈敏度、低輻射劑量及早期偵測骨骼病灶之能力，在臨床上應用的非常廣泛，能夠快速找出癌症骨轉移的位置，若加上 SPECT/CT 檢查，能夠更加精確診斷出病灶位置，甚至於提早發現其他部位的轉移，如本案例能夠讓臨床醫師改變治療方向的工具，是檢查癌症骨轉移的最佳利器。

PC-065

身心醫學科病患產生高泌乳激素之相關研究

林淑靜[1] 莊紫翎[1,2] 周詩謹[1] 廖建國[1] 張素雲[1] 薛伃婕[1] 王昱豐[1,2]

[1] 佛教慈濟醫療財團法人大林慈濟醫院核子醫學科
[2] 慈濟學校財團法人慈濟大學醫學系放射線學系

背景：臨床上，高泌乳激素血症 (Hyperprolactinemia, HPRL) 是服用抗精神病藥物後常引起的副作用之一。身心醫學科病患治療的藥物作用機轉大部分爲阻斷腦部多巴胺傳導路徑，使腦下垂體的泌乳細胞接收的多巴胺信號減弱，導致 Prolactin 分泌增加。當 Prolactin 發生異常時，與腦下垂體相關的內分泌賀爾蒙，特別是性賀爾蒙類，可能造成女性停經、月經週期異常甚至不孕，而男性會有男性女乳症、勃起功能障礙等等，而這些不良反應發生對身心醫學科患者造成的影響甚大。此篇主要探討身心醫學科病患服用抗精神病藥物後產生 HPRL 的患病率，並評估性別、年齡與 PRL 的相關性。

材料與方法：此研究收集 2014 年 1 月至 2019 年 3 月在本院接受 PRL 檢查的病人 (5,136 例)，依照科別分類進行回顧性研究，收集 331 例身心醫學科病患，皆服用抗精神病相關藥物，其中男性 42 例 (12.69%)，女性 289 例 (87.31%)，平均年齡 41.17 ± 11.56，年齡分布 19-87 歲。分別探討 Prolactin level 在性別和年齡中的差異。本院 Prolactin 女性正常參考範圍爲 2.64~37.2 ng/mL，男性爲 3.06~26.9 ng/mL，以此爲基準，男性 > 26.9 ng/mL，女性 > 37.2 ng/mL 定義爲 HPRL。

結果：所有科別發生 HPRL 病患，身心醫學科佔 32.5%，婦產科 28.3%，新陳代謝科 23.2%，身心醫學科居冠 (Fig 1)。Prolactin 異常中，女性佔 90.3% (456 例)，男性佔 9.7% (45 例)。性別分類中 Prolactin level，男性 50.34 ± 40.26 ng/mL，女性 86.00 ± 61.49 ng/mL，兩者有顯著性的差異 ($p < 0.001$)。各科別的男女在 Prolactin level 之比較，身心醫學科和新陳代謝科在性別上都具有統計學上的差異 ($p < 0.001$ 及 $p = 0.031$)。身心醫學科發生 HPRL 中女性 Prolactin level 明顯高於男性 (男性：41.59 ± 12.6 ng/mL，女性：94.96 ± 62.62 ng/mL)，兩者具有統計學上的差異 ($p < 0.001$) (Table 1)；Prolactin 異常中女性患者年齡≧ 45 歲與年輕患者 (< 45 歲) 的 Prolactin level 相差 27.46 ng/mL ($p = 0.001$)，年齡與 Prolactin level 呈現負相關 (Table 2,3)。結果顯示，Prolactin 異常在性別上因性賀爾蒙的不同造成男女之間的差異性，女性隨著年齡增加，賀爾蒙的變化使得 Prolactin 數值也發生不同的變化。在本院，身心醫學科服用精神病藥後的病人發生 HPRL 的機率遠高於其他科別。精神病藥物所產生的不良反應 (Adverse Drug Reaction, ADR) 影響病人的日常，往往造成病人用藥依從性降低，甚至中斷用藥，導致藥物療效降低或是精神疾病復發。

結論：我們建議身心醫學科病患服藥前應檢驗 Prolactin，用藥過程中定時檢驗 Prolactin，觀察病人在服藥過程中所產生的不良反應並記錄。若服藥過後病人有嚴重的副作用產生或血液中 Prolactin 數值異常，醫師應視情況調整其所用的藥物及劑量，給予合理的用藥，並持續監控病人的臨床徵狀和 Prolactin level。透過定時監測血液中 Prolactin 來降低抗精神病藥引起的 HPRL 症狀，減低副作用的發生，提升病人用藥上的安全及品質。

PC-066

血清 Vitamin B12 濃度與骨質密度之相關性探討

薛伃婕[1] 張素雲[1] 林淑靜[1] 廖建國[1] 王昱豐[1,2]

[1] 佛教慈濟醫療財團法人大林慈濟醫院核子醫學科
[2] 慈濟學校財團法人慈濟大學醫學系

目的：隨著世界人口的老齡化，骨質疏鬆症成爲一個主要的健康問題，而骨質密度 (BMD) 受內分泌代謝和營養因素以及年齡等許多因素之影響，儘管目前已知 Vitamin B12 對血液以及神經系統有影響，且在合成 DNA 扮演重要的角色，但關於 Vitamin B12 缺乏是否對骨質密度有影響仍然不確定的，考慮到血清 Vitamin B12 與成骨細胞功能之間的關係，它可能與骨質密度有關，因此我們探討兩者之間的相關性。

方法：收集 2020 年 5 月至 7 月於本院健康檢查之民眾，同時接受骨質密度以及血清 Vitamin B12 之檢查，共 282 名 (182 名女性和 100 名男性)。腰椎、髖關節和股骨近端的骨質密度使用骨質密度儀 (HOLOGIC Discovery Wi) 檢查，血清 Vitamin B12 濃度使用電化學發光免疫分析法 (ECLIA) 測量，正常值爲 > 197 pg/mL，並將其結果分爲 Vitamin B12 濃度正常以及不足兩組，利用進行統計，比較兩組骨質密度之差異。

結果：結果顯示 Vitamin B12 正常組別 (共 233 名)，血清含量平均值爲 549.8 ± 334.0 pg/mL，顯著高於不足者 (共 49 名) 的 145.6 ± 32.5 pg/mL ($p < 0.001$)，且不足的組別，在腰椎、左右兩邊髖關節的骨質密度及 T score 均顯著低於正常組別，且具有顯著性差異 ($p < 0.05$)，而股骨近端在兩組之間的骨質密度及 T- score 則不具有顯著性差異。推斷這可能由於股骨近端測量之範圍較腰椎、左右兩邊髖關節小，因此相對而言與 Vitamin B12 之相關性較不顯著。

結論：研究發現血清中 Vitamin B12 濃度與腰椎及髖關節的骨質密度之間有顯著相關性，Vitamin B12 不足可能是造成骨質密度降低的因素之一，且 Vitamin B12 主要來源爲肉類、奶類、海鮮、蛋黃等，因此純素食者也易缺乏此維生素，進而可能使骨質密度降低，然而，還需要更進一步的研究來探討 Vitamin B12 和其他生化標誌物與不同程度的骨質密度之間的關聯性。

PC-067

以手工圈畫 Tc-99m Trodat-1 SPECT/CT 計算多巴胺轉運體可用率再現性之研究

林渝馨　郭家怡　邱南津

成功大學附設醫院核子醫學科

背景介紹：Tc-99m Trodat-1 SPECT 是一項越來越被廣泛使用的檢查，除了以目視判讀以外，圈畫有興趣區 (region of interest) 以計算多巴胺轉運體可用率 (Dopamine transporter availability)，則能提供客觀的數值資料做參考，但是其客觀性則會受到 ROI 圈畫的影響。SPECT/CT 因有 CT 影像，故能幫助決定 ROI。本研究的目的即是在探討同與不同觀測者間手工圈畫 Tc-99m Trodat-1 SPECT/CT 計算多巴胺轉運體可用率的再現性。

方法：本研究連續收集 30 位臨床轉介進行 Tc-99m Trodat-1 SPECT/CT 檢查患者的影像，由二位技術師以手工圈畫 ROI 方式計算多巴胺轉運體可用率，每次影像檢查皆分析兩次。再分析同與不同觀測者間的變化性 (variability)，組內相關係數 (intraclass correlation coefficient, ICC)。

結果：多巴胺轉運體可用率的平均變化性於同觀測者爲 7.65% 和 9.06%，不同觀測者間爲 15.14%；ICC 於同觀測者爲 0.987 (95% 信賴區間：0.973 – 0.994) 和 0.994 (95% 信賴區間：0.986 – 0.997)，不同觀測者間爲 0.983 (95% 信賴區間：0.941 – 0.993)。

結論：本研究顯示 Tc-99m Trodat-1 SPECT/CT 藉由 CT 影像幫助決定 ROI，在計算多巴胺轉運體可用率上，於同與不同觀測者間有極佳的再現性。

PC-068

將 OCE 系統導入醫放實習生全身骨骼掃描之考核

林渝馨　郭家怡　丁若洵　施成霖　李世昌

國立成功大學附設醫院核子醫學科

背景介紹

在在核醫科的檢查當中，「全身骨骼掃描」爲最大宗的檢查項目。目前核醫科醫放實習生是以 mini-CEX 做爲全身骨骼掃描之評量方式，但在評分上可能因爲臨床教師之不同而產生不同評分標準，導致實習生表現與分數無法被客觀呈現。因此我們希望導入 OCE (Observational Competency Exams) 系統，以 SCPCL (Solo Case Procedure Check List) 表格來評估實習生之學習成效，使其獲得更一致性的考核結果。

方法

舉行試前討論會議

1. 制定全身骨骼掃描之 SCPCL 表格考核細項，針對檢查步驟做詳細分解，分解爲 25 個重要步驟
2. 臨床教師開會討論以釐清在 SCPCL 中各步驟之判定標準，使每位教師在評分上有一致的共識。

執行實習生考核

1. 臨床教師依照 SCPCL 表格之步驟對實習生進行考核，針對每一步驟是否確實執行給予分數。

考核後缺失講解

考核後統計分數，並與實習生講解考核中之缺失改善。

應用之效益

1. 此系統目前尚未應用於核醫科實習生考核上，我們期待透過此考核，能在評分上讓臨床教師有一致性標準外，亦能在評量前將整個檢查過程標準化及步驟化，讓每個實習生能得到一個有共同標準的評核結果。

建議應用層面

1. 將 OCE 系統導入實習生之考核，透過 SCPCL 表格之建立，不僅可使用於全身骨骼掃描檢查，更可實際應用於其他檢查項目。

PC-069

淋巴閃爍造影時間點對臨床診斷影響之探討

林渝馨　李碧芳　邱南津

成功大學附設醫院影像醫學部核子醫學科

背景介紹：目前淋巴閃爍造影 (lymphoscintigraphy) 常被用於臨床評估病患淋巴管阻塞程度，由於文獻回溯後發現淋巴造影時間點差異甚大，爲了解造影時間點對臨床診斷之影響，故針對淋巴閃爍造影時間點對臨床診斷之影響進行探討，找出造影最佳時間點，進而有效調整檢查流程。

方法：依照成大醫院核醫科制定之淋巴閃爍造影檢查標準作業程序內容，其掃描時間點爲表皮淺層注射後 0 分鐘、30 分鐘、60 分鐘及 3 小時進行造影，掃瞄速度分別爲 18 cm/min、12 cm/min、12 cm/min、10 cm/min，收集淋巴閃爍造影共 80 人進行分析探討，可得知四個造影時間點分別對臨床診斷之影響。

結果：經分析後發現其四個造影時間點與影像及報告顯示，第 0 分鐘之影像結果與最終報告結果差距最大、幫助最小，其它時間點與最終報告結果差異性小。

結論：本研究顯示第 0 分鐘結果與最終報告結果差距最大、幫助最小，且影響臨床診斷，因此若修改目前之標準作業程序內的造影時間點，更動第 0 分鐘造影是第一選擇。

PC-070

Comparison of the ^{18}F-FDG PET Derived Radiomic Features between Different Software

Yu-Hung Chen[1], Kun-Han Lue[2], Shu-Hsin Liu[1,2], Sheng-Chieh Chan[1]

[1]*Department of Nuclear Medicine, Hualien Tzu-Chi Hospital, Buddhist Tzu-Chi Medical Foundation, Hualien, Taiwan*
[2]*Department of Medical Imaging and Radiological Science, Tzu Chi College of Technology, Hualien, Taiwan*

Introduction: ^{18}F-FDG PET derived radiomic features are valuable for prognostic stratification in patients with cancers. However, reproducibility remains an issue. We thus compare the ^{18}F-FDG PET derived radiomic features between different software.

Methods: We conducted a retrospective study investigating 50 lung cancer patients who received ^{18}F-FDG PET for staging. We used Chang Gung Image Texture Analysis (CGITA) and Pyradiomics for feature calculation. We select the primary tumor with a fixed VOI threshold of 2.5 for analysis. Radiomic matrices include the SUV histogram (first-order features), Gray level Co-occurrence Matrix (GLCM), Gray level Run Length Matrix (GLRLM), Gray level Size Zone Matrix (GLSZM), and Neighboring Gray Tone Difference Matrix (NGTDM). We select those features with similar nomenclature or definition between two software for analysis. Features derived from the two software were compared using linear regression analysis and Bland-Altman analysis.

Results: We select four first-order features, 4 GLCM features, 3 GLRLM features, 3 GLSZM features, and 4 NGTDM features for analysis. The first-order features and GLCM features showed high linear fitness between the two software ($R2 > 0.99$ and $R2 = 0.88–0.95$, respectively). The features of GLRLM and GLSZM showed variable correlation ($R2 = 0.17–0.96$) with low R2 for run percentage (0.17) and zone percentage (0.40). Most of the NGTDM features showed suboptimal correlation between the two software ($R2 = 0.01–0.67$) except for the coarseness ($R2 = 0.97$).

Conclusions: The reproducibility varied across different radiomic features. We found a high level of correlation between different software for first-order and GLCM features. Otherwise, the use of radiomics features from the GLRLM, RLSZM, and NGTDM should be cautious.

PC-071

Tumor Glycolytic Heterogeneity Measured from ^{18}F-FDG PET is Associated with PD-L1 Expression in Esophageal Squamous Cell Carcinoma

Yu-Hung Chen[1], Ming-Hsun Li[2], Sung-Chao Chu[3], Kun-Han Lue[4], Shu-Hsin Liu[1,4], Sheng-Chieh Chan[1]

[1]*Department of Nuclear Medicine, Hualien Tzu-Chi Hospital, Buddhist Tzu-Chi Medical Foundation, Hualien, Taiwan*
[2]*Department of Pathology, Hualien Tzu-Chi Hospital, Buddhist Tzu-Chi Medical Foundation, Hualien, Taiwan*
[3]*Department of Hematology and Oncology, Hualien Tzu-Chi Hospital, Buddhist Tzu-Chi Medical Foundation, Hualien, Taiwan*
[4]*Department of Medical Imaging and Radiological Science, Tzu Chi College of Technology, Hualien, Taiwan*

Introduction: Immune checkpoint inhibitor (ICI) is one of the options for treating metastatic esophageal squamous cell carcinoma (SqCC). The treatment effect can be anticipated by PD-L1 expression or microsatellite instability (MSI). However, both methods require tissue sampling, which subjects to sampling error. We aim to examine the association of ^{18}F-FDG PET derived features with the PD-L1 expression level in esophageal SqCC.

Methods: We conducted a retrospective study investigating 39 patients with esophageal SqCC. Primary tumor specimens were stained with VENTANA PD-L1 (SP263) Assay, and the expression level (CPS) was dichotomized into < 10% and ≥ 10%. All patients received ^{18}F-FDG PET as well. We contoured the primary tumor and extracted 96 images features using the Pyradiomics 2.2.0 (image matrices included histogram, GLCM, GLSZM, GLRLM, NGTDM, GLDM, and shape features). We used ROC curve analysis to examine the predictive value of these image features. The results were expressed as area under the curve (AUC) and *p*-value. We used a multivariate logistic regression to seek the independent predictor of CPS.

Results: Among all these 96 image features, a higher GLSZM Small Area Low Gray Level Emphasis (GLSZMsalgle) was significantly assocaited with the PD-L1 expression CPS ≥ 10% ($p = 0.026$, AUC = 0.708). We used a cutoff of 0.0529 for GLSZMsalgle and after logistic regression analysis, a GLSZMsalgle ≥ 0.0529 was independently associated with CPS ≥ 10% ($p = 0.009$, OR = 6.533).

Conclusions: GLSZMsalgle derived from the ^{18}F-FDG PET image is associated with PD-L1 expression in esophageal SqCC. This image feature may serve as a biomarker for predicting ICI response in metastatic esophageal SqCC. A larger prospective cohort is needed to validate our preliminary results.

PC-072

由庫欣氏症候群的鑑別診斷探討醫檢師之角色 – 案例報告

張素雲[1] 薛伃婕[1] 林淑靜[1] 廖建國[1] 王昱豐[1,2]

[1] 佛教大林慈濟醫院核子醫學科
[2] 慈濟大學醫學系

背景：庫欣氏症候群 (Cushing's syndrome) 是由於患者體內糖皮質素 (glucocorticoid) 過多，而導致全身一系列代謝混亂和病理變化的一種疾病，此病依照患者糖皮質素的來源可分成內源性及外源性，其病徵於庫欣氏症的臨床表現十分多樣，加上有些常見症狀較難和其他疾病分辨。因此，臨床上可利用抽血檢驗促腎上腺皮質素 (Adrenocorticotropic hormone; ACTH) 和皮質醇 (cortisol)、24 小時尿液游離皮質醇 (24-h UFC)、深夜唾液皮質醇 (late-night salivary cortisol)、或隔夜 1 mg dexamethasone 抑制測試 (overnight 1mg DST)、正子掃描、CT scan 和 MRI 等方法輔助診斷。

案例報告：本院近日有一 49 歲男性病患，醫師懷疑是 Cushing's syndrome，於 2/27 抽血檢查 4 pm cortisol 之結果爲 22.58 μg/dL (參考範圍：8 AM: 4.7-23.3 μg/dl; 4 PM: 2.2-15.6 μg/dl)。3/4 經類固醇隔夜抑制測試 (over night dexamethasone suppression test, ONDST) 檢查，發現隔日早晨 9:15 cortisol 濃度爲 0.95 μg/dL，而 ACTH 爲 < 5.0 pg/mL (參考範圍：< 46 pg/mL)，於 4/1 再次檢驗 cortisol 濃度爲 11.45 μg/dL，而 ACTH 爲 35.5 pg/mL (表 1)，兩次檢驗結果 cortisol 及 ACTH 均正常，顯示 ACTH 及 cortisol 之濃度皆可受 dexamethasone 所抑制，這也說明病人可能不是庫欣氏症，此案例進一步諮詢主治醫師後，確認病人爲壓力及肥胖所引起的僞庫欣氏症候群 (Pseudo-Cushing's syndrome)。由於臨床檢驗爲診斷庫欣氏症之重要依據，因此本案例之檢驗結果均經負責之醫檢師複驗確認後核發。一般而言，醫檢師於審查檢驗結果與核發報告時通常會有以下準則；1. 核對病人、檢體、項目、數據，2. 查詢病歷，檢視與近 3 個月內的檢驗報告是否相符，3. 審查疾病相關群組檢驗項目報告間的相關性，此病患 ACTH 和 cortisol 數據於 3/5 和 4/1 截然不同，就醫檢師角度而言，前後報告差距過大，可能須考慮是否重新檢測、檢体是否拿錯、品管是否異常以及編號是否抄錯等問題，因此核發報告時確認結果的正確性至爲重要。

結論：由以上庫欣氏症候群鑑別診斷之案例，顯示醫檢師的角色極爲重要，實驗室提供正確檢驗數據，可幫助臨床醫師確診。日常作業中醫檢師雖無法得知病患臨床症狀來判斷報告是否吻合，但若能針對醫檢師個人檢驗業務職掌，充分學習了解檢驗項目和疾病之間的相關性，必要時再向醫師請教及學習，如此則能提升報告審查之能力，並提高報告核發的信心。

PC-073

評估完整型副甲狀腺激素 (Intact Parathyroid Hormone; I-PTH) 試劑在血清中不同時間測試結果之相關性

林秋美　陳素英　蕭莉茹　古琴鳳　陳宜伶
曾翠芬　陳怡如　劉怡慶　林家揚　張晉銓

高雄醫學大學附設中和紀念醫院核醫部

目的：完整型副甲狀腺激素 (Intact Parathyroid Hormone; I-PTH) 主要是檢測生物活性型爲 84 個胺基酸的多胜肽，其測定可作爲鈣代謝異常評估的重要要素。本研究目的：希望藉由評估試劑在血清中不同時間測試結果之探討，以期儘快提供檢測數據供臨床醫師儘早確立可靠的副甲狀腺失調診斷。

材料和方法：本研究檢體共收集了 36 個樣本數，樣本數分成三管，分別進行反應時間爲 Rapid (30 分鐘)、5 小時、Regular (18±2 小時) 等方法進行檢測。操作方法大致一樣，唯 Rapid 方法不測標準液 1，其他流程均相同。ELSA-PTH 測試原理爲 Two-site Sandwich 免疫放射測定法 (Immunoradiometric assay)，即檢體中的 PTH 濃度與結合 ELSA 上的放射性濃度成正比進行樣本檢測。試劑採用 ELSA-PTH, Cisbio Bioassays。

結果：I-PTH 其血清濃度 (平均值 ± 標準誤差) 於 Rapid、5 小時、Regular 檢測結果分別爲 53.04±14.10 (pg/ml)、49.56±11.55 (pg/ml)、46.87±11.84 (pg/ml)。本研究檢體爲單一樣本重複量測，統計方法採用 Paired sample *t*-test。Paired sample *t*-test 結果顯示 Rapid vs. 5 小時其 T 檢定值 = 1.197，顯著性 *p* 值 = 0.239 ＞ 0.05、Rapid vs. Regular 其 T 檢定值 = 2.049，顯著性 *p* 值 = 0.054 ≧ 0.05、5 小時 vs. Regular 其 T 檢定值 = 1.875，顯著性 *p* 值 = 0.069 ＞ 0.05。結果顯示時間長短不同其值差異性是呈現不顯著的。另統計配對相關性檢定於 Rapid vs. 5 小時、Rapid vs. Regular、5 小時 vs. Regular 其相關係數 R 值分別爲：0.994、0.988、0.993。綜合其結果表示時間長短不同其值差異性是不顯著且彼此間有高的相關性。

結論：本研究分析了 Rapid、5 小時、Regular 不同時間測試方法，其數據結果顯示三者之間數據的差異度是不明顯且彼此間相關性強。故時間方法的選擇可依各醫院臨床需求，協助提供檢測數據給臨床醫師儘早確立可靠的副甲狀腺失調診斷爲要。

PC-074

Quantitative Myocardial Perfusion in Chronic Total Occlusion of Coronary Artery

Kuan-Hsiu Lin, Gin Hu

Nuclear Medicine, Kaohsiung Veteran Hospital, Taiwan

Abstract:

An 81-year-old man with type B aortic aneurysm and severe coronary calcification on CT who complained about chest pain. Coronary angiography showed triple-vessel disease with chronic total occlusion (CTO) of LCX, distal RCA and mid LAD significant stenosis. Angioplasty with bare-metal stent was done over distal RCA. Staged coronary angioplasty with stent over mid-LAD was performed, but failed angioplasty to LCX two months later. Chest pain relieved after angioplasty and conventional myocardial perfusion imaging later was normal.

Under the condition of failed angioplasty to LCX, cardiologist requested quantitative myocardial perfusion with dynamic SPECT/CT (MyoFlow Q) to confirm myocardial ischemic status. Conventional myocardial perfusion imaging showed normal heart size and suspected diaphragm attenuation effect in inferior wall. MyoFlow Q also showed normal coronary flow capacity, including stress blood flow (SBF) and myocardial flow reserve (MFR). CTO in LCX with adequate collateral supply from other epicardial vessel was impressed and further angioplasty was not necessary. Quantitative myocardial perfusion gave us more information about the myocardial ischemic status in CTO patients who was suspected balanced ischemia.

PC-075

Comparison of Lung Ratio Value between ^{99m}Tc-MAA Plane Image and SPECT/CT

Ying-Hsuan Li, Ming-Che Chang

Department of Nuclear Medicine, Changhua Christian Hospital, Changhua, Taiwan

Introduction: Two modalities for predictive evaluation of post-lobectomy split lung function are compared: planar perfusion scintigraphy and SPECT/CT. The resulting ratios are assessed for consistency and variance.

Methods: Subjects received intravenous injection of 5 mCi ^{99m}Tc-MAA in the supine position, immediately followed by planar perfusion scintigraphy and SPECT/CT in consecutive order. The scintigraphy image was processed by software, with automated lobar segmentation partitioning each lung into three ROIs. Counts in each ROI was divided by the total counts in each lung to obtain the ratio value of each part. The sagittal SPECT dataset was manually partitioned into two and three lobe ROIs respectively for the left and right lung referencing the CT image. Counts in each lobe ROI were summed and calculated for their ratio values. For the operated lung segment, the two sets of lung ratio values were compared for their differences.

Results: Between 2018 and 2020, five subjects (3 males, ages 47 to 74) were observed with both planar scintigraphy and SPECT/CT modalities. The processed lung ratio values of the two modalities were compared in reference to the planned lobectomy fields. The two modalities presented result values with high difference, with two sets greater than 10%, two between 5% and 6%, with only one subject's lung ratio value set differing within acceptable range.

Conclusions: These results showed a lack of conformity between resulting lung ratio values obtained with planar scintigraphy and SPECT/CT modalities. The two methods presented values with differences greater than the accepted range. These results suggested only SPECT/CT can be utilized for analysis, and planar scintigraphy can be spared, as it does not provide accurate data and provides less value to the predictive evaluation.

PC-076

核醫受檢電腦叫號系統效益評估與經驗分享

吳忠順[1] 俞長青[1] 彭南靖[1,2]

[1] 高雄榮民總醫院核醫科
[2] 國立陽明大學醫學院

背景介紹：本科未使用電腦叫號前，受檢者於報到後在櫃台前等候區等待，櫃台人員量測心肌血流受檢者身高體重後，須將藥單送至核藥室，藥師再依據體重調配血管擴張劑及放射性同位素劑量，檢查時護理師、醫師及放射師需以人工叫名後執行注射及造影檢查。本研究主要在評估本科使用核醫受檢電腦叫號的效益及經驗分享。

方法：本科電腦叫號系統分別裝設於核醫櫃台、檢查室、注射室、第一至第四造影室及核藥室等八處。受檢者依報到順序給予受檢序號，再依所需流程使用電腦系統將受檢者分派到下一個地點後等待叫號。比較裝設前後櫃台人員、護理師、醫師及放射師花費的時間及效益、裝設後受檢者的滿意度及發生問題經驗的分享。

結果：裝設電腦叫號系統前，櫃台人員遞送藥單，每日需 20 分，裝設後櫃台人員將身高體重輸入的時間，每日需 1 分 40 秒，每日節省 18 分 20 秒。裝設前注射室醫師於注射室前叫受檢者進入注射的時間每日需 6 分 40 秒，裝設後按號碼燈等候受檢者進入，每日需 1 分 20 秒，每日節省 5 分 20 秒。裝設前護理師於檢查室前叫受檢者進入施打靜脈留置針，每日需 5 分，裝設後按號碼燈等候受檢者進入，每日需 1 分，每日節省 5 分。裝設前四間造影室放射師於造影或造影準備前至櫃檯前或走廊叫受檢者進入，每日需 53-80 分鐘，裝設後於造影室按號碼燈等候受檢者進入，每日需 2 分 40 秒，每日節省約 51-78 分。總計全科工作人員使用電腦叫號系統每日節省時間約爲 80-107 分鐘，每月節省時間約 30-39 小時。

以報到先後順序編號，工作人員若因受檢者檢查種類不同而調動順序，少數受檢者會因此產生質疑，須事先說明叫號規則並加強溝通。裝設後受檢者對於電腦叫號系統滿意度爲 97.9%，Likert 5 分量表爲 4.77 分。

結論：裝設電腦叫號系統最主要的功能是可以減少人工叫號所需花費的時間。櫃台人員可以大幅減少往返送藥單時間，避免櫃檯無人看守而引起受檢者抱怨，藥師即時獲知受檢者所需劑量，可加速受檢者流程。注射室醫師及檢查室護理師可於按號碼燈後等待受檢者空檔時核對檢查單等資訊，做注射前準備 (如注射針劑量測等)。放射師使用電腦叫號，可以增加受檢者看護時間並加速受檢者流程，提升檢查品質。而因受檢者不清楚叫號規則所引起的質疑，也都可以在溝通後得到諒解。

PC-077

The Evaluation of Sex-Specific Differences in Myocardial Blood Flow and Myocardial Flow Reserve under Caffeine Intake by ^{99m}Tc-sestamibi Dynamic SPECT/CT

Hung-Pin Chan[1,3], Wen-Hwa Wang[2], Chin Hu[1], [4]Ming-Hui Yang[1], Nan-Jing Peng[1,5]

[1]*Department of Nuclear Medicine, Kaohsiung Veterans General Hospital, Kaohsiung City, Taiwan*
[2]*Division of Cardiology, Department of Internal Medicine, Kaohsiung Veterans General Hospital, Kaohsiung City, Taiwan*
[3]*Department of Medical Imaging and Radiology, Junior College of Medicine and Management, Kaohsiung City, Taiwan*
[4]*Department of Medical Education and Research, Kaohsiung Veterans General Hospital, Kaohsiung City, Taiwan*
[5]*School of Medicine, National Yang-Ming University, Taipei city, Taiwan*

Introduction: Quantitative coronary blood flow could be collected by dynamic single-photon emission computed tomography/ computed tomography (Dynamic SPECT/CT) for diagnosis of CAD in previous studies. Caffeine decreased myocardial blood flow (MBF) and myocardial flow reserve (MFR) of LV by dipyridamole-induced vasodilation, and yielded false positive results in PET studied. It had similar results of our previous study demonstrated by Dynamic SPECT/CT. The purpose of this study is to investigate the sex difference under caffeine intake on Dynamic SPECT/CT in our patients.

Methods: Totally 57 patients was enrolled suspected CAD (32 patients) or abnormal CT angiography (CTA) (25 patients) in this study, including women (22 patients) and men (35 patients) who divided into 3 groups randomly: (1) 72 hours caffeine abstinence before study (non-caffeine group); (2) < 24 hours caffeine intake group (one caffeine tablet, about 200 mg); (3) more 24 hours Caffeine intake group. Rest (13 mCi ^{99m}Tc-sestamibi; MIBI)/dipyridomale-stress (30 mCi MIBI) Dynamic SPECT/CT one day protocol with gated SPECT performed on a dedicated Siemens Symbia-T2 SPECT/CT system. The quantitative data was analyzed by MyoFloQ software. Statistical analysis was performed with commercially available soft ware (SPSS) and $P < 0.05$ was considered statistically significant.

Results: Interesting, we found the rest blood flow of LV in women (1.15 ± 0.2 ml/min/g) "higher" than in men (0.96 ± 0.2 ml/min/g) with statistically significant ($P < 0.01$), including in LAD, RCA, or LCx territories, respectively. Women had "higher" stress ejection fraction (EF; 73% ± 12%) and rest EF (69% ± 14%) than men (stress EF 63% ± 10%, rest EF 58% ± 11%) ($P < 0.01$). Difference of stress EF and rest EF presented women "lower" than men but no statistically significant. Stress blood flow, myocardial flow reserve, and stress hear rate/ rest heart rate (HRR) had no difference between women and men. Caffeine intake < 24 hours decreased MBF and MFR, but no influence > 24 hours caffeine intake on both groups. Caffeine reduced "less" sMBF and MFR in disease vessels (> 50% stenosis or positive PCI results) by caffeine, as compared with those in non-disease vessels that similar effects on both groups.

Conclusions: Compared to men, women have higher rest blood flow, stress EF and rest EF on Dynamic SPECT/CT. No difference of stress blood flow, MFR, difference EF, and HRR was noted between both groups. No matter man or women could be reduced less sMBF and MFR in disease vessels by caffeine, as compared in non-disease vessels.

PC-078

An Incidental Infra-renal Aneurysm on Tc-99m Red Blood Cell Scintigraphy

Shih-Fu Wang, Yu-Ling Hsu

Department of Nuclear Medicine, Ditmanson Medical Foundation Chia-Yi Christian Hospital

Case Report:

A 80-year-old man with dark stool was referred to our department for Tc-99m gastrointestinal bleeding red blood cell scintigraphy/ Although no definite bleeding site was identified during the 8hr study, an incidental focus of persistent massive radioactive accumulation was observed throughout the study over infra-renal abdominal aorta. Abdominal CT revealed an infra-renal abdominal aortic aneurysm, measuring 7.26 x 6.07 x 12.1 cm.

Aortic aneurysms are the 13th leading cause of death in the United States. While aneurysms can occur along the entire length of the aorta, the infra-renal location is the most common. The incidence of men is about four times than that of women. The risk factors are patients with diabetes, smokers, hypertension, and high blood lipids. The indication for repair includes either symptomatic aneurysms or aneurysms with a diameter greater than 5.4 cm; in our case repairment should be considered.

Treatment options for the repair of infra-renal aortic aneurysms are open surgical repair (OSR) and endovascular aneurysm repair (EVAR). Currently, EVAR is the primary treatment method for the repair of infra-renal aortic aneurysms due to improved short-term morbidity and mortality outcomes.

Tc-99m RBC scintigraphy helps identify the aortic aneurysm as an incidental finding and may indicate different patient management. Therefore we must be aware of any imaging finding which is unusual on our daily work basis.

PC-079

Plasma Renin Activity 與 Plasma Renin Concentration 近三年之相關性比較

陳宜伶　蕭莉茹　陳素英　古琴鳳　林秋美　林家揚　張晉銓

高雄醫學大學附設中和紀念醫院核醫部

目的：PRA 換新試劑後，每過一段時間都會隨機作一些抽樣檢查，主要是臨床科醫師要求本室進行 PRA 與 PRC 的相關性比較，長久以來黃金標準判讀是 PRA，PRC 則是近十幾年來新開發檢驗試劑，因此有鑑於臨床科的需求進行監控評估其與 PRC 的相關性是否有大的差異性，也符合認證醫學實驗室提供對臨床客戶服務的要求及互動，藉以提升服務品質。

材料與方法：隨機採樣申請核醫科檢查 PRA 或 PRC 的檢體分別加做 PRA 或 PRC 來進行比較，並將 PRA DATA 分成四個部分來觀察 (Total、PRA < 1、PRA < 5、PRA < 10)。使用 SPSS PASW Statistics 18 統計軟體分析。

結果：此次樣本總共收集了 89 人，再將 PRA DATA 分成四個部分，PRA Total、PRA < 1、PRA < 5、PRA < 10；觀察此 4 組 PRA 與 PRC 的相關性；從統計分析中知道 4 組的 P-value 皆有高顯著性表現，相關性比較 PRA < 1、PRA < 10 兩組的相關性約在 P = 0.691；P = 0.665；PRA < 1 的相關性較前兩年相比相對好很多；PRA < 1 的斜率 Y = 29.355x 比前兩年差異不大外，其他三組與前兩年相較大些。

結論：我們發現 PRA < 1 中，樣本數 n = 59；pearson 係數爲 0.691 與前年 pearson 係數爲 0.319 比較相差大；斜率 Y = 29.355x 與去年 Y = 25.304x，前年 Y = 34.226x 差異不多。其他三組與前兩年差異性比較不大。

檢視這三年來 PRA 操作的穩定性發現在 PRA < 1 的部分，可從試劑標準品來看，早期試劑濃度可測定範圍爲 0、0.2、0.8、3.0、10.0、50.0 ng/mL (2011 年)；0、0.31、1.0、3.0、10.0、30.2 ng/mL (2018 年)；現在試劑濃度可測定範圍爲 0、0.29、0.95、2.85、9.5、28.5 ng/mL (2019 年)，我們觀察到試劑濃度範圍有在變窄，PRA 的參考值約在 0.3-4.88 ng/mL/hr 範圍所以 PRA < 5 以下仍值得我們持續觀察監控。

PC-080

Positron Emission Tomography in Mucosal Melanoma of Head and Neck: A Case Report

Kuo-Wei Ho, Ming-Fong Tsai

Department of Nuclear Medicine, Chiayi Chang Gung Memorial Hospital, Chiayi, Taiwan

Introduction: Mucosal melanoma is a rare clinical entity. A case of mucosal melanoma of hard palate who underwent fluorodeoxyglucose positron emission tomography/computed tomography (FDG PET/CT) was presented.

Case report: A 79-year-old man sufferred from progressive black mass at hard palate for several years. Biopsy was done over the mass and the pathology revealed mucosal melanoma of head and neck. Therefore, FDG PET/CT was arranged for evaluation of distant metastasis. The FDG PET/CT showed mildly FDG avid primary mass in the hard palate, and no abnormal FDG uptake to suggest nodal or distant metastasis, whereas an incidental focal thyroid FDG uptake at isthmus was identified. Surgical investigations with wide excision of the palate melanoma, bilateral neck dissection, and bilateral total thyroidectomy were performed. The pathological results revealed congruent staging of mucosal melanoma of head and neck as pT3N0 by AJCC 8th edition, and also confirmed the diagnosis of papillary thyroid carcinoma.

Discussion: Mucosal melanomas arise in extracutaneous sites from melanocytes present in mucosal membranes of the respiratory tract, gastrointestinal and urogenital tract. In the head and neck, the mucosal melanoma arises from the mucosal lining of the nasal cavity, sinuses, and in the oral cavity. Primary mucosal melanomas are rare, aggressive tumors accounting for 0.4–2% of all malignant melanomas and 4–10% of melanomas of head and neck. The pathogenesis of this malignancy is not well-known. Unlike in cutaneous melanomas where exposure to the sun is a well-known risk factor; it is not the case in mucosal melanoma as these arise on mucosal lining which are not exposed to sun. Because of the rarity of mucosal melanoma and lack of knowledge about their pathogenesis, there are no well-established treatment protocols. For early and localized mucosal melanoma, the primary modality of treatment is surgery with or without adjuvant radiotherapy postoperatively. FDG PET/CT demonstrates good overall accuracy in evaluation of patients with mucosal melanoma before undertaking curative resection. The main strength of PET/CT lies in detection of distant metastasis or unexpected synchronous malignancy due to extended whole-body field of view. We reported a patient with FDG PET/CT in accurate staging of mucosal melanoma of the head and neck and also in diagnosis of malignant thyroid incidentaloma.

PC-081

乳突甲狀癌病人之腎上腺皮質嗜酸細胞腺瘤：兩次正子掃描腎上腺有顯著 FDG 攝取增加，疑似轉移 -- 案例報告

吳麗君　顏玉安　李將瑄 *

奇美醫療財團法人奇美醫院

背景介紹：FDG 正子檢查可使用於偵測分化良好甲狀腺癌復發，而碘 131 掃描爲陰性的病人，而本案例歷經兩次氟化去氧葡萄糖 (FDG) 正子檢查，發現左腎上腺病灶 FDG 在兩次正子檢查攝取顯著增加，高度懷疑甲狀腺癌轉移。手術切除後病理証實爲良性之腎上腺皮質嗜酸細胞腺瘤 (oncocytic adrenal cortical adenoma)。腎上腺皮質嗜酸細胞腺瘤本屬罕見良性腫瘤，正子檢查案例更少，多屬意外發現。據我們所知，合併甲狀腺癌，以正子檢查時發現，只有三例報告。兩年期間之兩次正子檢查，FDG 攝取顯著增加，未曾有過文獻報告，故提出報告。

案例報告：一位 57 歲女性病患，因左側乳突甲狀腺癌施行甲狀腺全切除及頸部淋巴結切除，分期爲 T3N1a，術後服用 120 mCi 碘 131 做爲清除殘餘甲狀腺組織，清除後碘 131 掃描除頸部殘餘甲狀腺組織外，並無發現遠端轉移。病人之抗甲狀腺球蛋白爲陽性，甲狀腺球蛋白均低於 0.2 ng/mL。惟手術後一年後追蹤之頸部超音波及細胞抽吸証實左側鎖骨窩淋巴結轉移。再執行 150 mCi 碘 131 做爲治療，治療後碘 131 掃描在頸部及身體其他部位，並無發現攝取碘 131 病灶，故執行正子檢查。正子檢查發現左側鎖骨窩淋巴結及左腎上腺有 FDG 攝取病灶，胸部電腦斷層亦發現左側鎖骨窩淋巴結及左腎上腺病灶。因左側鎖骨窩太小，手術不易；及乳突甲狀腺癌合併左腎上腺轉移，或腎上腺本身惡性腫瘤均屬罕見，故採取追蹤觀察。惟手術後兩年追蹤胸部電腦斷層依然發現左側鎖骨窩淋巴結，及增大之左腎上腺病灶 (1.2×1.8 vs. 1.5×2.0 公分)。故再執行正子檢查。正子檢查發現左側鎖骨窩淋巴結及左腎上腺有 FDG 攝取病灶，而且左腎上腺病比起前次正子檢查，有顯著 FDG 攝取增加 (最大標準攝取值，2.2 vs. 3.2)。故執行頸部淋巴結切除及左腎上腺切除，病理証實左側鎖骨窩淋巴結轉移，及良性之左腎上腺皮質嗜酸細胞腺瘤。

討論：已知 FDG 正子檢查可使用於偵測分化良好甲狀腺癌復發，而碘 131 掃描爲陰性的病人。腎上腺是轉移的好發器官，惟乳突甲狀腺癌合併左腎上腺轉移呈屬罕見，且經常要合併肺或骨骼轉移。此案例執行兩次正子掃描，左腎上腺病有顯著 FDG 攝取增加，胸部電腦斷層亦發現增大之左腎上腺病灶，合理高度懷疑轉移，故執行手術切除，病理証實爲良性之左腎上腺皮質嗜酸細胞腺瘤。腎上腺皮質嗜酸細胞腺瘤本身已屬少見，但已知腎上腺皮質嗜酸細胞腺瘤是會攝取 FDG，我們推測此案例病理雖爲良性嗜酸細胞腺瘤，但在兩年期間仍有顯著增生，造成兩次正子掃描有顯著 FDG 攝取增加，兩次胸部電腦斷層病灶變大。

結論：雖然在兩年期間，兩次正子掃描有顯著 FDG 攝取增加，兩次胸部電腦斷層發現腎上腺病灶增大，本應高度懷疑轉移，病理卻爲腎上腺皮質嗜酸細胞腺瘤，未來有相似情況，仍應將嗜酸細胞腺瘤列入鑑別診斷。

PC-082

手術室施行同位素前哨淋巴結探索暨相關手術輻射劑量偵測分析結果

古瑋凱[1] 劉仁賢[1,2]

[1] 振興醫療財團法人振興醫院核子醫學部
[2] 國立陽明大學生物醫學影像暨放射科學系

背景介紹：前哨淋巴結同位素造影及手術中以輻射偵檢探針偵測聚積同位素的淋巴結，是探索前哨淋巴結的常規方法之一。檢查時，於患側乳房乳暈皮內注射 0.2 毫升含 0.5 毫居里 (mCi) 同位素藥劑 Tc-99m phytate 的生理食鹽水，旋即於 15 分鐘完成前哨淋巴結核醫造影。造影完成後，病患轉送至手術室進行前哨淋巴結探索手術。本文在探討手術過程中工作人員所接受之輻射暴露劑量是否符合輻射安全標準。

方法：本次檢查使用 0.5 mCi 之放射性同位素鎝製劑 (Tc-99m Phytate)。偵檢器廠牌：Thermo SCIENTIFIC，型號：RADEYE PRD-ER，依各醫護人員 (外科醫師、刷手護理師、麻醉護理師) 工作位置現場實測。手術時間約 60-90 分鐘，本次量測採最長時間 90 分鐘計。探索手術每週約 1-4 台，每年以 100 台計。

結果：手術室內外輻射背景值 0.07 μSv/hr (微西弗 / 每小時) (註：等同於北投區自然背景輻射)。麻醉護理師工作位置 0.30 μSv/hr，手術 90 分鐘接受 0.45 μSv.，每年手術 100 位最高接受 0.045 mSv.。刷手護理師工作位置 3.1 μSv/hr，手術 90 分鐘接受 4.65 μSv.，每年手術 100 位最高接受 0.93 mSv.。手術醫師工作位置 8.4 μSv/hr，手術 90 分鐘接受 12.6 μSv.，每年手術 100 位最高接受 1.26 mSv.。手術助理工作位置 0.17 μSv/hr，手術 90 分鐘接受 0.255 μSv.，每年手術 100 位最高接受 0.025 mSv.

結論：經實地量測，以每位工作人員每年執行 100 次同位素前哨淋巴結探索手術，如手術時間以 90 分鐘估算，除手術醫師年輻射曝露 (1.26 毫西弗) 略高於一般人 1 毫西弗年劑量限度外，其他工作人員的年輻射曝露亦未超過 1 毫西弗。如每次手術以 60 分鐘估算，均低於一般人年劑量限度 1 毫西弗。工作人員可安心執行前哨淋巴結探索手術。

PC-083

The Role of FDG PET-CT in Evaluation of Patients with Colon Cancer with Recurrence Suspected

Dung-Ling Yu, Shu-Fen Chen

Department of Nuclear Medicine, Mennonite Christian Hospital, Hualien, Taiwan

Introduction: The purpose of this study is to evaluate the role of FDG PET-CT in evaluation for the patient with colon cancer with recurrence suspected.

Methods: This study retrospectively collected 33 patients (M:F = 28:5, mean age = 63.2 y/o) with colon cancer after treatment with recurrence suspected. The recurrence was suspected by clinical findings, serum level of CEA elevated or equivocal findings on imaging or clinically. FDG PET-CT was performed on all of the patients and all of patients were followed up at least 6 months after PET-CT study for the confirmation of recurrence. The confirmation of recurrence is established either by pathological findings or by imaging findings if progression of the suspected lesions.

Results: 19 out of 33 patients (57.6%) were confirmed with recurrence. FDG PET-CT showed positive findings in 20 patients with true positive in 16 patients and false positive in 4 patients. FDG PET-CT showed negative findings in 13 patients with true negative in 10 patients and false negative in 3 patients. The sensitivity, specificity, positive predictive value and negative predictive value of 18F-FDG PET/CT in detecting the recurrence of colon cancer is 84.2%, 71.4%, 80.0% and 76.9% respectively. The overall accuracy is 78.8%.

Conclusions: Our study suggests FDG PET-CT is a useful tool in detecting recurrent lesions in patients with colon cancer with recurrence suspected.

PC-084

核子醫學輻射工作人員接受體外輻射之累積劑量探討與分析

蘇于婷　陳妍文　陳輝墉　王文祥

義大醫療財團法人醫院義大醫院核子醫學科

背景介紹：核子醫學根據不同的職務內容，分別有不同的專業技術人員，因核子醫學檢查之特殊性，均須使用放射性同位素製劑以進行各項影像檢查與治療，因此核子醫學所有工作人員均被定義爲輻射工作人員。依照工作內容不同，輻射工作人員受輻射曝露也截然不同，本文將針對核子醫學之輻射工作人員 (醫事放射師) 所接受體外輻射劑量高低進行原因之探討。

方法：6 位醫事放射師於工作期間將一般劑量配章 (Panasonic UD-802) 依規定置於胸前或腰際，肢端劑量配章視情況所需戴於手指上，每累積一個月將劑量配章送至相關機關進行當月累積劑量之判讀，可得各輻射工作人員一般劑量配章之 Hp (10) 與 Hp (0.07)，肢端劑量配章之 Hp (0.07)，收集 12 個月，分別將之相加爲年累積劑量。

結果：針對 6 位醫事放射師劑量之顯示分別給予代號 A、B、C、D、E、F，代號 A：一般劑量配章 Hp (10)-3.4 mSv、Hp (0.07)-3.59 mSv、肢端劑量配章 Hp (0.07)-3.67 mSv，B：Hp (10)-2.85 mSv、Hp (0.07)-3.5 mSv、肢端劑量配章 Hp (0.07)-2.22 mSv，C：Hp (10)-2.77 mSv、Hp (0.07)-2.77 mSv、肢端劑量配章 Hp (0.07)-1.92 mSv，D：Hp (10)-2.57 mSv、Hp (0.07)-2.6 mSv、肢端劑量配章 Hp (0.07)-3.86 mSv，E：Hp (10)-2.28 mSv、Hp (0.07)-2.5 6mSv、肢端劑量配章 Hp (0.07)-1.4 mSv，F：Hp (10)-1.5 mSv、Hp (0.07)-1.62 mSv、肢端劑量配章 Hp (0.07)-1.62 mSv。

結論：代號 A：一般劑量配章 Hp (10) 爲最高，其原因爲職務內容除執行影像檢查外，另包括專責處理輻防業務如：放射性廢水槽巡視、高劑量 I-131 治療病人之外釋劑量率偵測；F 各項年累積劑量爲最低，B 至 E 各項年累積劑量介於中間，其原因爲其職務內容除傳統核醫檢查外，尚包括每月輪替執行正子檢查。綜合以上，同爲醫事放射師，雖同樣執行病人檢查業務，但仍會因爲執掌不同的病人檢查內容或工作性質不同而有所高低。

PC-085

Incidental Gallbladder Carcinoma with Diffuse Bone Metastases in a Man with Initial Symptoms of Tarry Stool

Yi-Hsun Chen, Yu-Ling Hsu

Department of Nuclear Medicine, Ditmanson Medical Foundation Chia-Yi Christian Hospital

Case report: A 65-year-old man complained with tarry stool, coffee ground vomitus, dizziness, and general weakness went to our Emergency Department for help. Gastrointestinal bleeding was the first impression. However, his condition did not improve as clinicians expected. The following CT imaging incidentally showed a 6.7 x 5.4 cm mass between the second portion of duodenum and the gallbladder, and some enlarged lymph nodes were also noted at the hepatic hilar region. Malignancy was suspected. At the same time, the ^{99m}Tc-MDP whole body bone scan showed diffusely multiple bone metastases. The patient was then admitted for further treatment as cholecystectomy and hepatectomy. The pathology confirmed the disgnosis of poorly differentiated adenosquamous carcinoma of gallbladder, with live metastasis.

Discussion: Carcinoma of the gall bladder afflicts the elderly and constitutes 4% of gastrointestinal malignancies. Though jaundice may be a presenting feature, non-specific symptoms like chronic right upper quadrant pain, chronic cholecystitis, weight loss, anorexia, nausea and vomiting, delay the diagnosis. Primary carcinoma of gall bladder is a highly aggressive malignancy, most often detected in late stage in majority of the affected patients. It commonly spreads to the adjacent liver parenchyma and, via lymphatics, to mesenteric nodes. Extra-abdominal metastatic sites are extremely rare, with lung being the commonest site. Bone scintigraphy does not form a part of the routine work-up for carcinoma of the gall bladder since bone metastasis is rare. Incidence of skeletal metastasis in gallbladder cancer is very low (2.1%). Axial skeleton was the most common site of bone metastasis. Gallbladder cancer with skeletal metastasis portends poor prognosis with rapidly fatal course. We report a rare occurrence of diffuse bone metastases from an incidental gall bladder cancer patient, detected on ^{99m}Tc-MDP whole-body bone scan. Hence, bone scintigraphy still plays a very important role in gallbladder cancer staging.

PC-086

運用 FMEA 模式提升高價藥劑治療之跨部門協調流程效能 -- 以南部某醫院鐳 223 治療流程設計爲例

卓世傑　鄭揚霖　陳懿貞　張虹麗　張綉芳　梁育雅　顏玉安　李將瑄

奇美醫療財團法人奇美醫院核子醫學科

背景介紹：

由於標靶治療與免疫療法的蓬勃發展，台灣的核子醫學部門現正不斷的引進高價並需跨部門協調之癌症治療藥劑。例如，用以治療肝癌的釔 -90 (Yttrium-90) 與用於去勢抗性攝護腺癌 (Castration-Resistant Prostate Cancer, CRPC) 治療的鐳 -223 (Radium-223) 等治療藥劑。由於這類藥劑由臨床開立至實際治療病人，需要相當之訂藥準備時間與經常性跨部門的繁複協調，方得以順利的讓病人依時、依序的接受高醫療品質的治療。以鐳 -223 爲例，即關連到核子醫學科、藥局與各臨床開單科別等不同科別作業流程之合作。因此如何簡化、提升此類高價藥劑治療之經常性跨部門協調機制，以避免疏失，進而影響病人之醫療品質，是頗爲重要的。本研究即是提供一個運用 FMEA (Failure mode and effects analysis, FMEA) 模式來達到跨部門協調與合作流程提效能，以提升高價藥劑治療跨部門協調醫療品質之鐳 -223 治療開立流程專案經驗的案例。

方法：

1. 自發集合相關科別人員組成小組，成員爲核子醫學科、臨床開單科別與藥局等共 5 人進行專案討論。
2. 設定簡單與有效之鐳 -223 治療各相關科別跨部門協調 2 項專案目標：(1) 正常案例之協調與執行。(2) 異常案件之發現、提示與中止。
3. 利用 FAMA 模式檢視現行流程並繪製流程圖，再就各流程進行危害分析。
4. 就危害分析結果最高之流程，以根本原因分析 (Root Cause Analysis, RCA) 之方式，由小組以因果樹分析 (Why Tree Analysis) 方法，針對已實際發生協調不足導致未及訂藥之警訊事件 (Sentinel Events)，找出近端原因，再討論、歸納爲根本原因。
5. 由小組針對根本原因，討論可行與簡單之介入解決辦法。
6. 採取流程改善行動方案，並監測實行結果。

結果：

依討論結果決定實施 3 項介入策略：

1. 設立電腦程式管控鐳 -223 開單條件。
2. 確立鐳 -223 由開單至治療完成正常流程，需自動發出之 e-Mail 內容與對象，並由各收 e-Mail 科別交叉比對是否異常。
3. 建立 Line 群組，針對異常情形，即時提醒與中止。
4. 持續觀察並記錄實施成效，由小組視成效進行再精進或維持。
5. 自實施介入策略以來，已無發生未及訂藥之事件，並及時發現及修正 2 件異常開單情形。

結論：

運用 FMEA 模式，可以簡單、快速的找出舊流程的問題與可能造成的危害，並有可能針對各單位的特性設計適合與簡單的流程以提升效能與品質。因此運用 FMEA 模式來處理高價藥劑治療之跨部門協調流程，應該是可以深入探討的。不過本研究僅是針對南部某醫院鐳 223 治療流程設計專案的經驗，尚不足以做爲任何必須運用 FMEA 模式進行改善的結論

PC-087

於 ICU 病房注射放射性同位素後輻射劑量值之研究 – 以南部某醫院核醫科爲例

卓世傑　張虹麗　林凡珍　張南雄　陳興隆　梁育雅　顏玉安　李將瑄

奇美醫療財團法人奇美醫院核子醫學科

背景介紹：

執行核子醫學檢查前，依法病人必須到核醫科指定之注射場所，執行放射性同位素之注射。但有部分 ICU (Intensive Care Unit) 病人，因病況限制無法至核醫科指定之注射場所，執行放射性同位素之注射。惟如依法進行輻射安全評估，並經行政院原子能委員會審核許可，仍可由合格人員至 ICU 執行放射性同位素之注射。至 ICU 注射放射性同位素之行爲雖經輻射安全評估計算無虞，但其實際產生之輻射劑量仍有待驗證。本研究即爲實際量測 ICU 病人注射放射性同位素後，產生輻射劑量率之研究。

方法：

1. 收集南部某醫院核醫科，自 2018 年 10 月 30 日至 2019 年 11 月 20 日止，共 10 位注射 Ga-67 射性同位素之 ICU 病人資料，注射活度均爲 3 mCi。
2. 於病人注射放射性同位素後 1-5 分鐘，以手提輻射偵檢器偵測，側面 30、100 cm，後面 (腳部) 100 cm 及鄰床之四處輻射劑量值與臨床距離並記錄。
3. 以收集之 10 位病人臨床輻射劑量值進行統計分析，再以臨床輻射劑量率與臨床距離進行迴歸分析。

結果：

1. 注射後病人含背景值 (約爲 0.07-0.1 μSv/h) 之輻射劑量率分別爲，側面 30 cm：最高 9.1，3 最低 5.19 μSv/h，中位數 6.42，平均 7.04 μSv/h。側面 100 cm：最高 2.89，最低 1.3 μSv/h，中位數 2.18，平均 2.14 μSv/h。後面 (腳部) 100 cm：最高 0.77，最低 0.38 μSv/h，中位數 0.6，平均 0.58 μSv/h。臨床 (距離 200-300 cm)：最高 0.5，最低 0.15 μSv/h，中位數及平均都是 0.31 μSv/h。
2. 注射 Ga-67 病人之臨床輻射劑量率與臨床距離，以線性迴歸統計相關性之 R_2 爲 0.28。

結論：

本研究之結果顯示，病人於 ICU 病房執行注射後，其實測之輻射劑量率在側面 30 與 100 cm 處最高分別爲 9.1 與 2.89 μSv/h，平均則爲 7.04、2.14 μSv/h。至於後面 (腳部) 100 cm 及鄰床之輻射劑量率最高更僅爲 0.77 及 0.5 μSv/h。因此如以病人住院 7 日，工作人員每日於 30 cm 處執行病人照護工作 1 小時及通過 100 cm 處累計 30 分鐘計算，則 ICU 工作人員因照護病人所接受之劑量爲 63.7 μSv (9.1*7H)，僅爲一般人年許可劑量 1000 μSv 之 6.4% 以下。另如僅短暫通過病人，則工作人員接受之輻射劑量，幾乎可以忽略不計。至於臨床病人接受之輻射劑量平均更僅爲 0.31 μSv/h，所以臨床病人住院期間接受之輻射劑量，應不致超過一般人年許可劑量 1000 μSv 之限制。至於臨床輻射劑量率與臨床距離，以線性迴歸統計相關性之 R_2 亦僅爲 0.28，似乎表示，注射 3 mCi 之 Ga-67 病人於 200 cm 以上，其距離與輻射劑量率即無明顯之相關性。

PC-088

LUNG VANTILATION SCAN 病人偵測之 CPS 值與造影 COUNTER 數相關性之研究－以南部某醫院核醫科爲例

卓世傑　張南雄　林凡珍　陳興隆　鄭揚霖　顏玉安　李將瑄

奇美醫療財團法人奇美醫院核子醫學科

背景介紹：

執行 LUNG VANTILATION SCAN 時，必須先以高壓空氣灌注內含 ^{99m}Tc-DTPA 之一次性噴霧器，再讓病人經口部吸入，等肺部累積足夠活度後，病人再移至珈瑪攝影機平躺造影。依據美國核醫學會之程序指南 4.0 顯示，通常於噴霧器內使用的 ^{99m}Tc-DTPA 劑量約爲 900-1300 MBq (25-35 mCi)，而病人吸到肺部裡的活度大約爲 20~40 MBq (0.5-1 mCi)。由於實際吸入的活度難以量測，實務上大都未偵測活度，僅讓病人吸入 10-15 分鐘後，即將病人移至珈瑪攝影機平躺造影。但同樣吸入 10-15 分鐘 由於病人個體之差異，吸入活度可能參差不齊，導致造影品質良劣不一。本研究即爲嘗試以手提輻射偵檢器，偵測吸入病人背部之 CPS (COUNTER PER SECOND) 值與實際造影後之 COUNTER 數值是否有相關之研究。

方法：

1. 收集南部某醫院核醫科，自 2019 年 3 月 28 日至 2020 年 5 月 19 日止，共 16 位病人執行 LUNG VANTILATION SCAN 之資料。
2. 於病人吸入以高壓空氣灌注內含 ^{99m}Tc-25 mCi ＋ DTPA 之一次性噴霧器，10-15 分鐘結束時，以手提輻射偵檢器貼附背部，偵測其 CPS 值並記錄。
3. 於珈瑪攝影機之 LUNG VANTILATION SCAN 完成後，計算 POST 影像，左、右邊之平均 COUNTER 數值並記錄。
4. 以收集之 16 位病人 CPS 值與 POST 影像，左、右邊之平均 COUNTER 數值，分別以線性、對數與指數，進行統計迴歸分析。

結果：

1. 病人之 CPS 最高爲 300 最低爲 27，平均爲 202.13。LT-POST AVERAGE 數值最高爲 75 最低爲 1.80，平均爲 36.03。RT-POST AVERAGE 數值最高爲 79 最低爲 2.06，平均爲 38.49。
2. 以 CPS 及左邊之平均 COUNTER 數值分別進行線性、對數與指數統計迴歸分析，得到的 R_2 結果分別是，0.45、0.48 與 0.59，顯示 CPS 及左邊之平均 COUNTER 數有相當之相關性。
3. 以 CPS 及右邊之平均 COUNTER 數值分別進行線性、對數與指數統計迴歸分析，得到的 R_2 結果分別是，0.45、0.49 與 0.56，顯示 CPS 及右邊之平均 COUNTER 數有相當之相關性。

結論：

依本研究之結果顯示，以手提輻射偵檢器偵測吸入以高壓空氣灌注內含 ^{99m}Tc-25 mCi ＋ DTPA 噴霧器之病人背部，所得到的 CPS 值，對於南部某醫院核醫科之 LUNG VANTILATION SCAN 病人之 POST 影像，左、右邊之平均 COUNTER 數值，於統計嗥歸時其 R_2 有 0.45 以上之相關性。如以指數進行嗥歸統計，其左、右 R_2 相關性，更可高達 0.56 與 0.59。

所以執行 LUNG VANTILATION SCAN 前之病人吸入作業時，如以手提輻射偵檢器偵測 CPS 值，即可大致判斷病人吸入之活度是否足夠，而得以減少或增加病人吸入之時間，從而得到良好之影像。依據經驗顯示，吸入病人之 CPS 值如大於 200，於造影後，通常即可得到品質良好之影像。

PC-089

護理人員執行注射作業接受輻射劑量之研究 - 以南部某醫院核醫科爲例

梁育雅　卓世傑　張虹麗　張綉芳　鄭揚霖　陳懿貞　顏玉安　李將瑄

奇美醫療財團法人奇美醫院核子醫學科

背景介紹：

進行核子醫學相關檢查前，通常必須將放射性同位素經由注射之方式，注入病人體內，再經由珈瑪攝影機收集訊號以組成可供判讀之影像。而執行放射性同位素注射工作之人員，即多由護理人員擔任。但是對於護理人員執行注射作業所接受之輻射劑量，卻較少有實際之數據可供參考，因而頗值得研究。本研究即爲探究，護理人員執行注射作業，實際接受多少輻射劑量之研究。

方法：

1. 自 2019 年 8 月 20 日至 10 月 14 日及 2020 年 5 月 14 日至 6 月 5 日止，分兩階段，請南部某醫院核醫科之護理人員，於注射作業時佩戴劑量筆。
2. 第一階段之注射作業主要爲注射 Tl-201，2 mCi 每日約 7-10 支之注射作業， 第二階段之注射作業主要爲注射 Tc-99m，20 mCi 每次約 5-23 支之注射作業。
3. 收集兩階段不同注射作業，其起始、結束劑量與總陪同時間，各爲 36 筆與 48 筆資料。
3. 將每次之結束劑量減起始劑量，分別計算每次之實際接受劑量。
4. 將實際接受劑量除總作業分鐘後，再乘以 60 分鐘，即得到每小時接受劑量率。
5. 每小時接受劑量率，再減除背景值(0.07 μSv/h)後，即爲實際接受之輻射劑量率(小於零即視爲背景值)。

結果：

1. 第一階段注射 Tl-201，共 36 筆資料，計測作業時間平均爲 518.5 分鐘，最多爲 536 分，最少爲 405 分鐘，實際接受之輻射劑量率平均爲 0.19μSv/h，最高爲 1.32，最低爲 0 (18 筆)。
2. 第二階段注射 Tc-99m，共 48 筆資料，計測作業時間平均爲 230.9 分鐘，最多爲 470 分，最少爲 40 分鐘，實際接受之輻射劑量率平均爲 1.15 μSv/h，最高爲 6.73，最低爲 0。
3. 以第一階段注射 Tl-201，共 36 筆資料之作業時間與實際接受之輻射劑量率進行線性迴歸統計，R_2 僅有 0.004，顯示兩者之間似無相關性，迴歸線則略向右下方傾斜。
4. 以第二階段注射 Tc-99m，共 48 筆資料之作業時間與實際接受之輻射劑量率進行線性迴歸統計，R2 雖有 0.36，但兩者之相關性亦難稱顯著，迴歸線則較明顯的向右下方傾斜情形。

結論：

本文認爲依本研究之結果顯示，南部某醫院核醫科護理人員，執行注射作業所接受之輻射劑量有以下結論：

1. 執行 Tc-99m 等注射作業所接受之輻射劑量率，遠高於執行 Tl-201 注射作業之劑量率；其最高劑量率，分別爲 6.73 μSv/h 及 1.32 μSv/h，平均劑量率則各爲 1.15 μSv/h 與 0.19 μSv/h。
2. 作業時間長短與實際接受之輻射劑量率，並無明顯相關，其 R_2 分別爲 Tl-201 之 0.04 與 Tc-99m 之 0.36。
3. 作業時間與實際接受之輻射劑量率，進行迴歸統計後，分別向右下方傾斜之迴歸線似乎顯示，計測時間越短，劑量率越高，計測時間越長，劑量率則越低之現象。

惟因本研究之樣本較少，且實驗設計仍有不足，如需探究是否確有計測時間越短，劑量率越高，計測時間越長，劑量率則越低之現象或其原因，尚需更進一步的研究。

PC-090

Early Prediction of Outcomes in Patients with Advanced Lung Adenocarcinomas and EGFR Mutations Treated with EGFR TKIs by using ^{18}F-FDG PET/CT

Yu-Erh Huang[1], Ming-Szu Huang[2], Yu-Jie Huang[3], Ying-Huang Tsai[2], Jr-Hau Lung[4], Tzu-Chen Yen[5], Sheng-Chieh Chan[6], Kuo-Wei Ho[7], Ming-Feng Tsai[7], Chih-Feng Chen[8]

[1]Department of Nuclear Medicine, Tungs' Taichung MetroHarbor Hospital, Taichung, Taiwan
[2]Department of Chest, Chang Gung Memorial Hospital, Chiayi, Taiwan
[3]Department of Radiation Oncology, Kaohsiung Chang Gung Memorial Hospital, Kaohsiung, Taiwan
[4]Department of Research and Development, Chang Gung Memorial Hospital, Chiayi, Taiwan
[5]Department of Nuclear Medicine and Molecular Imaging Center, Chang Gung Memorial Hospital, Taoyuan, Taiwan
[6]Department of Nuclear Medicine, Hualien Tzu-Chi Hospital, Hualien, Taiwan
[7]Department of Nuclear Medicine, Chang Gung Memorial Hospital, Chiayi, Taiwan
[8]Department of Radiology, China Medical University Hospital, Taichung, Taiwan

Introduction: ^{18}F-FDG PET/CT was evaluated with respect to the role of early prediction of response and survival following epithelial growth factor receptor (EGFR) tyrosine kinase inhibitor (TKI) treatment in patients with advanced lung adenocarcinomas and EGFR mutations.

Methods: Thirty patients with stage IIIB/IV lung adenocarcinomas and EGFR mutations receiving first-line EGFR TKI treatment were evaluated in this study. EGFR mutation quantification before treatment was evaluated by measuring the delta cycle threshold (ΔCt) value. ^{18}F-FDG PET/CT was performed before and 2 weeks after EGFR TKI treatment. PET response was assessed by Position Emission Tomography Response Criteria in Solid Tumors (PERCIST) 1.0 criteria and the metabolic responders were represented by $MR_{PERCIST}$. For exploratory analysis, the maximum standardized uptake value normalized to lean body mass (SUL_{max}), metabolic tumor volume (MTV) and total lesions glycolysis (TLG) of up to 5 target lesions on PET were measured and calculated. The changes in the sums of SUL_{max}, MTV and TLG of the target lesions from the baseline to post-treatment PET scans were calculated and represented by $\Delta sumSUL_{max}$, ΔsumMTV and ΔsumTLG, respectively. Nonprogression after 3 months of EGFR-TKI treatment in CT based on Response Evaluation Criteria in Solid Tumors (RECIST) 1.1 criteria (nPD_{3mo}), progression-free survival (PFS) and overall survival (OS) served as the main outcome measures. The predictive abilities of the clinical (age, sex, smoking, initial serum CEA level, ΔCt value and classical EGFR mutations) and PET ($MR_{PERCIST}$, $\Delta sumSUL_{max}$, ΔsumMTV and ΔsumTLG) parameters with respect to nPD_{3mo}, PFS and OS were evaluated by using univariate and multivariate analysis.

Results: Based on CT RECIST 1.1 at 3 months, there were 6 progression and 24 non-progression patients. Median PFS and OS were 361 and 991 days respectively. At univariate analysis, $MR_{PERCIST}$ ($p = 0.009$), $\Delta sumSUL_{max}$ ($p = 0.004$), ΔsumMTV ($p = 0.005$) and ΔsumTLG ($p = 0.003$) were significantly associated with nPD_{3mo}. ΔsumSUL ($p = 0.010$) and ΔCt value ($p = 0.001$) value were significantly associated with PFS. ΔsumMTV ($p = 0.038$) was significantly associated with OS. At multivariate analysis, $MR_{PERCIST}$ was an independent predictor of nPD_{3mo} ($p = 0.015$). ΔCt value was an independent predictor of PFS ($p = 0.019$). ΔsumMTV ($p = 0.005$) and delta Ct value ($p = 0.014$) were independent predictors of OS.

Conclusions: ^{18}F-FDG PET/CT could early predict nPD_{3mo} and OS in patients with advanced lung adenocarcinomas and EGFR mutations treated with EGFR TKIs, while EGFR mutation quantification could predict PFS in such patients.

PC-091

FDG PET-CT in Detection of Infected Hepatic Cyst

Dung-Ling Yu, Shu-Fen Chen

Department of Nuclear Medicine, Mennonite Christian Hospital, Hualien, Taiwan

Case report: A 84 y/o female patient was admitted with chief complaints of general malaise and abdominal pain. The body temperature was 39.5°C, and laboratory examination showed leukocytosis with white cell count of 19,460/uL. Abdominal sonography and CT showed multiple hepatic cysts. Under impression of fever of unknown origin, FDG PET-CT was arranged for the evaluation of infection site. The result of FDG PET-CT showed a ring-shaped area of increased uptake of FDG in the surrounding area of the cyst at lower portion of right lobe of liver, and there was no any abnormal uptake of FDG in the surrounding areas of the other non-infected cysts. Infection of the hepatic cyst was impressed. After treatment of antibiotics, the fever was subsided.

Discussion: Infection of hepatic cyst is rare. The risk of the infection of hepatic cyst may be due to abdominal surgery, under hemodialysis, diabetes mellitus and in immunosuppressive condition. In our case there was no above-mentioned risk, therefore the cause of the infection was not clear. Diagnosis of infected hepatic cyst is depended on the imaging study. Sonography shows increased echogenicity in the infected hepatic cyst, but not a specific sign. CT scan showed thickened walls, heterogeneous densities or gas bubbles, but may not show in the early phase of the infection. FDG PET-CT has been used for imaging of infectious diseases because it has been studied that inflammatory cells are able to express high levels of glucose transporters and hexokinase activity. Our case showed prominent uptake of FDG in the infected area surrounding the hepatic cyst, giving strong evidence of infection. The treatments of the infected hepatic cyst are antibiotics or percutaneous drainage of the infected cyst.

Conclusion: Infection of hepatic cyst is rare but lethal and should be diagnosed as soon as possible. FDG PET-CT has the role to detect infection of hepatic cysts.

PC-092

Lung and Skeletal Tuberculosis Mimicking Lung Cancer with Multiple Bone Metastasis

Kuan-Hsiu Lin, Gin Hu

Nuclear Medicine, Kaohsiung Veteran Hospital, Taiwan

Abstract:

In Taiwan, the incidence of cancer and tuberculosis is 473/100000 and 2.3/100000. FDG-avid lesions in lung and bones is more likely due to lung cancer with bony metastasis than tuberculosis in PET scan. Tuberculosis typically attacks the lungs, but can also affect other organs and tissues of the body, such as lymph nodes, pleura, bone, GI tract, etc. The most common sites of skeletal tuberculosis are the weight-bearing bones and joints such as the vertebral column (40% to 50%), hip, knee, and elbow.

Here we report a 64-year-old male who was diagnosed with pulmonary tuberculosis (S/P video-assisted thoracoscopic biopsy) under anti-tuberculosis treatment. The first PET showed FDG-avid RML mass with multiple bony lesions over sternum, spine, left ribs, pelvis and left femur. The nature of FDG uptake was uncertain, and no definite malignancy was found clinically, except pulmonary tuberculosis under treatment. Biopsy of sternal osteolytic lesion showed inflammatory cells infiltration without malignant cells. After one year of anti-TB treatment, the second PET showed marked decrease in FDG uptake and size in RML mass and bony lesions. We favored pulmonary and skeletal tuberculosis in this case and TB should be kept in mind in Taiwan.

PC-093

Altered FDG Uptake in a Pediatric Hemophagocytic Lymphohistiocytosis Patient Receiving Corticosteroids Treatment: A Case Report

Xuan-Ping Lu, Jui-Hung Weng

Department of Nuclear Medicine, Chung Shan Medical University Hospital, Taichung, Taiwan

Introduction: Hemophagocytic lymphohistiocytosis is a syndrome of excessive immune activation characterized by fever, hepatosplenomegaly, pancytopenia, and the pathologic finding of hemophagocytosis in the bone marrow and other tissues. According to previous studies, FDG-PET/CT was sometimes performed for malignancy or infection detection in secondary hemophagocytic lymphohistiocytosis patients and diffuse increase in FDG activity in the liver, spleen, and bone marrow or lymphadenopathy were usually detected.

Methods: FDG-PET/CT scan was sometimes performed in secondary hemophagocytic lymphohistiocytosis patients for survey of possible primary malignancy or infection. We reported a child with hemophagocytic lymphohistiocytosis secondary to EBV infection, and FDG-PET scan was performed after fasting for 6 hours with a GE Discovery MI PET/CT scanner at 60 min after intravenous injection of F-18- FDG. The CT scan is low-dose without contrast enhancement. The scan area covers vertex to above knees. Images are reconstructed iteratively with attenuation correction.

Results: FDG-PET/CT scan demonstrated altered normal distribution of FDG with decreased activity in the liver and brain. Besides, no increased FDG activity in the spleen nor lymphadenopathy was shown on FDG-PET/CT scan. Tracing back her medical history, she had been treated with 6 milligrams of dexamethasone per day since 24 days before receiving FDG-PET/CT scan.

Conclusions: After reviewing articles about altered FDG uptake and glucocorticoids, glucocorticoids were known to affect cell glucose utilization which may lead to decreased FDG uptake in the brain. In addition, the anti-inflammatory effect of corticosteroids may contribute to this abnormal FDG-PET/CT scan.

PC-094

智慧型自助報到候診系統在核醫之應用

謝文彬　黃文盛

臺北榮民總醫院核醫部

背景介紹：因應核醫部每日檢查數量及人流量大，目前皆以人工方式進行病患報到及安排檢查室，檢查時病患自行至造影室報到再進行人工唱名叫號 (全名帶姓) 方式引導病人就診，無法有效保護病人隱私，且衛生福利部醫療機構醫療隱私維護規範中也有明文規定，呼喚病人應顧慮其權利及尊嚴。爲提昇診間運作效率及改善人工唱名叫號，目標爲建置核醫部檢查流程智能服務系統，以提升病患、造影室、櫃台服務人員工作效益與提升檢查流程便利性。

方法：配合核醫部現有軟硬體設備環境，並與現有醫療資訊系統介接，建置檢查室流程系統，病人使用健保卡自助報到，診間服務人員根據等候清單服務病人，系統記錄叫號時間便於後續管理及研究運用。建置自助報到系統，提供病患自助報到機與人工櫃檯報到方式，進行病患分流。系統給報到病患號碼，提供注射室及造影室叫號，不唱名保留病患隱私。提供造影室病患自助報到功能及造影室進行叫號功能。

結果：智慧型檢查自助化報到候診系統結果：委外開發軟硬體建置費約需 2,500,000 元，且技術與資訊安全可充分掌握。創新成效爲 一、病人自助報到減輕工作人員負擔、維護病人隱私；二、同時段多診病人同步報到及最佳化看診順序；三、工作人員根據資訊即時建議病人最佳看診順序。

結論：普查 189 位門診病人，對於自助報到系統及注射造影室電腦叫號系統流程，滿意度平均爲 91.66%，門診滿意度調查提升 27%；候診時間整體下降 10 分鐘至 15 分鐘。對於第一線櫃檯人員、醫師護理師、放射師滿意度平均爲 92.66%；門診滿意度提升 10.66%。此系統對提升服務效率及品質具臨床效益，期待此服務可提供病人更優質、便利的就醫環境，不需要人爲的立即介入，同時又可提高尖峰時間的服務效能。

PC-095

Gallium-67 Scintigraphy in the Detection of Inflammation Around Endograft for Thoracic Arch Aneurysm: A Case Report

Yu-Chien Shiau, Chia-Wen Lai, Ya-Huang Chen, Fang-Shin Liu, Yen-Wen Wu, Shan-Ying Wang

Division of Nuclear Medicine, Far Eastern Memorial Hospital, New Taipei, Taiwan

Introduction: Gallium-67 scintigraphy is reported to be a useful tool for detection and follow-up of inflammation focus. Inflammation of synthetic vascular graft is relatively difficult to diagnose by conventional methods. Gallium-67 scintigraphy could be useful in the diagnostic evaluation of graft inflammation. We report a case of inflammation around the endograft for thoracic arch aneurysm detected by Gallium-67 scintigraphy.

Case report: The 80 year-old female suffered from fever for 3 weeks and left flank pain radiated to neck. She was sent to ER of a hospital in central Taiwan. Pleural effusion, LLL pneumonia, and UTI were noted and treated in the hospital. CTA was done and showed a huge thoracic aortic arch aneurysm 8 x 7 x 5 cm. She was transferred to our hospital for operation, where operation with 1. Total arch endografting (Chimney for IA (11*100 mm H-Viabahn) & LCCA (8*150 mm H-Viabahn); Periscope for LSCA (8*150 mm Viabahn) 2. echo-guided bil CFA and LBA punctures 3. Endografting for AsAo & DsAo were done. In the OPD follow-up, she suffered from progressive dyspnea and fever off-and-on. CTA of the chest and abdomen showed type 1a endoleak at the ascending aorta status post coil embolization and thrombosis of the aneurysmal sac at aortic arch. Because of persistent fever and suspicious mycotic aneurysm, she was admitted for treatment and gallium-67 scan was arranged, which showed inflammatory activity in bilateral upper chest or around endograft. Based on the report of gallium-67 scan, blood culture was arranged and reported Proteus mirabilis. Antibiotic was adjusted to control the inflammation. The fever subsided and her condition went more smoothly. She was follow-up in OPD.

Conclusions: In this case we report Ga-67 scintigraphy in the diagnostic study of inflammation around endograft for thoracic arch aneurysm, which elucidate that the modality is a useful clinical tool for diagnosis and beneficial for treatment. In the future, we hope to gather more cases for more detailed statistical analysis.

PC-096

Prognostic Value of Interim ^{18}F-DOPA and ^{18}F-FDG PET/CT Findings in Stage 3-4 Pediatric Neuroblastoma

Kuan-Yin Ko[1,2], Ruoh-Fang Yen[3], Meng-Yao Lu[4]

[1]*Department of Nuclear Medicine, National Taiwan University Cancer Center, Taipei, Taiwan*
[2]*Graduate institute of Clinical Medicine, College of Medicine, National Taiwan University, Taipei, Taiwan*
[3]*Department of Nuclear Medicine, National Taiwan University Hospital, Taipei*
[4]*Department of Pediatrics, National Taiwan University Hospital, Taipei, Taiwan*

Introduction: The aim of our study was to figure out the prognostic value of imaging parameters derived from mid-therapy ^{18}F-DOPA and ^{18}F-FDG PET in pediatric patients affected with stage 3-4 neuroblastoma.

Methods: We enrolled 32 stage 3-4 pediatric neuroblastoma patients who underwent ^{18}F-DOPA and ^{18}F-FDG PET/CT scans before and after 3 cycles of chemotherapy. For each image, in addition to the measurement of metabolic and volumetric parameters, we applied metabolic burden scoring system to evaluate the extent of primary tumor and of soft tissue metastases and that of bone/bone marrow involvement. In time-to-event analyses, the score distributions were categorized in medians. We used Cox proportional hazards model and Kaplan-Meier curves to investigate the association between theses PET parameters and clinical outcome.

Results: Over a median follow-up of 47 months (range 3-137), 16 cases of disease progression and 13 deaths occurred. After adjustment for clinical factors, multivariate Cox proportional hazards models showed interim FDG/FDOPA SUV_{max} score $\geqq$ 0.57 [hazard ratio (HR) 8.8, 95% confidence interval (CI) 1.09-71.2] and interim FDOPA metastatic burden $\geqq$ 1.27 (HR: 7.05, 95% CI: 1.02-48.7) were negative factors for overall survival and only interim FDOPA metastatic burden (HR: 7.3, 95% CI: 1.5-35.5) was associated to progression free survival. Based on Kaplan-Meier analyses, interim FDOPA metastatic burden was associated with prognosis (log rank $p < 0.001$) and interim FDG/FDOPA SUV_{max} score was associated with overall survival rather than progression free survival (log rank $p = 0.03$).

Conclusion: Our results infer that mid-treatment FDG and FDOPA PET/CT have the prognostic prediction role in stage 3-4 neuroblastoma patients.

PC-097

An Incidental Finding of Floating Kidney on Technetium-99m Methylene Diphosphonate Bone Scintigraphy: An Interesting Case

Jing-Uei Hou[1], Yi-Ching Lin[1], Shih-Chuan Tsai[1,2]

[1]*Department of Nuclear Medicine, Taichung Veterans General Hospital, Taichung, Taiwan*
[2]*Institute of Radiological Science, Central Taiwan University of Science and Technology, Taichung, Taiwan*

Introduction: The nuclear medicine bone scintigraphy is a useful tool due to its high sensitivity for bone metastasis, infection, and trauma with a reasonable cost. Nowadays, the most commonly used radiopharmaceutical for bone scintigraphy is Technetium-99m methylene diphosphonate (Tc-99m MDP). After intravenous injection, Tc-99m MDP is quickly taken up into bone and mainly excreted in the form of urine through the urinary system [1]. Therefore, there is some radionuclide activity in the bilateral kidneys and can be seen on the bone scintigraphy. We report a rare case with a floating kidney that was incidentally found during a bone scan.

Case report: Our case is a 57-year-old female who was diagnosed with breast cancer about 5 years ago. She has regular follow up at our breast surgery outpatient department and received bone scan annually. No abnormal Tc-99m MDP uptake is demonstrated in the previous whole body bone scintigraphies.

This time, she received bone scan for survey of the tumor status. Neither bone pain, operation history of bone, nor abdominal pain was told. We acquired the whole body bone scintigraphy at 3 hours in the supine position after intravenous injection of 20 mCi of Tc-99m MDP. The anterior and posterior planar images revealed relatively higher radioactivity at the tip of left 12th rib. However, the left kidney is also seen at this location. To realize where the hot spot is at, we took a local view of abdomen in the upright position and found the hot spot is at the left kidney.

Otherwise, on the supine images, the right kidney is located between the L2 to L4 vertebrae. On the upright images, the right kidney is slipped at the level of L5 vertebra. The left kidney is located in its normal position (between the T12 to L3 vertebrae) on both the supine and upright images. Thus, this patient is then diagnosed with a right floating kidney.

Discussion: A floating kidney, also called nephroptosis, is a condition in which the kidney drops down into the pelvis more than two vertebral bodies (or > 5 cm) during a position change from supine to upright. It is more common in women than in men.

Most patients with a floating kidney is asymptomatic, though some of them may have abdominal pain, a feeling of 'a ball rolling' inside, or hematuria. The pain is typically relieved by lying down due to movement of the floating kidney may cause renal tract obstruction. Some symptomatic patients also mentioned that pregnancy could relieve the pain since the enlarged uterus providing support to the floating kidney.

The cause of the floating kidney is believed to the absence of peri-renal supporting connective tissue. To treat the symptomatic floating kidney, laparoscopic nephropexy has recently become available nowadays.

In our case, the right kidney drops down into the pelvis from L2 to L5 vertebra, suggestive of the right floating kidney. However, this patient is asymptomatic. No further treatment is recommended.

Key Words: Bone scan, Floating kidney, Nephroptosis.

PC-098

術後甲狀腺球蛋白急劇升高之病例報告

盧永承　杜東峻

戴德森醫療財團法人嘉義基督教醫院核子醫學科

背景介紹：結節性甲狀腺腫，係指發生在甲狀腺內的腫塊，通常分爲單一或多發性甲狀腺結節。甲狀腺結節絕大多數是良性，良性的甲狀腺結節可用甲狀腺素治療，使結節縮小。若在甲狀腺素的治療下，結節仍持續生長有惡性疑慮，則可考慮手術切除，或臨床發現結節太大，壓迫到氣管或食道而導致呼吸困難或吞嚥困難時，也建議以手術治療。Thyroglobulin (TG) 是一種僅由甲狀腺濾泡細胞合成的糖蛋白分子，這些以膠體形式儲存在甲狀腺濾泡中，爲甲狀腺素和三碘甲狀腺素的前驅蛋白質，整個過程由甲狀腺刺激激素調節。血清中 TG 的半衰期爲 65.2 小時，血清 TG 濃度與人體中甲狀腺組織的體積成正比。TG 常在下列三種情況下上升，包括 (1) 甲狀腺腫或甲狀腺功能亢進，(2) 甲狀腺發炎或損傷，(3) 甲狀腺癌 (但非髓質部癌)。

案例報告：患者爲 56 歲男性，因診斷爲無毒性多結節性甲狀腺腫大，最後決定執行雙側全甲狀腺切除術，術前的實驗室檢查，TSH 0.24 (參考區間 0.25-4.00 uIU/ml)，FT4 1.11 (0.7-1.8 ng/dl)，Anti-Tg Ab 10.65 (< 115 IU/ml)，Tg 67.95 (3.5-77 ng/ml)，甲狀腺功能正常，符合無毒性甲狀腺腫大之診斷。術後 3 天實驗室的檢查結果爲 TSH 0.28 uIU/ml，FT4 0.82 ng/dl，Anti-Tg Ab < 10 IU/ml，Tg 762.8 ng/ml，TG 濃度急劇上升有 10 倍多，術後 10 天又再次追蹤 TG，結果爲 33.05 ng/ml 已降到正常範圍。

討論：TG 濃度的三個主要決定因素是：(1) 存在甲狀腺組織的大小 (正常和惡性甲狀腺細胞)，(2) 存在甲狀腺損傷，例如細針抽吸檢查 (FNA)、甲狀腺切除術或放射性碘治療後或甲狀腺炎期間，(3) 激素影響，如促甲狀腺激素 (TSH)、人絨毛膜促性腺激素及 TSH 受體抗體 (TRAb)。本篇案例爲良性的甲狀腺腫大，所以 TG 急遽上升最有可能的原因爲手術後造成甲狀腺損傷所導致，另外甲狀腺球蛋白的半衰期爲 65.2 小時，所以甲狀腺完全切除後至少也需一個月後 TG 才能測不到，因此術後 3 天的甲狀腺球蛋白才會如此高，術後 10 天 TG 濃度即下降至術前一半的正常範圍內。

結論：TG 是甲狀腺癌術後一個重要的腫瘤標記，但術後何時才檢查甲狀腺球蛋白？臨床上通常會在手術後一年內，每 3 個月檢查一次包含甲狀腺功能檢查 (T4、FT4 及 TSH)，一年後每 6 個月檢查一次，如果一切正常，兩年後可以一年才檢查一次。就算是良性甲狀腺手術亦同，只要甲狀腺全切除理應測不到 TG 才對，太早測反而會造成病人的憂慮以及不必要的醫療浪費。

PC-099

Post-operative Serum Thyroglobulin for the Aid of Decision Making to use Low-dose Radioactive Iodine Ablation in Patients with Differentiated Thyroid Cancer

Yen-Hsiang Chang[1], Pei-Wen Wang[1,2]

[1]*Department of Nuclear Medicine, Kaohsiung Chang-Gung Memorial Hospital, Kaohsiung, Taiwan*
[2]*Department of Internal Medicine, Kaohsiung Chang-Gung Memorial Hospital, Kaohsiung, Taiwan*

Background: Postoperative (Post-op) serum thyroglobulin (Tg) provides valuable information about residual disease or remnant tissue in patients with differentiated thyroid cancer (DTC). However, the utility of post-op Tg to determine the use of radioactive iodine (RAI) is still on debate. From mid-2018, we started introducing serum Tg within 6 weeks postoperatively for aiding the decision making for low-dose (30 mCi) RAI ablation in our hospital. The study is to assess the short-term outcome of DTC patients receiving low-dose RAI ablation with or without the aid of post-op Tg.

Methods: We retrospectively reviewed the medical records of DTC patients receiving 30 mCi RAI for remnant ablation after total thyroidectomy from June 2018 to Aug 2019, with the exclusion of the presence of anti-Tg antibodies (TgAb). The short-term outcome at one year was classified into response-to-therapy categories according to dynamic risk stratification.

Results: From the 49 patients, 30 (61.2%) were ATA low-risk, 15 (30.6%) were intermediate, 3 (6.1%) were high risk, and 1 (2.0%) could not be classified. Twenty-one (42.9%) patients had post-op Tg for decision aid before RAI ablation and 28 (57.1%) did not. Overall, 90% (19/21) of patients with post-op Tg achieved no evidence of disease (NED) at one year, whereas 82.1 (23/28) of patients without post-op Tg for decision aid achieved NED. Of those with post-op Tg for decision aid, only one (4.7%) developed structural persistent/recurrent disease (SPD/RD), while 4 (14.3%) patients without post-op Tg for decision aid developed SPD/RD and 3 of them were ATA intermediate-to-high risk.

Conclusion: Post-op Tg may be used to aid the decision for low-dose RAI ablation. Low post-op Tg could predict good short-term outcome after receiving low-dose RAI. Due to high SPD/RD rate, low dose RAI shall not apply to those without the information of post-op Tg, especially ATA intermediate-to-high risk patients.

PC-100

A Rare PET Scan of Hepatic Schwannoma

Kuan-Hsiu Lin, Chin Hu

Nuclear Medicine, Kaohsiung Veteran Hospital, Taiwan

Abstract:

We reported a 78-year-old female with a liver tumor. MRI showed a 2.8 cm nodule in S7, hypointense in T1 and moderately hyperintensity on T2WI and DWI, and cholangiocarcinoma or metastasis were suspected. FED-PET scan showed increased FGD uptake of the S7 nodule (SUVmax: 4.7) and multiple FDG-avid lymphadenopathy in mediastinum and bi-hilar region about 1.7 cm in size (SUVmax: 4.5). Tumor markers were within normal range. The patient received CT-guided biopsy, which confirmed the diagnosis of Schwannoma from pathology. Radiofrequency ablation of the tumor was performed.

Schwannomas are benign, slowly progression neoplasms which composed of Schwann cells usually occurs in the upper extremities, trunk, head and neck, retroperitoneum, mediastinum and pelvis. Schwannomas which diagnosed from liver parenchymal cell is very rare. FDG-PET scan usually reveals high tumor-to-background ratios for hepatic schwannoma, which limits the utility of PET scan to differentiate schwannoma form malignant tumors. The diagnosis of hepatic schwannoma before biopsy or operation is difficult only by radiological images and PET scan. Hepatic schwannoma is extremely rare but should be in our checking list.

PC-101

Diaphragmatic Metastasis Revealed by FDG PET/CT Scan

Po-Ling Chang, Kuang-Tao Yang

Department of Nuclear Medicine Changhua Christian Hospital

Introduction: Diaphragm is a rare region for distant metastasis. We present a case of diaphragmatic metastasis of a patient with breast cancer.

Methods: The 50 year-old female patient was diagnosed with breast cancer on the right side and received surgery in 2016. Unfortunately, left breast cancer was diagnosed in 2019. Unfortunately, left breast cancer was diagnosed in 2019. A FDG PET/CT scan was performed before operation in January, 2019 and distant metastasis was not found. After operation, the pathologic stage was T3N1M0. Because of recurrence confirmed in May, 2019, the second FDG PET/CT was performed and revealed left axillary lymph nodes metastasis, distant metastasis involving the mediastinum and liver. Because of triple-negative results of pathology, the patient received chemotherapy with Epirubucin and Cyclophosphamide. The third FDG PET/CT showed more lesions in the left diaphragm, bones and para-aortic lymph nodes in November, 2019. However, the abdominal CT scan did not suggest diaphragmatic metastasis even though there was slight thickness in the left diaphragm. The patient was expired in December, 2019.

Results: At least four lesions were noted with increased metabolic activity in the left breast (SUV max: 8.4). An extensive area with markedly increased FDG activity was noted in the dome of the left diaphragm (SUV max: 6). Hypermetabolic lesions were also noted in the liver, paraaortic lymph nodes, left iliac, ischial bones and left femur.

Conclusions: Triple-negative breast cancer is considered aggressive. FDG PET/CT has potential to evaluate the response of treatment for breast cancer.

PC-102

How Tc-99m Whole Body Bone Scintigraphy Helps to Diagnose Pediatric Bone Tumors

Ya-Cing Hsu, Yu-Ling Hsu

Department of Nuclear Medicine, Ditmanson Medical Foundation Chia-Yi Christian Hospital

A 9-years-old boy was referred to our hospital for a palpable mass with pain at left ankle. He complained about the left lateral malleolar tip mass for several days also got sprain injury. Under the impression of probable tumor, Tc-99m bone scintigraphy was arranged The imaging showed only slight increase of radioactivity at left lateral malleolar region. It might be ankle bursitis, tumor of unknown nature, intraosseous ganglion, trauma/fracture, or osteoarthritis. Biopsy was then performed because of persisting symptoms. The pathological result revealed osteochondroma measuring 3 x 2.4 x 1.3 cm.

Osteochondroma is the most common type of non-cancerous bone tumor. It is a hard mass of cartilage and bone that generally appears near the growth plate. In most situation, osteochondromas do not spread beyond the affected bone, they may grow in size as child grows till child stops growing (around age 14 in girls and 16 in boys). Under general circumstances, osteochondromas create no problems and no treatment is needed. Once the tumor is causing significant pain, putting pressure on blood vessels or nerves, or very large in size, the surgery is necessary. The chance of this benign tumor turning into malignant condition is rare, but patient still have to keep eyes in it.

The interpretation of the bone images of children is challenging, since the normal growing skeleton will appear different from one age group to another. X-ray and CT imaging are the common and fast modalities, but their scanning methods can only provide us partial information. The major performance of osteochondroma only has a single lesion. Less commonly, it will occur as multiple tumors. In this situation, ^{99m}Tc-MDP wholebody bone scan plays an important role and will help us to get the whole picture of any bone tumor lesions.

PC-103

Incidental Finding of Tertiary Primary Malignancy Detect by Dual Phase 18F FDG PET/CT Images

Yi-Ching Lin[1,2], Shih-Chung Tsai[2]

[1]*Department of Public Health, China medical University, Taichung, Taiwan*
[2]*Department of Nuclear Medicine, Taichung Veteran General Hospital, Taichung, Taiwan*

Here we present a case with underlying hepatic cell carcinoma who underwent F-18 FDG PET/CT scan due to disease progression. Patient suffered from tea-color urine and yellowish skin discoloraiton for one month since this April. ERCP was performed and showed hepatic hilar tumor. HCC was diagnosed with bile duct involvement. Due to aggressive disease entity, F-18 FDG PET/CT scan was suggested. On early images of F-18 FDG PET/CT scan, moderate hypermetabolic mass in the left lobe of liver was demonstrated which indicated primary HCC. Two hypermetabolic nodules were also detected at left lower lung and left pulmonary hilar area, respectively. There's a small area with equivocal metabolism in the ascending colon. Therefore, dual phase of local scan was performed after 3 hours of FDG injection. The delayed images of this patient revealed higher FDG accumulation not only in the left lobe of liver, but significant and focal uptake at the ascending colon though there's no structurally abnormality detected by attenuated CT scan. Lung wedge resection and colon scope were all arranged after PET scan. Lung adenocarcinoma of left lower lung with pulmonary hilar lymph node involvement and moderately differentiated adenocarcinoma in ascending colon were diagnosed incidentally. Three synchronous primary tumor were detected by PET/CT scan in this patient. F-18 FDG PET/CT scan is a useful tool for cancer staging and detecting.

PC-104

Bone Involvements of Distal Extremities in Extranodal Nasal NK/T Cell Lymphoma on F-18 FDG PET/CT: A Case Report

Yu-An Yen, Li-Chun Wu, Chiang-Hsuan Lee

Department of Nuclear medicine, Chi-Mei Medical Center, Tainan, Taiwan

Introduction: We present a patient with extranodal nasal NK/T cell lymphoma with rare multiple bone involvement of distal extremities on F-18 FDG PET/CT.

Case report: A 39-year-old woman suffered from nasal obstruction for 3 months and a right nasal tumor was found in another hospital. Tumor excision was done and extranodal NK/T cell lymphoma was histopathologically proved. She then received CCRT but incomplete due to severe radiation mucositis and was referred to our hospital for help. F-18 FDG PET/CT was arranged for restaging, and it showed multiple hypermetabolic lesions in distal extremities including bilateral carpal bones and metacarpals, bilateral radius and ulna, bilateral distal humerus, bilateral distal femur, bilateral tibia and fibula and bilateral tarsal bones. Following MRI of lower extremity showed consistent with lymphoma, involving bilateral distal femur, bilateral tibia, bilateral fibula and bilateral tarsal bones. Bone marrow aspiration revealed No immunophenotypic evidence of non-Hodgkin lymphoma. The restaging was as stage IV involving multiple bones. After 4 cycles of chemotherapy, interim F-18 FDG PET/CT was performed and showed good response to therapy of lymphoma in the lower extremities.

Discussion: Extranodal NK/T cell lymphoma is practically FDG-avid that F-18 FDG PET/CT is used to be a standard imaging modality in the survey of this cancer. The clinical features of extranodal NK/T cell lymphoma are majorly localized disease invading the nose, sinuses, or palate; other extranodal sites involved are often upper airway, Waldeyer's ring, gastrointestinal tract, skin, testis, lung, eye, or soft tissue; muscle and uterus involvement were also been reported; bone marrow involvement could be found in about 10 percents of patients. However, bone involvement like this case is rare as per our knowledge and literature in the past. Besides, this case also demonstrated the importance of the whole body acquisition from the vertex to the feet of F-18 FDG PET/CT in patients with lymphoma.

PC-105

PET/CT 於 GIST 轉移吸收低下之案例報告

沈淑禎[2] 門朝陽[1] 曾柏銘[1] 呂建璋[2] 林雅婷[2] 蕭聿謙[3]

[1] 天主教中華聖母修女會醫療財團法人天主教聖馬爾定醫院正子造影中心
[2] 天主教中華聖母修女會醫療財團法人天主教聖馬爾定醫院核子醫學科
[3] 亞東紀念醫院核子醫學科

前言：PET/CT 常用於診斷及治療追蹤，GIST (Gastrointestinal stromal tumors) 通常有強的 FDG (18F-fluorodeoxyglucose) 吸收，我們報告一位 GIST 病人開完刀於追蹤期間，CT 疑似有肝臟及腹膜轉移而 PET/CT 卻發現低吸收的病人。

案例報告：病人，69 歲，男性，於 108 年 04 月因胃部不適開刀，診斷爲 GIST，並於 108.05 至 109.03 接受 Glivec 治療。病人於 109.02 治療追蹤期間電腦斷層發現有 5 cm 的 cystic tumor 在肝臟右葉，無明顯之 tumor stain 及 multiple soft tissue nodules 在上腹部的腸繫膜間，疑似肝臟及腹膜轉移。後續的正子檢查於肝腫瘤的位置吸收不高 SUVmax 2.24 (early)，1.91 (delay)，腹部 soft tissue nodule 吸收亦低，其中一個爲 SUVmax 1.64 (early)，1.67 (delay)；另一個爲 SUVmax 1.64 (early)，1.65 (delay)。第一次的 CT guide biopsy 病理報告爲：mesothelial hyperplasia，第二次的 CT guide biopsy 爲 GIST metastatic。

討論：PET/CT 用於診斷及治療期間的復發，一般來說優於 CT，文獻上報告的 PET/CT，其敏感度爲 86%，PPV 爲 98%，好發轉移的位置爲肝臟和腸繫膜。此病患在 liver cystic tumor 的 FDG uptake 並不高，判讀爲治療後的反應，但也無法排除爲 FDG 低吸收的之 GIST 轉移。而在上腹間低吸收之 peritoneal nodule 也是懷疑治療效果之反應，但依然無法排除其爲 FDG 低吸收之轉移，因此進一步安排做病理切片，此病患做了第二次 Guide biopsy 才證實其中 peritoneal nodule 爲 GSIT 轉移。此病例並無 baseline 的 CT，如 baseline 中的 FDG PET 吸收低下的話，並不適合做追蹤使用。

結論：這次報告的病例屬於非常少見之案例。PET/CT 對於早期的 imatinib 治療效果的評估具有良好的敏感度及特異性，一般來說優於電腦斷層。但對於低吸收的 Soft tissue nodule，如果沒有 baseline 的影像，並不能排除復發的可能，需進一步的組織切片證實。

PC-106

SPECT-CT 運用於分化不良甲狀腺癌之追蹤

呂建璋[1] 林雅婷[1] 曾柏銘[2] 沈淑禎[1] 門朝陽[2] 蕭聿謙[3]

[1] 天主教中華聖母修女會醫療財團法人天主教聖馬爾定醫院核子醫學科
[2] 天主教中華聖母修女會醫療財團法人天主教聖馬爾定醫院正子造影中心
[3] 亞東紀念醫院核子醫學科

背景介紹：甲狀腺癌的分類中，分化不良甲狀腺癌 (poorly differentiated thyroid carcinoma, PDTC) 非常少見，是一種介於未分化和濾泡性癌之間的甲狀腺癌，本院自 96 年至 109 年間僅有 2 位 PDTC 患者，由於 PDTC 臨床預後介於未分化和分化良好甲狀腺癌之間，需要及積極的治療與追蹤，本篇報告 SPECT-CT 運用於 PDTC I-131 治療後之影像追蹤，探討 SPECT-CT 的診斷價值。

方法：本例 PDTC 患者於 108 年 12 月接受甲狀腺切除手術，並於 109 年 1 月接受 150 毫居里之 I-131 治療 (治療前 Tg：81 ng/mL)。109 年 4 月因懷疑復發接受甲狀腺切除手術 (術前 Tg：> 495 ng/mL)，並於 109 年 8 月再次接受 I-131 治療 (治療前 Tg：136 ng/mL)，兩次治療 7 天後均執行全身掃描 (WBS)。第一次治療後掃描時，加馬攝影機爲 SPECT，患者接受 WBS 及頸部平面掃描，第二次治療後掃描，機型已更換爲 SPECT/CT，除 WBS 外，亦執行胸頸部 SPECT-CT。

結果：第一次治療後掃描，除甲狀腺殘餘組織外，WBS 於右側肺部及肝臟交界處發現疑似轉移病灶，無法確認病灶實際位置。第二次治療後掃描發現甲狀腺殘餘組織已減少，肺部及肝臟交界處仍發現轉移病灶，但此次掃描藉由 SPECT-CT 技術，可確認甲狀腺殘餘組織位置及大小，並證實轉移病灶位於兩側肺部下葉。

結論：I-131 掃描的影像解析度因其同位素特性，除甲狀腺、唾液腺及腸胃道的吸收，其餘身體組織的攝取活性不高，因而解剖位置不易判定，採用 SPECT-CT，可提高對於甲狀腺殘餘組織、淋巴轉移及遠端轉移病灶判定的準確度，利於未來追蹤評估 I-131 治療的效果。

PC-107

A Rare Case of Pimary Bone Endothelioid Hemangioma Mimicking Multiple Bone Metastases --- Case Report and Imaging Study by Bone Scan; SPECT/CT & PET/CT

Chao-Yang Men[1], Shu-Jane Shen[2]

[1]*PET/CT Center. St Martin De Porres Hospital, Chiayi, Taiwan, ROC.*
[2]*Dep. of Nuclear Medicine. St Martin De Porres Hospital, Chiayi, Taiwan, ROC.*

Introduction: Epithelioid hemangioma (EH) is a vascular tumor with ubiquitous distribution. Multiple bone lesions are very rare in total cases. In this case, the radiological and nuclear scans are described. We suggest that whole body bone scans, SPECT/CT & PET/CT could have additional values in diagnosis cases like this. Possible mistake for misdiagnosis of multiple bone metastases should be avoid if when PET/CT SUVmax is not over 4. The patient received L1, L4 & S2 vesselplasty and bone biopsy in two surgery by PET/CT scan localization of bone lesions. PET/CT scan seems could very similar pathology like angiosarcoma, epithelioid hemangioen dothelioma and epithelioid hemangioma by SUVmax higer or lower.

Case report: A 65 male who had sustained painful limitation over back for one year. Because of back pain increased. X-ray and MRI showed multiple spine metastasis. Whole body bone scan and SPECT/CT scan all support for this diagnosis. Bone biopsy even showed angiosarcoma at one medical center. By second opinion, another medical center confirmed diagnosis for primary bone endothelial hemangioma which is benign nature. We will discuss subtle change for those imaging study mimicking multiple bone metastases, & what we can learn about. PET/CT scan shows low SUVmax indicating that this is not a bone malignant disease, All 6 hot locations is less than 4. This patient was told not a malignant disease and went home happily.

Discussion: Epithelioid Hemangioma is usually found in adult patient most commonly with one solitary lesion & only 1/4 with multifocal location. Our patient is the most few location in spine with multiple foci. EH is mostly lytic and well define sclerotic margin & found incidentally. EH does not cause cortical bone destruction but associated with thick periosteol bone reaction. L spine & MRI initially suspected with multiple bone metastases (A; B; C) SPECT/CT also shows L1 osteolytic lesion (D). PET/CT shows not just L1 but also L5; S1 and pelvic bones involvement. (F). 1st bone scan and 2nd bone scan shows apparently progressive disease during three months in comparison (G & H). PET/CT scan result rejected other study with the diagnosis of multiple bony metastasis. PET/CT scan could not merely localization but also decide maligant possibility.

Conclusion: In this case, PET/CT shows the SUVmax of all 6 lesions is around 3, which lower than 4.5, with cutoff value of metastatic bone disease of PET/CT scan. This probably helps us to differentiate EH patient in the future due to very few cases to complete imaging study like this in the world. Avoid misdiagnosis like this in the future.

PC-108

Diffuse Uptake of F18DG in Spine Could Be Bone Marraw Reaction Rather Than Bone Metastases in Staging of Esophageal SCC---Case Report and Literature Review

Chao-Yang Men[1], Shu-Jane Shen[2]

[1]*PET/CT Center. St Martin De Porres Hospital, Chiayi, Taiwan, ROC.*
[2]*Dep. of Nuclear Medicine. St Martin De Porres Hospital, Chiayi, Taiwan, ROC.*

Background: There are many case report and research about why so high false positive rate of PET scan in staging esophageal SCC with bone metastases. Bone marrow hyperplasia and fat degeneration are two reasons. Others like using EGFR and blood transfusion or chemotherapy. We found this case septic shock caused it.

Case report: A 52 year-old male was diagnosis as M/3 esophageal SCC. PET/CT scan is for staging. Unexpectedly found F18DG with homogeneous distributed in whole spine (B & D). CT scan shows T4N0M1 with tumor invades adjacent structures also with suspicious lung infection or invasion (A). During admission he had RML pneumonia and septic shock with blood culture for gram positive streptococus. Short of breath and high fever were noted. O2 & antibiotics were given and patient was improved. The coronal CT scan also showed no osteolytic lesions but some DJD of L4; 5 spine only (C). PET/CT also shows diffusely TL spine hypermetabolism.

Discussion: We can seen this tumor is in carinal level with tumor invasion to neighbering structure but no evidence of bony invasion and the reason of F18DG homogeneous uptake in spine is due to bone marrow reaction like septic shock induced bone marrow hyperplasia. In this case, multiple consolidation with diffuse bronchovascular nodularity at RML, RLL & LLL lung may favor of lung metastases. A resarch of Mayrland university hospital showed when patient had septic shock, the SUVmax of bone marrow and pelvic bones will be increased to 3.2 even 4 and other organ will be decreased in their review. The SUVmax of T spine is 4.9 to 5.4. in our study, maybe slightly increased in comparison with their study. This is due to different stage of infection and antibiotic using time. Mixed with lung metastases is possible the other reason.

Conclusion: Complex etiology of F18DG avid in esopheal SCC should be traced. The reason of diffusely F18DG avid in esophageal patient is many, according to literature like use of EGFR, blood transfusion and postchemotherapy. New report for bone marrow hyperpalsia and fat degeneration should do bone biopsy to prove. Unlike this case, septic shock is the main cause of study due to blood culture. and it will be relieved by antibiotics should expect spine will be decreased in uptake if follow up PET scan. Though we cannot do anther study for sure diagnosis. We can use past research to confirm this condition if septic shock improved.

PC-109

因注射部位所引起之藥物堆積分析

曾柏銘[1] 呂建璋[2] 沈淑禎[2] 門朝陽[1] 林雅婷[2] 蕭聿謙[3]

[1] 天主教中華聖母修女會醫療財團法人天主教聖馬爾定醫院正子造影中心
[2] 天主教中華聖母修女會醫療財團法人天主教聖馬爾定醫院核子醫學科
[3] 亞東紀念醫院核子醫學科

背景介紹：核醫藥物是使用診斷用藥物混合不穩定之放射性同位素而成。診斷用藥物可以利用其特性，在注入身體後附著於特定器官，達到診斷的效果。然而核醫藥物殘留至留置針的狀況卻仍不停發生，進而引起影像品質及臨床醫師診斷結果下降。經過去年使用 PDCA 手法來降低骨骼掃描所導致之藥物殘留堆積問題後，我們想要藉由此經驗來分析正子藥物 (18F-fluorodeoxyglucose, FDG) 造成藥物堆積之原因。

方法：我們搜集了 2020 年 04-08 月曾經進行正子造影檢查之病人 (共 86 位，男 36 位，女 50 位)，分別以年齡、性別、不同種類之留置針 (Lock & T-connect)、以及生理食鹽水沖洗量 (10 cc & 20 cc)，來檢視造成正子造影藥物堆積的原因。

討論：我們原本認爲年齡 (本次收集之平均年齡爲 60 歲) 與留置針的種類是造成藥物堆積的主要原因 (因 T-connect 有雙接頭，在注射 FDG 時容易堆積至另一測接頭)，但我們在收集數據並使用 Mann-Whitney 分析後發現無論在年齡、性別、以及留置針的種類上皆無明顯差異，反而是生理食鹽水的沖洗量有著顯著的差異。在注射完 FDG 再沖洗 20 cc 的生理食鹽水後，其留置針上的 SUV 明顯低於沖洗 10cc 的生理食鹽水 (P = 0.023)。

結論：核醫藥物注射堆積一直是核醫科長久以來想改善的項目之一，雖由上述實驗中得知生理食鹽水沖洗量愈多則 FDG 堆積量愈低，但 20 cc 的沖洗量仍可有許多不同方法完成，例如將 20 cc 同時注入同一接頭，或分別以 10 cc 沖量 T-connect 之兩邊接頭。由於藥物注射當下護理師並無法由手感判定藥物是否堆積，故需利用許多不同的方法來進行測試，方可降低藥物洩露的機率。而我們也將繼續利用其它不同的方法進行測試，使得藥物堆積於留置針或血管的問題能徹底解決。

PC-110

利用 QCC 手法來降低骨骼掃描影像不良率

曾柏銘[1] 呂建璋[2] 沈淑禎[2] 門朝陽[1] 林雅婷[2] 蕭聿謙[3]

[1] 天主教中華聖母修女會醫療財團法人天主教聖馬爾定醫院正子造影中心
[2] 天主教中華聖母修女會醫療財團法人天主教聖馬爾定醫院核子醫學科
[3] 亞東紀念醫院核子醫學科

前言：全身骨骼掃描因具有便宜、可進行全身掃描及敏感性高等特性，一直爲核子醫學重點檢查項目之一，約佔總檢查量之 1/3-1/4。但進行骨骼掃描時需同仁及患者共同配合，如異物、污染、病人晃動、注射部位藥物殘留等皆會造成影像品質下降。如可降低骨骼掃描之影像不良率，則可讓影像更清晰、醫師更利於診斷，同時也可降低受檢病人之等待時間。

方法：我們搜集了 2018 全年骨骼掃描影像，逐一檢視並分析影像不良之原因，最後在全年 1086 件骨骼掃描案例中，共分爲異物、污染、病人晃動、解尿不完全、注射部位藥物殘留、藥物沉積於軟組織過多等六項影像不良原因，最後計算出 107 年件影像不良件數，不良率爲 9.9%。經由公式之計算，將骨骼掃描影像不良率目標值設定在 5.1%【目標值＝改善前 – (改善前 × 改善重點 × 圈員能力) 9.9%-(9.9%×80%×60%) ＝ 5.1%】。

討論：決定目標值後，我們利用要因分析圖及眞因驗證等方法，解析出眞因爲「檢查前未解尿」、「無法正確判斷留置針是否順暢致藥物洩露」、「生理食鹽水沖洗量不足致藥物蓄積於留置針」、「解尿時污染衣物」及「缺乏適合之衛教單張」5 項，並在對策實施與方法中，導入「藥物注射口訣 CDPRP 五步驟」、「整合病人檢查前解尿及更衣流程規範」及「優化骨骼掃描檢查各流程衛教單張」，使原本之影像不良率 9.9% 降至 3.9%，達成率 125%，進步率 60.6%。

結論：透過此次品管圈活動之跨團隊小組 (包含醫師、醫事放射師及護理師) 進行改善骨骼掃描影像品質，使同仁在活動過程中學習到發掘問題的能力及改善問題的技巧，進而標準化使小組成員執行骨骼掃描有所依據，並達成提升骨骼掃描影像品質之目標。

PC-111

使用 SPECT/CT 來評估早期腰大肌膿瘡的應用

曾柏銘[1] 沈淑禎[2] 呂建璋[2] 門朝陽[1] 林雅婷[2] 蕭聿謙[3]

[1] 天主教中華聖母修女會醫療財團法人天主教聖馬爾定醫院正子造影中心
[2] 天主教中華聖母修女會醫療財團法人天主教聖馬爾定醫院核子醫學科
[3] 亞東紀念醫院核子醫學科

背景介紹：腰大肌起源於腹膜後肌，從 T12 胸椎一直到 L5 腰椎的外側邊緣，最後以肌腱爲結束點並終止於骶骨小轉子。腰肌膿瘡是髂腰肌腔內液的聚集，常見於糖尿病及免疫力缺損的病人；也可能透過血液、連續的相鄰結構擴散或遠端的感染中漫延。腰大肌膿瘡是一種不常見的疾病，該病因其有腰痛症狀，在診斷上具有一定挑戰性。

案例分析：一名 88 歲，患有脊椎炎、輸尿管癌，合併有高血糖並長期洗腎之女性病患，長期於本院進行看診。該病患於 2020 年 05 月時因腰部疼痛而住院，骨科醫師懷疑有骨髓炎 (Osteomyelitis) 而開立 Tc-99m MDP 及 Ga67 Scan，我們使用 Siemens Evo Excel SPECT/CT，於檢查前一天注射 Ga67，並於檢查當日注射 Tc-99m MDP。在打藥後我們立即收集了 Dynamic 與 blood pool 影像，並於四小時的延遲平面影像中同時開啓 Ga67 與 Tc-99m 雙能峰 (亦即病人一次檢查即可收集兩種影像) 檢查。 在 Tc-99m MDP 及 Ga67 的平面影像中可見 L2-L4 脊椎有顯影，Ga-67 平面則顯示周圍之軟組織亦有不明顯的吸收增加；但在 SPECT/CT 影像中，則可看出在脊堆旁有明顯之 Ga-67，沿著腰大肌顯影，最後診斷爲腰椎之骨髓炎及腰大肌膿瘡。

討論：腰大肌膿瘡是一種在腰椎間的膿液，可爲原發性或繼發性，臨床表現常爲非特異性，因此，很容易形成誤診。典型的表現包括發熱，腰痛，以及大腿前部或腹股溝疼痛，某些患者甚至出現不明原因的發熱。但如果單純使用 Ga-67 掃描，則很容易被誤診，而使用 SPECT/CT 則明顯優於平面影像，因爲 CT 有可效的進行定位，並有衰減校正功能，可消除部份誤診的問題。

結論：膿瘡的臨床表現是可變的，且往往是非特異性的。在一般人群中，膿瘡在進行抗生素治療前需進行膿液引流，而影像學檢查則可有助於做出明確的診斷。有注射顯影劑的 CT 被認爲爲黃金標準，診斷率可達 80-100%，但在早期感染或膿瘡形成前 CT 是不明顯的。而 MRI 則可提供詳細的圖像，並能分辨出蜂窩性組織炎、膿腫、血腫、和腫瘤，但 CT 或 MRI 皆僅能提供有限區域的掃描。而 Ga67 在偵測腰大肌膿瘡的敏感度爲爲 92%，雖然特異性不佳，但 Ga67 掃描搭配 SPECT/CT 卻爲檢測感染性病變的一種有效方式，且 Ga67 可提供全身掃描資訊，爲病人提供更準確的診斷結果。

PC-112

False Negative of Bone Scan in Patient of Cholangiocarcinoma with Occult Bone Metastasis Near Left Hip

黃立壬　翁瑞鴻

中山醫學大學附設醫院核子醫學科

Introduction: The purpose of this study was to evaluate and investigate the fallacy of the diagnosis of bone metastasis and osteoarthritis in Tc-99m MDP bone scan in one specific 76 -year-old female Taiwanese patient diagnosed of cholangiocarcinoma with lung metastasis.

The patient complained of left thigh pain after rehabilitation in 2018 and was diagnosed with pathological fracture of the left femur 10 days later. This case study aims to emphasize the importance of differential diagnosis and the thinking process pertaining to the occult lesions in the bone scans. The nature of the lesion should be identified due to the difference of subsequent treatment of bone metastasis and osteoarthritis, and mistaking bone metastasis for osteoarthritis may cause instability of pelvic bone, hip joint and femur.

Materials and Methods: The study reviewed all of the patient's clinical data from 2017-09 in a 3-year period. The data included X-ray plain film images, computer tomography, MRI and Tc-99m MDP bone scan.

Results: The initial evaluation of bone meta status on 2017/09/29 and 2018/10/11 were overruled after a retrospect analysis of subsequent clinical findings, CT, MRI and bone scan images. Upon re-examining the past bone scans carefully, a photopenic area was noted near left proximal femur and next to an increased uptake focus. The photopenic area was overlooked at the very first time of the interpretation. The abnormal uptake may not be mistaken into OA if the adjacent photopenia had been taken into consideration. Another discrepancy upon reexamination was the metastatic lesion near the right iliac bone. The patient has already received XRT treatment for the right iliac lesion.

Conclusions: OA in hips is common in the elderly. However, adjacent pelvis and proximal femurs are also predisposed to metastasis. As compared to hot foci, cold or photopenic lesions are more easily overlooked on bone scan. We suggest that in oncology patients with existing metastasis, OA should not be taken for granted on the etiology of severe hip pain.

The lesions should also undergo further investigation if the lesions in question were not situated at the joint space or the lesions exhibit heterogeneous uptake, especially if osteoblastic sites were to appear directly next to osteolytic lesions. The possibility of metastasis should be confirmed or excluded with great care due to the fact that false interpretations may lead to inappropriate management and possible undesirable results.

PC-113

台灣南部某醫院血清維生素 D 不足盛行率探討

張素雲[1] 薛伃婕[1] 林淑靜[1] 廖建國[1] 王昱豐[1,2]

[1] 佛教大林慈濟醫院核子醫學科
[2] 慈濟大學醫學系

背景：維生素 D 爲一種人體中重要的脂溶性維生素，血清維生素 D 濃度不足可能導致骨質疏鬆症及骨折的發生，對於人體其他的健康狀態也有著顯著的重要性，包含了免疫調節作用及感染性疾病的預防、降低呼吸道感染、心血管及腎臟保護作用、部分癌症的預防及改善、代謝症候群的預防、糖尿病的改善等，維生素 D 就像防護罩，缺少時會影響身體的防禦能力，進而產生各種問題。本研究目的爲探討陽光充足的南部人們是否有維生素 D 缺乏的問題 。

材料方法：2019/01/01 至 2020/06/30 間，共收集 1,053 支健檢血液檢體，經隔夜空腹抽血，離心取上清液，並使用 ROCHE cobas e601 全自動化學冷光免疫分析儀檢測分析。當血清 25-OH 維生素 D 濃度低於 32 ng/mL 訂爲維生素 D 不足，濃度高於 32 ng/mL 以上則訂爲維生素 D 正常。統計分析採用 Tuckey test 分析 和 One-way ANOVA 分析，$p < 0.05$ 具統計上意義 ，進行分析四組年齡層 (< 50、51-60、61-70 及 ≥ 70 歲) 之間維生素 D 不足的盛行率。

結果：男性有 450 人 (平均年齡：53.6 ± 13.2)，維生素 D 不足者有 237 人 (52.7%)，女性有 603 人 (平均年齡：53.3 ± 13.0)，維生素 D 不足者有 453 位 (75.1%) (表 1、表 2)，女性維生素 D 不足遠大於男性，男性 Vit D 的結果值隨著年齡增長而有增加的趨勢 (表 3)，女性的 Vit D 結果值與年齡分組有顯著差異，發現≦ 50 歲的組別 (23.3 ± 8.6) 偏低與 51-60 歲、61-70、> 70 歲的數值有較大差異 (表 4)。其中男性 Vit D 不足的比率明顯較女性低的原因，可能和飲食習慣、南部日照時數較高、居民以從事農業、畜牧業居多較一般人容易接觸到陽光有關，而女性則可能因爲怕曬黑、少戶外活動、擦防曬油、撐傘、攝取不夠、吸收不良、停經等因素所致。

結論：根據台灣國民營養健康調查研究指出，「近七成台灣成年人缺乏維生素 D，即使連日照充足的南部，維生素 D 濃度也未達標準，女性狀況又比男性嚴重」。本研究結果顯示維生素 D 不足，男性約占五成、女性約七成，其中男性盛行率與全國國民營養健康調查結果略有不同，但仍佔相當大的比率。

PC-114

Nasopharyngeal Carcinoma with Bone Metastasis: A Case Report

Pei-Jung Li, Chia-Chi Chang, Po-Ling Chang

Department of Nuclear Medicine Changhua Christian Hospital

Introduction: The incidence of bone metastasis with Nasopharyngeal carcinoma (NPC) is relatively rare.

Methods: A 61-year-old man was a case of nasopharyngeal cancer diagnosed in 2018. Bone metastasis was found on a FDG PET/CT scan in 2019 because of elevated EBV viral load. On the follow up FDG PET/CT scan, marked resolution was noted. However, bone metastasis was found again on the FDG PET/CT in the delayed study. Before injected tracer ^{18}F-FDG, the patient was instructed to fast for more than 6 hours. The early phase image acquisition for whole body scan started at a mean time point of 60 minutes. (range: 50-70 mins) A delayed scan after tracer injection of duration about 100-150 mins. A transmission scan was obtained with two setting of images for attenuation correction.

Results: Areas with intensely increased ^{18}F-FDG uptake were noted in the left nasopharynx, left level II, V regions and right ilium (SUV max: 5.5) with increased SUVs in the delayed study (SUV max: 5.7). An area with increased ^{18}F-FDG uptake was noted in L3 (SUV max: 2.9) in the delayed study.

Conclusions: A whole body PET/CT scan was usually performed to evaluate distant metastasis. Most of the metastasis disease will be detected with a threshold of suv > 2.5. However, still obscurve lesions only be detected with an additional delayed scan. A specified PET/CT scan with or without whole body delayed scan may be recommended.

PC-115

以決策樹探討放射免疫分析實驗室廢水桶容量設置策略之研究－以南部某醫院 RIA 爲例

張淑芬　張朝鈞　卓世傑　顏吉龍　曾宜玲　段淑薰　李將瑄　顏玉安

奇美醫療財團法人奇美醫院核子醫學科 RIA

背景介紹：

放射免疫分析實驗室依照現行法規均必須設置廢水桶。而廢水桶之總容量，至少必須滿足每次桶滿後偵測濃度，降至法規許可排放濃度所需之儲存時間與維持正常作業量之需要。不過，在一定的空間中，究竟是設置少數大桶或多數小桶對實驗室之正常運作較爲有利，是頗值得探討的問題。本研究即爲以南部某醫院核醫科之操作量與偵測濃度統計結果爲基礎，運用決策樹方法來探討放射免疫分析實驗室廢水桶容量設置策略之研究。

方法：

1. 收集自 2008 年 5 月至 108 年 10 月儲滿，共 30 筆 RIA 廢水桶送驗檢測活度資料並與以統計。
2. 計算檢測出活度之各筆資料，衰減至低於〈游離輻射防護安全標準〉之下水道排放物月平均濃度水中排放物濃度管制限度 6.09×10^5 Bq/m^3 之單桶應留置日期。
3. 將各單桶應留置日期 * 總量比例 (1600L 桶 *0.25，300L 桶 *0.047)，以得出影響日數。
4. 以檢測活度比例 (機率) 與各影響日數爲基礎，製作決策樹圖。

結果：

1. 送驗之 30 筆資料，大桶 (1600L 桶) 有 13 筆，佔全體 43%，小桶 (300L) 有 17 筆，佔全部之 57%，檢測出放射性活度之資料共 8 筆，比例約爲全體之 27%，其中大桶有約 7 筆，達所有大桶之 54% 檢出活度，小桶僅有 1 筆檢出活度，約佔小桶全部之 6%。
2. 檢測出活度之 8 筆資料，應留置日期最多爲 477 日，最少爲 0 日，平均爲 261 日，中位數爲 466 日。
3. 以應留置日期 * 總量比例，得出之影響日數方面，小桶僅有 1 筆，日數爲 17.6 日，其餘 7 筆皆爲大桶，日數最高爲 119.3，最低爲 0 日，平均爲 61.1 日，中位數爲 45 日。
4. 決策樹圖顯示，小桶可能影響之作業日爲 1.1 日，大桶高達 33 日 (詳見下圖)。

結論：

依照南部某醫院 RIA 之廢水桶送驗檢測活度資料，所製作之決策樹圖顯示，相同之廢水總容積設置，小桶對實驗室之正常運作較大桶爲有利。如以本文之資料爲例，小桶可能影響之作業日僅爲 1.1 日，而大桶卻高達 33 日，所以可以容易明確的以設置多數小桶來作爲廢水桶設置的策略目標。事實上決策樹方式的優點主要即是對簡單選項的決策，以不複雜的計算，組織明確且可理解的規則，以得出明顯的決策依據。當然其缺點就是對多選項與影響不明確的選項較難得出明顯的決策依據。所以如何運用決策樹方法或是否適當，仍然必須視決策選項的多寡與能否明確得出影響程度而定。不過本研究所依據之數據僅爲單一醫院的資料，如需確認大、小桶設置何者爲優，仍需收集更多之資料，進行更深入之研究。

PC-116

放射免疫分析實驗室作業量與產生廢水放射性濃度關係之研究－以南部某醫院核醫科爲例

曾宜玲　張朝鈞　卓世傑　顏吉龍　張淑芬　段淑薰　李將瑄　顏玉安

奇美醫療財團法人奇美醫院核子醫學科放射免疫分析實驗室

背景介紹：

放射免疫分析實驗室於作業後，均會產生放射性廢水。而此廢水依法規規定，均需經偵測合於或儲放至低於法規允許之放射性活度濃度才能排放。因此如能預估廢水之放射性活度濃度，即可計算出所需之儲存空間與時間。一般認爲作業量應與產生廢水之放射性活度濃度呈正比關係，但國內卻並無相關之實證研究，殊爲可惜。本研究即爲以南部某醫院核醫科爲例，探究放射免疫分析實驗室作業量與排放廢水檢測放射性活度濃度關係之研究。

方法：

1. 收集自 2009 年 1 月至 108 年 10 月儲滿，共 29 筆 RIA 廢水桶送檢驗之放射性活度濃度資料。
2. 收集自 2008 年 1 月至 108 年 10 月每月操作檢體數量，共 142 筆資料。
3. 選取每月操作檢體數量最少之月份設爲 1，其餘各月份之數量依比例轉換。
4. 將送檢驗之放射性活度濃度資料，依每筆桶滿日至送檢驗之間隔日數，回推至桶滿日之活度濃度。
5. 依照前一次桶滿日至本次桶滿日之月數，計算前次至本次桶滿比例作業量之累積。
6. 將比例作業量之累積與還原性活度濃度資料進行統計分析。

結果：

1. 送檢驗之 29 筆放射性活度濃度資料中，僅有 7 筆檢測有活度，比例約 24%，且集中於前 6 筆資料，第 7 筆有活度之資料爲第 24 筆，其餘 78% 檢驗均無活度。
2. 檢驗有活度濃度之 7 筆資料，還原之活度濃度，最高與最低分別爲 297716、3332 Bq/L，平均 141512 Bq/L，中位數 153195 Bq/L，最高與最低之活度差距達 89 倍餘。
3. 以各桶之比例作業量累積與還原之性活度濃度資料進行線性迴歸統計，其 R2 僅 0.14。

結論：

本文之實證研究結果似乎顯示：

1. 比例作業量累積與還原之性活度濃度資料似無明顯之相關性，其線性迴歸之 R2 僅 0.14。
2. 送檢驗之資料共 29 筆，檢測有活度之資料僅 7 筆，且集中於前 6 筆，至第 24 筆才又出現第 7 筆，可能表示廢水活度濃度之發生爲隨機或與操作習慣有關。換言之，熟練與良好之工作習慣，或可減少廢水活度濃度之發生機率。
3. 不論濃度之發生爲隨機或與操作習慣有關，因活度濃度高低差距達 89 倍餘，所以每桶廢水需放置之時間，至少需預計較最低檢測值可排放日期，再加 6-7 個半衰期之時間。

惟因本研究之樣本較少，且實驗設計仍有不足，RIA 作業量與產生廢水放射性濃度之關係確認，尚需更進一步的研究。

PC-117

Lugol's Solution Overdose in a Patient Underwent I-131 NP-59 Adrenal Scan

Jiun-Ying Chern[1], Yen-Hwa Chang[2], San-Fan Yao[1], Ban-Hong Yang[1], Wen Sheng Huang[1]

[1]*Departments of Nuclear Medicine/National PET & Cyclotron Center, Taipei Veterans General Hospital, Taipei*
[2]*Departments of Urology, Taipei Veterans General Hospital, Taipei*

Introduction: I-131 NP-59 is a radiolabeled cholesterol analogue that binds to low density lipoproteins and is uptaken mainly by adrenal cortical cells. It has been used in practice for localizing hypersecretory adrenal cortical diseases. Oral lugol's solution prior to I-131 NP-59 is used to block I-131 thyroid uptake. While careful patient instructions, un-favored events remain. We present a case of lugol's solution overdose in preparing I-131 NP-59 scan.

Method: The NP-59 adrenal scan was prescribed for evaluating a right adrenal adenoma. The patient was informed to ingest lugol's solution, 0.5 mL/day 3 days prior and 3 days after the scan with a total dose of 3 mL. High dose dexamethasone suppression with 2 mg qid for 6 days was also prescribed. Abdominal SPECT/CT was performed on the day 3 after I-131 NP-59 iv injection. However, the patient swallowed all of the lugol's solution on day 3 prior to the scan.

Result: The patient experienced a dizziness, headache and mouth burning sensation minutes after 3 ml of lugol's solution ingestion, following by GI discomfort, chest tightness and dyspnea. She was sent to a hospital's emergency department. Lab tests including CBC/DC, electrolytes and cardiac enzyme revealed unremarkable. EKG and CXR also showed nothing particular. Serum TSH, Free T_4, T_3 and I-131 thyroid scan with 24 h uptake were performed 2 weeks after lugol's solution ingestion, showing normal data except mildly decreased Free T4 (3.9, normal: 4.5~9.0 ng/mL) (Table 1 & Fig. 1). The patient felt better after conservative treatment such as hydration and close follow-up.

Discussion and Conclusion: Lugol's solution containing 100 mg/ml of potassium iodide and 50 mg/ml of iodine was routinely used for I-131 NP-59 adrenal scan. While it contains a higher concentration of potassium, acute toxicity of lugol's solution is mainly caused by its iodine content. Patients may potentially experience metabolic acidosis, renal failure, hypotension, iodine-induced hyperthyroidism or even death. Treatment of iodide overdose was mainly supportive. Activated charcoal and laxatives can be given to prevent further iodide resorption. The patient ingested iodide only 6 mg iodine equivalent causing little side effect except mild biochemical hypothyroid state. Carefully oral and written patient instructions should be given to avoid unnecessary adverse effects.

PC-118

動脈鈣刺激肝靜脈取血檢測胰島素 (ASVS) 協助胰腺胰島素瘤術前定位的應用：病例報告

林淑靜 [1] 張素雲 [1] 薛伃婕 [1] 周詩瑾 [1] 廖建國 [1] 王昱豐 [1,2]

[1] 佛教慈濟醫療財團法人大林慈濟醫院核子醫學科
[2] 慈濟學校財團法人慈濟大學醫學系

簡介：胰島素瘤 (Insulinoma) 是一種罕見的胰臟腫瘤，又稱爲胰島 β 細胞腫瘤，生長的速度緩慢，因 80% 腫瘤通常小於 2 公分，一般影像學檢查如超音波、斷層掃描 (CT) 或核磁共振 (MRI) 都很難發現及定位。診斷胰島素瘤依據 Whipple triad：(一) 發作時血糖低於 40 mg/dL (正常血糖爲 80-120 mg/dL)；(二) 飢餓時會出現頭暈、盜汗、手抖等現象；(三) 給予糖食或注射葡萄糖溶液時可以緩解症狀。爲了確保手術時能準確定位腫瘤位置，Doppman 等人在 1989 年首次提出動脈鈣刺激肝靜脈取血檢測胰島素 (arterial calcium stimulation with hepatic venous sampling, ASVS) 做爲胰島素瘤的術前定位方法：胰臟動脈攝影時，分別由胃十二指腸動脈 & 上腸繫膜動脈 (以上兩者負責胰臟頭部之血流)、脾動脈 (負責胰臟體、尾部之血流)、肝固有動脈 (proper hepatic artery 負責肝臟部分血流，可偵測肝轉移) 等，直接注入 Calcium gluconate (0.00625 ～ 0.025 mEq/kg)。分別於注射前 0 秒、注射後 30、60、90、120、180 秒測量肝靜脈 (hepatic vein) 的胰島素濃度。若採集的濃度大於基礎值的 2 倍，就可由該動脈負責之血流區域來推斷出腫瘤的位置。

病例報告：一位 59 歲具高血壓及高血脂之女性患者，因冒冷汗、手抖及前兩天開車時意識喪失而到急診求診，到院時有高血壓 (179/115 mmHg)、低血糖 (42 mg/dL)、白血球增多 (9800/μL)、頭至腹部 CT 可見一甲狀腺結節 (5 mm) 及一肺右中葉小結節 (3 mm)。經給予葡萄糖症狀及血糖改善而後入院，住院期間於清晨反復性出現低血糖情形。在低血糖期間，Insulin 和 C-peptide 數值都有升高，Insulin：24.6 μIU/mL (正常：4-16 μIU/mL)，C-peptide：6.06 ng/mL (正常：1.1-4.4 ng/mL)，腹部 CT 及內視鏡超 (Endoscopic ultrasound, EUS) 檢查皆未發現明顯的腫塊病變，安排了動脈鈣刺激肝靜脈取血檢測 (ASVS)，以找出確切病變位置。檢驗結果顯示出遠端脾動脈 (distal splenic artery, dSA) 和近端脾動脈 (proximal splenic artery, pSA) 的胰島素水平升高，濃度大於基礎值的 2 倍，懷疑有多灶性的小胰島素瘤在胰臟體部和尾部。再經過腹部胰臟 MRI 影像檢查在胰線尾端發現一個 9 mm 大小的胰腺腫瘤，懷疑是單個胰島素瘤，術中超音波檢查發現在胰臟尾部有一 1.16 x 0.64 cm 結節腫塊、在胰臟體部有另一 0.5 cm 之可疑病兆，最終實施了將胰臟體部和尾部之全胰臟切除術，經病理切片報告爲 1 級神經內分泌腫瘤，結合臨床數據 (胰島素數值升高)，與胰島素瘤相符合，腫瘤分期 pT1。

結論：檢查血中的 Blood sugar，Insulin 和 C-peptide 濃度是檢查高胰島素低血糖症的第一步，第二步進行 ASVS 誘發胰島素功能性分泌檢驗 Insulin，提供疑似病灶的定位，最終病理組織的染色結果確認腫瘤型態，透過實驗室三步驟，提供臨床醫師對不易發現的高胰島素低血糖症的診斷，更能在手術中準確的定位病灶，使開刀更精準與完整。在執行 ASVS 誘發胰島素功能性檢驗胰島素時，醫檢師須在同一時間處理 30-40 支檢體，應更加注意檢體採集來源和時間點的標示，以提供準確有效的檢驗報告。

PC-119

Polystotic Fibrous Dysplasia Mimicking Multiple Bone Metastasis

Kuan-Hsiu Lin, Chin Hu

Nuclear Medicine, Kaohsiung Veteran Hospital, Taiwan

Abstract:

Fibrous dysplasia is a benign bone disorder, which abnormal fibro-osseous tissue replace normal bone. It can involve any bone and be divided into monostotic (single bone involved) and polystotic (multiple bones involved). In CT, the lesions are expansile, and well-defined with either ground-glass opacity (56%), homogeneously sclerotic (23%), or lystic (21%). ^{99m}TC-MDP Bone scan may show increased tracer uptake and FDG PET scan may reveal normal to markedly increased FDG uptake. It is difficult to differentiate bone metastasis from polystotic fibrous dysplasia only by bone scan and PET scan. CT image in combined PET/CT is helpful to provide more information of fibrous dysplasia.

We reported a 59-year-old man with left tonsillar cancer (T4aN2b). Whole body bone scan showed multiple bone lesions in left ribs, T- spine and pelvis, suspecting multiple bone metastasis. PET scan was arranged, which showed hot FDG uptake in left tonsillar mass (SUVmax: 16.5) and moderate FDG uptake in multiple bony lesions in C-spine, T-spine, left ribs and sacrum (SUVmax: 5.3). All of the bony lesions were on left side of body. In CT images of PET/CT, expansile osteolytic bony lesions with osteoblastic margin were noted, compatible with polystotic fibrous dysplasia instead of bony metastasis. Tnsillar cancer, T4aN2bMo was diagnosed. The patient received bio-CRT and no tumor recurrence was noted until now.

PC-120

Diffusely Increased Tc^{99m}-MDP Uptake by the Renal Cortex in a Patient with Multiple Myeloma

Ting-Yao Kuo, Kuang-Tao Yang

Department of nuclear medicine, Changhua Christian Hospital

Background: A 55-year-old male patient with a past history of hypertension and hyperlipidemia complained of back pain for 1 month. A lumbar spine magnetic resonance imaging (MRI) was performed and multiple and diffusely abnormal foci of low intensity were observed, which may be interpreted as multiple myeloma or bone metastasis.

Clinical, laboratory, and pathology findings: Blood examination revealed elevated levels of kappa free light chain of 2400 mg/L, kappa/lambda ratio of 1600, beta 2 macroglobulin of 4.45 mg/L, gamaglobulin fraction of 31%, and IgA of 2574 mg/dL. Serum creatinine and total Ca levels were 2.04 mg/dl and 11.5 mg/dL, respectively, while the eGFR was 34.07 min/1.73 m^2. In the past 2 month, his serum creatinine level was 1.06 mg/dl while his eGFR was 72.53 min/1.73 m^2. However, in the past 1 month, his total blood Ca was 10.0 mg/dL. Bone marrow biopsy revealed a plasmacytoid cell of 80% with CD38 and CD138 of 100% and CD56 of 95%. The final diagnosis was multiple myeloma with IgA gammopathy.

Image: A Tc^{99m}-MDP whole-body bone scan was performed to evaluate bone lesions. Two hot spots with mildly increased activity were noted in the bilateral 8th ribs. Linear shape regions with moderately and intensely increased activity were noted in the L1 and L2 vertebral bodies, which could be explained by simple or pathologic compression fractures. Interestingly, there was a diffusely increased uptake of Tc^{99m}-MDP by the renal cortex of the kidneys.

Discussion: The incidence of diffuse cortical renal uptake, also known as “hot kidney” on bone scintigraphy had been reported to be less than 1 percent (Ozdogan O et al, 2013, Acute Kidney Injury Secondary to NSAID Diagnosed on ^{99m}Tc MDP Bone Scan, Mol Imaging Radionucl Ther). Hot kidneys on bone scan had been reported in patients with hypercalcemia, hyperparathyroidism, chemotherapy, iron overload, acute renal injury due to acute tubular necrosis and NSAIDS, recent radiotherapy, use of antineoplastic drugs, and secondary to the aluminum breakthrough of ^{99m}Mo-^{99m}Tc generator. The exact mechanism leading to abnormal diffuse renal cortical tracer uptake had not been established. In patients with multiple myeloma, different mechanisms can lead to kidney injury such as light chain cast nephropathy, hypercalcemia, amyloidosis, or monoclonal immunoglobulin deposition disease or light chain proximal tubulopathy. In this case, eGFR was found to have decreased rapidly from 72.5 mL/min/1.73 m^2 (in the past two months) to 34 mL/min/1.73 m^2. The patient was more likely to develop acute kidney injury. Total blood Ca elevated from 10.0 mg/dL (in the past one month) to 11.5 mg/dL. The most possible reasons for the “hot kidney” sign may include: hypercalcemia, amyloidosis, or monoclonal gammopathy induced acute kidney injury considering the underlying disease. Further studies examining renal biopsy would be needed to elucidate the definite mechanisms. Whether the diffuse uptake of Tc^{99m}-MDP in the renal cortex is an early and useful sign of kidney injury in patients with multiple myeloma is worthy of investigation.

PC-121

Pitfalls of FDG PET/CT in Cancer Patients Treated with Immune Checkpoint Inhibitor Therapy

Pei-Ing Lee, Yu-Yi Huang, Bor-Tau Hung

Department of Nuclear Medicine, Koo Foundation Sun Yat-Sen Cancer Center, Taipei, Taiwan

Introduction: In recent years, immune checkpoint inhibitor (ICI) therapy has emerged as an important treatment option for several cancer types, such as melanoma, lymphoma and lung cancer. Due to its unique mechanism of action, ICI therapy is associated with distinctive immune-related adverse events (irAEs). These irAEs can affect any organ and system, and may clinically manifest as colitis, hepatitis, pneumonitis, thyroid or pituitary dysfunction etc. FDG PET has been proved to be a useful tool for assessing treatment response in cancer patients treated with ICI. However, irAEs occurred during ICI therapy may lead to pitfalls on FDG PET, thus causing misinterpretation and wrong decision making. The aim of this study is to review various irAEs detected by FDG PET/CT after ICI therapy at our institution.

Methods: In this retrospective study, patients treated with ICI therapy at our institution who had received both baseline and subsequent FDG PET/CT scans were included. Their FDG PET/CT findings were recorded and correlated with clinical and laboratory data.

Results: Twenty-three patients (9 male, 14 female) with 47 subsequent FDG PET/CT scans were included in this study. Their cancer types included melanoma, lymphoma, breast cancer, buccal cancer, sarcoma and prostate cancer. Nineteen patients were treated with PD-1 inhibitor (Pembrolizumab and Nivolumab) and 4 patients were treated with PD-L1 inhibitor (Azetolumab). Imaging features that were associated with irAEs were identified on 26 of 47 FDG PET/CT scans. Among them, colitis were demonstrated in 7 FDG PET/CT scans (15%), pneumonitis in 3 scans (6%), thyroiditis in 6 scans (13%), hypophysitis in 3 scans (6%), arthritis in 8 scans (17%) and mediastinal lymphadenopathy in 2 scans (4%).

Conclusions: IrAEs may be detected by FDG PET/CT in patients being treated with ICI therapy. It is critical for nuclear medicine physicians to recognize and distinguish abnormal FDG uptake associated with irAEs from hypermetabolic malignant lesions when using FDG PET/CT for monitoring treatment response of ICI therapy.

PC-122

比較新舊 CZT γ Camera 在心肌灌注造影之定量分析結果

魏文祺　林啓芬　蔣筱玲　胡蓮欣　黃文盛

臺北榮民總醫院核醫部

背景介紹：CZT γ camera 用在心肌灌注造影已有十年的歷史，其高空間解析力、高計數率及快速取像的優點，目前在臨床上的使用逐漸增加。本研究的目的是比較兩台機齡相距 9 年的新舊 CZT γ camera 在心肌灌注造影之影像分析結果是否一致。

方法：分析軟體結果一致性比較：將 50 筆以 GE DISCOVERY NM530C (舊機) 執行 Tl-201 心肌灌注造影之資料用 GE Xeleris 3.0 EC Toolbox 及 GE Xeleris 4.0 Emory Cardiac Toolbox 分析 stress、rest 的 ejection fraction (EF)、myocardial mass 及 TID ratio。新、舊機造影結果比較：30 位病人於注射 persantin 及 2 mCi ^{201}Tlcl 5 分鐘後先以舊 GE DISCOVERY NM530C (舊機) 執行 Tl-201 心肌灌注造影，間隔 10 分鐘後再以相同的造影條件用新 GE DISCOVERY NM530C (新機) 執行造影。影像分析用 Xeleris 4.0 Emory Cardiac Toolbox。分析 stress、rest 的 ejection fraction、myocardial mass 及 TID ratio。統計分析使用 Medcalc® version 19.5.1，統計方法用 Paired samples T-test，P 值小於 0.05 視爲有顯著性差異。

結果：分析軟體結果一致性比較：Xeleris 3.0 與 Xeleris 4.0 之 stress EF 分別爲 63.46±11.45% 與 63.26±11.58%，P = 0.24；rest EF 爲 62.08±12.54% 與 62.06±12.34%，P = 0.93；stress mass 爲 108.44±27.12g 與 108.00±27.41g，P = 0.94；rest mass 爲 105.06±27.13g 與 108.00±27.42g，P = 0.59；TID ratio 爲 1.10±0.21 與 1.10±0.22，P = 0.57。新、舊版本的分析軟體結果並無顯著性差異。新舊機造影比較：新、舊機的 stress EF 分別爲 70.60±5.50% 與 68.93±4.26%，P = 0.03；rest EF 爲 67.27±4.49% 與 67.87±5.58%，P = 0.41；stress mass 爲 101.47±15.24g 與 102.30±13.47g，P = 0.61；rest mass 爲 95.47±13.94g 與 96.90±13.16g，P = 0.36；TID ratio 爲 1.04±0.14 與 1.06±0.12，P = 0.61。新、舊機的 stress EF 在統計上有顯著性的差異，其原因可能是 persantin 對心臟作用隨時間增加而遞減所造成。

結論：新、舊 CZT γ camera 及不同版本的分析軟體對同一病人之心肌灌注造影之定量分析結果並不會有顯著性不同。

PC-123

利用 SPM 分析 PET/CT 與 PET/MR 全腦上的差異性

李建穎　楊邦宏　黃文盛

台北榮民總醫院核醫部暨全方位正子磁振造影中心

背景介紹：新型 SIGNA PET/MR 對於使用在腦部 PET/MR 組像的衰減校正 (AC) 的準確性，仍然是一個謎團，也是大家已知的問題。雖然爲了修正骨骼與空腔部位 AC 校正的不準確性，因而衍生出 ZTE AC 波續來彌補 Atlas 上的缺點。因此本研究目的探討 SIGNA PET/MR (ZTEAC) 與當前臨床 MIDR PETCT (CTAC) 在全腦上 SUV 值的差異性。

方法：我們選擇了 30 位受檢者，於商售的 PETCT (MIDR) 與 PETMR (GE SIGNA) 進行造影，所有的受檢者皆先靜脈注射 3.17 MBq/kg 的 F^{18}-FDG 後休息 60 分鐘進行 PETCT 造影，結束後立即至 PETMR 造影。PETCT 影像經過標準的 CTAC，當作標準值：PETMR 則使用 ZTE 波序，產生 ZTE-AC 衰減校正影像。兩組腦部影像利用 SPM (Statistical Parametric Mapping) 標準化分析處理，並進行配對 t 檢定 (Paired Sample t test)，分析兩台造影儀器 SUV 之差異性。

結果：利用 SPM 標準化分析處理，全腦數值顯示 PETCT (SUVmean = 4.96±2.17)，PETMR (SUVmean = 5.43±2.48)，差異度百分比爲 –10% (PETCT-PETMR)/PETCT)。利用配對 t 檢定顯示 cluster size >50, pValue = 0.001 結果。

結論：再利用 SPM 標準分析結果顯示全腦，PETMR SUV 值稍微高於 PETCT SUV 值，其中腦幹 ($p < 0.001$) 值爲相反區域。這是值得我們再深入探討的地方。

PC-124

全身正子造影之 SUV 值在 PETCT 與 PETMR 的表現

張嘉容　楊邦宏　黃文盛

臺北榮民總醫院核醫部

背景介紹：臨床上氟化去氧葡萄糖的全身正子造影用來追蹤是否癌症復發或是分期，而隨著正子儀器日新月異的發展，如何確保受檢者在不同正子儀器追蹤時，影像與 SUV 值是否能夠一致。本研究之目的在於比較使用不同 PET/CT 造影儀與 PET/MR 造影儀，全身氟化去氧葡萄糖造影中正常器官組織的 SUV 值之關係。

方法：本研究受試者於注射氟化去氧葡萄糖後 60 分鐘造影，進行常規 PET/CT 全身造影，分別使用 GE Discovery VCT (人數 23，年齡 59±12) 與 GE Discovery MIDR (人數 21，年齡 58±16)，接著再做 GE SIGNA PET/MR 全身造影。針對頸部，肺部，心肌，血池，肝臟，腰椎，腰大肌，股骨頭與臀大肌等部位之正常器官組織圈選 VOI (1 cm3)，以及頸部與肺部病灶組織圈選 VOI (1 cm3)。比較在各區域 PET/CT (VCT 與 MIDR) 及 PET/MR 之 SUV (Max/Average) 相關性與差異。

結果：比較在 PET/CT (VCT) 及 PET/MR 影像中，正常器官組織之心肌組織有非常好的相關性，在頸部及股骨頭) 有良好的相關性；而在 PET/CT (MIDR) 及 PET/MR 影像中，在頸部，肺部，心肌，血池，肝臟，腰椎與腰大肌皆有非常好的相關性，在股骨頭有良好的相關性；PET/CT (VCT) 的 SUV 在頸部，肺部，血池與肝臟略高於 PET/MR，在其他部位則無顯著差異於 PET/MR。PET/CT (MI DR) 的 SUV 在頸部，肺部，血池及肝臟略高於 PET/MR，在腰大肌及臀大肌則略低於 PET/MR，在其他部位則無顯著差異於 PET/MR。在 2 臺 PET/CT 與 PET/MR 影像中，病兆組織的頸部 $SUV_{Max}/SUV_{Average}$ 之 $R^2 = 0.88/0.82$ (VCT) 及 $R^2 = 0.89/0.90$ (MIDR)；肺部 $SUV_{Max}/SUV_{Average}$ 之 $R^2 = 0.99/0.97$ (VCT) 及 $R^2 = 0.90/0.91$ (MIDR) 皆有非常好的相關性。PET/CT (VCT) 及 PET/CT (MIDR) 僅肺部的病灶組織 SUV_{Max} 高於 PET/MR ($p = 0.01$ 與 0.048)。PET/CT (VCT) 與 PET/CT (MIDR) 相比的 $SUV_{Average}$ 皆略高 (頸部，肺部，血池，肝臟，腰椎，腰大肌與臀大肌) 或無顯著差異 (心肌與股骨頭)。

結論：在不同的 PET/CT 造影儀與 PET/MR 造影儀的氟化去氧葡萄糖全身正子造影中，正常器官組織大多有良好的相關性，在頸部與肺部病兆組織則是非常好的相關性。所以在正子檢查造影追蹤時，使用不同的 PET/CT 與 PET/MR 在定量上可以提供相似的結果。

PC-125

導入 TAF 認證對核醫儀器品管之影響

張嘉容　楊邦宏　陳苓仕　黃文盛

臺北榮民總醫院核醫部

背景介紹：TAF (Taiwan Accreditation Foundation; TAF) 認證是依據 ISO 15189 認證標準，建立品質與技術能力之規範要求。本研究主要在探討導入 TAF 認證對於核醫儀器品管之影響。

方法：本部核醫儀器包括 6 臺加瑪閃爍造影儀，2 臺 SPECT/CT 造影儀，1 臺 PET/CT 造影儀與 1 臺 PET/MR 造影儀。建立各儀器操作及品管作業程序，並依各廠牌品管數值 (如：溫度、溼度、能峰、均勻度等) 制定允收範圍。而根據 ISO 15189 認證標準，儀器使用期限內相關資料皆須保存，過去本部以紙本記錄，容易發生使用版本混淆及紀錄保存空間的限制，藉由建置線上表單，記錄每日儀器品管數值；當儀器異常發生時，進行線上通報。

結果：透過使用線上表單記錄每日儀器品管數值，可達無紙化管理，方便觀察及統計儀器品管數值狀態。若數值未在允收範圍或是發生儀器異常，線上通報可讓相關同仁及報告醫師即時了解儀器狀態並追蹤。

結論：透過導入 TAF 認證，能有系統性的管理核醫儀器品管，進而維持影像品質。

PC-126

評估全身型數位 CZT 半導體 SPECT 應用在 ^{99m}Tc-TRODAT-1 腦部檢查影像上的表現

陳苓仕　楊邦宏　黃文盛

臺北榮民總醫院核子醫學部

目的：核醫儀器科技日新月異，目的不外乎爲了追求更短的造影時間及獲得更好的影像品質。本實驗嘗試透過 ^{99m}Tc-TRODAT-1 SPECT 來評估 NM/CT 870 CZT 以不同造影條件在腦部影像上的表現。

材料與方法：利用注射 ^{99m}Tc-TRODAT-1 於 RSD Striatal Phantom 假體在 NM/CT 870 CZT 上使用四種不同條件造影。方法一 (傳統) : 兩個偵檢器各轉 360 度，每 3 度收 1 張，每張收 20 秒，總共約 45 分；方法二：兩個偵檢器各轉 180 度，每 3 度收 1 張，每張收 40 秒，總共約 45 分；方法三：兩個偵檢器各轉 180 度，每 3 度收 1 張，每張收 30 秒，總共約 35 分；方法四：兩個偵檢器各轉 180 度，每 3 度收 1 張，每張收 20 秒，總共約 25 分。在 Xeleris 工作站將方法一至四的資料重組三種不同影像重組條件，分別是 MZ Filter、BW Filter 及 Iterative Reconstruction with Attenuation Correction (IRAC)，其他條件參數都相同，再分別以本部已開發之 TRODAT Tool 軟體自動化分析紋狀體 (尾核、殼核) 攝取值活性比值，並比較之間的相關性。

結果：比較結果以方法一 (傳統) 的 MZ Filter 重組影像爲基準，方法二至四的 MZ Filter 重組影像的 R 平方值皆高於 0.75。以方法一 (傳統) 的 BW Filter 重組影像爲基準，方法二至四的 BW Filter 重組影像的 R 平方值皆高於 0.8。以方法一 (傳統) 的 IRAC 重組影像爲基準，方法二至四的 IRAC Recon 重組影像的 R 平方值皆高於 0.9。

結論：我們觀察到在三種不同影像重組條件的影像表現上，方法一 (傳統) 與方法二至四的相關性都很高。以此爲依據，或許未來可以縮短 ^{99m}Tc-TRODAT-1 SPECT 檢查所需花費的時間，減少病人因長時間維持同姿勢的不適感，也可以降低出現移動假影的風險，提供更好的影像品質。

PC-127

Imaging Response of Treatment in Multiple Brown Tumors: A Case Report

Chien-Wei Kuo

Department of Nuclear Medicine, Kaohsiung Veterans General Hospital, Kaohsiung, Taiwan
Department of Medical Imaging and Radiological Sciences, Kaohsiung Medical University, Kaohsiung, Taiwan

Introduction: Brown tumor, also known as osteitis fibrosa cystica, is the classical bone manifestation of hyperparathyroidism, showing a reparative cellular process rather than a true neoplasm. It has been reported in 3~4.5% of patients with primary hyperparathyroidism. We herein report a case of multiple brown tumors with significant response after surgical resection of parathyroid adenoma.

Case report: A 50-year-old female was found to have hypercalcemia, elevated serum alkaline phosphatase, creatinine levels and low bone mineral density in health examinations. Following lab data showed elevated intact parathyroid hormone level. The femur radiograph showed expansile radiolucent lesions. A Tc-99m MIBI parathyroid scan (including SPECT/CT), a thyroid/parathyroid MRI were arranged for hyperparathyroidism survey, and a F-18 FDG whole body PET/CT scan was arranged for tumor survey. A MIBI-avid mass lesion over the left upper thyroid zone was identified, and PET/CT showed multiple expansile osteolytic lesions with high FDG uptake in axial skeletons and all extremities. After parathyroidectomy, the pathology report showed atypical parathyroid adenoma. Therefore, the diagnosis of multiple brown tumors was impressed. After four years, parathyroid scintigraphy, bone scan, and F-18 FDG whole body PET/CT scan showed significant resolution of prior bone lesions.

Discussion: Brown tumor can expand beyond usual shape, causing palpable bony swelling, bone pain and pathologic fractures. Correction of hyperparathyroidism is effective to treat brown tumor. Bone scan and FDG PET/CT imaging can help to evaluate the response to treatment.

PC-128

An Excellent Modality in Detecting Bony Malignancy: Combined Irregular-Flux-Viewer with Artificial-Neural-Networks Systems

Chang-Ching Yu[1,2], Hung-Pin Chan[1,2], Chien-Yi Ding[2], Hueisch-Jy Ding[3], Nan-Jing Peng[1,4]

[1]*Department of Nuclear Medicine, Kaohsiung Veterans General Hospital, Taiwan*
[2]*Shu-Zen Junior College of Medicine and Management, Taiwan*
[3]*Department of Medicine Imaging and Radiological Science, I-Shou University, Taiwan*
[4]*National Yang-Ming University, School of Medicine, Taipei, Taiwan, R.O.C*

Aim: The Tc-99m MDP Whole Body Bone Scan (WBBS) has been widely used as a diagnostic modality for bone and joint changes in patients with oncologic diseases. The WBBS has high sensitivity but relatively low specificity owing to bone variation. The aim of this study was developed by combining the self-developing irregular-flux-viewer (IFV) with a computer-aided diagnosis (CAD) system to be capable of predicting bone lesions using planar WBBS.

Methods: A total of 766 patients with diagnoses of prostate, breast, or lung cancer were evaluated. Bone scintigraphy was performed from September 2015 to September 2019. All of the patients in the control group (388) were used in developing the image analysis techniques and training the artificial neural networks. An experimental group of 378 patients with breast or prostate cancer was used to evaluate the CAD system. Whole-body images (including anterior and posterior views) were also obtained after an injection of 99mTc methylene diphosphonate. Gradient Vector Flow (GVF) and Self-Organizing Map (SOM) methods were used in this study to analyze blood fluid-dynamics and IFV for evaluating the hot points. Two sets of artificial neural networks (ANN) were used to classify the images: (1) checking each hot spots and (2) whole bone scan. The image-processing techniques included algorithms for automatic segmentation of the skeleton and automatic detection and feature extraction of hot spots. Nuclear medicine physicians divided all cases into four categories: (1) benign, (2) malignant, (3) degenerate, and (4) healthy controls. We compared IFV values with BONENAVI version data.

Results: The analysis revealed the sensitivity of IFV system in prostate cancer was 94% with 92% in breast cancer and 88% in lung cancer. On the other hand, our modified modality had a higher sensitivity than original BONEVAVI version 2.0.5, and the new method showed a sensitivity of 88%, 86%, and 82% in prostate, breast lung cancer cases. The method was also accurate for distinguishing bone metastasis from degenerative or normal tissue (total classification accuracy = 93.33% $\pm$ 2.46%). The specificity was 92.26% (Fps was 7.74 per image) based on this new method.

Conclusion: The results have shown higher sensitivity and specificity of the combined IFV with ANN system, which could provide assistance for image interpretation and enhance WBBS prediction values.

PC-129

比較心肌血流灌注檢查與心臟冠狀動脈造影檢測冠狀動脈疾病之探討

張添信　陳慶元

佛教慈濟醫療財團法人台中慈濟醫院

背景介紹：根據衛生福利部資料統計 2017 年國人 10 大死因，心臟病位居第二位，莫約 200 萬國民有心臟疾病，其中約一半是冠心病，包括心絞痛、心肌梗塞。

核醫心肌血流檢查 (MPI) 爲檢測冠心病的其中一項檢測工具，在台灣根據 2016 年健保資料庫分析 MPI 一年約施行約 15 萬餘件，全民健康保險醫療費用審查注意事項，施行經皮冠狀動脈擴張 (CATH) 送審所需之基本資料需要包含放射核醫心臟血管造影檢查，非侵入性的核醫心臟提供一項快速的篩檢冠狀心臟疾病工具。

心臟冠狀動脈造影 (CTA) 利用血管注射顯影劑造影，來評估心臟冠狀動脈血管內阻塞或狹窄的嚴重度，提供另一項檢測冠心病工具，但健保目前尚未提供給付須自費負擔，以上兩項皆爲檢測冠心病之檢查工具，本篇探討兩項檢查工具優劣比較。

方法：回朔分析 3 年內有施行 MPI、CTA、CATH 之病人，且病人未曾有冠狀動脈疾病史或已知心臟相關疾病，三者檢測項目距離不能超過半年，最終驗證標準爲 CATH 的施行結果比較，總共收集 28 筆資料 (男性 24 位、女性 4 位) ，年紀爲 64.21 (±8.634) 歲，利用混淆矩陣及 ROC 曲線進行相關分析比較。

結果：CATH 的結果爲陽性 12 位、陰性 16 位，經由 SPSS 25 版統計軟體分析，發現 CTA 敏感度 (Sensitivity) 爲 75%，MPI 則爲 66.7%，曲線下面積 CTA 爲 0.688 及 MPI 爲 0.615，在特異性 (Specificity) 方面 CATH 爲 65.2%，MPI 爲 56.2%。

結論：核子醫學的 MPI 是在預測哪些病人有冠狀動脈狹窄，造成心肌缺氧、缺血現象，之後適合做 CATH 放置支架可以改善等結果，而 CTA 看血管鈣化造成冠狀動脈狹窄，與 CATH 觀測現象較爲接近，因爲阻塞與缺血、缺氧還是有著些許的差異，所以 MPI 的正確性需要增加其他標準來給予參考，例如分數血流儲備容積 (FFR)、心肌血流量 (MBF)、心肌血流儲備容積 (MCF) 等評估標準。

關鍵字：心肌血流灌注檢查、心臟冠狀動脈造影、混淆矩陣。

PC-130

The Prevalence of Osteoporosis in Patients with Low FRAX Risk

Yuh-Feng Wang[1,3], Pao-Liang Chen[1,2], Tzyy-Ling Chuang[1,3], Shih-Chin Chou[1], Jian-Guo Liao[1]

[1]*Department of Nuclear Medicine, Dalin Tzu Chi Hospital, Buddhist Tzu Chi Medical Foundation, Chiayi, Taiwan*
[2]*Department of Medical Research, Dalin Tzu Chi Hospital, Buddhist Tzu Chi Medical Foundation, Chiayi, Taiwan*
[3]*Department of Radiology, School of Medicine, Tzu Chi University, Hualien, Taiwan*

Background: In clinical practice for the bone mineral density evaluation, lumbar spine and bilateral hip areas, were included. However, the fracture risk assessment tool (FRAX) only adapt the hip areas as calculation factor. That is, for cases with osteoporosis in lumbar spine but normal in hip areas, FRAX might underestimate the risk of spinal fracture. The aim of this study analyzes the difference between low fracture risk (major osteoporotic fracture risk < 20%, and hip fracture risk < 3%) and high-risk group according to FRAX in osteoporotic patients.

Methods: This retrospective research study, outpatient records and dual-energy X-ray absorptiometry (DXA) with variable for FRAX (age, gender, height, weight, previous fracture, smoking, glucocorticoids, rheumatoid arthritis, alcohol and high fracture probabilities) from November 2014 to December 2019 were collected. Past history of spinal surgery and total hip replacement or incomplete medical records were excluded. 7148 cases, 1183 (17%) males and 5965 (83%) females, were included for analysis.

Results: There showed older, higher, heavier, higher cigarette and alcohol taking rate, lower rheumatoid arthritis rate and lower fracture probabilities in men than in women with significant difference ($p < 0.05$). Significant difference in the bone mineral density and fracture risk assessment tool fracture probabilities between normal, low bone density, and osteoporosis groups were also noted. In osteoporotic cases, older, shorter, thinner, less BMD/T-score of bilateral femoral neck and bilateral total femurs in high fracture risk group than low fracture risk group with significant difference ($p < 0.05$).

Some patients only have osteoporosis because of the lumbar bone density area, but the fracture risk assessment tool judges that the risk of fracture is low, and most of them are judged as osteoporosis because the lumbar spine T-score $\leqq -2.5$. However, there showed significant difference in item achieve between high and low fracture risk in osteoporotic cases.

Conclusion: In this study, the osteoporotic cases defined by lumbar vertebrae DXA results with fair bilateral hip DXA results are classified into low fracture risk group. Therefore, three areas (lumbar vertebrae and bilateral hips) DXA scan and 10-years fracture risk calculation for bilateral hips should be performed together to provide clinicians with accurate reference for patient treatment and medication.

PC-131

腎臟檢查半定量分析一致性評估成果

楊士頤　謝沁彣　郭家怡　丁若洵　邱南津

國立成功大學醫學院附設醫院影像醫學部核醫科

背景介紹：

核醫腎臟掃描檢查功能測定，藉由半定量方式分析，可由腎臟吸收及排出放射性藥物時的放射計數推算出腎臟功能並以數據表示。由人爲圈選左右腎臟 ROI，計算出左右腎臟放射計數 (counts 數) 之比例 (%)。所以會因爲不同人操作或每次圈選 ROI 之範圍大小而造成些微誤差。讓放射師圈選 ROI 減少誤差值及提升再現性，進行人員教育訓練及降低人與次數間所畫之 ROI 差異爲重要課題。

方法：

1. 資料庫中挑選二十個病例 (四十個腎臟)，包括了腎臟功能壞至好 (腎臟相對功能百分比由 15% 至 85%)，由有經驗者 (至少有兩年腎臟掃描影像半定量分析經驗) 的分析結果作爲標準，再由受測試者分析此四十個腎臟的腎臟相對功能百分比兩次，並與標準的結果做比較。
2. 以組內相關係數 (Intraclass Correlation Coefficient，簡稱 ICC) 評估此受測試者的同測試者再現性 (Intra-observer reproducibility) 和測試者間再現性 (Inter-observer reproducibility)，其所計算出來的 ICC 數值若達到 Landis 和 Koch 所定義的幾乎完美 (ICC 數值介於 0.81 至 1.00；Landis JR, Koch GG. The measurement of observer agreement for categorical data. Biometrics. 1977;33:159-174.)，則此受測試者通過檢測；若 ICC 數值有任一項低於 0.81 (不含)，則此受測試者未通過檢測。
3. 執行腎臟掃描影像半定量分析者，需先經過本一致性評估檢測通過後，始得依其分析結果供臨床使用，每年需再做檢測一次。檢測不通過者，經學習後再做測試，直至檢測通過後其分析結果才可採用。

結果：

實施此教案對策後，比對 108 年五位放射師，同測者再現性達合格標準 (ICC：0.81-1.0)，測試者間再現性也達合格標準 (ICC：0.81-1.0)，合格達成率 100%。

結論：

在臨床定量或半定量分析上會有所謂的量測不確定度，不同操作人員下，將可信度增加使臨床決策值更有意義是這次重要的課題。目前已將此評量方式文件化寫入核醫放射師人員訓練課題之一，採每年進行評估考核，不管是新進或在職同仁都得進行腎臟檢查半定量分析一致行評估，使教學及臨床合而爲一是我們的宗旨。

PC-132

The First Experience of F-18 PSMA-1007 PET for Prostate Cancer in National Taiwan University Hospital

Ching-Chu Lu[1], Yeong-Shiau Pu[2], Ya-Yao Huang[1], Ruoh-Fang Yen[1]

[1]*Department of Nuclear Medicine, National Taiwan University Hospital*
[2]*Department of Urology, National Taiwan University Hospital*

Background: Prostate cancer (PCa) is one of the most frequent malignancies in men worldwide. Prostate specific membrane antigen (PSMA), a type II transmembrane protein, is strongly overexpressed in PCa cells. Ga-68 labeled PSMA PET imaging has been reported to detect nodal/bone metastases and pathological origin in biochemical recurrence with very low PSA level and is better than conventional imaging studies. Nevertheless, cyclotron produced F-18 has the advantage over Ge-68/Ga-68 generator eluted Ga-68 in larger radioactivity amount, longer half-life (119 min versus 68 min), and higher physical spatial resolution. In addition, F-18 PSMA-1007 PET imaging shows very low urinary activity which decrease the confusion of urine activity from nodal metastases or local relapse. The aim of this abstract was to report the clinical utilization of F-18 PSMA-1007 for the first 22 PCa patients in our hospital.

Methods: F-18 PSMA-1007 were produced in a GE TracerLab Mx synthesizer using commercial cassettes and reagents from ABX GmbH (Radeberg, Germany). Twenty-two consecutive patients, who received PET imaging because of the following 3 situations: clinical status evaluation after years of active surveillance (AS) for 5 patients, primary staging (PS) with equivocal conventional imaging for 5 patients, and localization of biochemical failure (BCF) for 12 patients, were included. The PET imaging was acquired 120 minutes after tracer injection (average dose, 9.37 ± 1.19 mCi).

Results: For the 5 AS patients (age: 76.47 ± 4.08 years; Gleason score: 3 3 + 3, 1 3 + 4 and 1 4 + 3; AS period: 4.98 ± 2.97 years; PSA level at PET: mean 3.78 ± 3.00 ng/mL). The SUVmax of prostate lesions were 9.89 ± 6.17. Costal metastases were detected in a patient (SUVmax = 12.15; Gleason score 3 + 3; PSA level at PET: 8.234 ng/mL). For the 5 PS patients (age: 69.85 ± 7.64 years; initial PSA: mean 31.93 ± 42.54 ng/mL, range 7.95-107 ng/mL), 3 patients with equivocal costal lesions in bone scan were down-staged from M1 to M0, 1 patient was detected to have more metastatic bone lesions, and 1 patient has unexpected solitary sternal metastasis besides pelvic nodes. For the 12 BCF patients (age: 71.10 ± 10.06 years; PSA level at PET: mean 8.81 ± 17.36 ng/mL, range 0.023-61.66 ng/mL; prior therapies: 3 received cryotherapy, 1 received androgen-deprivation therapy, 8 received radiation beam therapy to prostate bed), 1 patient had no detectable lesion (PSA 0.18 ng/mL), 1 had local relapse (LR), 5 had bone metastases, 1 had LR with nodal metastases, 1 had LR and bone metastases, 1 had nodal and bone metastases and 1 had LR with nodal and bone metastases (PSA 0.687 ng/mL), and 1 (PSA 61.66 ng/mL) had LR, nodal, bone and liver metastases). The liver lesion was detected by contrast enhanced CT appeared a cold lesion on PET imaging because of high liver background.

Conclusions: F-18 PSMA-1007 PET has promising ability to detect metastases and recurrence of PCa. Further inclusion of more PCa patients to evaluate its clinical impacts is warranted.

PC-133

Clinical Decision Making Based on Myocardial Perfusion Imaging in Cardiology Patients

Nan-Jing Peng[1,2], Chin Hu[1], Yu-Li Chiu[1], Hung-Pin Chan[1], Guang-Yuan Mar[3]

[1]*Department of Nuclear Medicine, Kaohsiung Veterans General Hospital, Kaohsiung, Taiwan*
[2]*National Yang-Ming University, School of Medicine, Taipei, Taiwan*
[3]*Section of Cardiology, Department of Medicine, Kaohsiung Veterans General Hospital, Kaohsiung, Taiwan*

Introduction: Myocardial perfusion imaging (MPI) has been widely applied in clinical situation to detect coronary artery disease (CAD). The aim of this study was to determine how MPI results were used by cardiologists in clinical decision making.

Methods: We performed a retrospective analysis of patients referred for MPI from Jan. 2017 in our hospital. Based on the reports of MPI, they were divided into 3 groups: negative, equivocal, and positive. Stenoses equal to or greater than 50% on coronary angiography (CAG) were considered significant. Clinical decision was evaluated according to the medical records.

Results: In 2017, 4,177 MPI scans were performed. The reports showed positive in 614 (14.7%), equivocal in 439 (10.5%) and negative in 3124 (74.8%), respectively. Five hundred and ninety-six of the 4,177 (14.3%) patients received CAG within 3 months after MPI. The reports of MPI were positive in 265 (44.5%), equivocal in 169 (28.4%) and negative in 162 (27.2%), respectively. The positive predictive value (PPV) in patients with positive MPI was 92.5% (245/265) on CAG. However, 349 of 614 patients (56.8%) didn't receive CAG within 3 months after a positive MPI. Among them, 31% of patients refused the suggestion of doing CAG by cardiologists, 34% proceeded medical treatment due to old age, renal disease, etc., 12% doing CAG after 3 months, and the rest not doing CAG for other reasons. Furthermore, 162 of 3,124 patients (5.2%) performed CAG within 3 months after a negative MPI. The reasons included clinical indication (76%), the consideration of other imaging modalities or EKG (15%), and other causes 9%).

Conclusions: MPI scans were actually applied as a gatekeeper in our hospital. Clinical decision making depends on the patient's condition and the recent improving concepts. Although the high PPV, less than half of the patients received CAG within 3 months after a positive MPI.

PC-134

The Effect of Benign Prostatic Hyperplasia Combined with High Prostate Specific Antige on Bone Mineral Density

Pao-Liang Chen[1,2], Tzyy-Ling Chuang[1,4], Jian-Guo Liao[1], Yuh-Feng Wang[1,3,4]

[1]*Department of Nuclear Medicine, Dalin Tzu Chi Hospital, Buddhist Tzu Chi Medical Foundation, Chiayi, Taiwan*
[2]*Department of Medical Research, Dalin Tzu Chi Hospital, Buddhist Tzu Chi Medical Foundation, Chiayi, Taiwan*
[3]*Center of Preventive Medicine, Dalin Tzu Chi Hospital, Buddhist Tzu Chi Medical Foundation, Chiayi, Taiwan*
[4]*Department of Radiology, School of Medicine, Tzu Chi University, Hualien, Taiwan*

Background: The aim of this study was to evaluate and compare PSA levels > 4 μg/L with BPH (disease groups) and PSA levels < 4 μg/L with non-BPH (normal groups) and compare the correlation of bone mineral density between the differences groups.

Material and Methods: Evaluation was made of a total of 5,606 male who underwent normal group total 5323 (95%) and disease group total 282 (5%). The BPH diagnosised via ultrasound scan. The PSA level by serum of chemiluminescence immunoassay. PSA > 4 was abnormal.

Results: Disease groups was diagnosed in 282 patients and normal groups in 5,323 patients. The mean age of patients in both groups as 53.85 ± 12.10 years in the normal group 68.46 ± 7.72 years in the disease group ($p < 0.001$). The disease groups compare to normal groups significantly increased in the disease patients at lumbar spine area, but bilateral hips significantly decreased.

Conclusions: In conclusion one of these findings are worth summarizing the in disease group. The disease of increase lumbar spine BMD but bilateral hips were normal to osteoporosis. Our suggested, when male patients disease group, to evaluated BMD.

大會組織

主辦單位： 中華民國核醫學學會
台北榮民總醫院
行政院原子能委員會核能研究所
經濟部技術處

會　　長 黃文盛 會長

指導委員 (依姓氏筆畫順序，尊稱省略)

王安美、王昱豐、李將瑄、杜高瑩、林立凡、周大凱、邱南津、邱創新、吳東信、吳彥雯
陳宜伶、陳輝墉、翁瑞鴻、許幼青、曹勤和、黃文盛、黃英峰、黃奕琿、黃淑華、黃雅瑤
彭南靖、程紹智、詹勝傑、張智勇、楊邦宏、廖炎智、廖建國、鄭媚方、蔡世傳、樊裕明
顏若芳、謝德鈞

法律顧問　蔡雅琴

論文評選組 (依姓氏筆畫順序，尊稱省略)

召　集　人　王昱豐
執 行 秘 書　陳保良
壁報臨床組　林立凡、林明賢、汪姍瑩、程紹智、詹勝傑、劉嘉儒
壁報基礎組　田育彰、吳東信、張志賢、許幼青、黃奕琿、楊邦宏
口頭臨床組　王昱豐、邱創新、彭南靖、曹勤和
口頭基礎組　黃雅瑤、黃詠暉

秘書處 (依姓氏筆畫順序，尊稱省略)

秘 書 長　路景竹
執行秘書　柯冠吟、陳建榮、莊佩儒、蔡思盈
秘　　書　羅尉文、楊月桂

贊助廠商

士宣生技股份有限公司

大昇生物科技股份有限公司

元新儀器有限公司

台灣飛利浦股份有限公司

台灣拜耳股份有限公司

台灣諾華股份有限公司

西門子醫療設備股份有限公司

扶康健康事業有限公司

貝克西弗股份有限公司

奇異亞洲醫療設備股份有限公司

昶洋貿易股份有限公司

恩典科研股份有限公司

泰歷藥品儀器股份有限公司

常捷生醫科技股份有限公司

現代儀器股份有限公司

富特茂股份有限公司

量子輻射科技有限公司

臺灣新吉美碩股份有限公司

衛采製藥股份有限公司

龍霆科技企業有限公司